Elucidation of the mode of action of a furanone based antituberculosis compound

By

Andile H. Ngwane

Dissertation presented for the degree of Doctor of Philosophy in Medical Sciences (Medical Biochemistry) in the Faculty of Medicine and Health Sciences at Stellenbosch University

Supervisor: Prof. Paul van Helden
Co-supervisor Prof. Ian J.F. Wiid
Division of Molecular Biology & Human Genetics
Department of Biomedical Sciences

December 2012

Declaration

I, the undersigned, hereby declare that the work contained in this dissertation is my own original work, and has not, to my knowledge, previously in its entirety or in part been submitted at any university for a degree.

....

Andile H. Ngwane Date

Abstract

The prevalence of multi-drug resistant (MDR) and extensively drug-resistant (XDR) *Mycobacterium tuberculosis* has been increasing to alarming levels globally. This has been exacerbated by tuberculosis (TB) co-infection with HIV where the epidemic is endemic. South Africa as a developing country is hit hard by TB and efforts to develop TB drugs that are compatible with anti-retroviral medication and also effective against MDR/XDR, could help shorten the treatment duration of the current TB treatment regimens. This thesis presents the identification and characterisation of a novel furanone based compound (F1082) and its derivatives as leads for anti-TB drug development. Furanones are generally known for an array of biological activities ranging from antibacterial, antifungal and antitumor.

F1082 has an aromatic benzene structure and was identified from screening synthetic compounds against *M. tuberculosis*. It is potent against *M. tuberculosis* at minimum inhibitory concentration (MIC) of 8 µg/ml. It is selective for mycobacteria since it did not inhibit the growth of Gram-positive and Gram-negative bacteria at concentrations five times the MIC for *M. tuberculosis*. F1082 is generally bacteriostatic around MIC concentrations in its effects against *M. tuberculosis* however; it may be bactericidal at higher concentrations. It is as effective against MDR, XDR and clinical isolates of *M. tuberculosis* at the same concentration as the *M. tuberculosis* H37Rv reference strain. This suggests that F1082 may have a different mechanism of action compared to current TB drugs. It has been shown to have no antagonistic effect with the first-line anti-TB drugs and it has been shown to synergize with rifampicin by reducing the MIC of rifampicin. A drawback of F1082 is that it is cytotoxic to human cell lines, but this is presently being addressed through the synthesis of analogues that have shown improved activity and less cytotoxicity. The synthesis of more than 40 analogues has led to identification of 4 compounds that have more than five times higher activity and more than 100 times less cytotoxicity against human cell-lines.

Microarray analyses have identified possible metabolic pathway/s in *M. tuberculosis* that is/are affected by F1082. One subset of genes which showed the most prominent alteration encodes the siderophores, which are involved with iron homeostasis in the *M. tuberculosis* bacillus. Of these genes, 7 were of interest (*mbt*B, *mbt*C, *mbt*D, *mbt*E, *mbt*F, *mbt*H and *bfr*B) as they all fall in the same cluster and are involved in iron acquisition. Due to the involvement of iron we also show that F1082 generates oxidative stress that is metal (iron) dependent. From the results we conclude that F1082 is a promising antituberculosis lead compound with unique target properties and also specificity against mycobacteria.

Opsomming

Die voorkoms van veelvuldige middelweerstandige *M.tuberculosis* (MDR) en uiters middelweerstandige *M.tuberculosis* (XDR) is besig om toe te neem teen ‘n kommerwekkende tempo wêreldwyd. Hierdie situasie word vererger met die ko-infektering van *M.tuberculosis* en HIV. Suid-Afrika, as ontwikkelende land, word sleg benadeel met tuberkulose siekte. Antituberkulose middels wat kan saamwerk met bestaande antiretrovirale middels en ook effektief is teen MDR en XDR stamme, kan alles meewerk om die behandelingstyd van tuberkulose te verkort. In hierdie tesis identifiseer en karakteriseer ons ‘n furanoon-gebaseerde verbinding (F1082) en derivate daarvan as voorloper-middels vir anti-tuberkulose middelontwikkeling. Furanone is algemeen bekend vir ‘n verskeidenheid van biologiese aktiwiteite insluitende antibakteriële-, antifungale- en antitumor aktiwiteite.

F1082 bevat ‘n aromatiese benseenstruktuur en is oorspronklik geïdentifiseer gedurende die skandering van sintetiese middels teen *M.tuberculosis*. Dit het ‘n sterk werking teen *M.tuberculosis* met ‘n minimum inhibitoriese konsentrasie (MIC) van 8ug/ml. Dit is baie selektief vir mikobakterieë aangesien dit nie gram-positiewe of gram-negatiewe bakterieë teen 5 maal die MIC, soos vir *M.tuberculosis*, geïnhibeer het nie. F1082 is bevind om, by laer konsentrasies, bakteriostaties te wees

in sy aktiwiteit teen *M.tuberculosis* maar by hoër konsentrasies word ‘n meer bakteriosidiese effek waargeneem. F1082 is effektief teen MDR, XDR en kliniese isolate van *M.tuberculosis* en teen dieselfde konsentrasie soos vir die *M. tuberculosis* H37Rv verwysingstam waargeneem is. Dit impliseer dat F1082 dalk ‘n alternatiewe meganisme van werking het in vergelyking met die van die huidige TB teenmiddels. F1082 toon geen antagonistiese werking in kombinasie met die voorste anti-TB middels nie, maar toon wel sinergistiese werking in kombinasie met rifampisien. F1082 toon nog sitotoksiese aktiwiteit teenoor menslike sellyne, maar die sintese van derivate van F1082 toon tot dusvêr groter anti-TB aktiwiteit en verminderde sitotoksisiteit. Die sintese van meer as 40 homoloë het gelei tot die identifisering van vier verbindings met vyf keer hoër anti-TB aktiwiteit en honderd keer verminderde sitotoksisiteit teen menslike sellyne as F1082 self.

“Microarray” ontledings het ‘n aantal metabolise paaie geïdentifiseer waar F1082 ‘n effek kan uitoefen. Een stel gene wat die mees uitstaande effek toon kodeer vir siderofore wat betrokke is by yster homeostase in *M.tuberculosis*. Van hierdie gene was daar sewe van belang omdat hulle in dieselfde groep voorkom en almal betrokke is by ysteropname (*mbt*B, *mbt*C, *mbt*D, *mbt*E, *mbt*F, *mbt*H, *bfr*B). Weens die rol wat F1082 in ysterhomeostase speel, toon ons ook dat F1082 intrasellulêre oksidatiewe stres bevorder wat yster afhanklik is. Al ons resultate dui daarop dat F1082 ‘n belowende ant-TB voorloper verbinding is met spesifisiteit teen *M.tb* en unieke teikeneienskappe in *M. tuberculosis*.

Acknowledgements

I would like to give a special thanks to my Lord, who has carried me from the very beginning of life through the most difficult and unbearable situations. You watched over me as a child, raised me as a man, provided me with opportunities and made me who I am today, still a long way to learn, I thank my Lord.

I would like to give my sincere thanks to my parents for nurturing me and devoted their entire life time in raising me. My father (Mphumeleli, Rhadebe) you are my hero, you are the most disciplined man I ever came across and you kept us under one roof with the fatherly love. To my mother (Nokhaya, Magaba) you always inspired me, your intellectual ability to understand subjects you never learnt from school and your sense of humour kept us warm. Even this time around, without the roots of your teachings, I would not have made it. You were the heart of the family and beyond, rest in peace (lala ngoxolo) Mama.

Also I would like to give a special thanks to my brothers (Mzolisi and Msokoli), you made me become a man through all times, I look into you. To my sisters, (Nosipho, Nolufefe, and Nomthandazo), I have learnt a lot from you and gained respect for women. To my niece (Khelina), you have been my little sister since we grew up and to Palisa and Nandipha you made me to be a better uncle and Tamncinci. All of you have put a hand in shaping me to be a better person. This is not for me but to you all including my extended families, neighbours and to my community at large

To my son (Achilles), in all the odds you have been my hope and a living spirit for me to do even better. Your mother has been so supportive and I admire her through difficult times. I love you and may God bless you all.

My special thanks go to Prof. Lafras Steyn who accepted me in my MSc as this work extends from his initiative. To Prof. Ian Wiid and Paul van Helden, my success would not be a success without you. You were the pillar of this work. I extend my thanks to Prof. Gilla Kaplan, Prof. Rodriquez Masella

and to Kaplan's lab members at UMDNJ, you fulfilled my dream and best wishes to your careers. I am grateful to have worked with all the TB- TAP T80006 consortium members stretching across all deciplines involved in drug development. My special thanks go to Prof. Peter Folb, the driver of the project and Dr. Eliya Madikane for all the work taken and carried out as a project leader and Dr. Niresh Bhangwandin for finances and budgeting of this program. Lastly but not least to all my colleagues at Stellenbosch, I thank you for your support.

In every sector there are financial supporters, namely following agencies: the Innovation Fund (IF), Technology Innovation Agency (TIA) project TB-TAP T80006, Fogarty Fellowship and Novartis (Next Generation Scientist Program); collectively you have been generous in funding and providing training opportunities for skills development during my PhD, I thank you all.

Table of Contents

List of figures:

List of Tables

List of abbreviations

%	percentage
µg	microgram
µl	microliter
µM	micromolar
ADC	Albumin/Dextrose/Catalase
AIDS	Acquired Immunodeficiency Syndrome
Ala	Alanine
AMK	Amikacin
Asp	Aspartaten/ Aspartic acid
BCG	Bacille Camette-Guérin
BSA	Bovine Serum Albumin
CFU	Colony Forming Unit
DARQ	Diarylquinoline
DNA	Deoxyribinucleic acid
DOTS	Directly Observed Therapy-Short Course
DR	Drug-resistant
DS	Drug-susceptible
DST	Drug-Susceptibility Testing
EMB	Ethambutol
ETH	Ethionamide
g/l	grams per later
HIV	Human Immunodeficiency Virus
hrs.	hours
Ile	Isoleucine
INH	Isoniazid

KAN	Kanamycin
LB	Luria Broth
M	Molar
M.tb	*Mycobacterium tuberculosis*
MDR	Multidrug-Resistant
MHC	Major histocompatibility complex
MIC	Minimum Inhibitory Concentration
Min	minutes
MOTTS	mycobacteria other than tuberculosis
MTBC	Mycobacterium tuberculosis complex
nm	nanometre
OADC	oleic acid/albumin/dextrose/catalase
OD	optical density
ONPG	o-nitrophenyl-_-D-galactoside
PBS	phosphate buffered saline
PCR	polymerase chain reaction
PZA	Pyrazinamide
RIF	Rifampicin
RNA	ribonucleic acid
Rpm	revolutions per minute
RT-PCR	reverse transcriptase polymerase reaction
SDS	sodium dodecyl sulphate
STR	Streptomycin
TB	Tuberculosis
WHO	World Health Organisation
XDR	Extensively Drug-Resistant

CHAPTER ONE

Literature overview

1.1 Historical tuberculosis

Tuberculosis (TB) is a fascinating disease, and even today still poses a challenge to the medical fraternity. TB is an old disease identified in the past as Phthisis, Consumption, Pott's disease, The Great Plague, King's Evil or Lupus vulgaris. (Mathema *et al*., 2006; Daniel, 2006). *Tuber* is a Latin name referring to all forms of degenerative protuberances or tubercles and *tuberculosis* was the term for diseases causing such tubercles (Shikano *et al*., 2009). Although *tuberculosis* was probably described for the first time in Indian texts, pulmonary TB was known since the time of Hippocrates as phthisis, which is derived from the Greek for "wasting away". Scrofula, a less common manifestation of TB that affects the lymph nodes, especially of the neck and most common in children, was documented during the European Middle-Ages and it was believed that cure would come from the power of the divine touch of the king. Pott's disease or Gibbous deformity, causing skeletal abnormalities, has been identified in skeletal remains from ancient Egyptian and Aztec times.

In Western and Northern America, TB reached its peak during the18th and 19th centuries, during the age of Industrialisation (Holmberg, 1990). At that time there was a mass movement of people into cities, where people lived and worked in harsh, unhygienic conditions which favoured the spread of infectious diseases. The Industrial Revolution is known for its over-crowded factories, where people worked in polluted air workplaces, were poorly paid and worked and lived in cramped spaces also with poor or no aeration. People were undernourished and had little or no access to health care. As these conditions favoured TB, it gained a stronghold in the population and maintained its position as a major cause of death.

It is now accepted that tuberculosis existed in the Americas before European contact (Arriaza *et al*., 1995; Gómez i Prat and de Souza, 2003) although it has not yet been determined which species or genotype of *M. tuberculosis* was responsible. It is hypothesized that the disease reached the Americas via animals (Rothschild *et al*., 2001) or early nomads (Daniel, 2006) who crossed the Bering land bridge at least 10 000 years ago. The suggestion that more virulent strains of tubercle bacilli

originated in Europe and spread to the Americas during the colonial expansions from the fifteenth century onwards (Clark *et al*., 1987) has not yet been verified nor disproved.

1.2 Tuberculosis (TB): the disease

It is often stated that around 2 billion people, about one third of the world's population, are infected with tubercle bacilli. During 2007, 1.77 million people died from the disease according to the World Health Organisation (: http://www.who.int/tb). It is also reported that about 10% of infected people become ill over a life time with active tuberculosis (in absence of immunosuppression) which includes those with less effective immune systems such as the very young and old, or those who suffer from malnutrition. This high level of latent TB infection indicates a long-term co-existence of the human host and the bacterial pathogen (Hirsh *et al*., 2004).

Tuberculosis in mammals is caused by a group of closely related bacterial species termed the *Mycobacterium tuberculosis* complex family. This family includes *M. tuberculosis, M. africanum, M. canetti, M. bovis*, *M. caprae*, and *M. pinnipedii* (Smith *et al*., 2006). Other mycobacteria are wide-spread in the environment but members of the *M. tuberculosis* complex are obligate pathogens (Grange, 1996). Many of the mycobacteria, including *M. tuberculosis*, are very slow growing with an *in vitro* doubling time of approximately 24 hours (Grange, 1996) . The pathogenic species are able to survive and grow within macrophages (phagosome), which enables them to evade the host immune system (Malik *et al*., 2001). An active cell-mediated response is required to contain and kill the tubercle bacilli (Ernst, 1998).

Today, the principal causative agent of human tuberculosis is *M. tuberculosis*. *M. bovis* has a wide host range, although is the main cause of tuberculosis in bovidae. Unpasteurised milk and milk products are regarded as the main route of transmission of zoonotic TB caused by *M. bovis* in countries where there are no effective eradication programmes (O'Reilly and Daborn, 1995). In the past, and today in the absence of effective eradication programmes, it is estimated that *M. bovis* is responsible for about 6% of human deaths from tuberculosis (O'Reilly and Daborn, 1995). Other

members of the *M. tuberculosis* complex also cause human infections, such as *M. canetii*, *M. africanum*, although these tend to appear in specific geographic regions (Gagneux *et al*., 2006).

Tuberculosis infection may involve almost any organ in the body, but the most common clinical presentation is pulmonary tuberculosis, in which transmission is via infectious aerosols released from the lungs of an infected person (Chandir *et al*., 2010). In the alveolus of the lung, inhaled tubercle bacilli are ingested by the macrophages and are normally contained by the host immune response (Frieden *et al*., 2003). This can lead to granuloma formation and eventually to a calcified lesion (Dannenberg *et al*., 1994). Spread of the bacteria within a year of initial infection results in primary disease. However, it is thought by many that the organism may remain dormant but viable for decades. If the immune response is subsequently compromised, the bacteria may escape into the lungs causing re-activated pulmonary tuberculosis (Marais *et al*., 2009). In a minority of cases, the bacteria spread to other host tissues via the lymphatic system and blood, thereby becoming disseminated throughout the body, resulting in miliary or extra-pulmonary tuberculosis (EPTB) (Golden and Vikram, 2005). In immunocompetent adults it is estimated that primary EPTB disease occurs in 15-20% of all cases (Donoghue, 2009).

Infection of the lymph nodes results in swollen glands and is the most common clinical presentation of EPTB (Golden and Vikram, 2005). Cervical lymphadenitis and skin lesions were previously known as scrofula or lupus vulgaris. Pleural effusions, genito-urinary tract tuberculosis, meningitis, skeletal, ocular and abdominal tuberculosis are additional clinical presentations of the disease, especially in communities where no effective chemotherapy is available (Thwaites *et al*., 2008). Gastro-intestinal tuberculosis can result from swallowing infected sputum or by ingestion of infected animal products, resulting in the potential for transmission of infection via faeces and urine (Donoghue, 2009).

Despite half a century of anti-TB chemotherapy, it is often said that one third of the world's population asymptomatically still harbour a dormant or latent form of *M. tuberculosis* with a risk of disease reactivation (Figure 1.1). Reactivation of latent TB, even after decades of subclinical persistence, is a high risk factor for disease development particularly in immunocompromised

individuals such as those harbouring the human immunodeficiency virus (HIV), or on anti-tumour necrosis factor therapy or with diabetes (Barry *et al*., 2009).

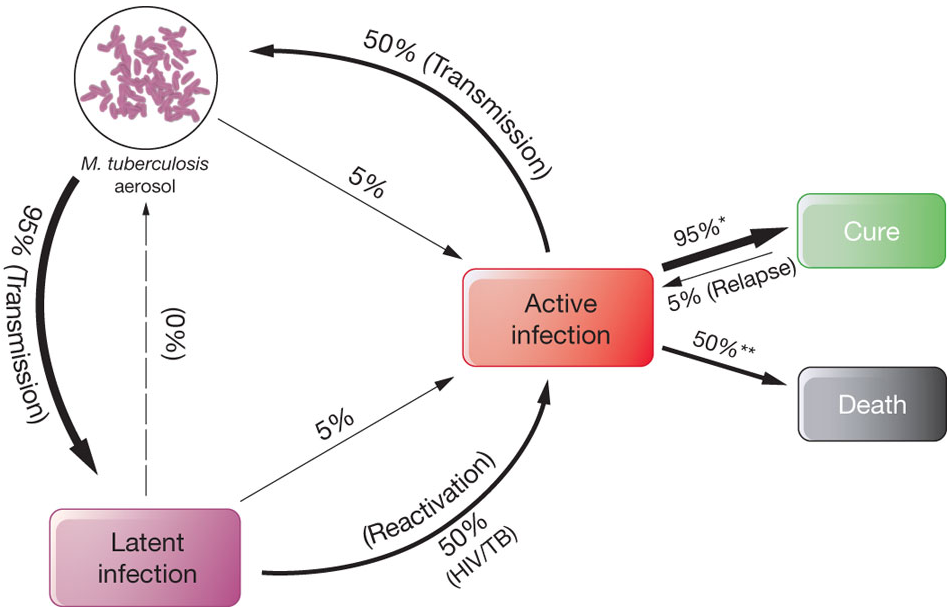

Figure 1.1 Stages of *M. tuberculosis* infection ("Koul *et al*., 2011")

Mycobacterium tuberculosis aerosol transmission and progression to infectious TB or non-infectious (latent) disease is shown (Figure 1.1). A sizeable pool of latently infected people may reactivate into active TB, years after their first exposure to the bacterium. In cases of drug-susceptible (DS)-TB with treatment compliance (denoted by asterisk), 95% of patients recover upon treatment, whereas 5% relapse. If untreated (denoted by double asterisks), high mortality results (Figure 1.1).

1.3 TB epidemiology

1.3.1 Incidence

There were an estimated 9.4 million incident cases (range, 8.9 million – 9.9 million) of TB globally (equivalent to 137 cases per 100 000 population) in 2009, as illustrated (Figure 1.2). The absolute number of cases continues to increase slightly from year to year, as slow reductions in incidence rates continue to be adjusted by increases in population. Estimates of the number of cases as published by

the WHO, (2010) indicate that women (defined as females aged ≥ 15 years old) account for an estimated 3.3 million cases (range, 3.1 million to 3.5 million), equivalent to 35% of all cases. Estimates of the number of cases need to be improved with more and improved reporting and more analysis of notification data disaggregated by age and sex. Most of the estimated number of cases in 2009 occurred in Asia (55%) and Africa (30%); smaller proportions of cases occurred in the Eastern Mediterranean region (7%), the European region (4%) and the region of the Americas (3%). The 22 high-burden countries (HBCs) that have received particular attention at global level since 2000 account for 81% of all estimated cases worldwide (Figure 1.2). The five countries with the largest number of incident cases in 2009 were India (1.6 – 2.4 million), China (1.1 – 1.5 million), South Africa (0.4 – 0.59 million), Nigeria (0.37 – 0.55 million) and Indonesia (0.35 – 0.52 million). India alone accounts for an estimated one fifth (21%) of all TB cases worldwide, and China and India combined account for 35% (WHO, 2010). Of the 9.4 million incident cases in 2009, an estimated 1.0 - 1.2 million (11-13% were HIV positive, with the best estimate of 1.1 million (12%) (Figure 1.2). These numbers are slightly lower than those reported in previous years, reflecting better estimates as well as reduction in HIV prevalence in the general population. Of these HIV-positive TB cases, approximately 80% were in the African region.

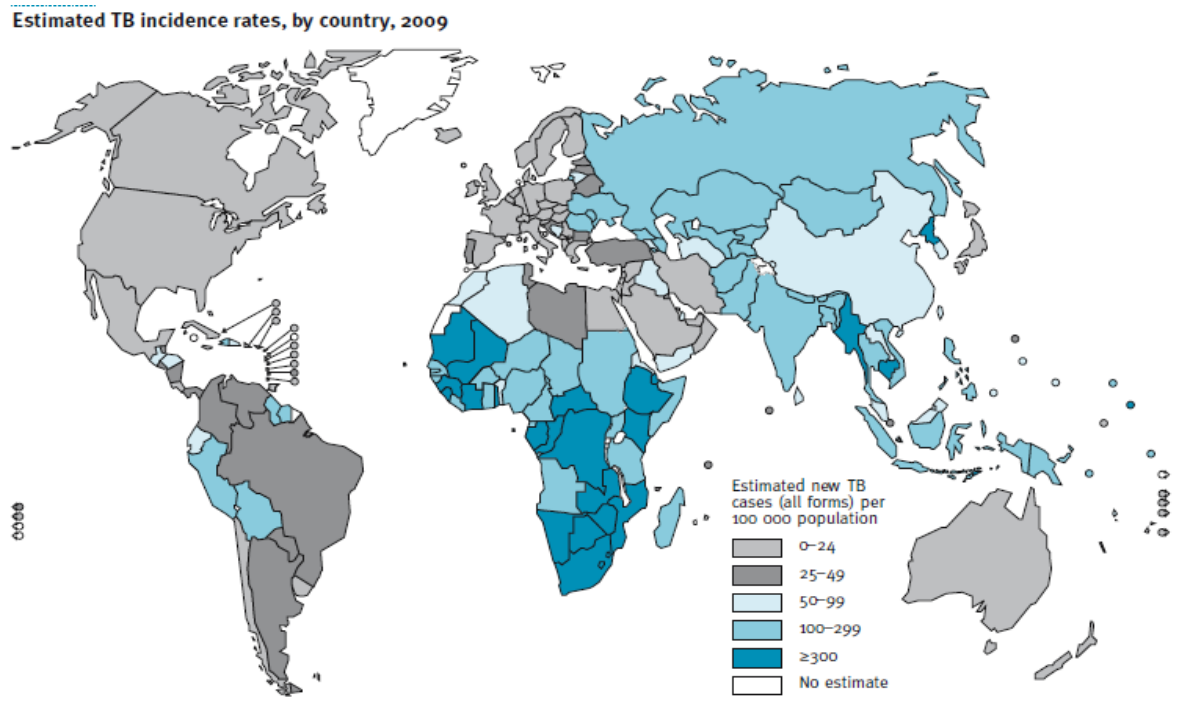

Figure 1.2 Estimated TB incidence rates, by country, 2009 (from WHO report 2010)

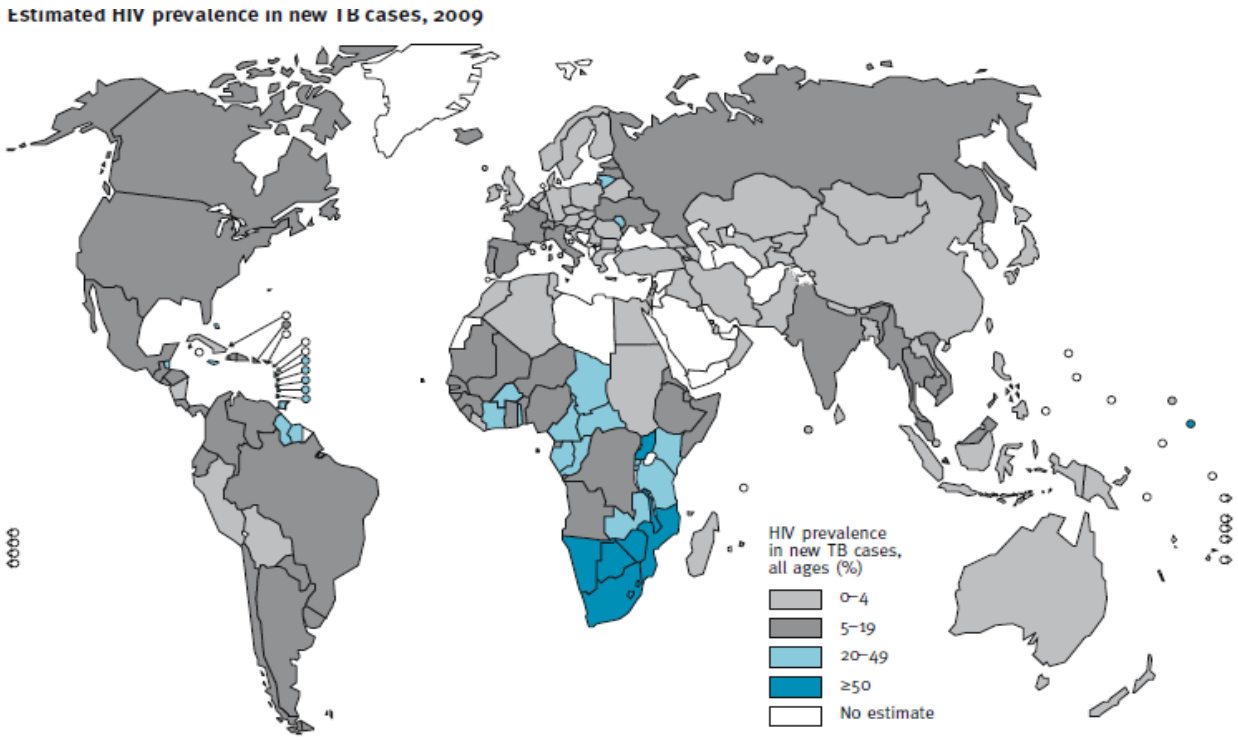

Figure 1.3 Estimated HIV prevalence in new TB cases, 2009 (from WHO report 2010)

1.3.2 Prevalence

In Wolrd Heath Organisation (WHO), 2010, there were 14 million TB (prevalent) cases estimated (range, 12 million to 16 million) for 2009, equivalent to 200 cases per 100 000 population (Figure 1.3). Prevalence is a robust indicator of the burden of the disease caused by TB when it is directly measured in a nationwide survey. When survey data are not available it is difficult to estimate its absolute level and trend. In those countries where surveys are done and repeated at periodic intervals, estimates of the prevalence of TB and trends in rates of TB prevalence will improve (WHO 2010).

1.3.3 Mortality

In 2009, an estimated 1.3 million deaths (range, 1.2 million to 1.5 million) occurred among HIV-negative cases of TB, including 0.38 million deaths (range, 0.3 – 0.5 million) amongst women WHO, 2010). This is equivalent to 20 deaths per 100 000 population (WHO, 2010). In addition there were an estimated 0.4 million deaths (range, 0.32 million – 0.45 million) among incident TB cases that were HIV-positive; these deaths are classified as HIV deaths in the 10th revision of the International Classification of Diseases (ICD-10). The number of TB deaths per 100 000 population among HIV-negative people plus the estimated number of TB deaths among HIV-positive people equates to a best estimate of 26 deaths per 100 000 population (WHO, 2010).

1.3.4 MDR-TB, XDR-TB and TDR-TB

The World Health Organisation (WHO) released statistics estimating the spread of multi-drug resistant tuberculosis (MDR-TB) defined as *M. tuberculosis* strains resistant to rifampicin and isoniazid and extensively resistant tuberculosis (XDR-TB) defined as MDR-TB that is also resistant to at least three of the six classes of second line agents. According to the WHO world report released in 2010 (Who, 2010), there were 440 000 estimated cases of multi-drug resistant TB (MDR-TB) in 2008 (range, 390 000 – 510 000). The 27 countries (15 in the European Region) that account for 86% of all such cases have been termed the 27 high MDR-TB burden countries. The four countries that had the

largest number of estimated cases of MDR-TB in 2008 were China (100 000; range, 79 000 – 120 000), India (99 000; range 79 000 – 120 000), the Russian Federation (38 000; range, 30 000 – 45 000) and South Africa (13 000; range, 10 000 – 16 000). By July 2010, 58 countries and territories had reported at least one case of extensively drug resistant TB (XDR-TB) (WHO, 2010).

Another important discovery raising concern is the identification of a form of incurable tuberculosis which was reported by a physician in India (Udwadia *et al*., 2012). Although reports call this latest form a "new entity" researchers suggest that it is instead another development in a long-standing problem. The discovery make India the third country in which a completely drug resistant form of the disease has emerged, following cases documented in Italy in 2007 (Migliori *et al*., 2007) and Iran in 2009 (Velayati *et al*., 2009). However, data on the disease, dubbed totally drug-resistant tuberculosis (TDR-TB), are sparse, and official accounts may not provide an adequate indication of its prevalence.

The term such as "total drug resistant" have not been clearly defined for tuberculosis. While the concept of "total drug resistance" is easily understood in general terms, in pratice, *in vitro* drug susceptibility testing (DST) is technicallt challenging and limitations on the use of results remain: conventional DST for drugs that define MDR and XDR-TB has been thoroughly studied and consensus reached on appropriate methods, critical drug concentrations that define resistance, and reliability and reproducibility of testing (WHO, 2008a). Data on the reproducibility and reliability of DST for the remaining second-line drugs (SLD) are either more limited or have not been established, or the methodology for testing does not exist. Most importantly, correlation of DST results with clinical response to treatment has not yet been adequately established. Thus, a strain of TB with *in vitro* DST results showing resistance could in fact, in patient, be susceptible to these drugs. The prognostic relevance of *in vitro* resistance to drugs without an internationally accepted and standardised drug susceptibility test therefore remain unclear and current WHO recommendations advise against the use of these results to guid treatment (WHO, 2008b).

Lastly new drugs are under development, and their effectiveness against these "total drug resistant" strains has not yet been reported. For these reasons, the term "total drug resistant" tuberculosis is not

yet recognised by the WHO. For now these cases are defined as extensively drug resistant tuberculosis (XDR-TB), according to WHO definitions.

1.4 Immune response to *M. tuberculosis*

Immediately after infection, alveolar macrophages and dendritic cells, which phagocytose *M. tuberculosis*, migrate through the lymphatic system towards the regional lymph node, forming the Ghon complex (Lin *et al*., 2009). Simultaneously, phagocytic cells can penetrate the pulmonary parenchyma, initiating an inflammatory focus to which other macrophages will be attracted (Flynn *et al*., 2011). In this case, the accumulation of inflammatory cells around the microorganism initiates the formation of granulomas, coordinated by T-lymphocytes. The T-cells become indispensable to the formation of stable granulomas, contacting mononuclear phagocytes and influencing their differentiation and activation status (Winau *et al*., 2006, Fallahi-Sichani *et al*., 2011). *M. tuberculosis* may be contained in this granuloma, and there is a belief that they may persist for decades, in latent form, without triggering activation of the disease (Barry *et al*., 2009).

Immunosuppression, either due to the poor health status of the individual (e.g. malnutrition, diabetes), HIV infection, or use of immunosuppressants, is thought to be a frequent cause of the multiplication of the bacilli enclosed in the granuloma and of the reactivation of TB (endogenous reaction), as compared to reinfection (exogenous) with *M. tuberculosis* (Kaufmann, 2005). Macrophages in the tissue constitute one of the first lines of defences against mycobacteria. After being phagocytosed, the bacilli remain within the phagosome. If there is phagosome-lysosome fusion, antigens can be processed and subsequently presented to T-helper (Th) lymphocytes ($CD4^+$), through the major histocompatibility complex class II (MHC II) molecules (also known as antigen presenting cells), which are found in macrophages, dendritic cells, and the B lymphocytes. It is known that the T-helper type 1 (Th 1) $CD4^+$ cells play a central role in the immune response to mycobacteria (Gallegos *et al*., 2008). However, cytotoxic T cells ($CD8^+$), which recognize antigens from the cytoplasm (tumour or viral), also participate in the immune response to *M. tuberculosis* (Palma *et al*., 2010). The $CD8^+$ T

cells can recognize peptide fragments bound to MHC class I cells, which are expressed in practically all differentiated or mature cells of the organism. In the case of mycobacteria, it has been demonstrated that apoptotic vesicles from infected cells containing antigens of the bacillus associated with MHC class 1 can specifically stimulate $CD8^+$ T cells (Winau *et al.*, 2006). Alternatively, in a phenomenon known as cross-presentation, antigens of intracellular pathogens can be presented via MHC class I cells, owing to the capacity of the phagosomes to fuse with the endoplasmic reticulum, and to the protein recruitment from the endoplasmic reticulum to the phagosome. Consequently, phagocytosed antigens can access the cytoplasm, suffer degradation by the proteases, known as proteasomes, return to the phagosome through transporters associated with antigen processing (TAPs), and bind to MHC class I molecules located in the phagosome, leading to the subsequent expression on the cell surface and to the recognition by $CD8^+$ cells(Margulies, 2009).

A complex cascade of events taking place in response to mycobacterial infection and human host immune response is depicted (Figure 1.4). Cytokines, molecules produced and secreted by different immunocompetent cells after some stimulus, are central component in the defence against mycobacteria. During immune response, the cytokines produced participate in the regulatory processes, as well as effector function (Cooper *et al.*, 2011).

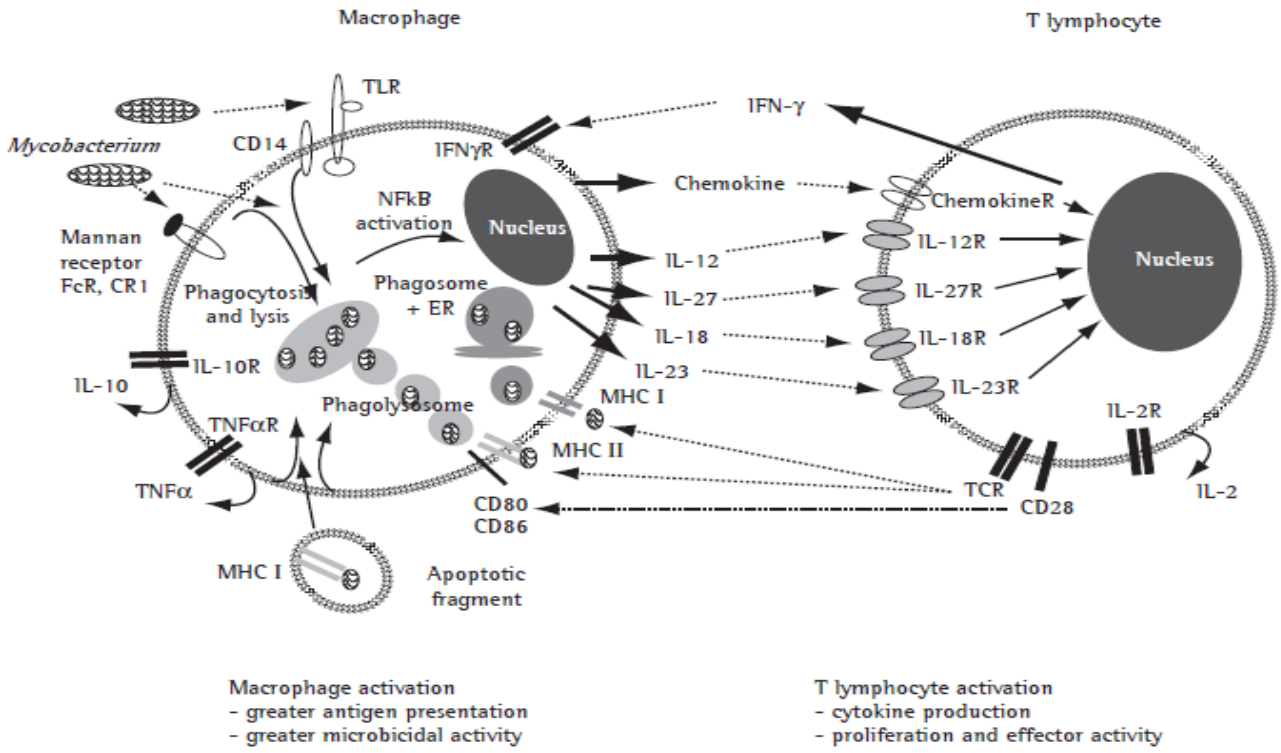

Figure1.4 Mechanism involved in the activation of macrophages and T lymphocytes by mycobacteria (from Teixeira *et al*., 2007).

Atypical lymphocytes ($CD4^-$ and $CD8^-$) have receptors containing gamma/delta polypeptide chains and recognize phosphoric components of *M. tuberculosis* (Tanaka *et al*., 1995), regardless of MHC class I or II, whereas the T lymphocyte receptor restricted only to CD1 can be stimulated by glycolipids derived from the cell wall of the mycobacteria (Cohen *et al*., 2009). Therefore the immune system can recognize and effectively respond to a broad spectrum of antigenic determinants of different biochemical characteristics. In this recognition, there is a hierarchy among the T cell subpopulations that contribute to the immune response to mycobacteria, and the $CD4^+$ and $CD8^+$ T lymphocytes are the most important in this hierarchy (Gallegos *et al*., 2008).

There is an enormously complex immune response to *M. tuberculosis* infection, and macrophages play an important role in this host response. These cells play two vital roles as the primary effector cells in killing and the habitat in which the mycobacteria reside. For the mycobacteria to survive and to develop a productive disease, they must develop strategies to evade the host immune system. Here,

we discuss some of the important strategies adopted by pathogenic mycobacteria to persist within macrophages as these areas may be exploited as targets for drug development.

An early microbicidal activity that any intracellular microbe will encounter within the macrophage is an oxidative burst (Russell, 2011). This is a nonspecific immune mechanism triggered by many microbes that results in the production of highly reactive chemical species known as reactive nitrogen intermediates (RNIs) and reactive oxygen intermediates (ROIs) (Ehrt and Schnappinger, 2009). Intermediate reaction products of O_2 en-route to water include superoxide (O_2), hydrogen peroxide (H_2O_2) and hydroxyl radicals ($OH\cdot$), and reactive products of these with halides and amines. With regard to RNIs the products correspond to molecular species in different oxidation states ranging from nitric oxide to nitrate (Nathan, 2008). From various studies it has been shown that the generation of the ROIs and RNIs is required for mycobacterial killing. However, it is unlikely that effective killing would be achieved without delivery of bacteria to acidic compartments (late endosome/lysosomes), as suggested by the studies of different laboratories (Flannagan *et al*., 2009). These findings and the lessons learned from mycobacterial immunology can direct one to potential weaknesses in the mycobacteria and can provide targets for development of new drugs from chemical compounds from synthetic libraries or natural products.

1.5 Tuberculosis (TB) disease prevention

1.5.1 BCG vaccination

The first BCG vaccination was carried out in 1921 (Grange *et al*., 1983). This vaccine, known as Bacille Calmette-Guerin (BCG), an avirulent *M. bovis* strain, was attenuated from the clinical isolates for over a decade by serial passages on glycerol saturated potato slices (Calmette, 1931). Due to the high demand, the original BCG was distributed globally, even before the establishment of an appropriate culture protocol (Aaby *et al*., 2000). Numerous BCG strains, with a variety of antigenic

and immunological differences, exist today in various parts of the world. BCG is currently used as a TB vaccine worldwide, and BCG vaccination is mandatory in many areas (Delogu and Fadda, 2009).

There have been significant advances in our understanding of the biology and the pathogenesis of tuberculosis. Unfortunately this increase in knowledge has not yet resulted in the development of a satisfactory vaccine; one that will overcome the problems associated with the current vaccine, BCG. Bacille Calmette-Guerin is an attenuated strain of *Mycobacterium bovis* and, although sometimes efficacious in laboratory models of disease (Smith, 1985), gives rise to variable protective efficacy in human populations (Andersen and Doherty, 2005). The increasing incidence of TB co-infection associated with HIV infection and the emergence of multidrug-resistant strains of *M. tuberculosis* has emphasized the importance of prevention through effective vaccination, possibly using a safe, non-viable subunit vaccine. Clearly a subunit vaccine would be preferable to overcome the difficulties associated with the use of a live vaccination such as BCG and to harness the relevant facets of the protective immune response to mycobacteria.

1.5.2 Problems associated with BCG

The efficacy of BCG in field trials has varied tremendously and in some geographical regions the vaccine has not shown any efficacy at all (Brandt *et al*., 2002). It is noteworthy that in the regions where BCG had the lowest efficacy such as South India (ten Dam, 1984) there is high level infection with mycobacteria from the soil or water sources (Herbert *et al*., 1994). More than 20 different species of mycobacteria were found in these studies and it would appear that many of these species share antigens with BCG. Several investigators have suggested that such prior exposure to environmental mycobacteria may provide varying levels of resistance against tuberculosis (Palmer and Long, 1966; Brandt *et al*., 2002). If so, one might expect low prevalence of disease, which is not necessarily the case (there is no control and this is speculation). However, sensitization provided by such exposure may have an adverse effect on the outcome of vaccination due to antagonistic interactions (Stanford *et al*., 1981). This issue remains to be resolved but, in general, the data collectively demonstrate the problem with the current BCG vaccine at least in tropical regions. Evidence in animal studies suggests

that immunity can be provided by mycobacterial species in the environment, but those isolated from South India provide only 50% of that afforded by BCG (Palmer and Long, 1966). Furthermore, the sensitization by environmental mycobacteria is acquired gradually and therefore does not provide sufficient immunity in early life. In individuals sensitized by environmental mycobacteria, subunit vaccination with *M. tuberculosis* antigens may be the optimal way to boost immunity provided by natural exposure.

A more recent development that has had a significant impact on the use of BCG is that of immunodeficiency due to the human immune deficiency virus (HIV). HIV imposes an obvious safety problem and limits the use of live BCG vaccine due to the risk of BCG-related pathology, as has been reported to occur up to 30 years after vaccination (Reynes *et al*., 1989) and may be common in HIV positive children (Hesseling *et al*., 2003). Furthermore, it is known that tuberculosis drives the progression of HIV infection to AIDS (Leroy *et al*., 1997; Goletti *et al*., 1996). Employing a vaccine based on live mycobacteria in a population already harbouring the HIV virus must therefore be considered carefully.

The antigenic similarity between BCG and *M. tuberculosis* is probably a major factor responsible for the efficacy of BCG (Fifis *et al*., 1991). However, this similarity creates problems for screening populations for tuberculosis with tuberculin PPD which contains multiple antigens shared between the vaccine and the pathogen (Farhat *et al*., 2006). As a result, BCG is not used in a number of countries that rely on tuberculin for diagnosis of tuberculosis. The ideal future vaccine would allow screening for tuberculosis to proceed without the potential pitfall of false positives within a vaccinated population.

1.6 Tuberculosis (TB) treatment

1.6.1 Evolution of antituberculosis drugs

Since the discovery of *Mycobacterium tuberculosis* by Robert Koch in 1882, a chronological development of antituberculosis drugs in relation to decades is shown (Figure 1.5). Antituberculosis drug development was catalysed in the 1940s when streptomycin was discovered and thought to provide the "magic cure" for tuberculosis (Fox *et al*., 1999). This enthusiasm was soon curbed when it became apparent that the final outcome of the "cures" with this single agent soon approached that of untreated patients. A decade later, isoniazid was discovered and when used in conjunction with streptomycin, rapid and durable cures were obtained (Fox *et al*., 1999). A combination of streptomycin with isoniazid and para-aminosalicylic acid resulted in the first combination therapy regimen which was given over 24 months (Schmitz and Kleine-Allekotte, 1960). Para-aminosalicylic acid was replaced in the mid-1960s by ethambutol, which was tolerated and reduced treatment duration to 18 months (Schmitz and Kleine-Allekotte, 1960). The introduction of rifampicin to combination therapy in the late 1960s offered a cure in more than 95% of patients and further reduced the treatment duration to 9 to 12 months (WHO 2009). Pyrazinamide was added in the 1980s and facilitated the modern-day short-course treatment.

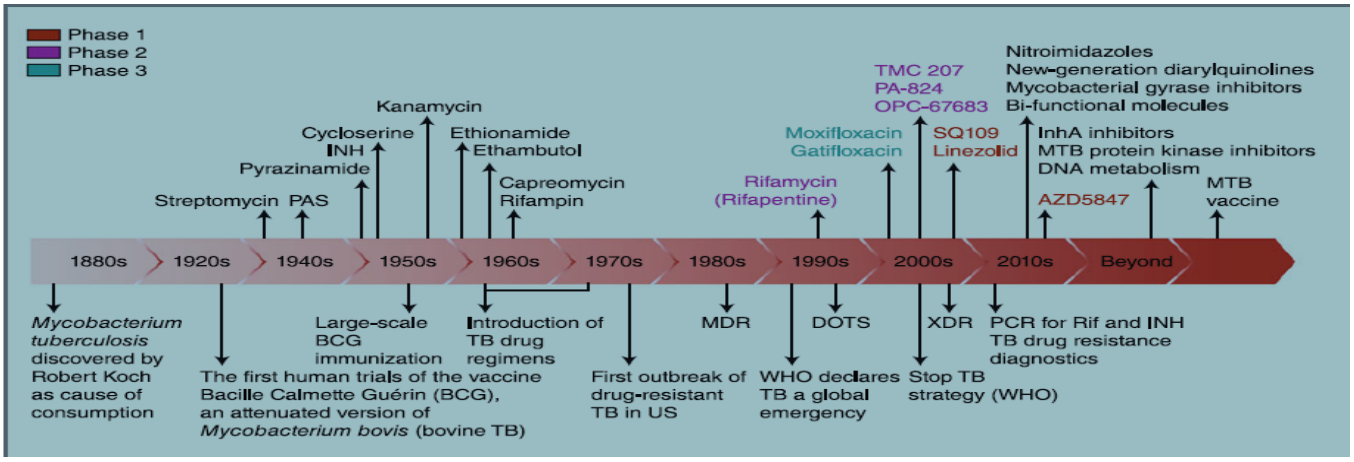

Figure 1.5 Time-line in TB and antituberculous drug development (from Lalloo and Ambaram, 2010**).**

1.6.2 Current TB treatment

Today many TB antibiotics are available which can, based on their activity, be classified into 3 groups: those with bactericidal activity, those with sterilizing activity, and those that prevent drug resistance. Bactericidal activity is the capacity of a drug to reduce the number of actively dividing bacilli in the initial therapy stage. Although rifampicin and streptomycin have some bactericidal activity, the most potent anti-TB drug is isoniazid (Hershfield, 1999). Sterilizing activity as in the case of rifampicin and pyrazinamide is the ability of the drug to eliminate the putative subpopulation of dormant bacteria from which clinical relapse can occur (Davies, 2010). Drug resistance is prevented by drugs that eliminate all bacterial populations and do not allow the emergence of resistant organisms. Most effective treatment regimens consist of at least two bactericidal ant-TB drugs (isoniazid and rifampicin) to kill actively growing *M. tuberculosis* populations, followed by a continuation phase for elimination of intermittent dividing and dormant bacteria (Frieden *et al*., 2003). A major challenge still remains: elimination of latent TB, which is a results from exposure *M. tuberculosis* that are alive in the body but remain inactive.The current treatment is ineffective in eliminating latent TB.

The therapy combination and duration is broadly classified into three categories. Category 1 consists of an initial phase of two months with daily (5/7) doses of INH, RIF, PZA and EMB. This is followed by a continuation phase of four months with daily (5/7) dose of INH and RIF, for newly smear-positive and seriously ill smear negative patients or seriously ill patients with extrapulmonary manifestations (Holland *et al*., 2009). Category 2 is recommended for previously treated smear-positive patients who come for re-treatment due to relapse, failure or default. The regimen consists of an initial phase of two months with daily (5/7) doses of INH, RIF, PZA, EMB and SM followed by a continuation phase of one month with daily (5/7) doses of INH, RIF, EMB with or without PZA. Category 3 is recommended for treatment of new smear-positive patients and those with extrapulmonary manifestations, but not seriously ill. The combination consists of an initial phase of

two months with thrice weekly doses of INH, RIF and PZA followed by a continuation phase of four months with thrice weekly doses of INH and RIF (Myers, 2005).

In an attempt to reduce the global burden of TB, the World Health Organisation (WHO) formulated the Millennium Development Goals (MDGs). The target of the MDGs is to halve TB prevalence and death rates by 2015 compared to that of 1990, and furthermore to completely eliminate TB by 2050. To achieve this, the WHO developed the Directly Observed Treatment, short-course (DOTS) strategy in the mid-90s, which was recommended internationally and consequently expanded worldwide (Hopewell *et al*., 2006). DOTS is a 6 months therapy regimen consisting of an initial 2 months treatment phase with four first-line drugs (isoniazid, rifampicin, pyrazinamide and ethambutol), followed by a 4 month treatment phase with only isoniazid and rifampicin. The addition of DOTS, where patients consume each dose of anti-TB drugs under supervision, to the treatment strategy is strongly recommended. This approach maximizes the probability of therapy completion, hence limiting the emergence of drug-resistance (Blumberg *et al*., 2003). Approximately 90% of the drug susceptible TB cases are cured when this regimen is fully adhered to (WHO, 2010). For MDR cases WHO recommends DOTS-plus, which includes adding second-line drugs to the conventional DOTS program (WHO, 2010).

1.6.3 Classification of TB drugs

Currently available TB drugs are classified by the World Health Organisation as first-line, second-line, and third-line drugs based on accessibility, efficacy and drug sensitivity (Lalloo and Ambaram, 2010). Table 1.1 is a practical classification of anti-TB drugs. Second-line drugs may be more toxic, less effective, and not routinely available in developing countries and are reserved for drug-resistant TB. Third-line drugs are generally still under development, or of unproven or diminished efficacy, more toxic, and/or very expensive (Falzon *et al*., 2011). Many are used for XDR-TB, for which treatment options are seriously limited. Drugs such as imipenem, metronidazole, co-amoxiclav, clofazimine, and perchlorperazine are used under exceptional circumstances despite lack of evidence

in many cases for their efficacy (Chambers *et al*., 2005). Global recognition of XDR-TB has prompted intensive clinical research into these and newer drugs for TB treatment.

Table 1.1 Classification of antituberculosis drugs

First-line	Second-line	Third-line
Rifampicin	Aminoglycosides	Rifabutin
Isoniazid	Amikacin	Macrolides
Ethambutol	Neomycin	Clarithromycin
Pyrazinamide	Polypeptides	Linezolid
	Capreomycin	Thiacetazone
	Viomycin	Thioridazine
	Emviomycin	Arginine
	Flouroquinolones	VitaminD
	Ofloxacin	Perchlorperazine
	Levofloxacin	
	Ciprofloxacin	
	Moxifloxacin	
	Thioamides	
	Ethionamide	
	Prothionamide	
	Para-aminosalicylic acid	

1.6.4 Challenges with the current treatment and the quest for new tuberculosis drugs.

At present, MDR-TB is treated by a combination of multiple drugs with therapies lasting up to 18-24 months; only four of these drugs were directly developed to treat TB (Gandhi *et al*., 2010). Suboptimal therapy leads to almost 30% of MDR-TB patients experiencing treatment failure (Mitnick *et al*., 2003). The treatment options for XDR-TB are even more limited, since XDR bacilli are

resistant not only to isoniazid and rifampicin, but also to flouroquinolones and injectables such as aminoglycosides. In addition, there are serious side effects with most XDR-TB and MDR-TB drugs, including nephrotoxicity, ototoxicity with aminoglycosides, hepatoxicity with ethionamide and dysglycemia with gatifloxacin (Ma *et al*., 2010). Thus the current situation necessitates the immediate identification of new scaffolds that can address emerging resistance and also requires the conduct of appropriate clinical trials, since historically, very few clinical studies have been performed to evaluate the efficacy of drugs in MDR-TB or XDR-TB patient cohorts. Improving diagnostics with wider coverage of drug susceptibility testing will also help address the high mortality of MDR/XDR-TB and curb the emergence of resistance.

TB accounts for about one in four of the deaths that occur among HIV-positive people (WHO 2010). Of the 9.4 million TB cases in 2009, 11-13% was HIV-positive, with approximately 80% of these co-infections confined to the African region (WHO 2010). The frequent co-infection of TB in HIV patients further complicates the selection of an appropriate treatment regimen because (1) increased pill burden diminishes compliance (2) drug-drug interactions lead to sub-therapeutic concentrations of antiretrovirals; and (3) overlapping toxic side effects increase safety concerns. The interaction between HIV drugs and TB antibiotics can occur because of rifampicin-induced increased expression of the hepatic cytochrome P450 oxidase system (CYP) (Niemi *et al*., 2003). This CYP induction results in increased metabolism and decreased therapeutic concentrations of many co-medications, such as HIV protease inhibitors (L'homme *et al*., 2009). Even in the presence of CYP 450 inhibitors such as ritonavir, normal trough levels of various classes of protease inhibitors cannot be rescued and consequently, standard protease inhibitor regimens, whether boosted or not, cannot be given with rifampicin. The only treatments for HIV-infected TB patients with minimal drug-drug interactions are non-nucleoside-reverse-transcriptase inhibitor (NNRTI) containing regimens. However, there are fewer options for patients with NNRT-resistant mutations and therefore new chemistry approaches are being used to identify new rifamycins, such as rifabutin, with reduced CYP-induction properties (Ma *et al*., 2010).

However the presence of ritonavir in the protease cocktail increases the serum concentration of rifabutin, thereby increasing its accompanying toxicity (Dye and Williams, 2010). In order to search for newer rifamycin analogues with minimal interaction with HIV and other co-medications, the upfront screening of newer molecules in a CYP profiling (pregnane-X receptor) assay can be performed (Goodwin *et al*., 1999). This receptor drives transcription of CYP genes and can identify chemical analogues with minimal interactions with drug metabolizing enzymes such as CYP450. Furthermore, availability of co-crystal structures of rifampicin with bacterial RNA polymerase (Campbell *et al*., 2001) might help to design molecules with better drug resistance profiles. In HIV patients harbouring MDR- or XDR-TB strains, drug-drug interaction studies of second-line antibiotics are not well established, (for example ethionamide, cycloserine, kanamycin, amikacin, capreomycin and para-amini salicylate) (Burman *et al*., 1999). Thus, there is a clear need for new studies to investigate the interaction of antiretrovirals with second-line TB drugs and with those currently in clinical development.

Confounding these issues is the association of TB with other chronic diseases such as diabetes, which is known to increase the risk of developing active TB three fold (Dye and Williams, 2010). The biological rationale for the slower response of diabetics to anti-TB drugs and for their increased risk of developing MDR-TB is poorly understood, although it is well known that cell-mediated immunity is suppressed in diabetes, which could explain higher TB rates. Attainment of bacterial culture negativity, relapse rates and mortality are significantly higher in diabetic TB patients (Touré *et al*., 2007). We therefore need to identify new TB molecules that are strongly bactericidal and have minimal drug-drug interactions with oral anti-diabetic drugs (Dooley and Chaisson, 2009). Diabetics also tend to have a high body mass index (BMI) and are often obese, which may in part lead to lower TB drug concentrations (Ruslami *et al*., 2010). Where there is a poor response to TB treatment in diabetic patients, therapeutic drug monitoring may be useful in TB management.

After decades of a standstill in TB drug development, the drug pipeline has begun to show promise over the last 10 years. The main criteria established by the TB Alliance are to select drug candidates

for further development and are: shortening of the current treatment, activity against MDR-TB, and lack of interactions with antiretroviral drugs. During the last few years, increasing awareness of the lack of Research and Development (R&D) for neglected diseases has led some pharmaceutical companies to establish an institute undertaking R&D activities on a 'non-profit-no-loss' basis. Other companies have engaged in tuberculosis R&D on a for-profit basis and with some success (Moran, 2005).

Major advances have been also made in tuberculosis basic research. Modern molecular and genetic analytical tools have become available for *M. tuberculosis* (such as targeted mutagenesis, array-based analysis of mutant libraries, techniques for conditional gene silencing and global gene expression profiling) and this has led to impressive improvement in the knowledge and understanding of the basic biology and physiology of *M. tuberculosis* (Wassenaar *et al*., 2009).

Despite these positive changes, there are still problems that need to be tackled. A critical question today is whether they are sufficient to bring improved treatment to patients in the next few years. The next important question is whether there are an adequate number of promising compounds in the TB pipeline for a broadly effective new treatment combination to be developed. Although different attrition rates might apply, the number of candidate compounds is still small compared to the drug pipelines for diseases of major concern to wealthy countries, such as cancer or cardiovascular diseases.

1.7 TB Drug discovery and development process

Mycobacterium tuberculosis is a difficult pathogen to combact and the drugs used are more tan 40 year old. Although cure rates are as high as 95% have been reported, they are not typical observed in stting where health facilities are afar in developing countries. If cure rates of 85% are achievable, it is reasonable to ask why TB still kills 1.7-1.8 million people every year (WHO, 2010). The most straighward answer to the question is that these drugs are not ideal for treating TB. However the most

answer is undoubtedly complex and is related not only to the current treatment but also rooted to socioeconomical issues. The most noteworthy accepted treatment for TB that is long lasting and involves multiple-drug combination is challenged by the fact that the current treatment is not efficacious and *M. tuberculosis* ability to develop resistance to any single agent. There is an urgent need todevelop new or improved drug for the treatment of TB. Drug discovery development for treatment of TBis slow and the time spent to identify lead compounds has been delays by much attrition applied in this process. Therefore drug discovery in TB treatment is an area of focus and requires collective effort.

Drug discovery and development is the mission of pharmaceutical research companies to the path from understatnding a disease to bringing a safe and effective new treatment to patients. Scientist work to piece together the basic causes of a disease at level of genes, proteins and cells. Out of this understanding emerge "targets" which potential new drugs might be able to affect. Researchers work to validate these targets, discover the right molecule (potential drug) to interact with the target chosen, test the new compound in the lab and clinics for safety and efficacy and gain approval and get the new drug into the hands of doctors and patients. The task of discovering and developing safe and effective drugs is even more promising as our knowledge of disease increases. As scientist work to harness his knowledge, it is becoming an increasingly challenging.

It takes about 10 to 15 years to develop one new medicine from the time it is discovered to when it is available for treatmenting patients (Figure 1.6). The average cost to research and develop each successful drug is estimated to be US $800 million to $1 billion. This number includes the costs of thousands of failures. For every 5, 000 to 10, 00 compounds that enter the research and development (R & D) pipeline, ultimately only one receives approval. These numbers defy imagination, but a depper understanding of the R & D process can explain why so many compounds don't make it and why it takes such a large, lengthy effort to get one medicine to patients. Success requires immense resources (the best scientific minds, highly sophisticated technology and complex project management. It also takes persistence and sometimes, luck. Ultimately, though the process of drug

discovery brings hope and relief to millions of patients. In the following discussion we unravel the process of TB drug discovery and how we have engaged ourselves in coming with a promising molecule to TB drug development pipeline.

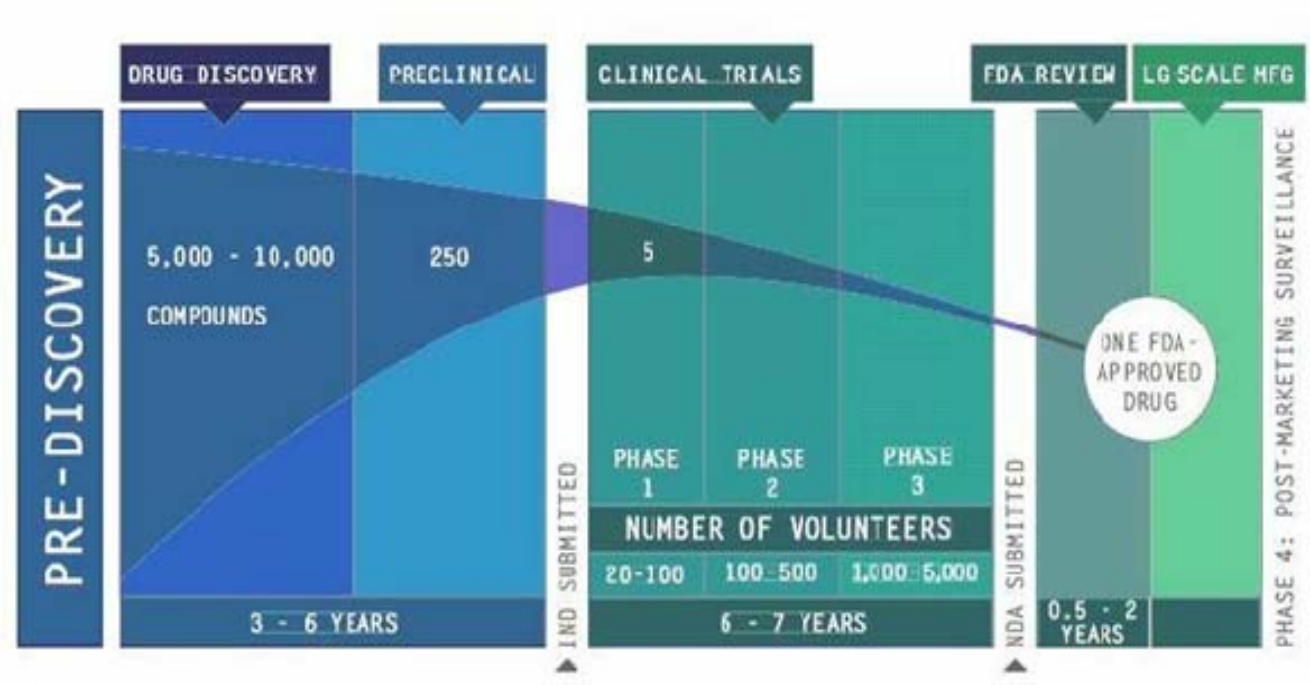

Figure 1.6 Tthe attrition rate of compounds as they travel through the drug development process over time (Adopted from PhRMA, 2008).

The complex nature of drug discovery and development requires a great knowledge of understanding

The special challenges with *M. tuberculosis* biology

TB drug research is mostly challenged by broad strectrum anti-bacterial drug research; identifying and developing a novel antibiotic is extremely difficult. The need for new antibiotics and the low success rate of finding such antibiotics (only two new antibiotics series have been brought to market in the last 40 years) and have been published (Fischbach and Walsh, 2009). Besides the fact that pharmaceutical companies have redirected their resources in drug discovery but still fall short of effective target-based “hits” (Payne *et al*., 2007). Furthermore aside from specific challenges, there are several barriers in TB area including: no well-established pharmarcokinetic (PK)-

pharmacodynamic (PD) paradigms; lack of validation and human-like pathology of animal model currently available for drug discovery; lack of adequate clinical laboratories for clinical trials; and the lack of adequate research funds.

1.7.1 Current TB drug under development

The major drugs currently under development are listed in Table 1with their mode of action (MOA). There are several reports on the advancement of these compounds under development (Palomino *et al*., 2009; Barry and Blanchard, 2010), and herein we provide a summary.

TMC207, a lead compound in diarylquinoline series and was originally discovered by Janssen Pharmaceutical (Koul *et al*., 2007). This compound is undergoing Phase II clinical development for both multi-drug resistant (MDR) and drug-sensitive (DS)-tuberculosis (TB) indications. Its MOA is by inhibiting the *M. tuberculosis* ATP synthesis by interacting with the subunit c of ATP synthase (Koul *et al*., 2007).TMC was identified from estimated 7, 000 compounds screened on a whole-cell based assay against surrogate strain *Mycobacterium smegmatis*. Its MOA was established by analyzing the whole genome sequence of laboratory generated drug-resistant *M. tuberculosis* mutants. It is active against dormant *M. tuberculosis* organisms. Although a large number of TMC207 have been synthesized by Tibotec and TB Alliance for further development, one challenge might be to overcome the lipophilic nature of the compound. This might affect the PK, drug formulation and potentially may have other consequences.

PA-824, is a derivative of **CGI-17341** whose anti-TB activity was already reported (Ashtekar *et al*., 1993). It is currently in Phase II clinical exploration against DS-TB patients. Its bacterial activity has been shown to be similar to that demonstrated by standard first-line drug regime (Diacon *et al*., 2010). The MOA of the compound has been shown to in *M. tuberculosis* **PA-824**-resistant mutants to involve reduction of the nitro-imidazole moiety by an F420-dependant enzyme (RV3547, deazaflavin-dependent nitroreductase) (Manjunatha *et al*., 2006).The generation of the des-nitro intermediates and cell killing has been the suggested bactericidal mechanism under anaerobic conditions. The exact

MOA under aerobic conditions is still a limitation, however, inhibition of mycolic acid biosynthesishas been suggested (Manjunatha *et al*., 2009). A diverse range of **PA-824**-derivatives have been synthesized (Kmentova *et al*., 2010) and some of them are in preclinical candidate stage of development.

OPC-67683, is also an analogue of CGI-17431, discovered and under development by Otsuka Pharmaceutical Company (Sasaki *et al*., 2006). It has a similar mode of action to Pa-824 (Matsumoto *et al*., 2006). OPC-67683 is reported to 4-16 times more potent than PA-824 *in vitro* and has no cross-resistance with TB first-line drugs. It is currently in Phase II clinical trials for MDR-TB patients.

Moxifloxacin and gatifloxacin, both are the most advanced compounds under development for TB drugs. They are in Phase III clinical trials. They are quinolones and both have 8-methoxyquinolone they were initially developed as broad-spectrum antibiotics and now being repurposed as anti-TB drugs. Fluoroquinolones in bacteria target gyrase and topoisomerase IV but in *M. tuberculosis* it is assumed they target solely gyrase since there is no evidence of topoisomerase IV (Diacon *et al*., 2011). Moxifloxacin and gatifloxacing are more potent *in vitro* than other quinolones such as ciprofloxacin and ofloxacin which are used as second-line drugs. They are both in Phase III clinical trials in DS-TB patients replacing either ethambutol or isoniazid in standard first-line treatment (Aristoff *et al*., 2010).

Rifampin and rifapentin, in recent years, efforts to use high dose of refampin (rifampicin) is under investigation whether it might contribute to treatment shortening (Diacon *et al*., 2007). Earlier trials of high-dose rifampin were reviewed and it was concluded that higher than standard rifampin dosing results in improved culture conversion rate (Steingart *et al*., 2011). Rifampetin is a newer analogue of the rifamycin class. It is more potent against *M. tuberculosis* and has a longer shelf-life in human compared with rifampin (Temple and Nahata, 1999). Rifapentine is currently evaluated in Phase II clinical trials. Rifamycin class of compounds inhibits *M. tuberculosis* RNA polymerase and resistance occurs by mutation in RNA polymerase (Aristoff *et al*., 2010). A challenge about this class of

compounds is that they induce cytochrome P456, this could affect the plasma levels of co-administered drugs.

Oxazolidinones, linezolid which represent the oxazolidinone class of antibiotics is one of the newly introduced antibiotics into the market and daptomycin representing lipopetide class of antibiotics. They are potent against Gram positive bacteria including methicilin-resistant *Staphylococcus aureus* (MRSA) and vancomycin-resistant *Enterococci*. It has also been shown that linozolid is active against *M. tuberculosis* by *in vitro* and in animal models (Alcalá *et al*., 2003). In *M. tuberculosis* it targets the ribosome and is active against MDR-TB clinical isolates. Linezolid has been used for MDR-TB and XDR-TB and additional Phase II clinical trials are ongoing (Fortún *et al*., 2005). Two oxazolidinones are also in clinical trial development include PNU-100480 from Pfizer and AZD5847 from AstraZeneca. It well known that linezolid adverse side effect results to hematological adverse effects (Gerson *et al*., 2002) and may not bet used fro treatment longer than 14 days. Therefore second-generation oxazolidinone agents will be the key to their development.

SQ109, is an anlogue of ethambutol that was prepared through recombinatorial chemistry (Protopopova *et al*., 2005). SQ109 is implicated in affecting cell wall biosynthesis and also active against ethambutol-resistant strains, however its precise MOA is not well known. It has been shown to have synergistic effect in combination with rifampin, isniazid, or **TMC207** (Nikonenko *et al*., 2007). The challenge with this molecule is low bioavailability, however Phase I sduties have been completed and recruitment for Phase II studies.

Meropenem and **clavulanic acid**, β-lactam antibiotics have been used for the first against *M. tuberculosis*. Deletion of the major β-lactamase of *M. tuberculosis,* BlaC, resulted in activity with of β-lactam antibiotics against *M. tuberculosis* (Flores *et al*., 2005). A combination of clavulanic acid, a β-lactamase inhibitor and meropenem, a carbapenem antibiotic was shown to be active and potent *in vitro* in XDR-TB strains under aerobic and anaerobic conditions (Hugonnet *et al*., 2009). By *in vitro* studies it has been shown that combination of any of the carbapenems (imipenem, meropenem and ertapenem) with clavulanic acid reduce the minimal inhibitory concentration (MIC) of carbapenem

from 8-16 to 1-4 µg/ml. *In vivo* studies of combination of imipenem or meropene with clavulanic acid improve survival of mice with less reduction of colony forming units when compared to isoniazid after 28 days of treatment.

Benzothiazones, a promising new class of antimycobateria is represented by BZT043 with an MIC against *M. tuberculosis* of 0.004 µg/ml (Igarashi *et al*., 2003). *In vivo* studies indicate that this compound reduces bacterial load by 1 to 2 logs in the lung and spleen of mice, respectively. By sequencing, resistant mutant strains, it appears that it targets the enzyme decaprenylphosphoryl-β-D-ribose 2'-epimerase (DprE1), which is involved in the biosynthesis of cell-wall component, arabinogalactan. The proposed MOA involves the reduction of the nitro group to a nitrosoresidue, that reacts with the cysteine group of DprE1 (Trefzer *et al*., 2010)

Caprezamycins, are closely related natural products of complex structure (Igarashi *et al*., 2003).They are active against DS and DR strains of *M. tuberculosis* with an MIC of 3.13 µg/ml. They are similar to other known lipo-uridine antibiotics, it is believed their MOA to be the inhibition of lipid biosynthesis, with specificity the inhibition of phospho-MurNAc-pentapetidetranslocase (MraY, translocase I) (Bugg *et al*., 2006). There is not enough data on PK properties and hence the compoud can only be given by injection and can only be used for DR-TB patients. Caprazmycins are still in preclinical development stage.

DC-159a, is an 8-methoxy-fluoroquinolone and was originally developed as a broad spectrum antibiotic, but was recently repurposed for TB treatment. It's been shown to be more potent than moxifloxacin and gatifloxacin by *in vivo* studies against DS *M. tuberculosis* strains and retained activity against 11 strains of quinolone-resistant *M. tuberculosis* strains (Disratthakit and Doi, 2010). It also shown to be active in both replicating and non-replicating phases (Ahmad *et al*., 2011).

Although many compounds show promise *in vitro*, not all compounds or molecules showing antimycobacterial activity either *in vitro* or in animal models end up evaluated in human clinical trials. Table 1.2 show some compounds that are currently undergoing clinical trials, opening the

possibility of eventually replacing one or more of the current first-line anti-TB drugs (Chen *et al*., 2006; Jia *et al*., 2005; Spigelman, 2007).

Table 1.2 Main TB drugs undergoing clinical evaluation

Drug type	Drug name	Phase	Mechanism of action	Sponsor	Reference
Diamine	SQ-109	I	Cell wall biosyntheisis but its exact MOA not established	Sequella	Reddy *et al*., 2010
Pyrrole	LL-3858 O	I	Multiple	Lupin	Kant, 2009
Nitromidazooxazine	PA-824	I	Multiple	Global TB Alliance	Manjunatha *et al*., 2009
Flouroquinolone	Gatifloxacin	III	DNA synthesis inhibition (inhibition of the gyrase)	EU/TDR	Rustomjee *et al*., 2008
Flouroquinolone	Moxifloxacin	III	DNA synthesis inhibition (inhibition of the gyrase)	Bayer/Global TB Alliance (GATB)	(Rustomjee *et al*., 2008
Diarylquinolone	TMC207	II	ATP synthesis inhibition (subunit of ATP synthase	Tibotec/J&J	Koul *et al*., 2007

1.7.2 Identification of new chemical scaffolds

The poor efficiency of identifying new TB drugs by screening pharmaceutical library collections has been linked to the limited chemical diversity within these collections (Payne *et al*., 2007). Additionally, most TB drugs and antibacterials in general do not follow Lipinski's 'rule of 5', which defines the optimal drug-like features; whereas pharmaceutical compound collections are biased

towards these properties (Projan, 2003). In spite of these challenges, the current TB clinical pipeline (Figure 1.7) is slowly expanding, although it is arguably inadequate for the development of a completely novel regimen. The key question remains how to search for new TB drugs and where to look for them?

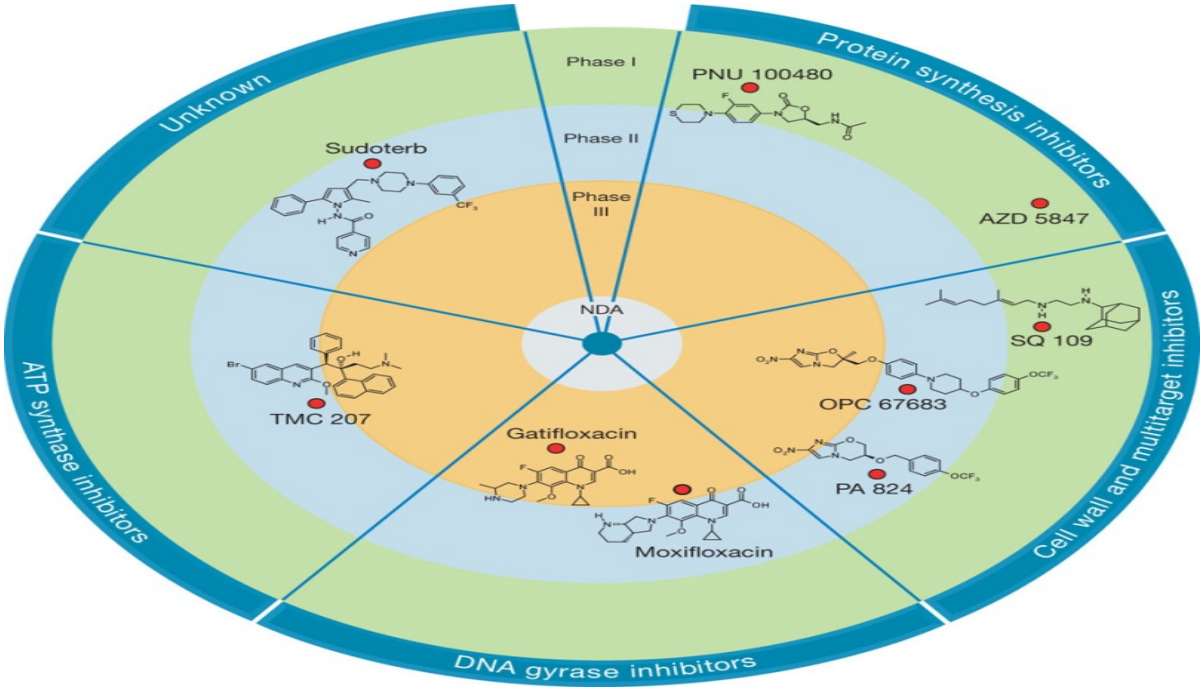

Figure 1.7 A representation of the current clinical pipeline for TB ("Koul *et al*., 2011")

1.7.3 Novelty in screening

Attempts to advance identification of new TB drugs targets have also been driven by the availability of the genome sequence of *M. tuberculosis* (Cole *et al*., 1998a), but unfortunately this approach has yet to lead to the identification of new advanced drug candidates. Genome-derived, target-based approaches have had little success in the antibacterial therapeutic area in general (Payne *et al*., 2007). The essentiality of a target for replication may be a prerequisite but it does not ensure its druggability, since for many essential targets we are unable to identify specific inhibitors with drug-like properties. For example, several high-throughput screening campaigns to identify inhibitors of isocitrate lyases (Cole *et al*., 1998a), which are key glyoxylate-shunt-pathway enzymes (Smith *et al*., 2003) found to be essential for mycobacterial intracellular growth and their long-term persistence in mice, were

discontinued owing to lack of druggability of these targets (Working group on New TB drugs, 2010). Secondly, we have often failed to understand how to convert good bacterial enzyme inhibitors into compounds that can easily penetrate the highly impermeable bacterial cell wall. Without proper understanding of these entry mechanisms of antibiotics across bacterial cell walls, any medicinal chemistry approach to engineer (via chemical modifications) a 'permeability property' into enzymatic inhibitor has proven to be quite challenging.

Over time, it has emerged that shifting the screening strategy from single-enzyme target to phenotypic screens at a whole bacterial cell level is a much more successful strategy (Payne *et al*., 2007). Such a strategy recognises a potential holistic interaction of a drug target(s) with one or more components in a bacterial cell and defines its essentiality in a more relevant physiological space. One of the drawbacks of the whole-cell-screening approach is that upfront knowledge regarding the mechanism of action remains largely unknown, thereby preventing any input from structural biology into medicinal chemistry efforts around the drug design. Another challenge of the whole-cell-screening is to determine the right *in vitro* growth conditions that are relevant for *in vivo* infections, as certain metabolic targets behave differently depending on the composition of the growth medium (Pethe *et al*., 2010). Whole-cell-screening can deliver many 'hits', but several of these may work via non-specific mechanisms (such as detergent effects) and have cytotoxic effects. As such, the key in whole-cell-screening campaign is to identify the quality of 'hits' by certain counter screening assays (for example cytotoxicity across several cell lines, monitoring non-specific membrane leakage, analysing red-blood haemolysis), so as to account for good selectivity and specificity.

The recent success with the whole-cell-screening approach is particularly exemplified by the identification of new TB drug candidates such as diarylquinolones (TMC207), which target ATP synthesis, and benzothiazinones (BTZ043), which targets cell wall arabinan synthesis (Andries *et al*., 2005; Koul *et al*., 2007; Makarov *et al*., 2009). An interesting feature of both these molecules is that they target the membrane-associated proteins that may be more easily accessible to drugs from the

periplasmic space (that is the target binding sites are exposed to the periplasm) and this to some extent may overcome certain issues of mycobacterial membrane permeability(Andries *et al*., 2005).

1.7.4 Nature as a source of medicinal compounds

Over thousands of years, natural products have been used in attempts to treat and prevent human diseases. Natural product "medicines" originated from various source materials including terrestrial plants, terrestrial microorganisms, marine organisms, terrestrial vertebrates and invertebrates (Newman *et al*., 2000). The importance of natural products in modern medicine has been discussed in recent reviews and reports (Newman *et al*., 2000; Koehn and Carter, 2005; Paterson and Anderson, 2005). The value of natural products in this regard can be assessed using 3 criteria: (1) the rate of introduction of new chemical entities of wide structural diversity, including those serving as templates for semisynthetic and total synthetic modification, (2) the number of diseases treated or prevented by these substances, and (3) their frequency of use in the treatment of disease.

An analysis of the origins of the drugs developed between 1981 and 2002 showed that natural products or natural product-derived drugs comprised 28% of all new chemical entities (NCEs) launched onto the market (Newman *et al*., 2003). In addition, 24% of these NCEs were synthetic or natural mimic compounds, based on the study of pharmacophores related to natural product (Newman *et al*., 2000). This combined percentage (52% of all NCEs) suggests that natural products are important sources of new drugs and are also good lead compounds suitable for further modification during drug development. The large proportion of natural products in drug discovery has stemmed from the diverse structures and the intricate carbon skeletons of natural products. Since secondary metabolites from natural sources have been elaborated within the living systems, they are often perceived as showing more "drug-likeness and biological friendliness than totally synthetic molecules" (Koehn and Carter, 2005), making them good candidates for further drug development (Balunas and Kinghorn, 2005; Jones *et al*., 2006; Drahl *et al*., 2005).

Scrutiny of medical indication by source of compounds demonstrated that natural products and related drugs are used to treat 87% of all categorized human diseases (Scott *et al*., 2004; Keating and Figgitt, 2003), including antibacterial, anticancer, anticoagulants, antiparasitic, and immune suppressant agents among others (Newman *et al*., 2003). There was no introduction of any natural product or related drug for 7 drug categories (anaesthetics, antianginal, antihistamine, anxiolytic, chelator and antidote, diuretic, and hypnotic) from 1982 to 2002 (Newman *et al*., 2003). In the case of antibacterial agents, natural products have made significant contributions as either direct treatments or templates for synthetic modification. Of the 90 drugs of that type that became commercially available in the United States or were approved worldwide from 1982 to 2002, 79% can be traced to a natural product origin (Newman *et al*., 2003).

The number of natural product drug discovery programs has steadily declined since the 1980s, primarily because pharmaceutical companies have shifted to using synthetic libraries that are more amenable to high-throughput screening and simplified synthesis. Despite this, between 1981 and 2002, approximately 50% of all new chemical entities approved by U.S. Food & Drug Administration (FDA) were natural products, natural products derivatives, or synthetic mimetic related to natural (Koehn and Carter, 2005). They were prescribed predominantly as anti-allergy/pulmonary/respiratory agents, analgesics, cardiovascular drugs and for infectious diseases. Another study found that natural products or related substances accounted for 40%, 24%, and 26%, respectively, of the top 35 worldwide ethical drug sales from 2000, 2001, and 2002 (Butler, 2004). Current drug discovery from terrestrial plants depend mainly on bioactivity-guided isolation methods, which, for example, have led to discoveries of the important anticancer agents, paclitaxel from *Taxus brevifolia* and camptothecin from *Camptotheca acuminate* (Kinghorn, 1994). Other NCEs discovered or modified from terrestrial plants include: (1) Apomorphine hydrochloride, which is a potent dopamine receptor agonist used to treat Parkinson's disease (Deleu *et al*., 2004); (2) Tiotropium bromide used for the treatment of bronchospasm in the United States (Koumis and Samuel, 2005); (3) Nitisinone: this drug has been used for the treatment of hereditary tyrosinaemia type 1(HT-1) (Mitchell *et al*., 2001); (4) Galantamine hydrobromide is used as a selective acetylcholinesterase inhibitor for Alzheimer's

disease treatment (van Agtmael *et al*., 1999); (5) Arteether use as an antimalarial agent (van Agtmael *et al*., 1999).

1.7.5 South African approach to the use of indigenous plant for drug development

The idea for the development of African indigenous plants or plant compounds as medicines led to the formation of a consortium funded by the Government of South Africa and thus the National Drug Development Platform (NDDP) was established (http://www.sahealthinfo.org/noveldrug/partnership). The NDDP brings together a multi-disciplinary research and development team in a consortium which has the combined technical skills, research facilities and strategic capability required to develop novel drugs from medicinal plants. The platform further provides for the establishment of new agro-processing businesses in rural communities for supply of plant material required for new drugs. The primary goal of NDDP was to evaluate the use of medicinal plants used by traditional healers and to develop drugs for neglected disease such as tuberculosis, malaria and diabetes at low cost for the benefit of the poor and needy people (Douwes *et al*., 2008).

Due to continuing indications that the global pharmaceutical industry is suffering from declining productivity (fewer) new medicines are introduced despite increased spending on research (Script reports, 2001: Natural Product Pharmaceuticals: A diverse approach to drug discovery). Yet there is an increasing need for innovation in selecting therapeutic agents and finding lead compounds. The vast majority of current drug discovery carried out by pharmaceutical industry relies on molecular approaches, involving defined molecular targets. Molecular approaches in turn are dominated by high throughput screening. Pharmaceutical companies with the best and most diverse chemical collections will ultimately dominate the industry (Strohl, 2000). Broadly speaking, chemical diverse collections can only come from two sources of large numbers of compounds: combinatorial chemistry and natural products (Taniguchi and Kubo, 1993). Although combinatorial chemistry can provide large numbers of compounds for high throughput screening such compounds tend to have limited structural

diversity. By contrast, natural products provide a wealth of small molecules with drug-like properties and with incredible structural diversity (Balick, 1990)

The rationale of the scientific approach is based on the use of indigenous natural products and by indigenous people. To achieve the goals of the project is making use of collaboration with South African scientist as consortium in a coordinated plan. The consortium incorporates microbiology, chemistry, pharmacology, botany and traditional medicinal practices. As a member of the consortium my role as a microbiologist was to perfom biological assays in order to guide chrmist in synthesis of compounds and working with other divisions to provide a TB drug candate compound.

Mycobacterium tuberculosis *Vernonia staehelinoides* (blouteebossie)

Figure 1.8 Pictures of opposing effects: how a persistent problem of TB disease (*M. tuberculosis*) can be solved by natural occurring plant (blouteebossie) product from which furanone (F1082) was original identified.

As part of a national programme to identify and develop novel antibiotics (antimalarial and antituberculosis) agents from indigenous medicinal plants, bioassay-guided fractionation of the dichloromethane extract of the leaves of *Vernonia staehelinoides* (Figure 1.8) led to the isolation of two structurally-related hirsutinolides, displaying *in vitro* antiplasmodial activity. The compounds lacked selectivity (cytotoxicity *vs*. bioactivity) but the results led to the identification of mucochloric and mucobromic acids as privileged 2(*5H*)-furanone substructures (Pillay *et al*., 2007). Halogenated

furanones were first discovered to inhibit bacterial colonization of the red algae *Delisea pulcra* (Manefield *et al*., 2002) and have also been shown to act as biofilm inhibitor for several bacterial species in laboratory experiments (Hentzer *et al*., 2002; Rice *et al*., 2005; Lönn-Stensrud *et al*., 2007). 'Biofilms are defined as matrix-enclosed bacterial populations adherent to each other/or to surfaces or interfaces' (Costerton *et al*., 1995). Furanones have been suggested to interfere with the quorum sensing system in Gram-negative bacteria (de Nys *et al*., 2006). The furanone ring system is a widely recognised component of natural products exhibiting a wide range of interesting biological activities such as antibacterial, antifungal, antiviral, anticancer, anti-inflammatory, vasodilation and anti-convulsant (Alam *et al*., 2010; Hashem *et al*., 2007). These furanones are the subject of study in this thesis for anti-*M. tuberculosis* activity.

The synthesis of the three most active compounds is depicted (Figure 1.9). Mucobromic and mucochloric acids were transformed to the respective ethyl carbonates, exemplified by F952, by treatment with ethyl chloroformate in the presence of diisopropylethylamine at low temperature (Zhang *et al*., 2002; Gondela and Walczak, 2011). The carbonates were obtained in average yield of 50%. Two sequential nucleophilic substitution reaction of the carbonate and β-halo (bromine) group by selected phenols and 4-aminoquinoline diamine, respectively, delivered the target compounds in moderate to high (un-optimized) yields (Scheme 1).

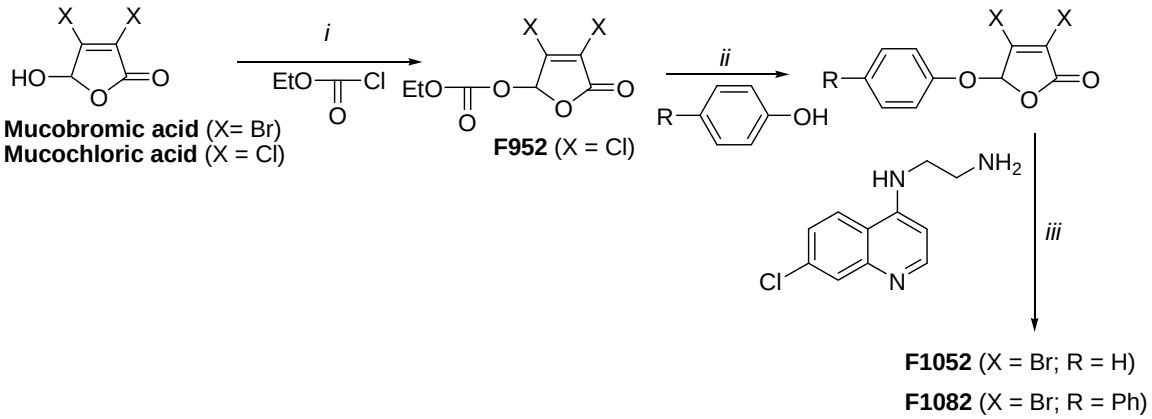

Figure 1.9 *Reagents and conditions*: (i) 1.05 equiv. of ethyl chloroformate, CH_2Cl_2, -10°C, 1.5 h, 49-50%; (ii) 1.1 equiv phenol, 0.3-1.0 equiv CsF, CH_2Cl_2, 25°C, 72-80%; (iii) 1.5-2.0 equiv amine, *N*-

methylpyrrolidine, 55-78%. Derivatives of the F1082 were synthesized based on the chemical structure of the compound by the Jenny-Lee Pandayan at CSRI, Pretoria as illustrated in Appendix AI.

This thesis investigates the possible mechanism of action of a furanone based compound (F1082) and future development through synthesis of derivatives

Scientific rational

The special feature of this project is that the compounds original from indigenous plants and is done by researchers in the developing word. The exploration of indigenous plants for medical value to solve complex problem of tuberculosis is a country's worth.

Hypothesis

If F1082 inhibits the growth of *M. tuberculosis*, we therefore hypothesize that there is a mechanistic manner by which F1082 articulates its inhibitory activity.

1.10 Aim of the study

To evaluate a furanone based compound (F1082) and derivatives as potential candidates for antituberculosis drug development and to elucidate the mechanism by which F1082 exerts its antimycobacterial activity.

1.10.1 Objectives

I. Activity testing

- To determine the minimal inhibitory concentration (MIC) of F1082 against *M. tuberculosis.*
- To generate and carry out activity testing of F1082 and analogues against *M. tuberculosis* H37Rv, pan-susceptible, MDR and XDR clinical isolates of *M. tuberculosis.*
- Evaluate whether F1082 is bactericidal or bacteriostatic in its effect.
- To evaluate F1082 in combination with existing anti-TB drugs.
- To evaluate F1082 cytotoxicity in human cell-line.

II. Cellular targets of F1082

- Identification of *M. tuberculosis* genes and metabolic pathway/s affected by F1082 activity using microarray technique.
- Confirmation of the microarray data by qPCR.

III. Detection of mutation targets

- Generate deletion mutants of target genes identified with microarray.
- Determine the survival ability of the deletion phenotypes under F1082 treatment.

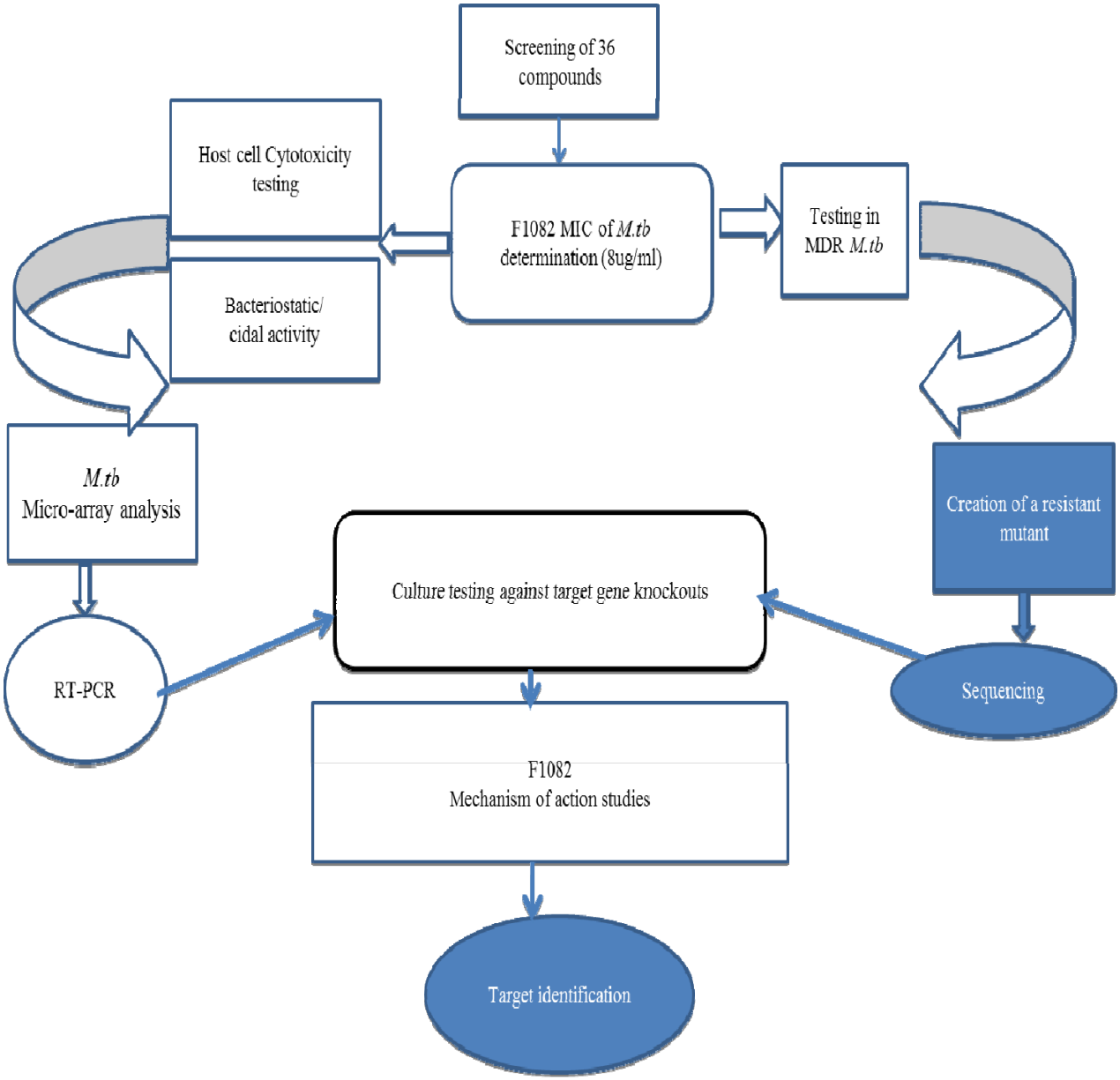

Figure 1.10 Schematic representation of the project outline with possibilities for further studies or development.

The blue coloured segments indicate areas which have not been fully determine during the time by which this report was written. It must be indicated that although mutants were attempted to be created but due to inhibitory activity of the compound not able to kill bacteria no mutants were generated and hence sequencing was not performed. The need for resistant mutant to the compound is a grey areas that when discovered could provide greater understanding of the underlying mechanism of action of this compound.

CHAPTER TWO

F1082 activity testing against *M. tuberculosis* by *in vitro* culture assays.

2.1 Introduction

With the findings observed from this chapter, one may expect to be able to deduce whether there is any cross resistance of F1082 to the current TB-drugs. In clinically practice drugs that have the same mechanism of action are difficult to develop as there is a tendency that resistance to one drug may confer resistance to the other (Blaschitz *et al*., 2011). Clinical experience is that inadequate exposure to anti-TB drugs may result in the emergence of resistant mycobacteria (Zhao and Drlica, 2008). However the mechanism by which drug resistance is induced is not always known. The term 'phenotypic drug-resistance' is used to indicate drug-tolerant mycobacteria that exhibit reduced susceptibility to anti-TB drugs without known genetic mutations. Phenotypic drug resistance might, for instance, due to increased efflux pump activity, porin loss, permeability decrease or drug-modifying enzymes, resulting in reduced intracellular drug concentrations (Gumbo *et al*., 2007). 'Genotypic drug-resistance' indicates resistance associated with known mutation in the genome of *M. tuberculosis* and relates to known levels of resistance. Therefore drugs or compounds that have or show different mechanisms of action are more preferred for development. The techniques and assays utilised for this work involve the use of the BACTEC 460 system [which is being discontinued by the manufacturer (Becton and Dickison) in 2012].

A major obstacle in TB eradication is the ability of TB bacilli to transition to a non-replicating (latent) state in which metabolism is reduced to extremely low basal levels. This status is currently defined as dormancy or non-replicating persistence (NRP). Besides latent bacteria, a part of the bacterial population in patience with active tuberculosis also persists in a non-replicating state, and there is an obvious need for the eradication of this population. The maturing granuloma exposes the pathogen to harsh microenviroment characterised by limited nutrients, low oxygen and low pH, which does not support rapid growth but rather induces a state of dormancy in bacteria (Voskuil *et al*., 2003). There is evidence of both macrophage physiology and the nature of TB granuloma which suggest that hypoxia is the major factor for inducing NRP state of the tubercle bacilli. There is evidence that some very specific adaptation to oxygen depletion occur to make it possible for hypoxic NRP state to exist.

Current available anti-TB drugs are not particularly effective against a subpopulation of "persistent" bacilli (Wayne, 1994), however in nowadays there are compounds that are specific for NRP include (OPC67683, Kanamycin/amikacin, metronidazole, TMC207). It is therefore imperative to find drugs that can target this population. In this study, the Wayne model of persisters was also used to evaluate the F1082 activity against non-replicating persisters.

All compounds have the capacity to be toxic depending upon dosage (Rozman and Doull, 2001). This realisation allowed for a significant advance in the field of early medicine. This observation also makes toxicity testing necessary and critical in practice to identify and define safety thresholds for all new chemotherapeutics. The advent of *in vitro* cytotoxicity testing has greatly streamlined this process and is now considered to be a necessary or important activity. *In vitro* cytotoxicity testing has become an integral aspect of drug discovery because it is a convenient, cost effective, and predictive means of characterising the toxic potential of new chemical entities. In this study, we used a viability assay (MTT) described later for toxicity testing.

In this chapter, the aim is to: 1) determine the MIC of F1082 against *M. tuberculosis* H37Rv; 2) compare the activity of F1082 against clinical isolates [including multi-drug resistant (MDR)] clinical isolates of *M. tuberculosis;* 3) to evaluate the activity of F1082 with anti-TB drugs against non-replicating persisters (NRP), generated by Wayne model; 4) to determine F1082 activity in combination with current anti-TB drugs and 5) to assess the cytotoxicity of F1082 in THP1 cell line.

2.2 Materials and Methods

2.2.1 Minimal inhibitory concentration (MIC) determination of F1082 and derivatives

Susceptibility of an *M. tuberculosis* reference strain, H37Rv and clinical isolates was done using the BACTEC 460 TB-system (Becton Dickinson, USA) as proposed by (Siddiqi *et al*., 1981). The methodology is easy to perform, rapid, robust and suitable for screening the number of compounds that were checked in this work.

2.2.1.1 Bacterial strains and growth conditions

M. tuberculosis H37Rv (ATCC 27294) was obtained from the American Type Culture Collection (Rockville, Md). Clinical isolates of *M. tuberculosis* were obtained from our in-house Divisional strain collection (Ang *et al*., 2008). All isolates were confirmed to be genotypically unrelated according to IS6110 genotyping. Isolates were identified as drug resistant by mutational analysis and genotyping testing (Ang *et al*., 2008). Stock cultures in 15% glycerol were prepared from log phase culture at an optical density (OD_{600nm}) of 0.6 (2 x 10^8 CFU/ml) see section 2.3.2 (Figure 2.5). Cultures for experimental treatment were initiated by diluting a frozen stock inoculum 1:200 into fresh Middlebrook 7H9 supplemented with 10% oleic acid-albumin-dextrose- catalase, v/v (OADC; Difco Laboratories, Detroid); 0.05% Tween 80, v/v (Sigma, St. Louis, Mo) in a vented, screw cap, tissue culture flask and cultured to log phase (OD_{600} 0.6) at 37°C. The growth conditions for the non-replicating persisters (NRP) are detailed in section 2.2.3 of this chapter.

Table 2.1 *M. tuberculosis* strains/isolates used for susceptibility and combinational testing

Strain	Description	Mutant	Functional use
H37Rv	*M. tuberculosis* laboratory strain (ATCC 27294)		Base-line susceptibility test
R1129	*M. tuberculosis* clinical isolate resistant to INH	*katG* 315 ACA (Ser 315 Thr)	Combinational effect
R5182	*M. tuberculosis* clinical isolate resistant to RIF	*rpoB* 531(TTG Ser 531 Leu)]	Combinational effect

2.2.1.2 Antibiotics

F1082 (Figure 2.1) and derivatives (Appendix A) thereof were provided by Dr Chris Parkinson, CSIR, Pretoria, South Africa. Isoniazid, rifampicin and ethambutol were purchased from Sigma-Aldrich (St Louis, MO, USA). Stock solutions of isoniazid and ethambutol were prepared in distilled and deionised water at 10 mg/ml, sterilized by filtration (0.22 µm filter) and stored frozen at -80˚C. Stock solutions of rifampicin, at 10 mg/ml were prepared in 100% DMSO and stored at -80˚C. Stock solution of F1082 was prepared in dimethyl sulfoxide (100% DMSO) at 15mg/ml and stored at -80˚C.

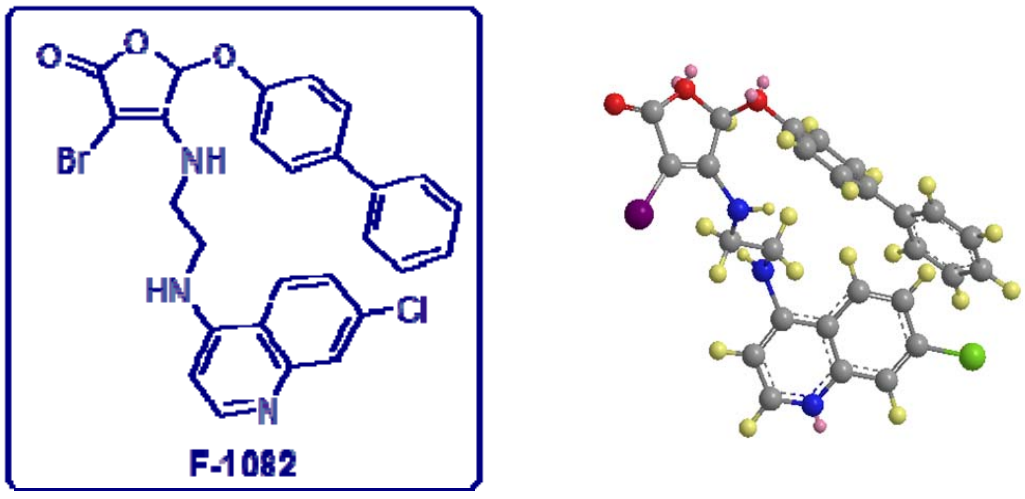

Figure 2.1 The chemical and crystal structure of F1082

2.2.1. 3 Minimum inhibitor concentration determination by BACTEC 460 System

The growth of mycobacteria can be determined within one week by the extent of oxidation of [^{14}C] palmitic acid (in a liquid Middlebrook 12B medium) to $^{14}CO_2$ which is measured in the BACTEC 460 instrument (Collins and Franzblau, 1997). Owing to the quantitative nature of the data, the relative activity of various samples can be compared by testing at only 1 or more concentrations and determining a percent inhibition of $^{14}CO_2$ production relative to drug-free undiluted controls (Cantrell *et al* 1998). Alternatively, multiple concentrations can be tested and the MIC calculated (Cantrell *et al*., 2004).

The BACTEC 460 system (Becton Dickinson) was used to determine the MIC for each individual compound and to study the combined effects of compounds (drugs) on *M. tuberculosis* survival *in vitro* (Siddiqi *et al* 1981). *M. tuberculosis* H37Rv or RIF^R or INH^R *M. tuberculosis* isolates were grown on 12B. The growth of the bacilli, expressed as the growth index (GI), was monitored daily by measuring the release of $^{14}CO_2$ after the bacteria consumed ^{14}C-labelled palmitic acid in the medium. Drug free controls, including the undiluted and the 1:100 diluted bacterial inocula, were included in each experiment to monitor bacterial growth. When the GI value of the 1:100 inoculum vial reached ΔGI of 30 or greater the results were interpreted. Delta (Δ) GI is defined as the difference in GI values between the latest and the previous reading. The MIC of a given drug was defined as the lowest concentration at which the GI of the drug vial was less or equal to the GI of the 1:100 control. The BACTEC drug susceptibility testing was completed within 5-8 days.

2.2.2 Growth kinetics of *M. tuberculosis* (exposed to F1082)

To monitor the optimal bacterial growth kinetics: log phase cultures of H37Rv were diluted 1:6 in OADC supplemented 7H9 growth medium and OD_{600} measured daily for 15 days. For colony forming unit (CFU) determination, tenfold serial diluted suspensions were plated on 7H11 agar daily. The bacterial growth by CFU and the OD_{600} was compared to determine optimal culture conditions for our experimental design.

For growth kinetics by CFU enumeration, *M. tuberculosis* H37Rvcultures at 1.3 x 10^6 CFU/ml were exposed to antimycobacterial agents. The concentration range for F1082 was 2 to 128 µg/ml and for INH 0.2-5 µg/ml, using two fold increasing concentrations. *M. tuberculosis* H37Rv cultures exposed to compounds (and solvents as controls) were incubated for 21 days at 37°C and CFUs were counted at day 1, 2, 5, 10 and 21 as described (Bakker-Woudenberg *et al*., 2005). A bacteriostatic effect is defined as the lowest concentration that inhibited visible growth at day 21. Bactericidal effect is defined as killing capacity of the agent expressed as the lowest concentration that resulted in ≥ 99% killing at day 1, 2, 5, 10 or 21.

To determine the bactericidal or bacteriostatic effect of the drug/compound at different concentrations after 1, 2, 5, 10, and 21 days of exposure, the bacterial suspensions were centrifuged at 10 000 rpm on a bench top centrifuge for 4 minutes at room temperature, washed in 7H9 broth supplemented with OADC and centrifuged again. Samples were tenfold serially diluted and plated onto 7H11 agar supplemented with OADC. After 15 to 21 days of incubation at 37°C, CFU numbers were counted and the values were used to plot a dose response curve for each concentration (Figure 2.6 and Figure 2.7).

2.2.3 Non-replicating persisters (NRP)

Popular working models suggest that unfavourable micro-environmental conditions inside the human lesion, such as oxygen and nutrient, are external triggers that terminate growth of subpopulations of tubercle bacilli and render them phynotypical resistant drug. Most antibiotics are more effective against replicating than nonreplicating bacteria (Hobby and Lenert, 195; Levin and Rozen, 2006). However, a major problem in TB treatment is to eradicate a persistent or nonreplicating subpopulation of bacteria (McCune *et al*., 1966; Muñoz-Elías *et al*., 2005). Indeed in vitro models using oxygen depletion in nutrient nutrient-rich medium (Wayne model) or nutrient starvation in oxygen-rich medium (Loebel model) have demonstrated the survival of *M. tuberculosis* for extended periods in a non-replicating and drug-tolerant state (Betts *et al*., 2002). Therefore since F1082 is a novel compound we want to evaluate its activity on NRP as this provides fundal information for any new

drug under development. For non-replicating persistence, *M. tuberculosis* H37Rv was used for all conditions. A volume of 20 ml single seeding of bacteria from stock cultures was grown in Dubos Tween-Albumin (DTA) broth, prepared according to the manufacturer's instruction from Dubos broth base (Difco, Detroit, Mich), to an optical density of 580 nm (OD_{580}) of 0.4. This corresponds to a cell density of about 2.5 x 10^8 CFU/ml. The stock was dispensed in small aliquots of 1 ml in 2 ml screw cap tubes and stored at -70°C. When a working culture was needed, a seed culture was thawed and 100 µl was inoculated into 10 ml of DTA and incubated at 37° C with agitation until it reached an OD_{580} of 0.4 (2.5 x 10^8 CFU/ml) with shaking at 250 rpm.

The 10 ml working culture was incubated at 37°C with shaking at 250 rpm. This shaking should produce a small vortex at the top surface of the medium, maximizing aeration. The screw caps were slightly loosened (about 1/8 to 1/4 turn) and held in place with a small strip of tape. Growth rate was monitored on a daily basis until it reached an OD_{580} of 0.4 and this culture was used as seed culture for non-replicating persistence experiments. In a number of experiments, Wayne and Hays (1996) have noted that the NRP stage 1 lasted until the A_{580} reached values between 0.4 and 0.45 before shifting into NRP 2 plateau.

2.2.3.1 Limitation of Aeration for Shift down to NRP Stages

For liquid cultures we used 20 x 125 mm screw-cap test tubes, with a total capacity of 25.5 ml. An 8 mm long Teflon-coated magnetic stirring bar was placed in each of the tubes containing 17 ml DTA medium, leaving an air head space of 8.5 ml, corresponding to ratios of headspace air volume to liquid volume of 0.5. These proportions are hereafter referred to as headspace ratio (HSR). Each tube was inoculated with 170 µl of working culture from 2.2.3 (OD_{580} = 0.4) to yield a calculated initial optical absorbance (OD_{580}) of 0.004. The tubes were closed tightly with a tightly fitting rubber vaccine cap. The rubber caps were used since reagents were to be injected into the tubes during the course of the experiment. Since the experiment was planned to last more than 21 days, the caps were sealed with Parafilm. The tubes were placed in plastic racks on the Biostire 4 magnetic stirrer (Wheaton, Millville, N.J.) at 120 rpm in a 37°C incubator. The OD_{580} was determined daily, taking

care not to agitate the tubes while transferring them to the spectrophotometer. Growth curves using the optical measurements were plotted on a logarithmic scale to permit clear definition of the two deflection points, i.e., from aerobic growth into microaerophilic NRP stage 1, and then into anaerobic NRP stage 2 (Wayne and Hayes, 1996) see (Figure 2.2). Aerobic growth occurs for approximately 60 hours. After which the mycobacteria shift to the microaerophilic NRP-1 stage until oxygen is completely depleted. When the culture is about 160 hours old the mycobacteria shift down to anaerobic NRP-2 stage.

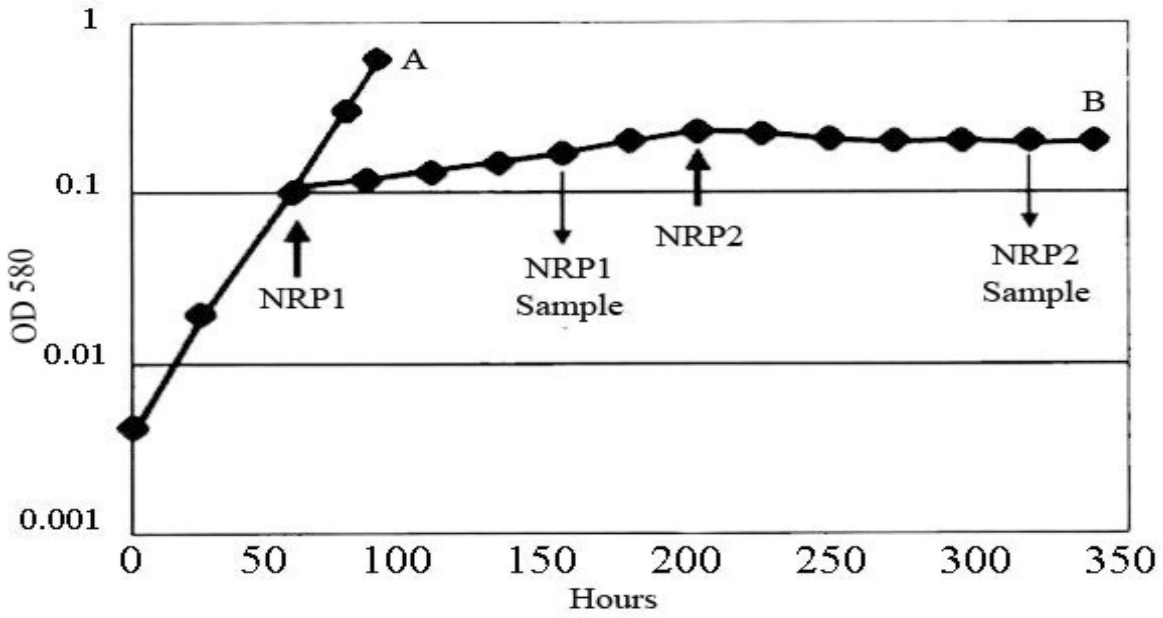

Figure 2.2 *In vitro* model of hypoxically induced nonreplicating persister of *M. tuberculosis.* Arrows indicate the start of NRP-1 (microaerophilic) and NRP-2 (anaerobic) and the sampling points for markers assessment of each stage. (A) aerobic growth (B) hypoxic culture and NRP growth (from Mitchison, 2004).

2.2.3.2 Initiation of Shift up and Synchronized Replication from the NRP State

To permit bacilli in the NRP state to resume replication, it is necessary to reintroduce oxygen into the system. On recovery from the hypoxic condition, bacilli exhibit synchronized replication (Wayne and

Hayes, 1996). *M. tuberculosis* H37Rv under NRP state with drugs concentrations was allowed to replicate by allowing air in sealed tubes and was grown for 18 days (Figure 2.8).

2.2.3.3 Determination of the Colony Forming Units (CFUs)

Colony counting was performed as described above (section 2.2.2) with the following changes. In preparation for counting of colonies on agar, dilutions of liquid culture were made in DTA medium. Dubos oleic-albumin (DOA) agar was prepared from Dubos oleic agar base (Difco) supplemented with Dubos oleic albumin complex to final concentrations of 50 µg/ml of oleic acid and 5 mg/ml albumin and then dispensed in 3 ml amounts into each of the 12 wells of sterile Falcon no. 3043 tissue culture plates (Becton Dickinson, Lincohn Park, NJ). These agar plates were inoculated (in triplicate) with 20 µl of selected dilutions of test culture and the plates were incubated at 37°C. Colonies were counted twice weekly: the closed plates were inverted and colonies were counted under a dissecting microscope at a magnification of x10, using transmitted light. The readings were discontinued after the counts were stable for a week or all showed diminishing counts due to spreading and fusion of colonies.

2.2.3.4 Non-replicating persisters (NRPs) assay

The Wayne model (Wayne and Hayes, 1996), based on the well-established principle of culturing hypoxic persister cells under gradual oxygen depletion was used to evaluate whether F1082 affects the metabolic recovery of non-replicating persisters (NRPs) and its ability to kill hypoxic NRP cells. F1082 was tested in duplicate in low oxygen Wayne model system as described by (Lenaerts *et al*., 2005a). Briefly, mid log cultures of *M. tuberculosis* H37Rv were diluted 100-fold in Dubos medium and grown at 37°C with low stirring for 24 days in tubes sealed with silicone rubber septa. After 24 days (anaerobic conditions) drugs [F1082, isoniazid (INH), and rifampicin (RIF)] were injected through the septa of the 24-day-old cultures at final concentrations of 8 and 64 µg/ml for F1082 and 10 and 50 µg/ml for INH and RIF and incubation continued for another 4 days. These concentrations have been previously used to evaluate several anti-TB drugs in this model and were adopted here for

direct comparison (Lenaerts *et al*., 2005b). Oxygen consumption was monitored in cultures containing methylene blue at 1.5 µg/ml. Reduction and decolourization of this dye served as a visual indication of oxygen depletion. Regrowth of bacteria from NRP state was achieved by re-aeration (exposure to oxygen) of the sample tubes. Fresh air was reintroduced into hypoxic cultures by loosening the caps for exit from dormancy. This exposure to air allowed dormant bacilli to regrow (2.2.3.2). Regrowth was monitored by measuring OD_{580} and the values were used to plot a re-growth curve for each drug concentration (Figure 2.8).

2.2.4 Chequerboard synergy assay

Any new candidate anti-TB drug should be tested in combination with other antibiotics to assess any antagonistic, additive or synergistic effects. How F1082, a new compound with unique attributes, interacts with existing first line anti-TB agents is important to understand, as this could allow the design of efficacious therapeutic drug combinations and minimize undesired side effects in a new combination therapy. Using the chequerboard titration in which a series of dilutions of two antibiotics are studied for the effects on bacterial growth inhibition at all possible concentrations, both alone and in combination, the nature of the interaction between the two antibiotics can be determined algebraically (Holfer *et al*., 1987). The effects of drugs in combination were evaluated based on GI values using the technique that was described previously (Hoffner *et al*., 1987). To assess the effect of each drug and in combination, BACTEC 460 system (described in section 2.2.1.3) was used

2.2.4.3 Data analysis

The interaction between two antibiotics in combination can be described as synergistic, additive, no effect or antagonistic. Synergy is defined as $x/y < 1/z$, where x is the GI of the test vial with the combination of drugs, y is the lowest GI of the single drugs of the combination and z is the number of drugs combined. In order to translate the experimental data into the classification of drug-drug interactions, the quotient x/y (where x is the data obtained when two antibiotics are in combination and y is the data with the lower value of the two agents when tested separately at the same

concentration) can be used. If the x/y value is equal to 1, it is interpreted that one of the drugs in the combination is inactive. If *x/y* is less than 0.5 for a two drug combination, it implies that the two drugs when used together are more effective than when they are used separately, suggesting synergistic effects. If *x/y* values fall between 0.5 and 0.75, an additive effect may exist between the two drugs, suggesting a weak enhancement between them. If *x/y* values are greater than 2, it suggests antagonistic interaction between the two drugs. If the window between x/y is greater than 1 and less than 2 this may be interpreted as the transition area from no effect to antagonistic. By applying the simple algorithm as described by (Hoffner *et al*., 1987), we can evaluate the potential outcome of the two drugs in combination.

2.2.5 Cytotoxicity

THP-1 cells are human monocyte cells which originated from the peripheral blood of a male with acute monocytic leukemia (Tsuchiya *et al*., 1980). These monocytic cell lines can be differentiated *in vitro* to macrophage-like cells for toxicity experiments and a model that resembles TB infection in human macrophages (Sly *et al*., 2001).

2.2.5.1 Growth of THP-1 cells

A 1:10 dilution from frozen stock of THP-1 human macrophage cell line (ATCC TIB-202) was cultured in RPMI 1640 (Gibco-BRL) supplemented with 10% heat-inactivated foetal bovine serum (FBS) with penicillin-streptomycin (100 U/ml), complete medium (CM). The cells were then transferred into a 50 ml tissue culture flask (Nunc, Easy Flask 200 Filt. Nunclon #092974), and examined under the light microscope. The cells were further diluted by additional complete medium to achieve approximately 50% cell confluence and the cells were incubated at 37˚C in 5% CO_2. The cells were inspected daily and when > 90% confluence was achieved they were further diluted. Depending on the final amount of the cells required it would be 1:1 or a 1:10 dilution, the dilution ratio refers to the dilution of the cells in the new media for growth and colony expansion.

The cells were transferred to a 50 ml tube and centrifuged for 5 minutes at 1200 rpm in a bench-top centrifuge (Eppendorf 5810 R, Hamburg, Germany). About 10 to 15% of residual complete medium was used for subsequent growth of the cells as it contains secreted hormones and growth factors which stimulate cell proliferation and keep the cells at optimum growth rate. The rest of the complete medium was discarded and freshly made complete medium was added to the cells for the final volume required before diluting into tissue culture flasks.

2.2.5.2 Preparation of THP1 cells for storage

An 80% confluent culture of cells was pelleted by low speed centrifugation, (1000 rpm) in a bench-top centrifuge (Eppendorf 5810 R, Hamburg, Germany) for 5 minutes, resuspended in FBS and cooled on ice for 5 minutes. A 20% v/v DMSO dilution was made in unsupplemented RPMI and cooled on ice for 5 minutes. The cells were frozen at a final concentration of 10% DMSO by combining the cell mixture and 20% DMSO solution in an equal volume. Aliquots of 1ml in 2ml Eppendorf tubes were wrapped in paper towel to allow cells to cool slowly in the -80°C freezer (to store cells for up to a month) or liquid nitrogen tank (for long term storage)

2.2.5.3 Preparation of THP1 cells from frozen stock

Frozen THP1 cell stocks were thawed at 37˚C as quickly as possible and diluted in approximately 10 ml complete RPMI medium, to dilute the DMSO in which the cells were frozen. The cells were pelleted by low speed centrifugation (1000 rpm for 5 minutes) in a bench-top centrifuge (Eppendorf 5810 R, Hamburg, Germany), and then resuspended in 10 ml complete RMPI medium and aliquoted into cell culture flasks to be incubated as described in section (2.6.1).

2.2.5.4 Differentiation of the THP-1 cells

The human monocyte cell line THP-1 was maintained in RPMI 1640 medium (Gibco-BRL) supplemented with 10% fetal bovine serum (FBS; Gibco-BRL) and 1 mM sodium pyruvate (Sigma).

In order to transform the cells into macrophages, the cells were subcultured four times without sodium pyruvate and then seeded into 6-well microplates (Costar Corning) at a concentration of 2 x 10^6 cells per well in complete RPMI 1640 supplemented with phorbol-12-myristate-13-acetate (PMA; Calbiochem Bioscience) at a concentration of 6.25 ng/ml. Cell cultures were washed twice with RPMI 1640 every 48 hours for no longer than 4 days. Before starting the experiment, the number of cells was counted by haemocytometer.

2.2.5.5 Colorimetric MTT (tetrazolium) assay

The yellow dye 3(4,5-dimethylthiazol-2-yl)-2,5-diphenyl tetrazolium bromide (MTT) is reduced by mitochondrial dehydrogenase in living cells to produce insoluble purple MTT formazan crystals (Garn *et al*., 1994) which, after solubilisation, can be measured spectrophotometrically. This property has been used to assess the viability of cells. For the assay we used 5 x 10^5 cells/ml counted by haemocytometer. We used the 96-well plate for cytotoxicity testing as shown in Figure 2.3. Briefly, 100 µl of cell suspension was added to rows A-G, subsequently another 100 µl of CM was added to rows A-G and 200 µl of CM to row H (serves as blank). The cells were incubated for 24 hours and were examined under the microscope to check that the cells settled. F1082 dilutions were done in CM to concentrations of (200; 20; 2; 0.2; 0.02; 0.002) µg/ml. The medium was then removed from all the wells, leaving a thin film of CM covering the cells. Row G serves as a positive control (no drug) and row H as blank (no cells), 200 µl of CM were added to row G and H. An aliquot of 100 µl of drug in triplicate was added, starting from row E, subsequently adding 100 µl of CM to wells containing F1082 concentrations, thus the final concentration range (0.001 to 100) µg/m. The plate was covered with a sterile lid and incubated for 48 hours at 37°C. To develop the plate, 25 µl of sterile MTT was added to each well and the plate was incubated for a further 4 hrs. The plate was shaken at 200 rpm in a microplate shaker (ORBIT P4, Bio Express) for 10 minutes. The medium was carefully aspirated from each well, 100 µl of DMSO was added to each well and the plate was shaken for 5 minutes on a microplate shaker to dissolve the formazan crystals. The absorbance at 540 nm was read immediately thereafter on an automatic microplate reader (Model 450. Bio-Rad Laboratories, Ltd., WatFord,

England). Inhibitory concentration (IC_{50}) data were obtained from a dose-response curve plotted using Graphpad prism 5. Inhibitory concentration 50 (IC_{50} Human) was defined as the concentration of the compound required to reduce a 50% decrease of cell growth compared to control cultures. A selectivity index (SI), corresponding to the ratio between anti-tuberculosis and cytotoxic activities, was calculated according to the following formula:

$SI_{M.\ tuberculosis} = IC_{50\ Human}/IC_{50\ M.\ tuberculosis}$

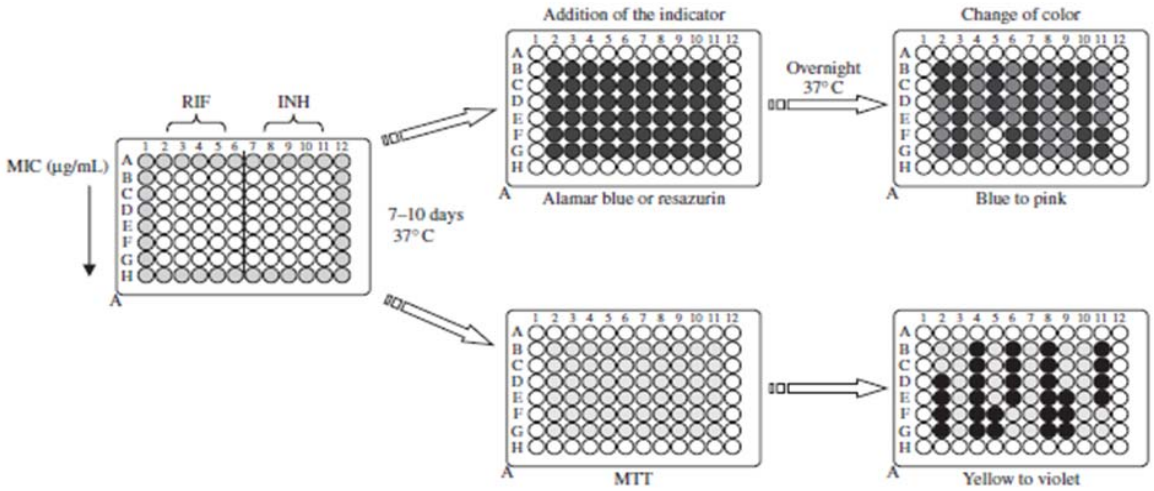

Figure 2.3 Ninety-six well micro plate to indicate the use of the plate for multiple purposes, showing the column and row positions (adapted from Martin *et al.*, 2007)

2.3 Results and Discussion

2.3.1 Determination of the minimal inhibitory concentration of F1082 against H37Rv and clinical isolates of *M. tuberculosis*.

M. tuberculosis was grown in the BACTEC 460 system in the presence of various concentrations of F1082 (ranging from 2 to 8 µg/ml) and the GI was monitored on a daily basis (Figure 2.4). Three controls were used i.e. (1) Neat (bacterial growth with no antibiotics), (2) 1:100 diluted bacterial culture (representing 99% bacterial inhibition) and (3) rifampicin at 2 µg/ml (RIF) representing a negative control. All concentrations of F1082 showed some degree of growth inhibition of *M. tuberculosis* when compared or the same to the neat; however the concentration of F1082 that was comparable to the 1:100 control was 8 µg/ml and was therefore considered as the MIC of the compound (MIC was defined as the lowest concentration of the compound that gave 99% growth inhibition).

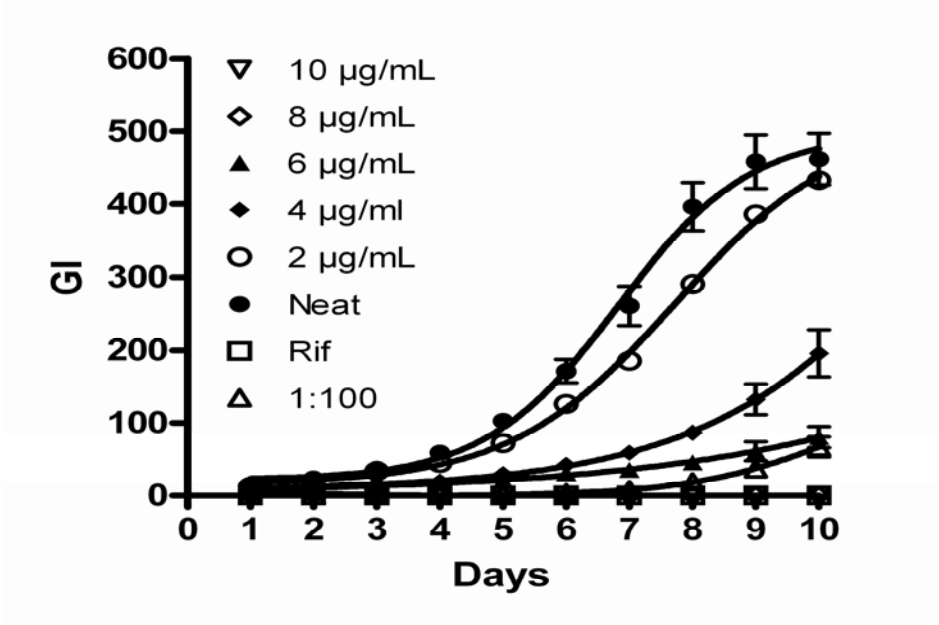

Figure 2.4 Inhibition of *M. tuberculosis* H37Rv growth with various concentrations of F1082

The activity of derivatives of F1082 (n = 42) were tested against *M .tuberculosis* in the BACTEC 460 system. All the derivatives were tested at a baseline screen of 45 µM, which was three times the MIC of F1082 (8 µg/ml = 14.52 µM calculated from molecular weight of F1082). The basis for screening at that concentration was to select compounds that showed activity and not simply toxicity. Compounds that showed activity were used to determine an MIC and cytotoxicity data in the same way as for F1082. Promising compounds include JP 206, JP 210, JP 216, and JP 223 (Table 2.2) as they showed improved activity with less cytotoxicity when compared to F1082. These compounds warrant testing in MDR-MTB isolates and in animal models furthermore their mechanisms of action remains to be determined. The list of all compounds tested with their activity and cytotoxicity data is shown in Appendix AII.

Table 2.2 Activity of F1082 and derivatives against H37Rv, pan-susceptible, and MDR clinical isolates of *M. tuberculosis* and cytotoxicity data.

ND-represent 'not done' as some of these compounds were under synthesis and we did not have enough at the time this work was reported.

	MIC (µM)					Cytotoxicity (IC_{50},µM)
	H37Rv	INH, EMB RIF resistant	INH mono-resistant	RIF mono-resistant	22 pan-susceptible clinical isolates	Chinese ovary Hamster cells
F1082	14.52	14.52	14.52	14.52	14.52	< 10
JP206	2.8	ND	ND	ND	ND	68
JP210	11.25	ND	ND	ND	ND	>100
JP216	5.6	ND	ND	ND	ND	82
JP223	5.6	ND	ND	ND	ND	83

The activity of F1082 against clinical isolates of *M. tuberculosis* including MDR was also tested in order to evaluate whether there is any comparable resistance or cross-resistance in line with the

current TB front-line drugs. All clinical isolates were tested using F1082 at a concentration of 8 µg/ml. All clinical isolates showed susceptibility (more than 90 % inhibition) to F1082 equivalent to that of *M. tuberculosis* H37Rv (Table 2.3). These results suggest that F1082 has a different mechanism of action to the current anti-TB drugs and that there is unlikely to be any cross-resistance with the current TB front-line drugs. This is encouraging, because a new mechanism of action of a novel compound could provide new scaffolds or targets to which anti-TB drugs could be developed. However, the challenge is to determine the specific target or pathway which it inhibits.

Table 2.3 Susceptibility testing of *M. tuberculosis* clinical isolates with F1082 (8 µg/ml)

Drug susceptibility	Number *M. tuberculosis* isolates	Percentage inhibition (%)
INH and RIF susceptible	20	>90
INH, RIF and EMB susceptible	1	>90
INH mono-resistant	2	>90
RIF mono-resistant	1	>90
INH and RIF resistant	1	>90
INH, RIF and EMB resistant	1	>90

2.3.2 Growth kinetics of *M. tuberculosis* H37Rv

In order to design experiments and use bacteria that are in the same growth phase under similar conditions, we had to establish the relationship between optical density (OD_{600nm}) and viable cell counts (by colony forming units, CFU). This enabled us to design experiments that are comparable and reproducible. A direct and proportional relationship between the CFU and the OD_{600nm} was observed in log phase. However, in the stationary phase, the CFU continues to increase, levels off and then declines, whereas the OD_{600} levels off before the CFU (Figure 2.5). For our experiments we chose to use bacteria that are at log phase (OD_{600} of 0.2-0.3 2 x 10^6 CFU/ml). At this phase, the bacteria are actively growing and are affected by compounds that target actively growing bacteria.

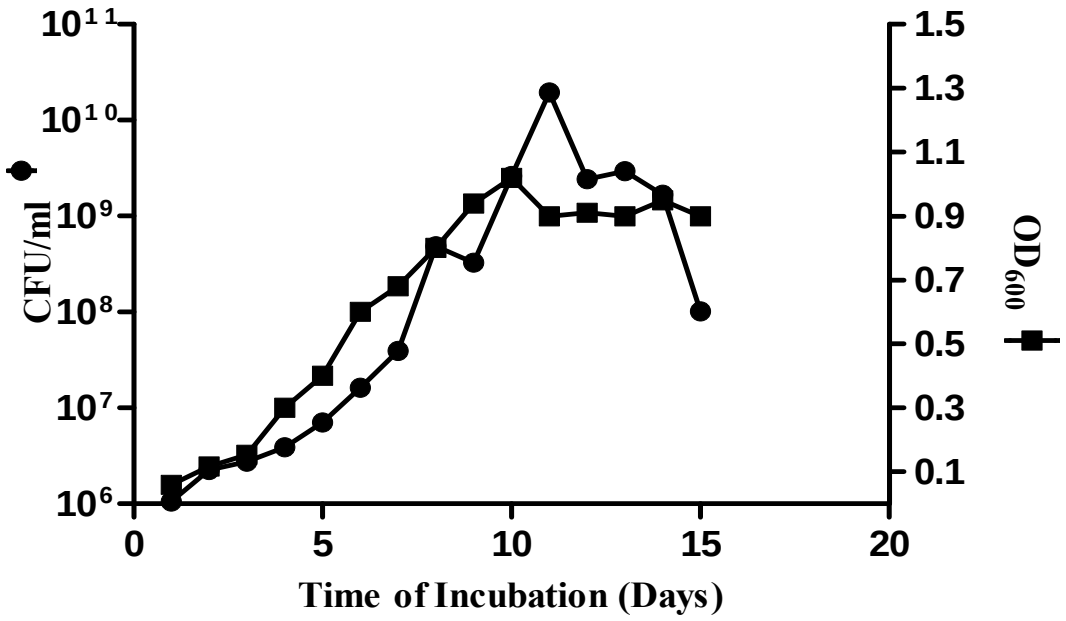

Figure 2.5 A correlation between the optical density (OD_{600}) and the colony forming units (CFU/ml) of *M. tuberculosis* H37Rv in the absence of drug.

For the time-kill assay, we monitored concentration-dependent and time dependent effects of anti-TB drugs. Isoniazid (INH) was used as a control at concentrations ranging from 0.2 to 5 µg/ml and F1082 at concentrations ranging from 2 to 128 µg/ml over a period of 21 days. The *M. tuberculosis* H37Rv growth curves were plotted for INH (Figure 2.6) and F1082 (Figure 2.7). Exposure of log phase *M. tuberculosis* to INH resulted in a concentration and time dependent effect (Figure 2.6). A four-fold log reduction of bacteria was observed after 48 hours at 5 µg/ml (INH) showing a bactericidal effect of the drug. Substantial killing by INH was not observed when *M. tuberculosis* was in the late log phase of growth after 120 hrs. The rise in the CFU/ml in isoniazid treated group after 120 hours of drug exposure may be explained by the selection of isoniazid-resistant mutant given the relatively high starting concentration of > 10^6 organism which was chosen intentional for subsequent microarray experiments. This bacterial population exceeds the spontaneous isoniazid resistant mutation rate of *M. tuberculosis* in vitro (Karakousis *et al*., 2008). This is consistent with the literature that INH does not affect non-replicating *M. tuberculosis* (Bryk *et al*., 2008).

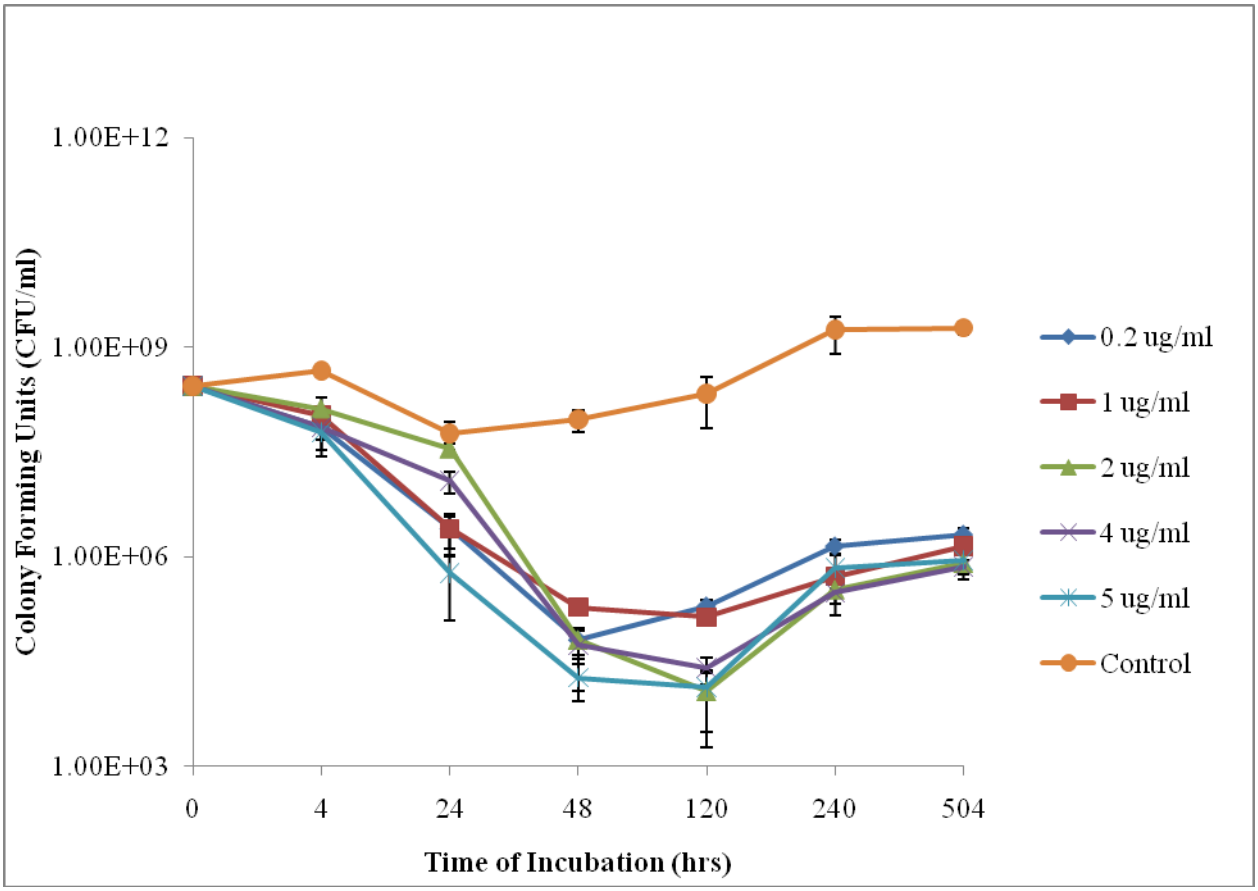

Figure 2.6 Time dependent dose response curve of *M. tuberculosis* H37Rv with INH

When *M. tuberculosis* was grown in the presence of various concentrations of F1082, we observed a different scenario. There was no sharp reduction of bacterial load, but a transient reduction of CFUs of approximately two-fold between 4 and 24 hours, which was concentration dependent (Figure 2.7). After 24 hours, bacteria resumed growth at all concentrations of F1082. However we observed a subsequent growth suppression of bacteria by two-fold after 48 hours in a concentration dependent manner. This effect may indicate that F1082 may have more than one target by which it exerts its effect. Since we observe a transient reduction of two log units of viable bacteria at first, we concluded that F1082 has a bacteriostatic effect (Kaur *et al*., 2009). This suggests that F1082 inhibits the growth of *M. tuberculosis* rather than is bactericidal. However, high concentrations (128 µg/ml) as shown in

Figure 2.7 appear to exhibit further bacterial load reduction, suggestive of bactericidal effect at this concentration.

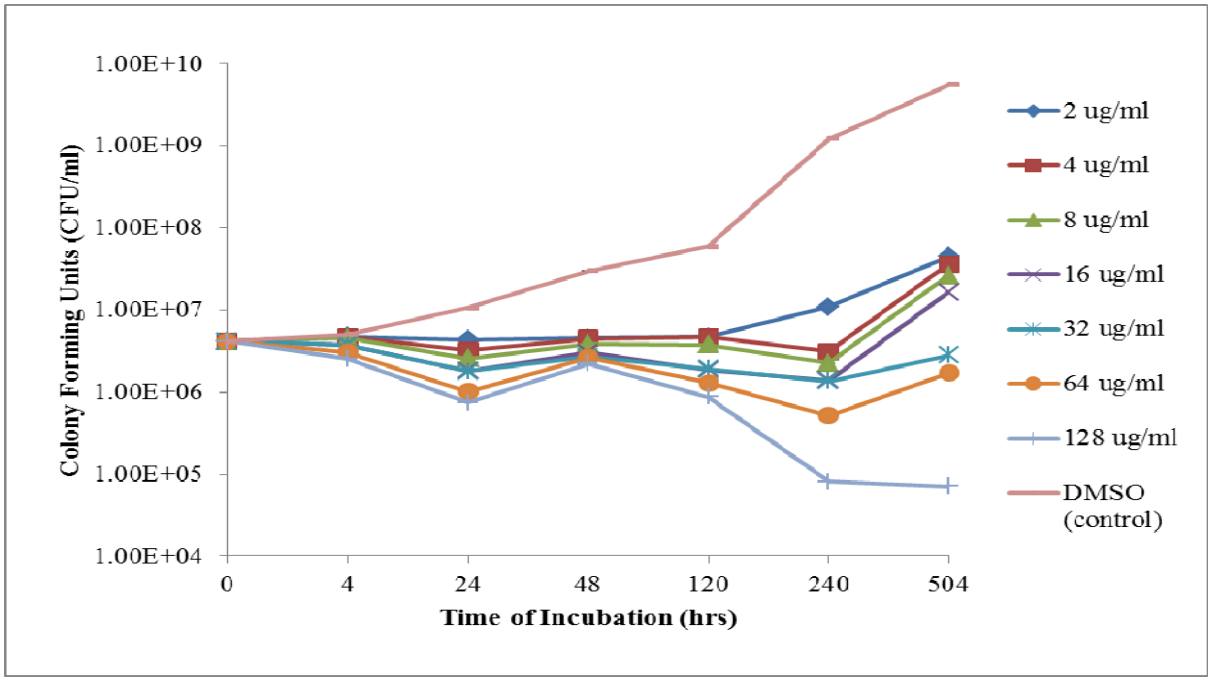

Figure 2.7 Time dependent dose response curve of *M. tuberculosis* H37Rv with F1082

2.3.3 Non-replicating persisters (NRPs)

M. tuberculosis was grown under oxygen limitation to establish non-replicating persisters as described by the Wayne-type model (Lenaerts *et al.*, 2005a) and was subsequently exposed to different compounds. The *M. tuberculosis H37Rv* cultures were revived from 28 days of oxygen limitation, exposed to oxygen by loosening the tightened sealed tube caps, shaken at 250 rpm and the OD_{580} measured daily for 18 days. A growth response curve was plotted as shown in Figure 2.8

The control cultures, including the DMSO control, grew with a long lag phase (about 5 days) as the cultures were adapting and changing from a non-replicating to a replicating state under sufficient oxygen (Figure 2.8). RIF exerted its bactericidal activity (at concentration of 10 and 50 µg/ml) by

killing the NRP and no re-growth was observed as was also observed by Hurdle *et al*., (2008). Since INH lacks the killing effect on non-replicating bacteria, re-growth of *M. tuberculosis* was observed even at 50 µg/ml of INH (Figure 2.8). F1082 also failed to kill non-replicating bacteria, since re-growth was observed even at a concentration of 64 µg/ml, which is 8 x MIC. This is not uncommon with bacteriostatic compounds as they inhibit growth rather than killing bacteria (Kohanski *et al*., 2007). These results were further confirmed with CFU counting and were consistent with RIF killing 99.6% of the bacterial population at 10 µg/ml, INH killing 22% at 50 µg/ml and F1082 10% of the bacteria at 64 µg/ml.

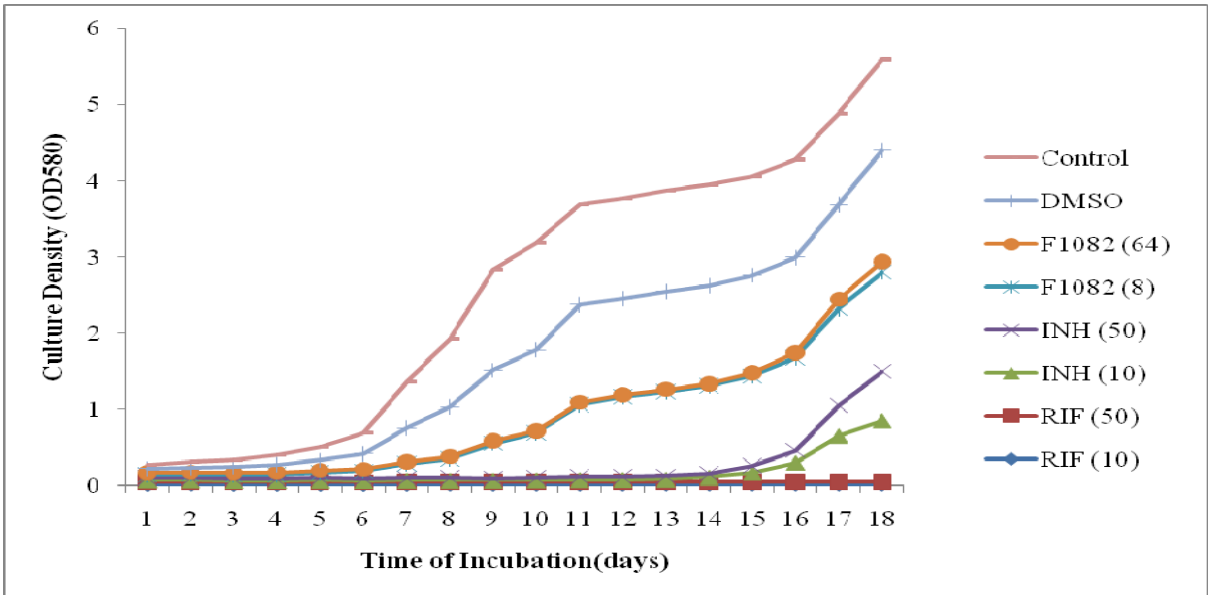

Figure 2.8 A re-growth dose response curve of *M. tuberculosis* H37Rv after 28 days of oxygen limitation.

2.3.4 Testing for Synergy

In this study, we investigated the interaction of F1082 in combination with other anti-TB drugs *in vitro*. The activity of F1082 in combination with rifampicin (RIF), isoniazid (INH) and ethambutol (EMB) was evaluated (in duplicate) against *M. tuberculosis* H37Rv and clinical RIF mono-resistant clinical isolate by a chequerboard titration method in the BACTEC 460 system, to assess whether F1082 may enhance the efficacy of existing TB drugs in a synergistic manner. Synergistic effect is

defined as when the activity of two drugs in combination is greater to the sum of their independent activity when studied together; additive effect as the activity of two drugs in combination is equal to the sum (or a partial sum) of their independent activity when studied separately; and antagonistic effect as the activity of the two drugs in combination is less to the sum (or partial sum) of their independent activity when studied separately.

The MIC of a drug is defined as the lowest concentration that inhibits the growth of 99% of bacterial inocula, thus it is clear that synergistic, additive or antagonistic effects of combination drugs must be evaluated at individual drug concentrations that are less than the level of the MIC for effects to be observed. The concentration of each individual drug used, as well as the quotient values for combination of F1082 with isoniazid, ethambutol and rifampicin at drug concentrations below the MIC values (Table 2.4). The concentration of each of the drugs used in combination was expressed as a fraction of the MIC value. This table includes only the combinations at which synergy or additive effects were observed. F1082 at 0.5 x MIC showed synergy with rifampicin (0.2 µg/ml), an additive effect for both isoniazid (0.04 µg/ml) and ethambutol (0.4 µg/ml), when MIC fractions (Table 2.3) were used. No antagonistic effect was observed with any of the two-drug combinations tested in this study.

Table 2.4 Synergy quotients for F1082 tested in two-drug combinations with isoniazid (INH), rifampicin (RIF) or ethambutol (EMB) against *M. tuberculosis* H37Rv.

Synergy quotients (*x/y*) in drug combinations (drug + 0.5 x MIC F1082)			
Drug	INH*	RIF**	EMB***
Dose	0.8 x MIC	0.5 x MIC	0.25 x MIC
Interaction	0.65[b]	0.11[a]	0.75[b]

MICs: INH, 0.05 µg/ml; RIF, 0.4 µg/ml; EMB, 1.6 µg/ml; F1082, 8 µg/ml. *0.04 µg/ml; **0.2 µg/ml;***0.4 µg/ml.

[a] Synergy was defined as $x/y < 1/z$, where x is the growth index (GI) of the test vial with combination

of drugs, y is the lowest GI of the single drugs of the combination and z is the number of drugs combined. For a two-drug combination, a quotient of < 0.5 was indicative of synergistic effect, a quotient of 1 indicated no interaction, a quotient of > 2 would show an antagonistic effect and a quotient of < 0.75 but > 0.5 indicated an additive effect.

[b]Additive effect. < 0.75 but > 0.5

2.3.4.1 Interaction of F1082 with rifampicin in *M. tuberculosis* H37Rv (RIF MIC of 0.4 µg/ml).

When F1082 was used with rifampicin, we observed marked synergy between the two drugs as indicated by the average quotient values (Table 2.5) in *M. tuberculosis* H37Rv. F1082 at 0.5 x MIC showed synergy with rifampicin at concentrations as low as 0.25 x MIC. Additive effect was observed when 0.25 x MIC F1082 was combined with 0.5 x MIC rifampicin. Interestingly, the combination with both drug combinations below 0.5 MIC (0.25 MIC F1082 + 0.25 x MIC rifampicin) showed no interaction so therefore there is no undesired antagonistic effect for these drugs at concentrations tested in this study..

Table 2.5 Synergy quotients for F1082 tested in combination with rifampicin (RIF) against *M. tuberculosis* H37Rv

MIC fraction F1082[a]	MIC fraction RIF[b]	Quotients (mean x/y ± SD)[c]	Interaction interpretation
0.5	0.5	0.11 ± 0.098	synergy
	0.25	0.39 ± 0.268	synergy
0.25	0.5	0.63 ± 0.388	additive
	0.25	1.04 ± 0.086	No interaction

[a]MIC of F1082 = 8 µg/ml

[b]The average MIC of RIF from two experiments (0.4 µg/ml). The MIC fractions used in the table represent the concentrations used in combinations in respect to the MIC of that particular experiment.

[c]Data obtained from two separate experiments. Please refer to the Table 2.3 footnotes for x/y quotient definition.

2.3.4.2 F1082 and rifampicin interaction in *M. tuberculosis* rifampicin mono-resistant (RIF^R) strain (RIF MIC > 100 µg/ml).

To examine whether the synergistic interaction between F1082 and rifampicin also facilitated inhibition of growth of drug-resistant *M. tuberculosis* strains, we evaluated drug interaction with RIF^R *M. tuberculosis* clinical isolates. The rifampicin MIC for RIF^R *M. tuberculosis* was more than 100 µg/ml, much higher than the average MIC for drug susceptible *M. tuberculosis* H37Rv (0.4 µg/ml). The RIF^R phenotype did not affect the MIC of F1082 for this strain: MIC was 8 µg/ml, the same value as that determined for rifampicin-susceptible (RIF^S) *M. tuberculosis* H37Rv. The RIF^R results [Figure 2.9 (a)] show that bacteria grew with minimum growth inhibition of 36 % in the presence of 100 µg/ml of rifampicin compared to DMSO control. Adding 0.25 x MIC (2 µg/ml) of F1082 to this culture inhibited (47 %) growth. The scaling down of RIF concentration to 0.25 x MIC (2 µg/ml) F1082 gave 98 % inhibition even at 6.25 µg/ml [Figure 2.9 (a)]. The *x/y* quotients for rifampicin at 100, 50 and 25 µg/ml were (0.95, 0.74 and 0.68), respectively, indicating no effect and additive effect. Synergistic effects were observed at 12.5 and 6.25 µg/ml rifampicin (x/y = 0.12 and 0.21, respectively) between F1082 and rifampicin (Table 2.5).

Table 2.6 F1082 tested in combination with rifampicin (RIF) againat RIF monoresistant isolate

RIF-monoresistant isolate	RIF (µg/ml)				
F1082 (2 µg/ml)	100	50	25	12.5	6.25
Interaction	0.95	0.74	0.68	.012	0.21
Iterpretation	No effect	additive	additive	synergy	synergy

However, 0.5 x MIC of ethambutol did not show any additive or synergistic activity with rifampicin on strain RIF^R [Figure 2.9 (b)]. This could be interpreted that EMB invariable with RIF, however no antagonistic activity was observed at the concentrations tested. In both cases (RIF^S and RIF^R combination with F1082), the concentrations to MIC ratio at which the synergy between F1082 and rifampicin was observed, was similar to those obtained for the RIF^R strain, implying that the synergistic interaction was independent of drug susceptibility status. These results strongly suggest that the synergy between F1082 and rifampicin was specific for the combination of drugs and that the enhanced drug interactions inhibited *M. tuberculosis* growth in both RIF^S and RIF^R strains.

The synergy observed between F1082 and RIF has a possible explanation: RIF is an efficient inducer of cytochrome P450 (CYP) (Bolt, 2004). The CYP is a superfamily of haem-containing enzymes involved in a wide array of NADPH/NADH-dependent reactions, in addition they play pivotal roles in biosynthesis of compounds such as sterols, steroids and fatty acids, as well as detoxification of xenobiotics and chemicals (Kelly *et al*., 2003). Rifampicin is a potent inducer of a variety of CYP in human hepatocytes, as well as in peripheral blood lymphocytes (Haas *et al*., 2005; Rae *et al*., 2001). The complete genome of *M. tuberculosis* reveals at least 20 CYP, but precise functions for these genes and enzymes remain to be elucidated (McLean *et al*., 2006). Like their mammalian counterparts, the mycobacterial CYP were induced by rifampicin but not by isoniazid treatment (Ramachandran and Gurumurthy, 2002). Therefore, the haem-containing enzyme of CYP may interact with F1082 and produce a more active metabolite of F1082. It is also possible that the expression levels of the currently unknown primary target/s of F1082 is/are tightly regulated at transcriptional level. Since rifampicin is an inhibitor of DNA transcription could be synergising with F1082. However these speculations could be clarified once the target/s of F1082 has /have been identified.

(a)

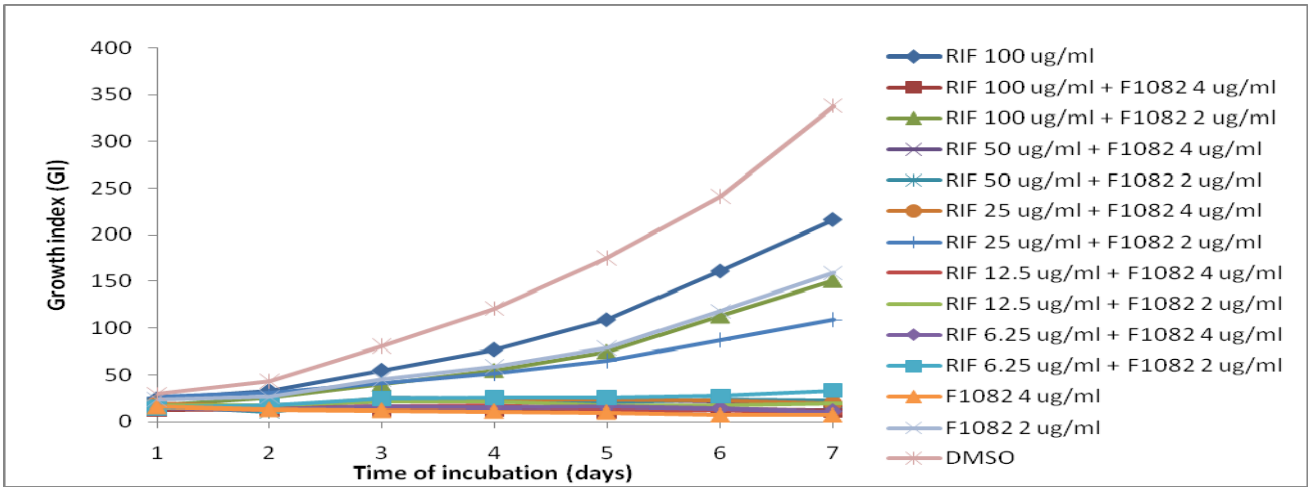

(b)

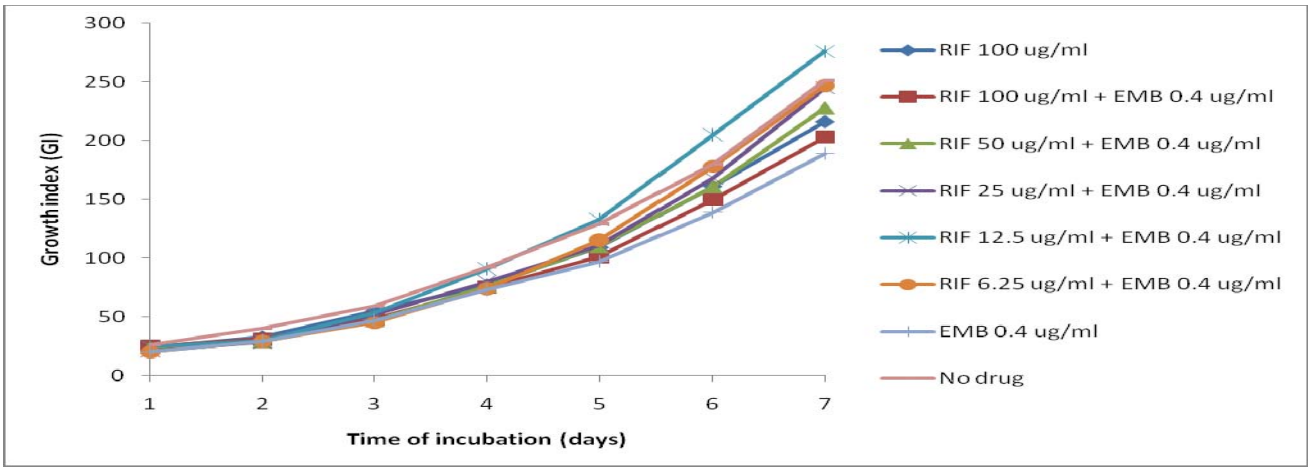

Figure 2.9 Growth profile of RIF^R *M. tuberculosis* treated with rifampicin (RIF) in combination with (a) F1082 and with (b) ethambutol EMB

The experiment was carried out in BACTEC 460 as described in Materials and Methods (section 2.2.1.2). GI readings were obtained daily until the 1:100 inoculum control vial reached a ΔGI value >30 at day 7. The MIC of RIF and F1082 in the RIF^R strain were > 100 µg/ml and 8 µg/ml, respectively..

2.3.5 Cytotoxicity

In order to determine the specificity of F1082 activity, it was considered necessary to obtain the general cytotoxicity on human cell line (THP1). THP-1 cells were chosen because they differentiate into phagocytes (Tsuchiya *et al*., 1982), which are predominant cells in the chronic inflammatory response. For this, the antiproliferative activity of F1082 was evaluated on human monocytic THP1 cells using the microculture tetrazolium (MTT) assay. This method is based on the ability of viable cells to convert the tetrazolium salt (MTT) to colored formazan (Ali-Vehmas *et al*., 1991; Yajko *et al*., 1995). The IC_{50} for F1082 was estimated to be 1 µg/ml (Figure 2.10). This is the concentration that kills 50% of the THP-1 cells.

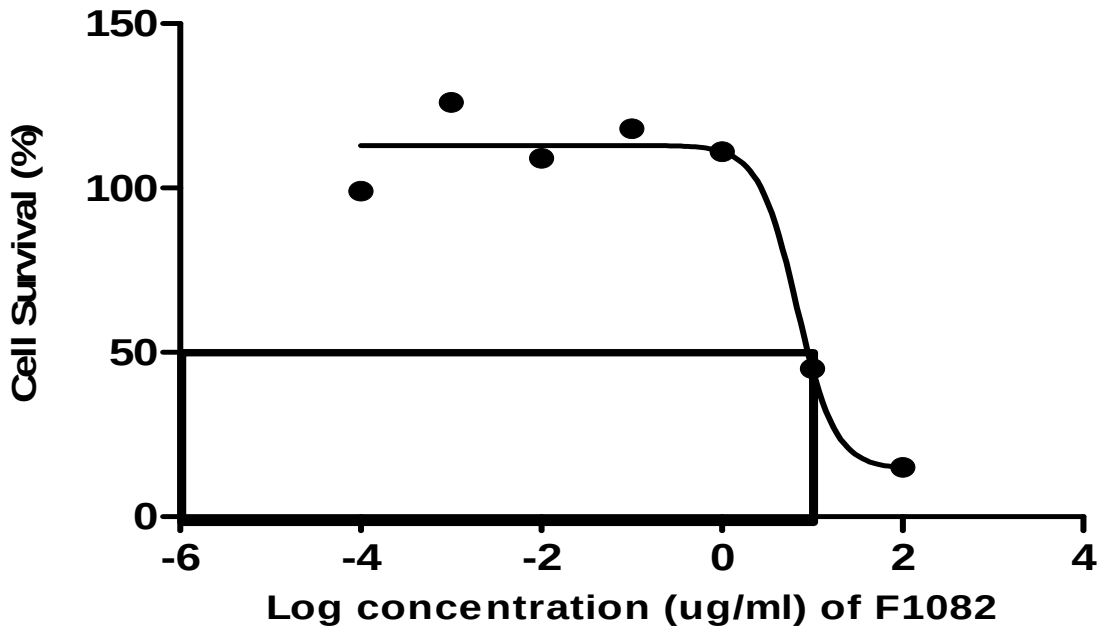

Figure 2.10 Cytotoxic effect of F1082 on the THP-1 cell line.

The selective index (SI) of F1082 was calculated as a quotient of the IC_{50} value of the THP-1 over the IC_{50} of *M. tuberculosis* and was found to be 0.25 (Table 2.7). For TB drug development an SI of ≥ 10

is considered significant by the TB-Alliance. This indicates that F1082 is more damaging to THP1 cells than *M. tuberculosis*. Clearly this is not a good indicator, as a compound should be at least 10 fold more active against *M. tuberculosis* than against a mammalian cell line.

The complex chemical structure of F1082 is depicted and possible degradation components that may be attributed to the observed cytotoxicity (Figure 2.11). The observed cytotoxicity could be attributed to a number of reasons. Firstly the lactone is hydrolytically labile under both acidic and basic conditions (Figure 2.11). Any opening of the lactone would result in hemiacetal formation and rapid release of the phenolic component. This would result in an aldehyde becoming available. Aldehydes are powerful cross-linking groups for proteins, reacting with free amino groups (lysines, thiols etc.). This could result in a loss of protein function resulting in toxicity. Secondly, the NH groups may be metabolically labile and may result in either toxic metabolites. Lastly the bromide may generate stable radicals. In published data, furanones (chlorohydroxyfuranones) induce genetic alterations in numerous biological systems *in vitro*, causing chromosomal aberrations in rodents (Harrington-Brock *et al*., 1995) and DNA damage (Brunborg *et al*., 1991). Therefore suggesting that F1082 may also be cytotoxic to human cell line.

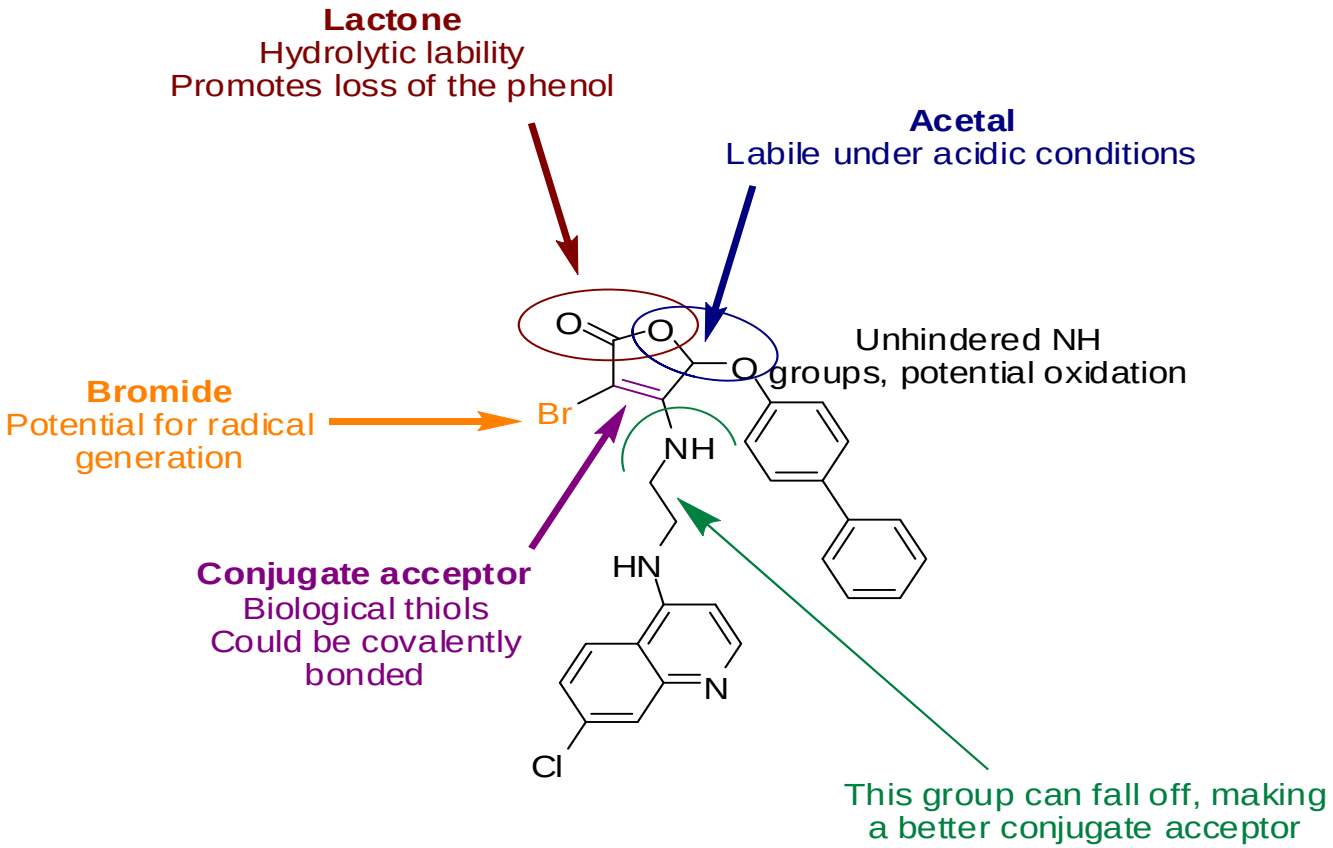

Figure 2.11 Depicts the structure of F1082 and possible degradation components

In order for F1082 to be used or developed into an anti-TB candidate drug, the cytotoxic effect has to be reduced but the antibiotic activity maintained. Derivatives are being synthesised by removal of the bromine group in the 2(5H) furanone, since this may contribute to cytotoxicity. Re-structuring of precursor molecules could perhaps provide us with a furanone based or similar compound with less cytotoxicity.

Table 2.7 *In vitro* antituberculosis activity, cytotoxicity and selective index (SI) values for F1082

Compound	*M. tuberculosis* IC_{50} (µg/ml)	THP1 IC_{50} (µg/ml)	SI[a]
F1082	4	1	0.25

[a]SI, cytotoxicity THPI IC_{50}/*M. tuberculosis* IC_{50}

In conclusion, F1082 has shown some potential as a compound that can be developed into an anti TB candidate drug. Although it has a higher MIC (8 µg/ml) than compared to current anti-TB drugs, it also must be taken into account that in combination with current anti-TB drugs (RIF) there is synergism of potency. F1082 was shown to synergize with rifampicin. Another important characteristic about F1082 is that it is active against MDR strains of *M. tuberculosis*, suggesting a different mechanism of action with the current anti-TB drugs. This suggests that F1082 has a greater chance of being used with the current anti-TB drugs in combating MDR and perhaps XDR-TB strains of *M. tuberculosis.* Unfortunately, F1082 shows high toxicity against a human cell-line. The cytotoxic characteristic of the compound might be overcome by synthesis of derivatives that are less cytotoxic. The use of F1082 as a candidate can provide new anti-mycobacterial targets and its scaffold can be used to try to synthesise improved compounds with higher potency activity and less cytotoxicity. In the next chapter we investigate the manner by which F1082 inhibits the growth of *M. tuberculosis* using gene expression profiling.

Appendix A

I. First Generation Compounds based on F1082

JP-001 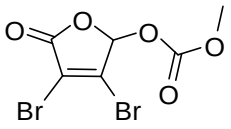	JP-002 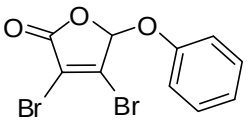	JP-003 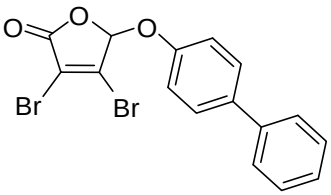
JP-004 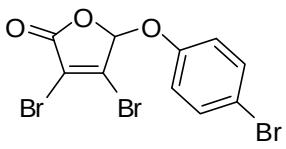	JP-005 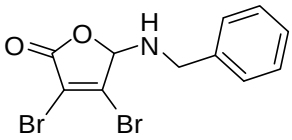	JP-008 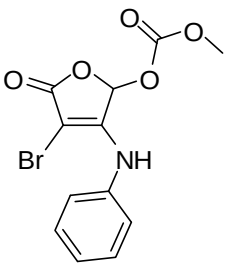
JP-009 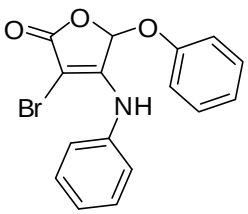	JP-010 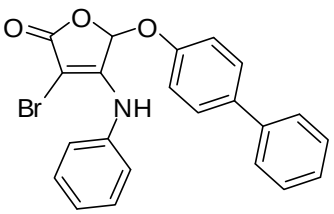	JP-011 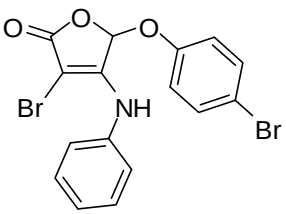

First Generation Compounds based on F1082

JP-022 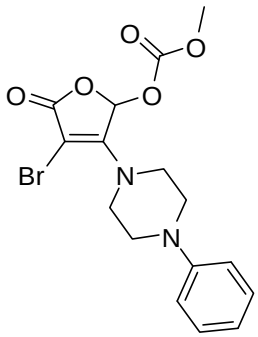	JP-023 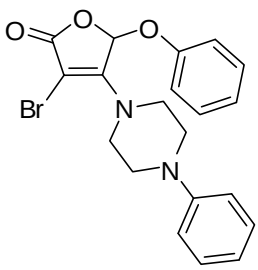	JP-025 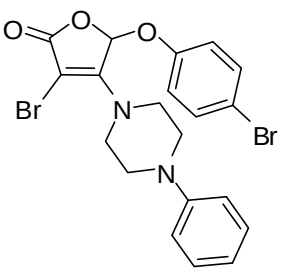
JP-043 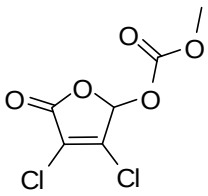	JP-044 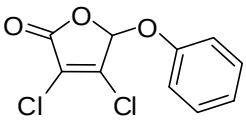	JP-046 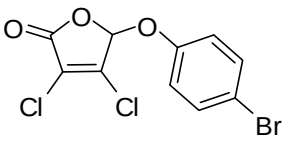
JP-047 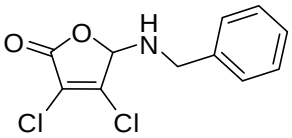	JP-048 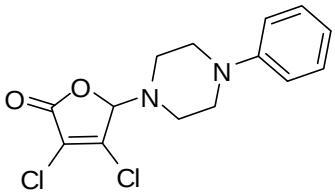	JP-050 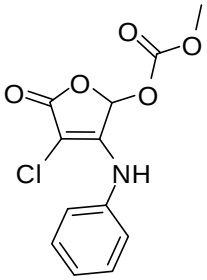

First Generation Compounds based on F1082

JP-051 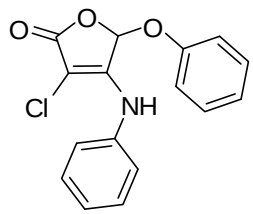	JP-053 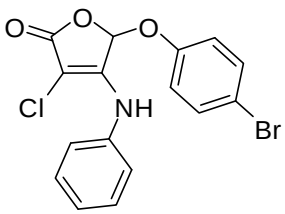	JP-064 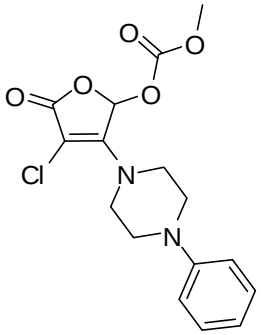
JP-065 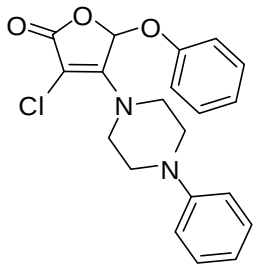	JP-067 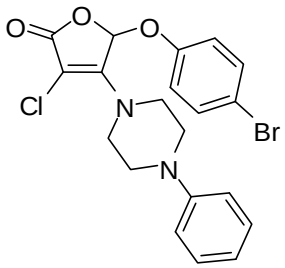	JP-085 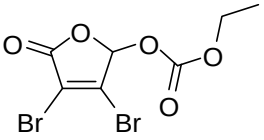
JP-091 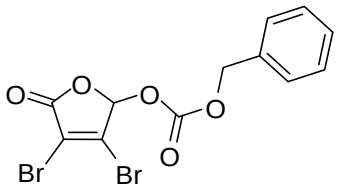	JP-097 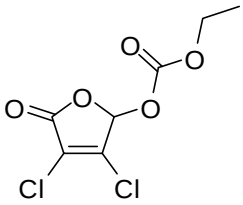	JP-103 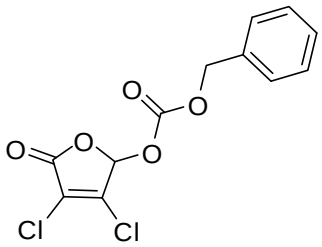
JP-115 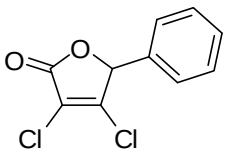	JP-127 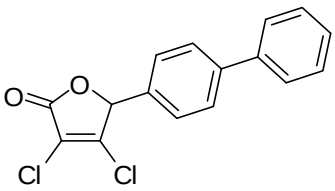	JP-133 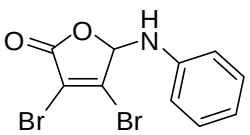

First Generation Compounds based on F1082

JP-134 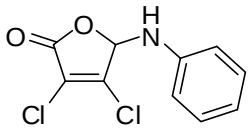	JP-193 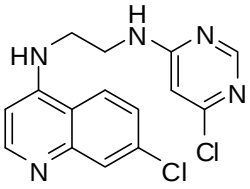	JP-194 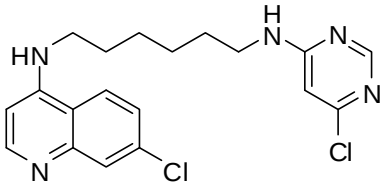
JP-195 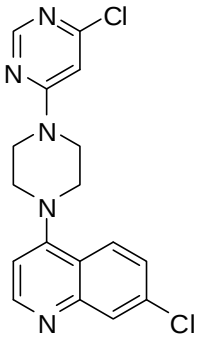	JP-196 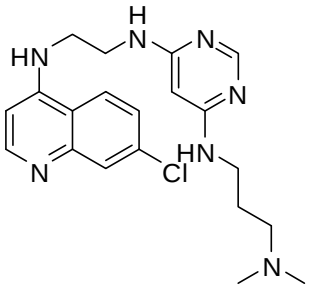	JP-197 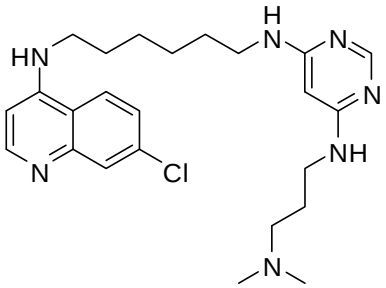
JP-198 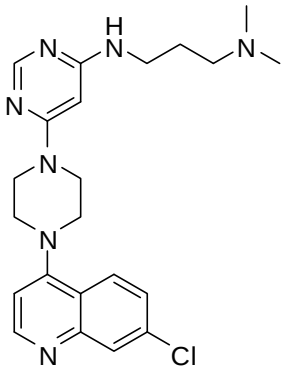	JP-200 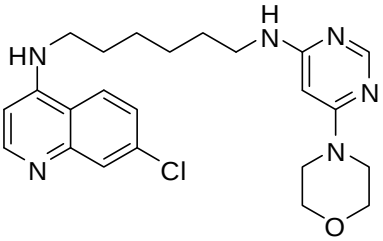	JP-201 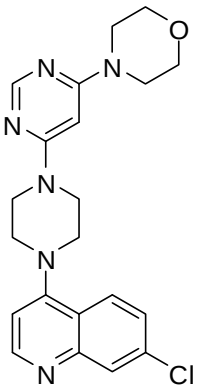

First Generation Compounds based on F1082

JP-203 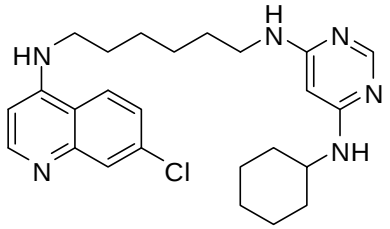	JP-204 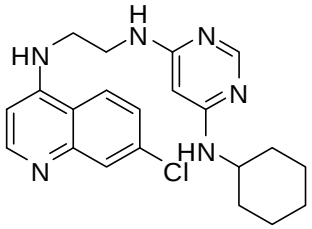	JP-205 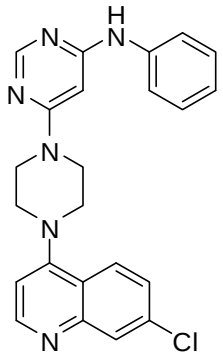
JP-206 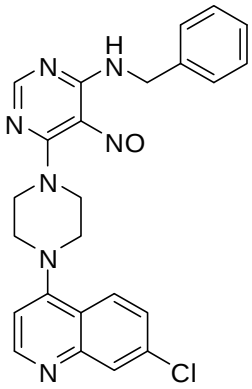	JP-207 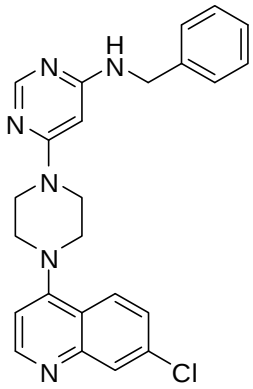	JP-208 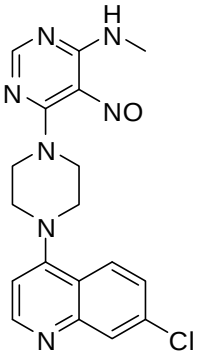
JP-209 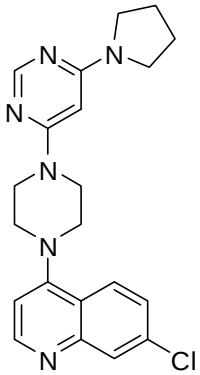	JP-210 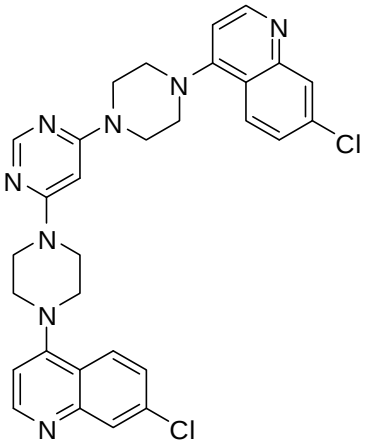	JP-211 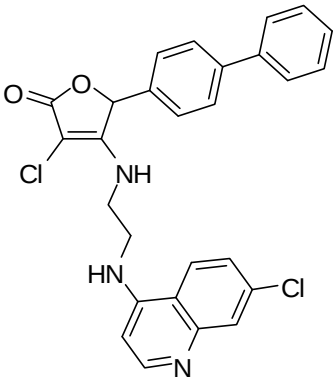

First Generation Controls First

JP-C001 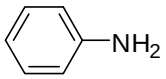	JP-C002 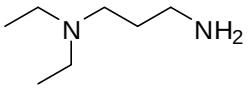	JP-C003 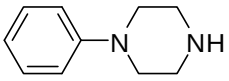
JP-C004 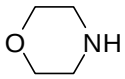	JP-C005 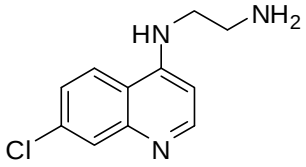	JP-C006 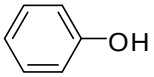
JP-C007 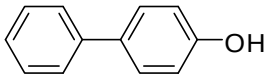	JP-C008 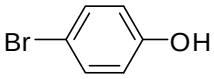	JP-C009 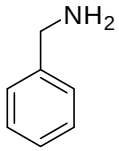
JP-C010 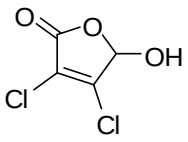	JP-C011 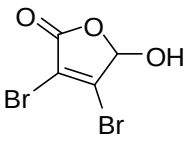	JP-C012 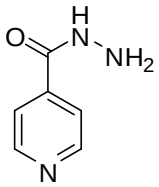
JP-C013 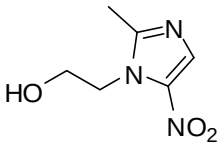	JP-C015 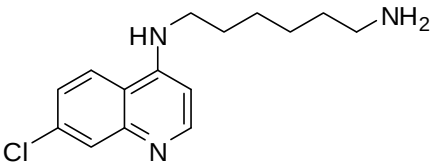	JP-C016 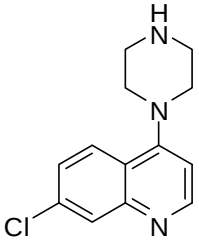

First Generation Controls First

JP-C017 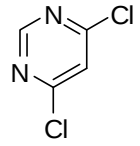	JP-C018 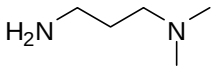	JP-C019 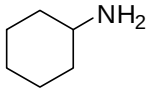
JP-C020 	JP-C021 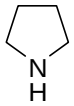	

II. Activity and cytotoxicity results of F1082 derivative

Compound Code	Percentage Inhibition *M. tuberculosis* H37Rv				*In vitro* Cytotoxicity (CHO line)
	45 uM	22.5 uM	11.25 uM	5.625 uM	IC_{50} Value
JP-001	0 %				52.9 uM
JP-002	0 %				88.4 uM
JP-003	0 %				84.1 uM
JP-004	68.9%				91.4 uM
JP-005	0 %				38.8 uM
JP-008	0 %				45.4 uM
JP-009	61.2 %				> 100 uM
JP-010	2.2 %				54.0 uM
JP-011	5.5 %				76.0 uM
JP-022	0 %				> 100 uM
JP-023	9.9 %				> 100 uM
JP-025	32.6 %				> 100 uM
JP-043	9.9 %				64.5 uM
JP-044	33.1 %				87.1 uM
JP-046	25.9 %				88.9 uM
JP-047	5.6 %				22.2 uM
JP-048	17.3 %				86.5 uM
JP-050	0 %				89.6 uM
JP-051	92.4 %				30.85 uM
JP-053	53.1 %				> 100 uM

Compound Code	Percentage Inhibition *M. tuberculosis* H37Rv	*In vitro* Cytotoxicity (CHO line)	Compound Code	Percentage Inhibition *M. tuberculosis* H37Rv	*In vitro* Cytotoxicity (CHO line)
JP-065	46.8 %				> 100 uM
JP-067	36.9 %				> 100 uM
JP-085	0 %				51.5 uM
JP-091	3.3 %				79.5 uM
JP-097	0 %				> 100 uM
JP-098	0 %				83.6 uM
JP-103	1.6 %				85.5 uM
JP-115	26.7 %				63.6 uM
JP-127	31.6 %				> 100 uM
JP-133	48.4 %				54.7 uM
JP-134	36.5 %				51.9 uM
JP-193	68.9 %				45.5 uM
JP-194	98.5 %	99 %	98 %	82 %	13.5 uM
JP-195	93.8 %				> 100 uM
JP-196	30.9 %				> 100 uM
JP-197	64.1 %				29.8 uM
JP-198	43.6 %				82.5 uM
JP-200	58.5 %				42.3 uM
JP-201	47.4 %				25.4 uM
JP-203	98.4 %	98 %	91 %	70 %	23.5 uM
JP-204	83.1 %				45.1 uM
JP-205	97.7 %	71 %	55 %	39 %	22.1 uM
*JP-206	95.7%	99 %	99 %	97 %	68.6 uM
JP-207	96.5 %	89 %	50 %	45 %	10.7 uM
JP-208	98.1%	82 %	49 %	32 %	42.1 uM
JP-209	38.7 %				11.6 uM
*JP-210	78.4 %				> 100 uM
JP-211	99.6 %	99 %	93 %	52 %	9.53 ± 0.10 ug/mL
JP-212	0 %				14.5 uM
JP-213	0 %				48.3 uM
JP-214	0 %				18.9 uM
JP-215	0 %				> 100 uM
*JP-216	98.1 %	98.1 %	98.1 %		82.8 uM
JP-217	0 %				47.9 uM
JP-218	0 %				40.3 uM
JP-219	4.3 %				> 100 uM
JP-220	0.7 %				44.8 uM
JP-221	0 %				36.1 uM
JP-222	8.5 %				32.1 uM
*JP-223	99.7 %	99.7 %	99.7 %	99.0 %	83.4 uM
JP-224	29.7 %				36.9 uM
JP-C001	35.8 %				> 100 uM

Compound Code	Percentage Inhibition *M. tuberculosis* H37Rv	*In vitro* Cytotoxicity (CHO line)	Compound Code	Percentage Inhibition *M. tuberculosis* H37Rv	*In vitro* Cytotoxicity (CHO line)
JP-C003	1.0 %				> 100 uM
JP-C004	3.4 %				> 100 uM
JP-C005	0.2 %				92.9 uM
JP-C006	1.5 %				> 100 uM
JP-C007	0 %				> 100 uM
JP-C008	0 %				> 100 uM
JP-C009	12.9 %				> 100 uM
JP-C010	12.2 %				60.2 uM
JP-C011	0 %				> 100 uM
JP-C013	24.2 %				> 100 uM
JP-C015	43.9 %				14.6 uM
JP-C016	35.3 %				> 100 uM
JP-C017	10.8 %				> 100 uM
JP-C018	17.7 %				> 100 uM
JP-C019	60.9 %				> 100 uM
JP-C020	16.7 %				> 100 uM
JP-C021	11.7 %				> 100 uM
JP-C022	0 %				> 100 uM
JP-C023	0 %				> 100 uM
JP-C024	0 %				> 100 uM
F-1082	99.7 %	100 %	99 %	82 %	1.82 ug/mL
DMSO	0 %	0 %	0 %		
Emetine					0.12 ± 0.07 ug/mL or 0.042 ug/mL

All compounds were tested for activity against *M. tuberculosis* H37Rv and for cytotoxicity against CHO cell line. Compounds that showed more than 90% activity at 45 µM and had greater cytotoxicity data (IC_{50} >50 µM) warranted MIC determination and * indicates compounds that were considered to be promising**.**

CHAPTER THREE

M. tuberculosis microarray gene profiling by F1082

3.1 Introduction

The sequencing of the complete genome of *M. tuberculosis* (Cole *et al*., 1998b) has provided an invaluable resource for TB research and has facilitated functional genomics studies such as transcriptomics and proteomics that enable investigation of the biology of *M. tuberculosis* at a whole genome level (Betts, 2002). The use of DNA microarray is one such approach and has many potential applications within the drug discovery process, from target identification and validation through hit generation and lead optimization (Barry *et al*., 2000).

Target selection may be critical for the development of new drugs, but understanding the dynamics of the metabolic response to interruption of target function may also be important. An organism responds to changes in its environment by altering the level of expression of critical genes that transduce such signals into metabolic changes favouring continued growth and survival (Boshoff *et al*., 2004). Analysis of the transcriptional response by microarray can provide clues to such adaptive responses (Agarwal *et al*., 2003; Betts *et al*., 2003 and Wilson *et al*., 1999). Co-ordinately regulated sets of genes (regulons) are often controlled by single transcriptional regulators that function as a genetic master switches, committing the bacterium to a major alteration in metabolism (Boshoff *et al*., 2004). Induced genes could be predicted to either compensate for inhibition of the target pathway or respond to the toxic effect of the drug and lead to the proposal that RNA response profiles could serve as a fingerprint of a given drug's mode of action (Wilson *et al*., 1999). In this study, we applied genome wide expression profiling in order to search for the mode of action of F1082.

For the design and full run of the study conducted, a pilot study was performed with regard to F1082 as to establish concentrations to be used. At initial we planned to start the experiment at with F1082 at subinhibitory concentration (4, 8 and 64 µg/ml). The rational was based on the fact that we identify gene xpression levels at low concentration i.e. half MIC, and 8 times the MIC. In our preliminary results we only saw 5 genes that were differentially regulated at this concentration. These include Rv3161, Rv3160, Rv3159, Rv1813c and Rv3839. Based on the fact that these genes are regulated in

the same way as by 8 µg/ml and also due to the expensive nature of microarray we decided to do two concentrations (8 and 64 µgml). The following methodologies describe how this study was performed and carried out to reach to our conclusions.

3.2 Materials and Methods

3.2.1 Bacterial strains and growth conditions

M. tuberculosis H37Rv (frozen stock, 2 x 10^8 CFU/ml) 1:10 dilution was initially inoculated into five 25 cm^2 tissue culture flasks containing 10 ml of Middlebrook 7H9 media supplemented with (OADC) and were cultured at 37 °C for 5 days. Each culture was transferred into 75 cm^2 tissue culture flasks containing 50 ml of 7H9 media (1:6), incubated at 37°C and shaken continuously on an orbital shaker until the OD_{600} reached 0.3, which corresponded to 1.3-1.99 x10^6 CFUs (Chapter 2, Figure 2.5).

Each culture of *M. tuberculosis* H37Rv from the same flask was split into 2 volumes (20 ml) in two 75 cm^2 tissue flasks. Each 20 ml received F1082 at 8 µg/ml and an equal amount of the DMSO solvent in which F1082 was dissolved. Similarly, flasks were set up for F1082 at 64 µg/ml and INH at 5 µg/ml, however, INH was dissolved in water. The final percentage DMSO used for all concentrations was less than 1% (0.64%) and these served as reference controls for each time point per concentration see (Table 3.2). The concentrations used for F1082 were chosen based on the MIC of 8 µg/ml and a pilot study that showed that this was the lowest concentration that gave reasonable chnges in gene expression. The highest concentration (64 µg/ml) was used to assess the overall effect of the drug. Isoniazid was used as a control drug at 5 µg/ml and 5 hours of incubation (Fu and Shinnick, 2007). Cultures were incubated for 4 or 24 hours for F1082, also based on a pilot study, and the fact that *M. tuberculosis* generation time ranges from 24 to 36 hours (Fontán *et al*., 2008). Bacterial cultures (20 ml) were harvested by centrifugation at (5000 rpm for 5 minutes) in a bench-top centrifuge (Eppendorf 5810 R, Hamburg, Germany) at room temperature (25°C). After removing the supernatant, pellets were immediately frozen on dry ice and stored at -80°C until RNA extraction.

3.2.2 RNA isolation

The frozen bacterial pellets were resuspended in 2 ml TRIZOL (Invitrogen) and mixed well by pipetting. The mix was transferred as 1 ml aliquots into 2 ml tubes containing 0.5 ml of Zirconia beads (0.1mm in diameter). The cells were lysed using a bead beater (MP Biosciences) set at 6.5 W for 30 seconds and thereafter cooled on ice for another 30 seconds. Each cycle was repeated three times. The samples were centrifuged at 14000 rpm for 15 minutes at 4°C in a bench-top centrifuge and the aqueous phase was removed from the beads. A volume of 300 µl of chloroform were added to each sample, the sample was gently mixed by inverting for 10-15 seconds and thereafter centrifuged at 14000 rpm at 4°C for 15 minutes in a bench-top centrifuge. The clear top-layer (approximately 600 µl) was transferred into new tubes (1.5 ml) with rubber O-ring caps. Nucleic acids were precipitated by addition of 0.6 % v/v (approximately 360 µl) of absolute ethanol (ice cold, -20°C). The RNA was isolated using the MACHEREY-NAGEL kit (GmbH & Co.KG, Germany) as instructed.

Briefly, for each sample, one NucleoSpin RNAII column was placed in a 2 ml centrifuge tube. All centrifugation steps were carried out in a bench top centrifuge. The lysate (precipitated nucleic acids) was pipetted up and down 2-3 times, loaded onto the column and then centrifuged for 30 seconds at 11 000 rpm. The column was placed in a new collecting tube. To desalt the silica membrane, 350 µl of membrane desalting buffer (MBD) was added and the column was centrifuged for 1 minute at 11 000 rpm to dry the membrane.

DNA digest was performed by preparation of DNase reaction mixture in a sterile micro-centrifuge tube: DNase reaction mixture was prepared by mixing 10 µl of reconstituted (r) DNase in 90 µl of reaction buffer for rDNase in a sterile 1.5 ml centrifuge tube for each isolation. The tube was mixed by flicking and 95 µl of DNase mixture was applied directly on the centre of the silica membrane of the column and incubated at room temperature for 15 minutes. The silica was washed and dried in three steps: (1) two hundred microliters of RA2 buffer was added to the NucleoSpin RNAII column, centrifuged for 30 seconds at 11 000 rpm and the column was placed in a new collecting tube (RA2 buffer inactivates the rDNase). (2) Six hundred microliters of RA2 buffer was added to the

NucleoSpin II column, centrifuged for 30 seconds at 11 000rpm, discarded the flow-through and placed back into the collecting tube. (3) two hundred and fifty microliters of RA3 buffer was added to the column, centrifuged for two minutes at 11 000 rpm to dry the membrane completely. The column was added into a nuclease-free 1.5 microcentrifuge tube. Pure RNA was eluted in 60 µl water (RNase-free), by column centrifugation at 11 000rpm for 1 minute.

The purity of RNA was estimated by the ratio of the readings at 260 and 280 nm (A260/A280) using Nanodrop. Agarose gel electrophoresis was used to assess the integrity of and relative proprtion of mRNA with ribosomal RNA using Nanodrop. The agarose gel electrophoresis revealed prominent 23S and 16S ribosomal bands, indicating that the RNA was not degraded. Extracted mRNA in water was stored at -80°C until use. All RNA samples were sent and furher checked through quality and quantity test before microarray byCenter for Applied Genomics.

3.2.3 Microarray Processing

Microarray processing was perfomed by the Center for Applied Genomics, Public Health Research Institute, UMDNJ-New Jersey Medical School (Newark, NJ, USA) on receival of 3 ng/ml of samples and experimental design. In principle, microarray analysis was perfomed as follows with minor changes and is indicated in Institutes public website (refer <http://www.cag.icph.org/downloads_page.htm>). *M. tuberculosis* oligoarrays were printed at the Center for Applied Genomics, Public Health Research Institute, UMDNJ-New Jersey Medical School (Newark, NJ, USA). These microarrays consisted of 4295 70-mer oligonucleotides representing 3924 open reading frames (ORFs) from *M. tuberculosis* strain H37Rv and 371 unique ORFs from *M. tuberculosis* strain CDC 1551 that are not present in H37Rv. The arrays were prepared by spotting oligonucleotides (Tuberculosis Genome set version 1.0, Operon Biotechnologies) onto poly-L-lysine coated glass microscope slides using an Omnigrid 100 Arrayer and SMP3 pins.

3.2.3.1 cDNA synthesis and labelling

Total RNA (3 µg each) was reverse transcribed into cDNA using Superscript II in the presence of Cyanine-3 (Cy-3) or Cyanine-5 (Cy-5) dUTP by a modification of a published procedure (Voskuil *et. al*, 2003). The RNA was incubated with a reaction mix containing a final concentration of 0.17µg/µl random hexamers, 0.96x first strand buffer, 9.6 mM DTT, 0.44 mM dATP, dCTP and dGTP, 0.02 mM dTTP, 0.06mM Cy-3 or Cy-5 dUTP and 9.4 units Superscript II for ten minutes at 25°C followed by ninety minutes at 42°C. The labelled cDNA probes were then purified and concentrated to 5 µl using a Microcon YM10 filter and TE buffer pH 8.0.

3.2.3.2 Hybridization

Prior to hybridization, slides were blocked by submersion in a solution of 3% BSA and 0.1% SDS for 1 hour in a glass chamber placed in a 42°C water bath. After blocking, the slides were washed with water for 2 minutes, followed by washing in 100% isopropanol for 2 minutes, and dried by centrifugation at 500 x g for 3 minutes. The purified cDNA probes were mixed with 10 µl hybridization solution containing a final concentration of 0.5 µg/µl tRNA, 2.0X SSC, 0.25% Formamide and 0.1% SDS and applied to the array. The probes were covered by a flat 22 x 22 mm coverslip and hybridized in sealed hybridization chambers for sixteen hours in a 50°C water bath. After hybridization, the coverslips were removed from the slides by submerging into a solution of 2X SSC/0.1% SDS. The slides were washed with vigorous agitation for 1 minute in a solution of 1X SSC/0.05% SDS, following by 2 minutes in a solution of 0.06X SSC, and dried by centrifugation at 500 x g for 1 minute. The complete protocol can be found in (APPENDIX 3A). For each pair of RNA samples, dye flips were performed as follows: (1) the test RNA was labelled with Cy3 and the control RNA with Cy5, or (2) the test RNA was labelled with Cy5 and the control RNA with Cy3, and the results were compared.

3.2.4 Microarray Analysis

The slides were scanned using an Axon 4000A scanner at 532 nm (for Cy3) and 635 nm (for Cy5) with a 10 micron resolution. Images were processed using GenePix Pro 5.1 software (Molecular Devices Corporation, Union City, CA). Data were filtered by removing all spots that were below the background noise or flagged as 'bad'. Spots were considered to be above the background noise if the median intensity of at least one of the channels was greater than twice the median local background for the spot. The chips were normalized by the print-tip Lowess method (Dudoit and Speed, 2000). The ratio of the average median intensity of Cy5 over the average median intensity of Cy3 was determined for each spot and the fold relative change values were calculated.

The experimental design was perfomed as as follows: The concentration and the time points were chosen based on our own pilot studies and by overviewing of the published data on microarray studies. To ensure that the primary effects of the compound were captured we used the MIC (8 µg/ml) and 8 times the MIC (64 µg/ml) as our high dose for global effect (Table 3.1). RNA isolated from solvent treated cultures at each time point was pooled and used as the reference to which each sample from a corresponding time point was compared by co-hybridization. In order to test reproducibility within slides and dye-bias, each sample was split twice, labelled in separate reactions with Cy3 and Cy5 and hybridised to a single array. In simple terms, RNA samples from F1082 treated and RNA from DMSO counterparts were split into two. RNA from the F1082 treated sample labelled with Cy3 was co-hybridised with RNA from DMSO treated sample labelled with Cy5 and then dyes were flipped with F1082 treated sample labelled with Cy5 and DMSO treated sample labelled with Cy3 (Figure 3.1). Three biological replicates from separate experiments were used for this study. Figure 3.1 shows the organisation and labelling of our samples for this study.

Triplicate cultures were treated with either 1 x or 8 x MIC of F1082, and RNA was isolated from these as well as from the solvent-treated control samples after 4 or 24 hours of incubation. RNA isolated from multiple solvent-treated cultures at each time point was pooled and used as the reference to which each sample from a corresponding time point was compared by cohybridization. Each

triplicate sample was hybridized twice, with the flours (dyes) reversed for the second batch of hybridizations. The whole genome was printed twice on each slide, hence giving a total of twelve measurements per gene for each treatment. Genes were considered differentially expressed if there was a fold change of at least 1.5 fold up or down. A one-class Significance Analysis of Microarrays (SAM) analysis (Tusher *et al*., 2001) was performed with the MEV 4.3 software (Saeed *et al*., 2003) to find genes with changes that occurred consistently in all replicates. A median FDR (false discovery rate) of zero, and a mean change of at least 1.5 fold were considered the cut-off values for significance. Genes with value changes in response to compound treatment (n-fold) of more or less than 1.5 times those in the solvent-treated control were retained as compound-induced or compound-suppressed changes, respectively

Table 3.1 Experimental design for microarray analysis

	Samples per concentration		
Time of treatment	F1082 (8 µg/m)l	F1082 (64 µg/ml)	INH (5 µg/ml)
4 hrs	DMSO control Test sample	DMSO control Test sample	DMSO control 5 hrs Test sample
24 hrs	DMSO control Test sample	DMSO control Test sample	

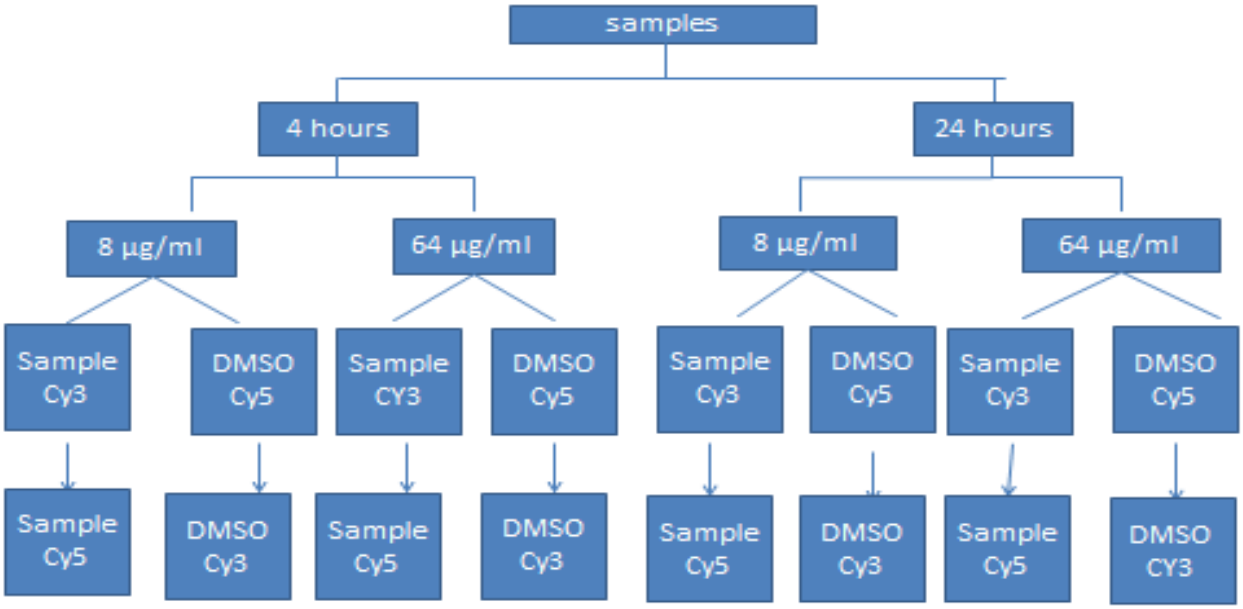

Figure 3.1 RNA sample organisation and labelling for microarray analysis and dye flip for each experiment. INH experiment was performed in the same way and can be represented by one time point and one concentration of F1082 as depicted in the above figure.

3.2.5 Microarray validation by relative quantification of mRNA by real-time PCR

1. cDNA conversion:

Each cDNA pool was prepared following the protocol for SuperScript™ III First-Strand synthesis SuperMix for qRT-PCR (Invitrogen™). Briefly a reaction mixture (20 µl) included 1 µg RNA, 2X RT Reaction Mix, RT Enzyme Mix and DEPC-treated water. Each reaction mix was gently mixed and incubated at 25°C for 10 minutes for primer to anneal then at 50°C for 30 minutes for cDNA synthesis. The reaction was terminated by heating to 85°C for 5 minutes then chilled on ice. Addition of 1 µl (2U) of *E. coli* RNase H and incubation at 37°C was performed immediately to remove RNA template from the cDNA. The cDNA was diluted to 10% in DEPC-treated water and stored at -20°C until use.

2. Candidate gene selection and primer design:

A set (n = 11) of genome-directed primers designed to prime all ORFs of interest in the *M. tuberculosis* genome was used for reverse transcription (Table 3.2). These genes were chosen based on the fact that they were highly upregulated and random selection of genes that were differentialy regulated to validate the microarray data. Forward and reverse primers for real-time PCR amplification were designed with Primer Express Software (Primer 3 version 0.4.0). Real-time PCR was performed on eleven genes, namely (*Rv3159c, Rv3160c, Rv0676c, Rv2358, Rv2190c, Rv0652, Rv2246, Rv3804c, Rv1094, Rv0724,* and *Rv1592c*) (Table 3.1).

Table 3.2 List of RT-PCR and PCR oligonucleotide primers used to amplify genes selected for microarray validation.

Name	Primer sequence (5' to 3')	Length of the primer	Tm [°C]	G+C (%)	Product length
Rv3159c **f**	gaaaccgaggctttggaaac	20	60.97	50	
Rv3159c **r**	gaggttattgtcgccgttgt	20	60	50	173
Rv3160c **f**	ccggccatctacaaacactt	20	59.99	50	
Rv3160c **r**	atggaaaccagcacataggg	20	59.81	50	191
Rv3161c **f**	gacacgttgacctgccaata	20	59.57	50	
Rv3161c **r**	gatccacaccaatccattcc	20	59.99	50	153
Rv0676c **f**	gacacgttgacctgccaata	20	59.99	50	
Rv0676c **r**	gatccacaccaatccattcc	20	59.79	45	207
Rv2358 **f**	agccagaaactgaccgagaa	19	61.67	63.16	
Rv2358 **r**	gtcgaaatccgcaatatggt	20	59.83	50	237
Rv2190c **f**	gtttctttgcgagcttcacc	20	60	50	
*Rv2190*c **r**	cgagcttttcgttgagatcc	20	59	50	162
Rv0652 **f**	caaggaaatgaccctgttgg	20	60.34	50	
Rv0652 **r**	gatcacgtcgaactcggact	20	60.27	55	160

Name	Primer sequence (5' to 3')	Length of the primer	Tm [°C]	G+C (%)	Product length
Rv2246 **f**	gaccgtgcagaagtacatgc	20	59.32	55	
Rv2246 **r**	gttgttggtggacatcacga	20	60.43	50	244
Rv3804c **f**	agcttgttgacagggttcgt	20	59.77	50	
Rv3804c **r**	cactttggaattggaccttga	21	59.96	42.86	210
Rv1094 **f**	ccgagaagtacacgcaggtc	20	60.85	60	
Rv1094 **r**	gtaacgaggttggcgaagaa	20	60.25	50	175
Rv0724 **f**	ggaggcggacttgttctaca	20	60.25	55	
Rv0724 **r**	cgaccccggataactgacta	20	59.95	55	232
Rv1592c **f**	gagtacgcaccggacctaga	20	60.28	60	
Rv1592c **r**	taccgttgtcatctccgtca	20	60.11	50	225
16S rRNA **f**	ggactgagatacggcccagact	20	60	60	
16S rRNA **r**	cgcgacaaaccacctacga	22	65	60	271

3. RT-qPCR design and analysis

Relative quantitative PCR was performed in MxPro4000 Multiplex quantitative PCR System (Stratagene, Santa Clara, CA) using SYBR® GreenER™ qPCR SuperMix Universal (Invitrogen™) following the manufacturer's instructions. All PCR reactions were carried out in duplicate with the following PCR conditions: 10 minutes at 95° followed by 40 cycles of 30 seconds at 95°C for denaturation, and 30 s annealing at 55°C, and 30 seconds extension at 72°C. Each cDNA preparation included a primer for 16S rRNA and ROX (contained in SYBR green mix as an internal reference dye) internal controls. Levels of the target RNAs were normalized for 16S rRNA in the same sample and evaluated as [Target mRNA]/[16S rRNA] by the instrument.

The fluorescence emission was detected for each PCR cycle and the threshold cycle (C_T) values were determined. The C_T value was defined as the actual amplification cycle when the fluorescence signal

increased above the background threshold. Average C_T values from duplicate PCR reactions were normalized to average C_T values for 16S rRNA from the same cDNA preparations. The ratio of expression of each gene in F1082 treated vs. vehicle (DMSO only) treated sample was calculated as

$2^{-(\Delta\Delta CT)}$ of that treatment where C_T is the threshold cycle and $\Delta\Delta C_T$ is the difference C_T [(test gene) − C_T (house keeping gene)], for treated sample minus vehicle sample. Assays were carried out in triplicate from three different experiments.

For statistitical significancy; all values were presents as mean ± standard deviation or mean standard error of means of three independent samples with multiple samples. Comparisons between experimental conditions were analysed by the Student's *t*-test. Differences were considered statistically significant when $P \leq 0.05$.

3.3 Results and Discussion

3.3.1 *M. tuberculosis* gene signature profile from exposure to isoniazid (INH).

INH was initially used as model compound to validate the microarray technology as the genes associated with this compound mechanism of action is already known (Boshoff *et al.*, 2004). The result shown in Table 3.3 is mainly based on the presence or absence of the characteristic gene-expression signature of FAS-II inhibition, rather than based on individually differentially regulated genes observed in the experiments. The most highly induced genes in response to INH were members of the *kas* operon (Rv2243-Rv2247). Isoniazid has been previously been shown to upregulate this operon, which contains five FAS-II components including *kasA* and *kasB* (Slayden *et al*., 2000; Vilchèze *et al*., 2000; Betts *et al*., 2003b; Fu and Shinnick, 2007). Amongst the induced seven genes, four genes belong to a functional class category of lipid metabolism, one to cell wall and cell processes and the other two remaining fall into conserved hypothertical. The fact that most genes induced belong to lipid metabolism and cell wall processes indicate that INH affects the pathway of the cell wall biosynthesis. Different laboratories have used different conditions depending on their

primary need but all came to produce the gene signature profile of INH. Our microarray data under the conditions we used confirmed these findings and showed that the *kas* operon is induced even by 5 µg/ml INH treatment (Table 3.3). At this stage we gained confidence that our micro array data is reliable by reproducing what is in literature. From this onwards we decided to persue our main objectives with F1082 and INH was no further used in microarray studies. Therefore test experiments with F1082 under conditions outlined in materials and methods (Figure 3.1) were performed.

Table 3.3 *M. tuberculosis* genes regulated by INH treatment at 5 µg/ml

Gene ID	Gene name	Fold change	Description	Functional category(ies)
Rv0411c	*glnH*	2.2	Probable glutamine binding protein	Cell wall and cell processes
Rv3413c	Rv3413	3.1	Hypothetical protein	Conserved hypotheticals
Rv1592c	*sucC*	3.1	Probable succinyl-CoA synthase	Conserved hypotheticals
Rv2246	*kasB*	2.8	β-ketoacyl synthase	Lipid metabolism
Rv2245	*kasA*	2.8	β-ketoacyl synthase	Lipid metabolism
Rv2244	*acpM*	2.9	Acyl carrier protein	Lipid metabolism
Rv2247	*accD6*	2.1	Acetyl-CoA carboxylase	Lipid metabolism
Rv1886c	*fbpB*	-3.1	Secreted antigen 85-B	Lipid metabolism
Rv1094	*desA*	-1.7	Possible acyl-[ACP] desaturase	Lipid metabolism

3.3.2 *M. tuberculosis* gene signature profile from exposure to F1082

In order to determine the mode of action of new or novel compounds, it is necessary to identify the genes that are regulated by the compound prior to a generalized response. Hence we used the lowest concentration (8 µg/m, F1082) at the earliest time point (4 hours) to determine the specific gene signature profile of F1082. Twenty four (24) hour time point, was also used since *M. tuberculosis* replicates within 24-36 hours (Fu and Shannick, 2007). It is not only the gene signature profile that is

important in order to understand the mechanism of action, but also the general response that is of importance. For this reason we included a concentration that was 8 times MIC (64 µg/ml) over 4 and 24 hours of treatment.

The total number of genes significantly regulated at each concentration and time point and the overlapping of these gene sets is displayed (Figure 3.2). Numbers within the sectors indicate the total number of genes regulated uniquely or in common by either 1 x or 8 x MIC treatment of F1082 at either 4 or 24 hours ($P < 0.05$). A cut-off of a minimum of 1.5 fold change was used and SAM statistical software was used to establish statistical significance. The Venn diagrams (Figure 3.2) indicate that many genes are uniquely regulated by one concentration and that there are time scale dependencies. There were 26 genes by 8 µg/ml for both time points, 179 genes by 64 µg/ml at 4 hours and 193 genes by 64 µg/ml that were uniquelly differentially regulated. Genes that were commonly regulated by 8 µg/ml and 64 µg/ml at 4 hours were only 10. There is a greater overlap of genes regulated by F1082 at 8 and 64 µg/ml (24 genes). Genes common to all concentrations and time points are only 77 and can be used as global gene expression Most of the genes regulated by 8 µg/ml are a subset of those regulated by 64 µg/ml at both time points (Table 3.4). This could suggest that these genes are a primary response to F1082 treatment, before a more general response ensued.

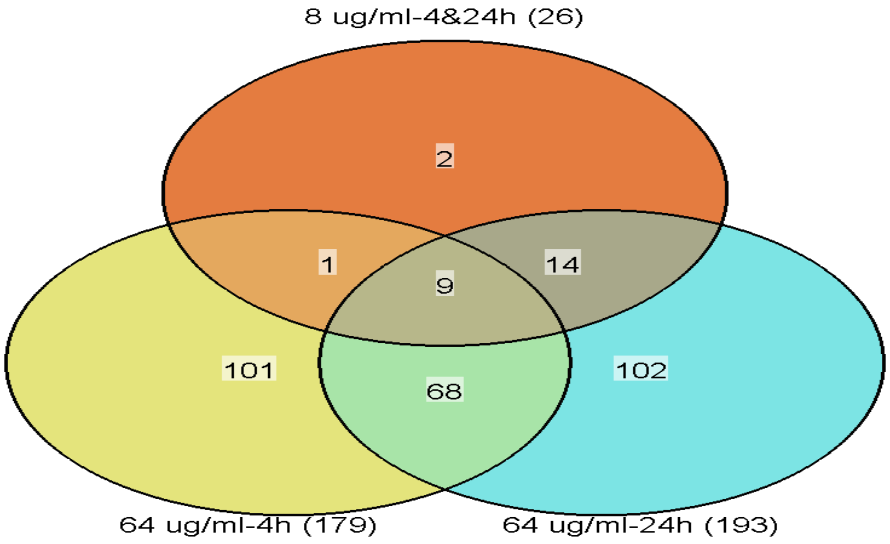

Figure 3.2 Representation of the significant differentially expressed genes, unique to, and common in *Mtb* H37Rv after 4 and 24 hours exposure at 8 and 64 µg/ml F1082

The twenty four genes regulated by F1082 and presumed to form part of the gene signature profile for F1082 fell into several categories (Table 3.4). One group encodes proteins that are annotated to be directly involved in either iron acquisition (*mbtB, mbtC, mbtD, mbtE, mbtH, and mbtI*), also called the mbt cluster, composed of 10 genes, and iron storage genes (*bfrB*). All the genes involved in iron acquisition were regulated by the lower concentration (8 µg/ml) only, at both time points (4 and 24 hours) but only the late time point (24 hours) at the highest concentration (64 µg/ml). This could suggest that we see F1082 primary effect at a delayed time point as F1082 has inhibitory activity not necessarily killing the bacteria. When *M. tuberculosis* is faced with low iron conditions, it up-regulates the mbt cluster for siderophore biosynthesis and down regulates the iron storage genes (*bfrA* and *bfrB*) (Quadri *et al*., 1998). From our data we noted that the *mbt* cluster was up-regulated by more than two fold whereas the iron storage genes (*bfrB*) were down-regulated by more than one 1.5 fold. This could mean that *M. tuberculosis* "senses" low iron conditions under F1082 treatment.

The second group of genes encoded (annotated) proteins are involved in detoxification. Molecules with aromatic characteristics in general have been reported to be potent inducers of monooxygenases, dioxygenases, certain methylases, efflux systems, and the associated carboxylic acid degradation gene (Boshoff *et al*., 2004). Since F1082 is an aromatic compound, this result is consistent in that there was high induction of genes involved in drug detoxification and efflux mechanisms (Rv3160c- Rv3161c, upregulated by more than 20 fold). We considered that induction of these genes could be a non-specific effect of F1082. The other group of genes involved included conserved hypothetical proteins and members of the PE/PPE family proteins with no known specific function. The last group involve up-regulation of the sigma (σ) factors (SigB and SigE). *In M. tuberculosis*, the response to cell envelope damage is regulated by σ^E and the response to oxidative stress and heat shock is regulated by σ^H, and σ^B is a component of both regulons (Manganelli *et al*., 2002). We speculated that F1082 could be interfering with iron acquisition either by being an iron chelator or directly affecting genes regulating iron acquisition; alternatively, it could be that F1082 exerts its effect by generation of oxidative stress.

Table 3.4 A list of 24 *M. tuberculosis* genes whose regulation is affected by 8 µg/ml and 64 µg/ml of F1082. These genes were classified into different functional categories according to TubercuList

Gene ID	Gene name	Fold change	Description	Functional category(ies)
Rv3839	Rv3839	2.5	Conserved hypothetical protein	Conserved hypotheticals
Rv1087	Rv1087	1.4	Conserved hypothetical protein	Conserved hypotheticals
Rv1813c	Rv1813c	-1.9	Conserved hypothetical protein	Conserved hypotheticals
Rv3161c	Rv3161c	27.5	Possible deoxygenase	Intermediary metabolism and respiration
Rv2122c	irgL	2.4	Probable phospho-ribosyl-AMP pyrophosphatase	Intermediary metabolism and respiration
Rv3841	bfrB	-1.5	Possible bacterioferritin	Intermediary metabolism and respiration
Rv3020c	esxS	2.1	ESAT-6 like protein	Cell wall and cell processes
Rv3402c	Rv3402c	2	Conserved hypothetical protein	Cell wall and cell processes
Rv0431	Rv0431	-1.9	Putative tuberculin related protein	Cell wall and cell processes
Rv3524	Rv3524	-1.5	Putative conserved membrane protein	Cell wall and cell processes
Rv3159c	Rv3159c	10.9	PPE family protein	PE/PPE
Rv0280	PPE	-2	PPE family protein	PE/PPE
Rv1387	Rv1387	-2.2	PPE20- PPE family protein	PE/PPE
Rv1386	Rv1386	-3.6	PPE family protein	PE/PPE
Rv2377c	mbtH	2.4	Putative conserved protein	Lipid metabolism
Rv2380c	mbtE	3	Polypeptide synthase (Mycobactin)	Lipid metabolism
Rv2381c	mbtD	2.4	Polyketide synthase	Lipid metabolism
Rv2382c	mbtC	3.2	Polypeptide synthase	Lipid metabolism
Rv2383c	mbtB	1.7	Phenyloxazoline synthase	Lipid metabolism
Rv2386c	mbtL	1.5	Putative isochorismate synthase	Lipid metabolism
Rv3252	alkB	-1.6	Probable alkane-1-monooxygenase	Lipid metabolism
Rv2710	sigB	2.7	RNA polymerase sigma factor B	Information pathways
Rv1221	sigE	1.5	Alternate RNA polymerase sigma factor E	Information pathways
Rv3160c	Rv3160c	30.8	Possible TETR family transcriptional regulatory protein	Regulatory protein
Rv3269	Rv3269	1.8	Conserved hypothetical protein	Virulence, detoxification, adaptation

The genes that are marked yellow are commonly regulated as in *M. tuberculosis* and are involved in acquisition and storage of iron and may be part of gene signature profile of F1082.

Mining the transcriptome data in the context of functional categories yielded particularly interesting results when applied to genes whose expression was repressed in *M. tuberculosis* following F1082 treatment (Figure 3.3). The expression of more than an anticipated number of genes belonging to the Intermediary metabolism and respiration, Information pathways and Lipid metabolism categories were repressed after 24 hours post inoculation. These results indicate that in response to F1082 treatment, a significant reduction of the expression of genes belonging to many key biosynthetic pathways is observed. These results indicate that F1082 treatment causes a later/ secondary effect in the expression of specific such as transcriptional regulators that mediate the pathogen's response to cell membrane damage, coupled with a silencing in expensive energetic processes such as lipid-metabolism, and DNA, RNA and protein synthesis. One such transcriptional factor is σ^B, which has been shown to protect *M. tuberculosis* against membrane damaging stress (Fontán *et al*., 2009) and whose expression was induced in response to F1082 (64 µg/ml) after 24 hours of post inoculation.

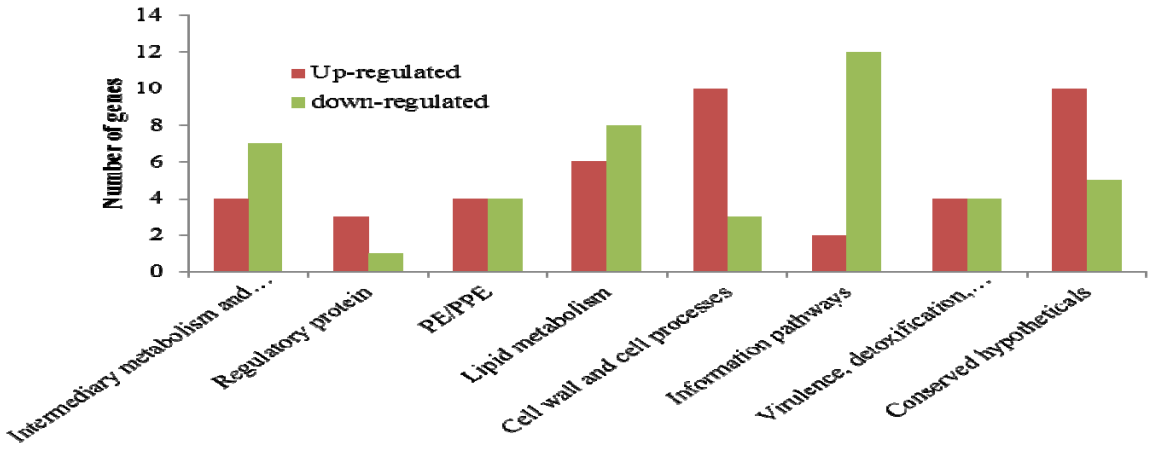

Figure 3.3 Distribution of the common 77 *M. tuberculosis* genes, where expression changes are between 4 and 24 hours at 64 µg/ml to F1082 exposure, into functional categories.

Genes differentially regulated common to 8 and 64 µg/ml were distributed in functional categories according to TubercuList (http://genolist.pasteur.fr/TubercuList/).

3.3.2.1 *M. tuberculosis* genes whose expression was affected by high concentration of F1082 (64 µg/ml)

When we investigated the global gene expression change induced by F1082 at a high concentration (64 µg/ml), we observed that almost all the genes that were differentially regulated at 8 µg/ml were a subset of genes altered by a high concentration (64 µg/ml). This clearly showed that as the concentration of F1082 increases, more genes were affected in terms of expression but the genes that were affected by low concentration consistently were also affected at high concentration (Figure 3.2). This suggests that the gene signature profile of the compound or mode of action is still the same. For the microarray data analysis, two paradigms were used to analyze the data, one having been to look at the genes that were differentially regulated between the control and the treated and the other one was to look at genes that are coordinately regulated. When we used the initial paradigm, genes that were down regulated at high concentration were all involved in information pathways. These genes are all involved in ribosomal protein synthesis (Table 3.5) and this suggests that F1082 inhibits the growth of *M. tuberculosis* somehow by interference with transcription and translation therefore cell replication is interrupted.

Table 3.5 *M. tuberculosis* genes from Information pathways suppressed by F1082 (64 µg/ml).

Gene ID	Gene name	Fold change	Description	Functional category (ies)
Rv0704	*rplB*	-2.1	Probable 50s ribosomal protein	Information pathways
Rv0700	*rpsJ*	-2.2	30s ribosomal protein	Information pathways
Rv3442c	*rpsI*	-2.2	Probable 30s ribosomal protein	Information pathways
Rv0718	*rpsH*	-2.2	30s ribosomal protein	Information pathways
Rv0009	*ppiA*	-2.3	Probable iron regulated protein	Information pathways
Rv0714	*rplN*	-2.3	Probable 50s ribosomal protein	Information pathways
Rv0652	*rplL*	-2.5	Probable 50s ribosomal protein	Information pathways
Rv2412	*rpsT*	-2.5	Probable 30s ribosomal protein	Information pathways
Rv0701	*rpsC*	-2.6	Probable 50s ribosomal protein	Information pathways
Rv0667	*rpoB*	-1.8	DNA directed RNA polymerase	Information pathways
Rv0706	*rplV*	-1.9	Probable 50s ribosomal protein	Information pathways
Rv2890c	*rpsB*	-2.0	Probable ribosomal protein	Information pathways
Rv2710	*SigB*	3.1	RNA Polymerase sigma factor B	Information pathways
Rv1221	*SigE*	2.3	alternate RNA Polymerase sigma factor E	Information pathways

3.3.3 Validation by RT-qPCR

We validated by quantitative RT-PCR, the DNA array data for selected *M. tuberculosis* genes that were found to be differentially expressed by F1082. The RNA used was the same as was used in microarray analysis. RT-qPCR confirmed that these were induced, to a level 2 to 10 times above control and genes that were down-regulated were similarly suppressed (Figure 3.4). The expression values of the genes from microarray in Table 3.6 were compared with expression values from quantitative RT-qPCR (B). The expression of each gene in every condition has been normalised to the expression of the reference gene 16S rRNA. Induction is expressed as ± standard deviation (error bars) of the ratios from three biological replicates. The induction levels as measured by RT-qPCR were generally higher than those observed using DNA microarray, probably due to greater sensitivity and dynamic range achievable using quantitative PCR technique rather than two-color microarrays.This was most apparent with genes Rv3159 to Rv3161, for which induction levels measured using RT-qPCR were up to 30 times higher than those observed using microarray.

Table 3.6 *M. tuberculosis* genes selected from microarray data for qPCR validation

F1082 (64 µg/ml) Gene	Rv3159c	Rv3160c	Rv3161c	Rv0676c	Rv2358	Rv2190c	Rv0652	Rv2246	Rv3804c	Rv1094	Rv0724
Fold change (4 hours)	8.3 ± 1.2	16.1 ± 0.2	23.6 ± 0.6	3.8 ± 0.5	2.3 ± 0.9	-3.6 ± 1.3	-2.3 ± 0.9	-1.7 ± 0.7	-2.1 ± 1.5	-1.8 ± 0.8	2.3 ± 0.9
Fold change (24 hours)	6.7 ± 0.9	7.5 ± 0.5	16.9 ± 0.8	3 ± 0.7	2.4 ± 1.4	-4 ± 0.8	-2.8 ± 1.5	-2.9 ± 0.9	-2.2 ± 0.5	-2.9 ± 0.6	2 ± 1.2

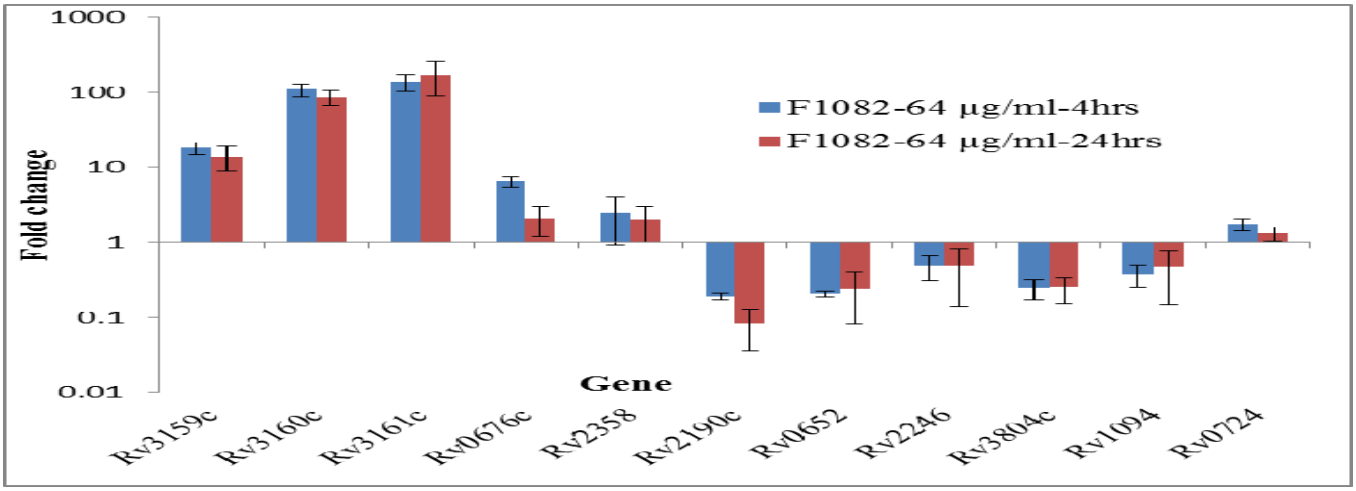

Figure 3.4 Validation of *M. tuberculosis* genes expression by quantitative RT-PC. Fold induction is expressed as means ± standard deviations (error bars) of the ratios from three biological replicates.

Summary

We used microarray to examine the effect of F1082 on *M. tuberculosis* growth. This has provided a gene signature expression profile of INH and F1082 from which the pathways involved in their activities can be drawn. As have been mentioned from our results that we were able to reproduce the gene signature profile of IHN, the FAS II operon induction. In conclusion, although F1082 has affected quite a number of genes including upregulation of the efflux pump for detoxification of

antibiotics, it appears that the iron acquisition pathway has been greatly affected by the low concentration (8µg/ml) and high concentration (64 µg/ml). The induction of efflux detoxication genes such Rv3159-3161did not attrct much of our attention as these genes are upregulated by most aromatic compounds. Our interest was more into genes that are coordinately regulated, the *mbt* cluster of the genes and other genes that are involved in iron macquisition and storage.This prompted us to look at the role of iron in *M. tuberculosis* and iron acquisition and regulation as controlled by the IdeR. It has been postulated that the up-regulation of the siderophore biosynthetic genes in activated macrophages is not only by low intracellular iron condition but also by inactivation of IdeR (Schnappinger *et al*., 2003). In the next chapter we investigate the putative role of F1082 in upregulation of the iron acquisition genes and possible mechanism of action of this compound.

Appendix 3A

Probe Preparation/Hybridization Using TB RNA and Random Primers

Synthesis and Labeling of cDNA

Bring 1.5µg of RNA to a volume of 11µl (in a PCR tube) with nucleotide-free water and add 2.2µl (2mg/ml) random primers (pulse centrifugation to collect contents).

Heat for 2 minutes at 98°C, snap cool on ice.

(Keep on ice) and add 11.1µl of the following reaction mix:

5.0µl 5X First-Strand buffer

2.5µl 100 mM DTT

2.3µl low dTdNTP mix (5mM A,G,C and 0.2 mM T stock)

1.5ul Cy3 or Cy5

Then add 1.2ul Superscript, vortex to mix and spin to collect contents

Incubate 10 min at 25°C followed by 90 min at 42°C in PCR machine.

**Can freeze or leave at 4°C overnight if necessary

Prime a microcon10 column (YM10 from Millipore) with 400µl TE and centrifuge for 10 min at 10,000 x g. Empty flow-through in collection tube and return primed column. Add both reactions (cy3 and cy5) to column and centrifuge at 10,000 x g until ~25µl remaining (~20-30 min). Wash with 200µl TE and spin until almost dry (<5µl).

Recover cDNA by inverting microcon into new collection 1.5 ml tube and centrifuge at half max speed 1 min.

Bring sample to 5µl with TE.

Prehybridization

1. Prepare Pre-hybridization Solution (Fresh Each Time)

**this volume is based on a glass dish with a base measurement of 11x8cm. This dish allows for a pre-hybridization of 1-4 slides. Adjust volume accordingly based on size of dish and/or number of slides.

106.0ml dH2O

3.0g BSA

1.2ml 10%SDS

Add Prehybridization solution to a glass slide-staining dish and place post-processed slides array side up into solution. Make sure there are no bubbles on the surfaces of the slides.

Place the staining jar containing the Prehybridization solution and slides into a water bath and hybridize for 1 hour at 42^{o}C.

Take the prehybridized slides out of the Prehybridization solution and place into a slide holder submerged in a slide-washing tray containing nuclease-free water. Wash slides for 2 minutes with constant shaking up and down.

Transfer slide rack to a slide washing tray containing isopropanol and wash for 2 minutes with constant shaking up and down.

Take the slides in the isopropanol bath to the centrifuge to keep the slides wet until you can dry them rapidly. Centrifuge at 600 rpm in a 50 ml conical flask for 3 minutes to dry.

**Complete this step within one hour of hybridization

Hybridization

Add the following to the 5µl labeled cDNAsample.

0.5µl 10 mg/ml tRNA

1.0µl 20X SSC

2.5ul Formamide

1.0µl 1% SDS

Heat to 98 ^{o}C for 2 minutes. Spin in centrifuge for 1 min at 12,000 Xg. Let cool for 5 min.

Pipette cooled 10µl hybridization solution on microarray. Apply 22 x 22 coverslip to cover array (if bubbles appear under the cover slip, they will slowly migrate to the edges provided that the volume is accurate).

Optional: Apply thin wall of rubber cement around the 4 corners of the coverslip to avoid movement. This step is recommended if water bath is not perfectly level.

Hybridize in standard hybridization chambers with ~40 µl water under each slide (20 ul under both ends of each slide) overnight in 50^{o}C water bath

**Bubbles (especially large ones) can be troublesome for arrays since they can cause areas of non-hybridization. To avoid bubbles, do not use the blowout feature of the pipette when adding the probe to the slide. Also, clean your coverslips with alcohol and lint-free wipes before placing over probe.

IV. Post Hybridization washes (next day)

Remove cover slip while array is submerged in first wash solution (2XSSC + 0.1% SDS), transfer to submerged microscope slide staining racks and rinse for 1 min in 1X SSC+0.05% SDS with agitation/shaking.

Rinse in 0.06X SSC with shaking. Transfer to another submerged staining rack and wash 2 min in fresh 0.06X SSC with gentle shaking.

Centrifuge 3 min at 1000 rpm in a 50 ml conical flask (array edge up) to dry. Scan immediately.

V. Reagents

Name	Stock Concentration	Source	Catalog #
Random Hexamers	2.0ug/ul	IDT	Custom oligos
5X First-Strand Buffer	From Kit	Invitrogen	Superscript Kit: 18064-014
0.1M DTT	From Kit	Invitrogen	Superscript Kit: 18064-014
Superscript II RT	From Kit	Invitrogen	Superscript Kit: 18064-014
Low dTdNTP mix 5mM A,G,C and 0.2mM T	100mM (each)	Invitrogen	10297-018
Cyanine 3-dUTP	25nmol/25ul	Perkinelmer	NEL578
Cyanine 5-dUTP	25nmol/25ul	Perkinelmer	NEL579
Milipore YM10 Microcon centrifugal columns		Fisher	42406
TE	TE pH8.0	Ambion	9849
BSA	BSA Fraction V, heat shock 50g	Roche	100360
SDS	10%	Ambion	9822
Isopropanol	99+%	Sigma	I-9516

Name	Stock Concentration	Source	Catalog #
tRNA		Invitrogen	15401011
20X SSC		Ambion	9763
Formamide		Sigma	F-9037
Corning coverslips (22x22)		Fisher	12-524B

Appendix 3B

A list of all *M. tuberculosis* genes expressed under F1082 treatment

1. *M. tuberculosis* gene regulated by 8 µg/ml for both time points (4 & 24 hours) of post inoculation. Significance Analysis of microarray was used for each concentration and time point each performed in triplicate. Av: average; FC: fold change; STDEV: Standard deviation.

	ID	Gene name	Function	Category	Av/FC	STDEV
1	Rv2020c	*esxS*	ESAT-6 LIKE PROTEIN	Cell wall and cell processes	2.093953	0.179233
2	Rv3402c	Rv3402c	CONSERVED HYPOTHETICAL PROTEIN	Cell wall and cell processes	2.012823	0.521572
3	Rv0431	Rv0431	PUTATIVE TUBERCULIN RELATED PROTEIN	Cell wall and cell processes	-0.86101	0.927315
4	Rv3524	Rv3524	PUTATIVE CONSERVED MEMBRANE PROTEIN	Cell wall and cell processes	-1.48663	1.212765
5	Rv3839	Rv3839	CONSERVED HYPOTHETICAL PROTEIN	Conserved hypotheticals	2.518153	0.924702
6	Rv1057	Rv1057	CONSERVED HYPOTHETICAL PROTEIN	Conserved hypotheticals	1.425914	1.858394
7	Rv1813c	Rv1813c	CONSERVED HYPOTHETICAL PROTEIN	Conserved hypotheticals	-1.95528	2.792233
8	Rv2710	*SigB*	RNA POLYMERASE SIGMA FACTOR B	Information pathways	2.715585	1.952806
9	Rv1221	*SigE*	ALTERNATE RNA POLYMERASE SIGMA FACTOR E	Information pathways	1.496848	1.227774
10	Rv3161c	Rv3161c	POSSIBLE DEOXYGENASE	Intermediary metabolism and respiration	27.54526	24.38284
11	Rv2122	*IrgL*	PROBABLE PHOSPHO-RIBOSYL-AMP PYROPHOSPHATASE	Intermediary metabolism and respiration	2.428293	0.920567
12	Rv3841	*BfrB*	POSSIBLE BACTERIOFERRITIN	Intermediary metabolism and respiration	-1.57729	1.304538
13	Rv2382c	*MbtC*	POLYPEPTIDE SYNTHASE	Lipid metabolism	3.20911	1.288678
14	Rv2380c	*MbtE*	POLYPEPTIDE SYNTHASE (MYCOBACTIN)	Lipid metabolism	2.981983	1.070068
15	Rv2381c	*MbtD*	POLYKETIDE SYNTHASE	Lipid metabolism	2.433865	0.597357
16	Rv2377c	*MbtH*	PUTATIVE CONSERVED PROTEIN	Lipid metabolism	2.169838	0.464288
17	Rv2383c	*MbtB*	PHENYLOXAZOLINE SYNTHASE	Lipid metabolism	1.71465	0.135848
18	Rv2386c	*MbtI*	PUTATIVE ISOCHORISMATE SYNTHASE	Lipid metabolism	1.3324	1.045023

	ID	*Gene name*	Function	Category	Av/FC	STDEV
19	Rv3252	*alkB*	PROBABLE ALKANE-1-MONOOXYGENASE	Lipid metabolism	-0.06073	1.235364
20	Rv3159c	Rv3159c	PPE FAMILY PROTEIN	PE/PPE	10.93322	5.072333
21	Rv0280	*PPE*	PE-PPE FAMILY PROTEIN	PE/PPE	-2.01427	0.461642
22	Rv1387	Rv1387	PPE20-PPE FAMILY PROTEIN	PE/PPE	-2.16936	0.515985
23	Rv1386	Rv1386	PE FAMILY PROTEIN	PE/PPE	-3.62666	1.281864
24	Rv3160c	Rv3160c	POSSIBLE "TET R" FAMILY TRANSCRIPTIONAL REGULATORY PROTEIN	Regulatory protein	30.76966	30.33673
25	Rv3269	Rv3269	CONSERVED HYPOTHETICAL PROTEIN	Virulence, detoxification, adaptation	1.778381	1.22058

2. *M. tuberculosis* gene regulated by F1082 (64 μg/ml at 4 hours) of post inoculation

	ID	Gene name	Function	Category	AV/FC	STDEV
1	Rv0227c	Rv0227c	UNKNOWN	Cell wall and cell processes	-2.14486	0.253084
2	Rv0418	*lpqL*	UNKNOWN; HYDROLYZES PEPTIDES AND/OR PROTEINS	Cell wall and cell processes	-1.84473	0.231635
3	Rv0559c	Rv0559c	POSSIBLE CONSERVED SECRETED PROTEIN	Cell wall and cell processes	1.740238	0.222031
4	Rv0676c	*mmpL5*	UNKNOWN. THOUGHT TO BE INVOLVED IN FATTY ACID TRANSPORT	Cell wall and cell processes	3.247001	2.090757
5	Rv0677c	*mmpS5*	UNKNOWN.	Cell wall and cell processes	5.34875	2.30678
6	Rv0821c	*phoY2*	INVOLVED IN TRANSCRIPTIONAL REGULATION OF ACTIVE TRANSPORT OF INORGANIC PHOSPHATE ACROSS THE MEMBRANE	Cell wall and cell processes	1.663298	0.107193
7	Rv0847	*lpqS*	PROBABLE LIPOPROTEIN LPQS	Cell wall and cell processes	1.905438	0.297441

	ID	Gene name	Function	Category	AV/FC	STDEV
8	Rv0867c	*rpfA*	MAY BE PROMOTE THE RESUSCITATION AND GROWTH OF DORMANT, NONGROWING CELL.	Cell wall and cell processes	-2.11903	0.174592
9	Rv1037c	*exsI*	UNKNOWN	Cell wall and cell processes	-1.70708	0.147981
10	Rv1072	Rv1072	UNKNOWN	Cell wall and cell processes	2.447351	0.470731
11	Rv1411c	*lprG*	UNKNOWN	Cell wall and cell processes	1.782393	0.267503
12	Rv1614	*lgt*	PROLIPOPROTEIN MODIFICATION	Cell wall and cell processes	-2.04061	0.281786
13	Rv1857	*modA*	PROBABLE MOLYBDATE-BINDING LIPOPROTEIN MODA	Cell wall and cell processes	-1.87352	0.091365
14	Rv2053c	Rv2053c	PROBABLE TRANSMEMBRANE PROTEIN	Cell wall and cell processes	2.083238	0.259944
15	Rv2091c	Rv2091c	UNKNOWN	Cell wall and cell processes	2.17082	0.548018
16	Rv2115c	Rv2115c	UNKNOWN. Involved in protection against reactive nitrogen intermediates	Cell wall and cell processes	2.334079	0.423334
17	Rv2272	Rv2272	UNKNOWN	Cell wall and cell processes	-1.75163	0.18104
18	Rv2450c	*rpfE*	PROBABLE RESUSCITATION-PROMOTING FACTOR RPFE	Cell wall and cell processes	-3.60328	1.011716
19	Rv2743c	Rv2743c	UNKNOWN	Cell wall and cell processes	2.526051	0.640498
20	Rv3006	*lppZ*	UNKNOWN	Cell wall and cell processes	1.761933	0.221079
21	Rv3036c	*TB22.2*	PROBABLE CONSERVED SECRETED PROTEIN TB22.2	Cell wall and cell processes	1.856761	0.132504

	ID	Gene name	Function	Category	AV/FC	STDEV
22	Rv3197	Rv3197	PROBABLE CONSERVED ATP-BINDING PROTEIN ABC TRANSPORTER	Cell wall and cell processes	2.279493	0.237291
23	Rv3524	Rv3524	UNKNOWN	Cell wall and cell processes	-2.13909	0.614227
24	Rv0057	Rv0057	UNKNOWN	Conserved hypotheticals	-2.02752	0.204432
25	Rv0164	TB18.5	UNKNOWN	Conserved hypotheticals	-1.96143	0.121362
26	Rv0250c	Rv0250c	UNKNOWN. POSSIBLY DOWN-REGULATED BY HSPR	Conserved hypotheticals	1.943959	0.225218
27	Rv0293c	Rv0293c	UNKNOWN	Conserved hypotheticals	2.163719	0.266863
28	Rv0313	Rv0313	UNKNOWN	Conserved hypotheticals	1.84183	0.27179
29	Rv0466	Rv0466	UNKNOWN	Conserved hypotheticals	-2.01962	0.399045
30	Rv0516c	Rv0516c	UNKNOWN	Conserved hypotheticals	2.539985	0.897858
31	Rv0635	Rv0635	FUNCTION UNKNOWN	Conserved hypotheticals	-1.94149	0.239289
32	Rv0678	Rv0678	UNKNOWN	Conserved hypotheticals	2.44694	1.064667
33	Rv0724	Rv0724A	UNKNOWN	Conserved hypotheticals	2.171285	0.425157
34	Rv0898c	Rv0898c	UNKNOWN	Conserved hypotheticals	2.432205	1.444775
35	Rv0937c	Rv0937c	UNKNOWN	Conserved hypotheticals	1.549623	0.036306
36	Rv1057	Rv1057	UNKNOWN	Conserved hypotheticals	3.914258	0.93924
37	Rv1059	Rv1059	UNKNOWN	Conserved hypotheticals	1.784418	0.219353
38	Rv1130	Rv1130	UNKNOWN	Conserved hypotheticals	2.905394	0.535371
39	Rv1331	Rv1331	UNKNOWN	Conserved hypotheticals	1.900691	0.262327
40	Rv1592c	Rv1592c	UNKNOWN	Conserved hypotheticals	-2.83567	0.773827
41	Rv1709	Rv1709	UNKNOWN	Conserved hypotheticals	-1.75427	0.115468
42	Rv2050	Rv2050	UNKNOWN	Conserved hypotheticals	2.165823	0.384023
43	Rv2052c	Rv2052c	UNKNOWN	Conserved hypotheticals	4.461768	2.767002
44	Rv2405	Rv2405	UNKNOWN	Conserved hypotheticals	1.988194	0.344172

	ID	Gene name	Function	Category	AV/FC	STDEV
45	Rv2627c	Rv2627c	UNKNOWN	Conserved hypotheticals	-1.65633	0.157207
46	Rv2641	*cadI*	UNKNOWN	Conserved hypotheticals	2.108186	0.146417
47	Rv2694c	Rv2694c	UNKNOWN	Conserved hypotheticals	3.400801	1.098051
48	Rv2744c	35kd ag	CONSERVED 35 KDA ALANINE RICH PROTEIN	Conserved hypotheticals	3.895726	1.191273
49	Rv2747	Rv2747	GCN5-RELATED N-ACETYLTRANSFERASE	Conserved hypotheticals	1.74522	0.25303
50	Rv3412	Rv3412	UNKNOWN	Conserved hypotheticals	1.744778	0.211103
51	Rv3747	Rv3747	UNKNOWN	Conserved hypotheticals	-2.73691	0.915266
52	Rv3748	Rv3748	UNKNOWN	Conserved hypotheticals	-2.1328	0.586852
53	Rv3822	Rv3822	UNKNOWN	Conserved hypotheticals	1.600105	0.014313
54	Rv0430	Rv0430	UNKNOWN	Conserved hypotheticals	-1.99441	0.509638
55	Rv0009	*ppiA*	PPIASES ACCELERATE THE FOLDING OF PROTEINS	Information pathways	-2.41061	0.221555
56	Rv0053	*rspF*	BINDS TOGETHER WITH S18 TO 16S RIBOSOMAL RNA.	Information pathways	-2.46591	0.29265
57	Rv0055	*rpsR1*	TRANSFER RNA BINDING. IT APPEARS TO BE SITUATED AT THE DECODING SITE OF MESSENGER RNA.	Information pathways	-1.97819	0.485315
58	Rv0056	*rsplI*	BINDS TO THE 23S RRNA.	Information pathways	-2.04093	0.346984
59	Rv0652	*rplL*	PROBABLE 50S RIBOSOMAL PROTEIN L7/L12 RPLL (SA1)	Information pathways	-2.33791	0.195555
60	Rv0667	*rpoB*	DNA-DIRECTED RNA POLYMERASE (BETA CHAIN) RPOB	Information pathways	-1.96706	0.325744
61	Rv0683	*rpsG*	PROTEIN S7 BINDS SPECIFICALLY TO PART OF THE 3' END OF 16S RIBOSOMAL RNA	Information pathways	-1.70907	0.102503
62	Rv0700	*rpsJ*	30S RIBOSOMAL PROTEIN S10 RPSJ (TRANSCRIPTION ANTITERMINATION FACTOR NUSE	Information pathways	-2.22706	0.331334
63	Rv0701	*rplC*	PROBABLE 50S RIBOSOMAL PROTEIN L3 RPLC	Information pathways	-2.8227	0.338625
64	Rv0702	*rplD*	PROBABLE 50S RIBOSOMAL PROTEIN L4 RPLD	Information pathways	-1.99993	0.210684
65	Rv0703	*rplW*	PROBABLE 50S RIBOSOMAL PROTEIN L23 RPLW	Information pathways	-2.44792	0.251863
66	Rv0704	*rplB*	PROBABLE 50S ribosomal protein L2 RPLB	Information pathways	-2.15861	0.248816
67	Rv0705	*rpsS*	PROTEIN S19 FORMS A COMPLEX WITH S13 THAT BINDS STRONGLY TO THE 16S RIBOSOMAL RNA	Information pathways	-2.57109	0.527435

	ID	Gene name	Function	Category	AV/FC	STDEV
68	Rv0706	*rplV*	PROBABLE 50S RIBOSOMAL PROTEIN L22 RPLV	Information pathways	-1.95896	0.415036
69	Rv0707	*rpsC*	PROBABLE 30S RIBOSOMAL PROTEIN S3 RPSC	Information pathways	-2.58143	0.344279
70	Rv0708	*rplP*	PROBABLE 50S RIBOSOMAL PROTEIN L16 RPLP	Information pathways	-1.81911	0.136984
71	Rv0709	*rpmC*	PROBABLE 50S RIBOSOMAL PROTEIN L29 RPMC	Information pathways	-2.19868	0.319817
72	Rv0714	*rplN*	PROBABLE 50S RIBOSOMAL PROTEIN L14 RPLN	Information pathways	-1.96694	0.448699
73	Rv0715	*rplX*	PROBABLE 50S RIBOSOMAL PROTEIN L24 RPLX	Information pathways	-2.11051	0.294595
74	Rv0718	*rpsH*	PROBABLE 30S RIBOSOMAL PROTEIN S8 RPSH	Information pathways	-2.1371	0.498698
75	Rv0721	*rpsE*	PROBABLE 30S RIBOSOMAL PROTEIN S5 RPSE	Information pathways	-1.88354	0.247095
76	Rv0722	*rpmD*	PROBABLE 50S RIBOSOMAL PROTEIN L30 RPMD	Information pathways	-1.59247	0.067732
77	Rv0723	*rplO*	PROBABLE 50S RIBOSOMAL PROTEIN L15 RPLO	Information pathways	-1.9892	0.227835
78	Rv1221	*sigE*	ALTERNATIVE RNA POLYMERASE SIGMA FACTOR SIGE	Information pathways	1.80489	0.36104
79	Rv1298	*rpmE*	INVOLVED IN TRANSLATION	Information pathways	-1.60805	0.069438
80	Rv1630	*rspA*	PROBABLE RIBOSOMAL PROTEIN S1 RPSA	Information pathways	-1.80495	0.266426
81	Rv2069	*sigC*	INVOLVED IN PROMOTER RECOGNITION, TRANSCRIPTION INITIATION.	Information pathways	-1.73223	0.172544
82	Rv2412	*rpsT*	PROBABLE 30S RIBOSOMAL PROTEIN S20 RPST	Information pathways	-2.70561	1.000659
83	Rv2710	*sigB*	RNA POLYMERASE SIGMA FACTOR SIGB	Information pathways	2.877154	0.655779
84	Rv2841c	*nusA*	PROBABLE N UTILIZATION SUBSTANCE PROTEIN A NUSA	Information pathways	1.918749	0.223708
85	Rv2890c	*rspB*	PROBABLE 30S RIBOSOMAL PROTEIN S2 RPSB	Information pathways	-1.85639	0.272286
86	Rv3442c	*rpsI*	PROBABLE 30S RIBOSOMAL PROTEIN S9 RPSI	Information pathways	-2.10591	0.779982
87	Rv3443c	*rplM*	PROBABLE 50S RIBOSOMAL PROTEIN L13 RPLM	Information pathways	-2.13444	0.349073
88	Rv3457c	*rpoA*	PROBABLE DNA-DIRECTED RNA POLYMERASE (ALPHA CHAIN) RPOA	Information pathways	-2.00649	0.307426
89	Rv3458c	*rpsD*	PROBABLE 30S RIBOSOMAL PROTEIN S4 RPSD	Information pathways	-1.67463	0.119311
90	Rv3460c	*rpsM*	PROBABLE 30S RIBOSOMAL PROTEIN S13 RPSM	Information pathways	-2.15981	0.339098
91	Rv3462c	*infA*	PROBABLE TRANSLATION INITIATION FACTOR IF-1 INFA	Information pathways	-1.84949	0.272725
92	Rv3598c	*lysS*	LYSYL-TRNA SYNTHETASE 1 LYSS	Information pathways	-1.76318	0.173022
93	Rv3646c	*topA*	DNA TOPOISOMERASE I TOPA	Information pathways	-1.77926	0.137459

	ID	Gene name	Function	Category	AV/FC	STDEV
94	Rv3923c	*rnpA*	RIBONUCLEASE P PROTEIN COMPONENT RNPA	Information pathways	-1.84334	0.114949
95	Rv0717	*rpsN1*	PROBABLE 30S RIBOSOMAL PROTEIN S14 RPSN1	Information pathways	-1.72332	0.165787
96	Rv1945	Rv1945	UNKNOWN	Insertion seqs and phages	2.164855	0.545776
97	Rv0077c	Rv0077c	UNKNOWN; PROBABLY INVOLVED IN CELLULAR METABOLISM	Intermediary metabolism and respiration	7.40796	4.82858
98	Rv0155	*pntAa*	FUNCTIONS AS A PROTON PUMP ACROSS THE MEMBRANE	Intermediary metabolism and respiration	-2.22465	0.20165
99	Rv0315	*Rv0315*	INVOLVED IN EXOPOLYSACCHARIDE BIOSYNTHESIS/DEGRADATION	Intermediary metabolism and respiration	-4.00494	1.191568
100	Rv0317c	*glpQ2*	POSSIBLE GLYCEROPHOSPHORYL DIESTER PHOSPHODIESTERASE GLPQ2	Intermediary metabolism and respiration	-1.60156	0.074614
101	Rv0462	*lpdC*	NVOLVED IN ENERGY METABOLISM	Intermediary metabolism and respiration	-1.77957	0.172944
102	Rv0467	*icl*	INVOLVED IN GLYOXYLATE BYPASS (AT THE FIRST STEP), AN ALTERNATIVE TO THE TRICARBOXYLIC ACID CYCLE	Intermediary metabolism and respiration	1.249717	1.207101
103	Rv0510	*hemC*	INVOLVED IN PORPHYRIN BIOSYNTHESIS BY THE C5 PATHWAY	Intermediary metabolism and respiration	-1.94294	0.347216
104	Rv0560c	Rv0560c	POSSIBLE BENZOQUINONE METHYLTRANSFERASE (METHYLASE)	Intermediary metabolism and respiration	8.608646	5.363083
105	Rv0636	Rv0636	UNKNOWN	Intermediary metabolism and respiration	-1.68351	0.117666

	ID	Gene name	Function	Category	AV/FC	STDEV
106	Rv0848	*cysK2*	POSSIBLE CYSTEINE SYNTHASE A CYSK2	Intermediary metabolism and respiration	2.280215	0.667022
107	Rv0897c	Rv0897c	UNKNOWN; PROBABLY INVOLVED IN CELLULAR METABOLISM.	Intermediary metabolism and respiration	1.743603	0.174047
108	Rv1131	*gltA1*	INVOLVED IN TRICARBOXYLIC ACID CYCLE (KREBS CYCLE) [CATALYTIC ACTIVITY	Intermediary metabolism and respiration	4.05827	0.831812
109	Rv1304	*atpB*	PROBABLE ATP SYNTHASE A CHAIN ATPB (PROTEIN 6)	Intermediary metabolism and respiration	-1.88764	0.26711
110	Rv1307	*atpH*	PROBABLE ATP SYNTHASE DELTA CHAIN ATPH	Intermediary metabolism and respiration	-1.87421	0.396862
111	Rv1471	*trxB*	PROBABLE THIOREDOXIN TRXB1	Intermediary metabolism and respiration	2.123795	0.233627
112	Rv1475c	*can*	INVOLVED IN TRICARBOXYLIC ACID CYCLE [CATALYTIC ACTIVITY	Intermediary metabolism and respiration	-1.74941	0.228654
113	Rv1497	*lipL*	PROBABLE ESTERASE LIPL	Intermediary metabolism and respiration	2.44596	0.516323
114	Rv1611	*trpC*	PROBABLE INDOLE-3-GLYCERON PHOSPHATE SYNTHASE trpC	Intermediary metabolism and respiration	-1.72631	0.108178
115	Rv1612	*trpB*	PROBABLE TRYPTOPHAN SYNTHASE, BETA SUBUNIT trpB	Intermediary metabolism and respiration	-2.18738	0.435589

	ID	Gene name	Function	Category	AV/FC	STDEV
116	Rv1613	*trpA*	PROBABLE TRYPTOPHAN SYNTHASE, ALPHA SUBUNIT trpA	Intermediary metabolism and respiration	-1.83088	0.172585
117	Rv1855c	Rv1855c	POSSIBLE OXIDOREDUCTASE	Intermediary metabolism and respiration	1.558758	0.037439
118	Rv2043c	*pncA*	CONSERVED AMIDES SUCH AS NICOTINAMIDE TO CORRESPONDING ACID	Intermediary metabolism and respiration	1.903435	0.324548
119	Rv2211c	*gcvT*	PROBABLE ANIMOMETHYLTRANSFERASE GcvT	Intermediary metabolism and respiration	-2.07647	0.380197
120	Rv2220	*glnA1*	GLUTAMINE SYNTHETASE GLNA1 (GLUTAMINE SYNTHASE) (GS-I)	Intermediary metabolism and respiration	-2.04807	0.502865
121	Rv2460c	clpP2	PROBABLE ATP-DEPENDENT CLP PROTEASE PROTEOLYTIC SUBUNIT 2 CLPP2	Intermediary metabolism and respiration	2.623966	0.669298
122	Rv2952	Rv2952	THOUGHT TO CAUSE METHYLATION	Intermediary metabolism and respiration	-2.05237	0.256055
123	Rv2958c	Rv2958c	POSSIBLE GLYCOSYL TRANSFERASE	Intermediary metabolism and respiration	-1.93967	0.379021
124	Rv2959c	Rv2959c	THOUGHT TO CAUSE METHYLATION	Intermediary metabolism and respiration	-2.7926	0.851517
125	Rv2987c	*leuD*	PROBABLE 3-ISOPROPYLMALATE DEHYDRATASE (SMALL SUBUNIT)	Intermediary metabolism and respiration	-2.17163	0.405632

	ID	Gene name	Function	Category	AV/FC	STDEV
126	Rv2988c	*leuC*	PROBABLE 3-ISOPROPYLMALATE DEHYDRATASE (LARGE SUBUNIT) LEUC	Intermediary metabolism and respiration	-1.87118	0.192825
127	Rv3002c	*ilvN*	PROBABLE ACETOLACTATE SYNTHASE (SMALL SUBUNIT) ILVN	Intermediary metabolism and respiration	-2.13677	0.509705
128	Rv3161c	Rv3161c	POSSIBLE DIOXYGENASE	Intermediary metabolism and respiration	25.49128	26.30773
129	Rv3837c	Rv3837c	PROBABLE PHOSPHOGLYCERATE MUTASE	Intermediary metabolism and respiration	1.891065	0.373739
130	Rv0129c	*fbpC*	SECRETED ANTIGEN 85-C FBPC (85C) (ANTIGEN 85 COMPLEX C) (AG58C) (MYCOLYL TRANSFERASE 85C)	Lipid metabolism	1.7287	0.179517
131	Rv0243	*fadA2*	FUNCTION UNKNOWN, BUT INVOLVED IN LIPID DEGRADATION	Lipid metabolism	1.847155	0.142639
132	Rv0270	*fadD2*	FUNCTION UNKNOWN, BUT INVOLVED IN LIPID DEGRADATION	Lipid metabolism	1.619445	0.081922
133	Rv0468	*fadB2*	BUTYRATE/BUTANOL-PRODUCING PATHWAY [CATALYTIC ACTIVITY	Lipid metabolism	1.753015	0.305655
134	Rv0642c	*mmaA4*	METHOXY MYCOLIC ACID SYNTHASE 4 MMAA4 (METHYL MYCOLIC ACID SYNTHASE	Lipid metabolism	-1.7029	0.127587
135	Rv0643c	*mmaA3*	METHOXY MYCOLIC ACID SYNTHASE 3 MMAA3 (METHYL MYCOLIC ACID SYNTHASE	Lipid metabolism	-1.98273	0.345851
136	Rv0947c	Rv0947c	FUNCTION UNKNOWN; THOUGHT TO BE INVOLVED IN MYCOLIC ACID BIOSYNTHESIS	Lipid metabolism	-2.09224	0.607665
137	Rv1094	*desA2*	POSSIBLE ACYL-[ACYL-CARRIER PROTEIN] DESATURASE DESA2	Lipid metabolism	-1.7626	0.149297
138	Rv1665	*pks11*	POSSIBLE CHALCONE SYNTHASE PKS11	Lipid metabolism	-1.86442	0.317725
139	Rv1886c	*fbpB*	SECRETED ANTIGEN 85-B FBPB (85B) (ANTIGEN 85 COMPLEX B) (MYCOLYL	Lipid metabolism	-3.13589	1.304213
140	Rv2243	*fadD2*	CATALYZES MALONYL-COA-ACP TRANSACYLASE (MCAT) ACTIVITY USING HOLO-ACPM AS SUBSTRATE FOR TRANSACYLATION	Lipid metabolism	-2.06329	0.567616
141	Rv2246	*kasB*	3-OXOACYL-[ACYL-CARRIER PROTEIN] SYNTHASE 2	Lipid metabolism	-1.62817	0.138421

	ID	Gene name	Function	Category	AV/FC	STDEV
142	Rv2500c	*fadE19*	POSSIBLE ACYL-CoA DEHYDROGENASE FADE19 (MMGC)	Lipid metabolism	1.979723	0.227066
143	Rv2947c	*pks15*	POLYKETIDE SYNTHASE POSSIBLY INVOLVED IN LIPID SYNTHESIS	Lipid metabolism	-1.76768	0.256155
144	Rv2950c	*fadD29*	FUNCTION UNKNOWN, BUT INVOLVED IN LIPID DEGRADATION	Lipid metabolism	-1.83998	0.330412
145	Rv3804c	*fbpA*	SECRETED ANTIGEN 85-A FBPA	Lipid metabolism	-2.09282	0.238717
146	Rv3825c	*pks2*	PROBABLE POLYKETIDE SYNTHASE PKS2	Lipid metabolism	1.785388	0.112709
147	Rv1386	*PE15*	UNKNOWN	PE/PPE	-1.88178	0.225971
148	Rv1806	*PE20*	PE FAMILY PROTEIN	PE/PPE	2.140563	0.746306
149	Rv2431c	*PE25*	UNKNOWN	PE/PPE	-2.03352	0.293417
150	Rv3159c	*PPe53*	UNKNOWN	PE/PPE	8.920608	8.033187
151	Rv0872c	*PE PGRS15*	UNKNOWN	PE/PPE)	2.752313	1.076616
152	Rv0078	Rv0078	POSSIBLY INVOLVED IN TRANSCRIPTIONAL MECHANISM	Regulatory proteins	1.9027	0.269015
153	Rv1129c	Rv1129c	INVOLVED IN TRANSCRIPTIONAL MECHANISM	Regulatory proteins	1.938548	0.36358
154	Rv2358	Rv2358	INVOLVED IN TRANSCRIPTIONAL MECHANISM	Regulatory proteins	2.258721	0.615515
155	Rv2359	*furB*	PROBABLE FERRIC UPTAKE REGULATION PROTEIN FURB	Regulatory proteins	1.943689	0.256762
156	Rv2745c	Rv2745c	POSSIBLY INVOLVED IN TRANSCRIPTIONAL MECHANISM	Regulatory proteins	4.144364	1.557585
157	Rv3160c	Rv3160c	POSSIBLY INVOLVED IN TRANSCRIPTIONAL MECHANISM	Regulatory proteins	16.87395	11.10883
158	Rv0251c	*hsp*	RIBOSOMAL SUBUNIT. POSSIBLY A MOLECULAR CHAPERONE	Virulence, detoxification, adaptation	2.355203	0.800261
159	Rv0440	*groEl2*	PREVENTS MISFOLDING AND PROMOTES THE REFOLDING AND PROPER ASSEMBLY OF POLYPEPTIDES UNDER STRESS.	Virulence, detoxification, adaptation	-2.19329	0.473026
160	Rv0563	*htpX*	PROBABLE PROTEASE TRANSMEMBRANE PROTEIN HEAT SHOCK PROTEIN HTPX	Virulence, detoxification, adaptation	3.804163	0.948096

	ID	Gene name	Function	Category	AV/FC	STDEV
161	Rv1932	*tpx*	HAS ANTIOXIDANT ACTIVITY. COULD REMOVE PEROXIDES OR H(2)O(2)	Virulence, detoxification, adaptation	-1.69969	0.137077
162	Rv2190c	Rv2190c	UNKNOWN	Virulence, detoxification, adaptation	-3.60516	0.41591
163	Rv2428	*ahpC*	ALKYL HYDROPEROXIDE REDUCTASE C PROTEIN AHPC	Virulence, detoxification, adaptation	-3.47518	1.485351
164	Rv3269	Rv3269	CONSERVED HYPOTHETICAL PROTEIN	Virulence, detoxification, adaptation	2.144943	0.621441
165	Rv3417c	*groEL1*	60 KDA CHAPERONIN 1 GROEL1	Virulence, detoxification, adaptation	-1.76904	0.174847
166	Rv3648c	*cspA*	PROBABLE COLD SHOCK PROTEIN A CSPA	Virulence, detoxification, adaptation	-1.89202	0.267815
167	Rv3922c	Rv3922c	POSSIBLE HEMOLYSIN	Virulence, detoxification, adaptation	-1.98405	0.280321

3. *M. tuberculosis* gene regulated by 64 µg/ml at 24 hours of post inoculation

	ID	Gene name	Function	Category	Av/FC	STDEV
1	Rv0116c	Rv0116c	UNKNOWN	Cell wall and cell processes	0.308579	0.557829
2	Rv0188	Rv0188	UNKNOWN	Cell wall and cell processes	3.454465	1.33538
3	Rv0284	Rv0284	UNKNOWN	Cell wall and cell processes	1.89602	0.617859
4	Rv0287	*esxG*	UNKNOWN	Cell wall and cell processes	2.785722	1.270164
5	Rv0288	*esxH*	LOW MOLECULAR WEIGHT PROTEIN ANTIGEN 7 ESXH (10 kDa ANTIGEN)	Cell wall and cell processes	2.257887	1.034699
6	Rv0292	Rv0292	UNKNOWN	Cell wall and cell processes	2.667309	1.046146
7	Rv0676c	*mmpL5*	UNKNOWN. THOUGHT TO BE INVOLVED IN FATTY ACID TRANSPORT	Cell wall and cell processes	3.019831	1.105876
8	Rv1072	Rv1072	UNKNOWN	Cell wall and cell processes	3.010396	1.327689
9	Rv1073	Rv1073	UNKNOWN	Cell wall and cell processes	1.878788	0.639475
10	Rv1303	Rv1303	UNKNOWN	Cell wall and cell processes	-1.47838	1.306097
11	Rv1463	Rv1463	PROBABLE CONSERVED ATP-BINDING PROTEIN ABC TRANSPORTER	Cell wall and cell processes	2.163168	0.942712
12	Rv1884c	*rpfC*	PROBABLE RESUSCITATION-PROMOTING FACTOR RPFC	Cell wall and cell processes	-3.86179	2.717854
13	Rv1997	*ctpF*	PROBABLE METAL CATION TRANSPORTER P-TYPE ATPASE A CTPF	Cell wall and cell processes	-1.29187	1.282785
14	Rv2053c	Rv2053c	PROBABLE TRANSMEMBRANE PROTEIN	Cell wall and cell processes	2.890922	1.607423

	ID	Gene name	Function	Category	Av/FC	STDEV
15	Rv2091c	Rv2091c	UNKNOWN	Cell wall and cell processes	1.690154	0.606482
16	Rv2115c	Rv2115c	UNKNOWN	Cell wall and cell processes	2.007678	0.846804
17	Rv2450c	*rpfE*	PROBABLE RESUSCITATION-PROMOTING FACTOR RPFE	Cell wall and cell processes	-1.68642	1.497623
18	Rv2688c	Rv2688c	PROBABLE ANTIBIOTIC-TRANSPORT ATP-BINDING PROTEIN ABC TRANSPORTER	Cell wall and cell processes	2.076917	0.659206
19	Rv2743c	Rv2743c	UNKNOWN	Cell wall and cell processes	1.887702	0.485809
20	Rv2846c	*efpA*	POSSIBLE INTEGRAL MEMBRANE EFFLUX PROTEIN EFPA	Cell wall and cell processes	-3.44348	2.282469
21	Rv3019c	*esxR*	UNKNOWN	Cell wall and cell processes	2.35757	1.111639
22	Rv3020c	*esxS*	UNKNOWN	Cell wall and cell processes	3.405513	1.3425
23	Rv3036c	*TB22.2*	PROBABLE CONSERVED SECRETED PROTEIN TB22.2	Cell wall and cell processes	1.700149	0.553723
24	Rv3197	*Rv3197*	PROBABLE CONSERVED ATP-BINDING PROTEIN ABC TRANSPORTER	Cell wall and cell processes	1.740114	0.598303
25	Rv3270	*ctpC*	PROBABLE METAL CATION-TRANSPORTING P-TYPE ATPASE C CTPC	Cell wall and cell processes	1.951628	0.670036
26	Rv3402c	Rv3402c	THOUGHT TO BE INVOLVED IN CELL PROCESS	Cell wall and cell processes	1.839049	0.585625
27	Rv3766	Rv3766	UNKNOWN	Conserve hypothetical	1.65081	0.556115
28	Rv3767c	Rv3767	UNKNOWN	Conserve hypothetical	1.548992	0.497318
29	Rv3706c	3706c	UNKNOWN	Conserve hypothetical	4.270889	2.043633
30	Rv3839	Rv3889	UNKNOWN	Conserve hypothetical	1.827095	0.773945

	ID	Gene name	Function	Category	Av/FC	STDEV
31	Rv3879c	Rv3879c	UNKNOWN	Conserve hypothetical	1.816651	0.827142
32	Rv0079	Rv0079	UNKNOWN	Conserve hypothetical	-1.45402	1.363151
33	Rv0080	Rv0080	UNKNOWN	Conserve hypothetical	-1.6969	1.582253
34	Rv0108c	Rv0108c	UNKNOWN	Conserve hypothetical	-1.94938	1.130768
35	Rv0164	TB18.5	UNKNOWN	Conserve hypothetical	-1.78315	1.568015
36	Rv0289	Rv0289	UNKNOWN	Conserve hypothetical	1.916764	0.884446
37	Rv0678	Rv0678	UNKNOWN	Conserve hypothetical	2.192649	0.958524
38	Rv0692	Rv0692	UNKNOWN	Conserve hypothetical	-2.18124	1.97288
39	Rv0724	Rv0724A	UNKNOWN	Conserve hypothetical	1.730289	0.757193
40	Rv0950c	Rv0950c	UNKNOWN	Conserve hypothetical	-1.33937	1.234598
41	Rv1057	Rv1057	UNKNOWN	Conserve hypothetical	2.792005	1.673761
42	Rv1078	*pra*	UNKNOWN	Conserve hypothetical	-1.43453	1.329032
43	Rv1331	Rv1331	UNKNOWN	Conserve hypothetical	1.58741	0.698234
44	Rv1462	Rv1462	UNKNOWN	Conserve hypothetical	1.69537	0.628539
45	Rv1466	Rv1466	UNKNOWN	Conserve hypothetical	3.598182	1.500445
46	Rv1535	Rv1535	UNKNOWN	Conserve hypothetical	2.069276	0.794238
47	Rv1592c	Rv1592c	UNKNOWN	Conserve hypothetical	-3.02859	1.986183
48	Rv1636	TB15.3	UNKNOWN	Conserve hypothetical	-1.40747	1.247084
49	Rv1670	Rv1670	UNKNOWN	Conserve hypothetical	1.72018	0.567502
50	Rv1738	Rv1738	UNKNOWN	Conserve hypothetical	-4.41426	3.934279
51	Rv1813c	Rv1813c	UNKNOWN	Conserve hypothetical	-3.84729	3.291971
52	Rv1870c	Rv1870c	UNKNOWN	Conserve hypothetical	-1.5493	0.832972
53	Rv2004c	Rv2004c	UNKNOWN	Conserve hypothetical	-2.328	2.368567
54	Rv2005c	Rv2005c	UNKNOWN	Conserve hypothetical	-1.85736	2.10947
55	Rv2028c	Rv2028c	UNKNOWN	Conserve hypothetical	-2.2641	2.165947
56	Rv2030c	Rv2030c	UNKNOWN	Conserve hypothetical	-7.64199	5.685122

	ID	Gene name	Function	Category	Av/FC	STDEV
57	Rv2032	*acg*	MAY HAVE A ROLE FOR BACTERIA WITHIN THE HOST ENVIRONMENT	Conserve hypothetical	-3.14219	2.761482
58	Rv2050	Rv2050	UNKNOWN	Conserve hypothetical	2.175217	0.838504
59	Rv2052c	Rv2052c	UNKNOWN	Conserve hypothetical	4.365885	2.56016
60	Rv2271	Rv2271	UNKNOWN	Conserve hypothetical	-1.35344	1.349987
61	Rv2325c	Rv2325c	UNKNOWN	Conserve hypothetical	1.516453	0.521006
62	Rv2405	Rv2405	UNKNOWN	Conserve hypothetical	1.98052	0.895512
63	Rv2623	*TB31.7*	UNKNOWN	Conserve hypothetical	-4.61677	6.032121
64	Rv2624c	Rv2624c	UNKNOWN	Conserve hypothetical	-1.99781	1.815636
65	Rv2626c	Rv2626c	UNKNOWN	Conserve hypothetical	-3.9021	3.769517
66	Rv2627c	Rv2627c	UNKNOWN	Conserve hypothetical	-4.12147	5.859899
67	Rv2628	Rv2628	UNKNOWN	Conserve hypothetical	-2.59259	2.681199
68	Rv2630	Rv2630	UNKNOWN	Conserve hypothetical	-1.98005	1.775833
69	Rv2676c	Rv2676c	UNKNOWN	Conserve hypothetical	1.504228	0.48085
70	Rv2694c	Rv2694c	UNKNOWN	Conserve hypothetical	3.0403	1.015513
71	Rv2744c	35kd ag	CONSERVED 35 KDA ALANINE RICH PROTEIN	Conserve hypothetical	3.925886	1.504433
72	Rv2840c	Rv2840c	UNKNOWN	Conserve hypothetical	1.632055	0.517419
73	Rv3126c	Rv3126c	UNKNOWN	Conserve hypothetical	-1.19456	1.088076
74	Rv3127	Rv3127	UNKNOWN	Conserve hypothetical	-3.48938	2.682606
75	Rv3131	Rv3131	UNKNOWN	Conserve hypothetical	-3.33124	2.355824
76	Rv3484	*cpsA*	UNKNOWN	Conserve hypothetical	-1.24897	1.153071
77	Rv3642c	Rv3642c	UNKNOWN	Conserve hypothetical	1.575123	0.509848
78	Rv3747	Rv3747	UNKNOWN	Conserve hypothetical	-1.54665	1.633619
79	Rv0430	Rv0430	UNKNOWN	Conserve hypothetical	-1.4261	1.288258
80	Rv0009	*ppiA*	PPIASES ACCELERATE THE FOLDING OF PROTEINS	Information pathways	-1.30988	1.221769
81	Rv0570	*nrdZ*	PROBABLE RIBONUCLEOSIDE-DIPHOSPHATE REDUCTASE	Information pathways	-2.59018	2.405685
82	Rv0652	*rplL*	PROBABLE 50S RIBOSOMAL PROTEIN L7/L12 RPLL (SA1)	Information pathways	-2.233	1.319094

	ID	Gene name	Function	Category	Av/FC	STDEV
83	Rv0667	*rpoB*	DNA-DIRECTED RNA POLYMERASE (BETA CHAIN) RPOB	Information pathways	-0.53004	1.125775
84	Rv0700	*rpsJ*	30S RIBOSOMAL PROTEIN S10 RPSJ (TRANSCRIPTION ANTITERMINATION FACTOR NUSE	Information pathways	-0.03154	0.793014
85	Rv0701	*rplC*	PROBABLE 50S RIBOSOMAL PROTEIN L3 RPLC	Information pathways	-1.40706	1.297251
86	Rv0703	*rplW*	PROBABLE 50S RIBOSOMAL PROTEIN L23 RPLW	Information pathways	-1.2395	1.140483
87	Rv0704	*rplB*	PROBABLE 50S ribosomal protein L2 RPLB	Information pathways	-1.33021	1.160337
88	Rv0706	*rplV*	PROBABLE 50S RIBOSOMAL PROTEIN L22 RPLV	Information pathways	-0.01838	0.697287
89	Rv0714	*rplN*	PROBABLE 50S RIBOSOMAL PROTEIN L14 RPLN	Information pathways	-1.92754	1.714155
90	Rv0715	*rplX*	PROBABLE 50S RIBOSOMAL PROTEIN L24 RPLX	Information pathways	-1.41734	1.348857
91	Rv0716	*rplE*	PROBABLE 50S RIBOSOMAL PROTEIN L5 RPLE	Information pathways	-1.51144	1.361296
92	Rv0718	*rpsH*	PROBABLE 30S RIBOSOMAL PROTEIN S8 RPSH	Information pathways	-1.67088	1.475071
93	Rv1221	*sigE*	ALTERNATIVE RNA POLYMERASE SIGMA FACTOR SIGE	Information pathways	2.183545	0.889734
94	Rv2412	*rpsT*	PROBABLE 30S RIBOSOMAL PROTEIN S20 RPST	Information pathways	-0.50767	1.102222
95	Rv2710	*sigB*	RNA POLYMERASE SIGMA FACTOR SIGB	Information pathways	2.296367	2.672677
96	Rv2890c	*rspB*	PROBABLE 30S RIBOSOMAL PROTEIN S2 RPSB	Information pathways	-1.53677	1.479332
97	Rv3052c	*nrdI*	PROBABLY INVOLVED IN RIBONUCLEOTIDE REDUCTASE FUNCTION	Information pathways	1.712417	0.558376
98	Rv3442c	*rpsI*	PROBABLE 30S RIBOSOMAL PROTEIN S9 RPSI	Information pathways	-0.00528	0.685922
99	Rv0336	Rv0336	THOUGHT TO BE REGULATED BY Rv2720|LEXA	Insertion seqs and phages	-1.30287	1.145501
100	Rv0077c	Rv0077c	UNKNOWN; PROBABLY INVOLVED IN CELLULAR METABOLISM	Intermediary metabolism and respiration	2.069728	1.10689
101	Rv0291	*mycP3*	THOUGHT TO HAVE PROTEOLYTIC ACTIVITY	Intermediary metabolism and respiration	1.608456	0.580266
102	Rv0315	Rv0315	INVOLVED IN EXOPOLYSACCHARIDE BIOSYNTHESIS/DEGRADATION	Intermediary metabolism and respiration	-1.5705	1.897698

	ID	*Gene name*	Function	Category	Av/FC	STDEV
103	Rv0560c	Rv0560c	POSSIBLE BENZOQUINONE METHYLTRANSFERASE (METHYLASE)	Intermediary metabolism and respiration	8.167123	5.609433
104	Rv0848	*cysK2*	POSSIBLE CYSTEINE SYNTHASE A CYSK2	Intermediary metabolism and respiration	1.630602	0.52215
105	Rv1177	*fdxC*	FERREDOXINS ARE IRON-SULFUR PROTEINS THAT TRANSFER ELECTRONS IN A WIDE VARIETY OF METABOLIC REACTIONS	Intermediary metabolism and respiration	-1.27341	1.1338
106	Rv1304	*atpB*	PROBABLE ATP SYNTHASE A CHAIN ATPB (PROTEIN 6)	Intermediary metabolism and respiration	-3.09786	2.655309
107	Rv1305	*atpE*	PROBABLE ATP SYNTHASE C CHAIN ATPE (LIPID-BINDING PROTEIN)	Intermediary metabolism and respiration	-1.3961	1.406573
108	Rv1306	*atpF*	PROBABLE ATP SYNTHASE B CHAIN ATPF	Intermediary metabolism and respiration	-2.77336	2.55119
109	Rv1307	*atpH*	PROBABLE ATP SYNTHASE DELTA CHAIN ATPH	Intermediary metabolism and respiration	-1.20709	1.100842
110	Rv1308	*atpA*	PROBABLE ATP SYNTHASE ALPHA CHAIN ATPA	Intermediary metabolism and respiration	-1.66703	1.546506
111	Rv1310	*atpD*	PROBABLE ATP SYNTHASE BETA CHAIN ATPD	Intermediary metabolism and respiration	-1.19907	1.075943
112	Rv1464	*csd*	PROBABLE CYSTEINE DESULFURASE CSD	Intermediary metabolism and respiration	3.767939	1.473816

	ID	Gene name	Function	Category	Av/FC	STDEV
113	Rv1465	Rv1465	POSSIBLE NITROGEN FIXATION RELATED PROTEIN	Intermediary metabolism and respiration	2.055772	0.809375
114	Rv1612	*trpB*	PROBABLE TRYPTOPHAN SYNTHASE, BETA SUBUNIT TRPB	Intermediary metabolism and respiration	-1.21941	1.073177
115	Rv1736c	*narX*	PROBABLE NITRATE REDUCTASE NARX	Intermediary metabolism and respiration	-1.68648	1.959071
					-2.47411	3.080402
					-5.50719	5.790081
					-3.44152	5.068395
119	Rv2122c	*hisE*	THOUGHT TO BE INVOLVED IN HISTIDINE BIOSYNTHESIS	Intermediary metabolism and respiration	1.924921	0.648981
120	Rv2124c	*metH*	PROBABLE 5-METHYLTETRAHYDROFOLATE--HOMOCYSTEIN METHYLTRANSFERASE METH	Intermediary metabolism and respiration	1.564868	0.579201
116	Rv1812c	Rv1812c	PROBABLE DEHYDROGENASE	Intermediary metabolism and respiration	3.059531	1.239747
117	Rv2007c	*fdxA*	INVOLVED IN ELECTRON TRANSFER	Intermediary metabolism and respiration	2.224867	0.985802
118	Rv2029c	*pfkB*	INVOLVED IN GLYCOLYSIS: CONVERTS SUGAR-1-P TO SUGAR-1,6-P	Intermediary metabolism and respiration	1.576235	0.546357

	ID	Gene name	Function	Category	Av/FC	STDEV
124	Rv2959c	Rv2959c	THOUGHT TO CAUSE METHYLATION	Intermediary metabolism and respiration	-1.43967	1.287455
125	Rv3161c	Rv3161c	POSSIBLE DIOXYGENASE	Intermediary metabolism and respiration	13.58208	9.364385
126	Rv3206c	*moeB1*	POSSIBLY INVOLVED IN MOLYBDOPTERIN METABOLISM	Intermediary metabolism and respiration	1.495546	0.466619
127	Rv3596c	*clpC1*	PROBABLE ATP-DEPENDENT PROTEASE ATP-BINDING SUBUNIT CLPC1	Intermediary metabolism and respiration	1.563453	0.501396
128	Rv3841	*bfrB*	INVOLVED IN IRON STORAGE	Intermediary metabolism and respiration	-2.52993	1.586847
129	Rv0642c	*mmaA4*	METHOXY MYCOLIC ACID SYNTHASE 4 MMAA4 (METHYL MYCOLIC ACID SYNTHASE	Lipid metabolism	-1.43369	1.373953
130	Rv0824c	*desA1*	PROBABLE ACYL-[ACYL-CARRIER PROTEIN] DESATURASE DESA1	Lipid metabolism	-4.01504	2.708589
131	Rv1094	*desA2*	POSSIBLE ACYL-[ACYL-CARRIER PROTEIN] DESATURASE DESA2	Lipid metabolism	-2.61738	1.569879
132	Rv1886c	*fbpB*	SECRETED ANTIGEN 85-B FBPB (85B) (ANTIGEN 85 COMPLEX B) (MYCOLYL	Lipid metabolism	-3.40309	3.158262
133	Rv2243	*fadD2*	CATALYZES MALONYL-COA-ACP TRANSACYLASE	Lipid metabolism	-1.53594	1.664022
134	Rv2244	*acpM*	INVOLVED IN FATTY ACID BIOSYNTHESIS (MYCOLIC ACIDS SYNTHESIS	Lipid metabolism	0.003447	0.818778
135	Rv2245	*kasA*	INVOLVED IN FATTY ACID BIOSYNTHESIS (MYCOLIC ACIDS SYNTHESIS	Lipid metabolism	-1.98833	1.405819
136	Rv2246	*kasB*	3-OXOACYL-[ACYL-CARRIER PROTEIN] SYNTHASE 2	Lipid metabolism	-2.46937	1.769753
137	Rv2377c	*mbtH*	PUTATIVE CONSERVED PROTEIN MBTH	Lipid metabolism	2.005751	0.723677
138	Rv2380c	*mbtE*	PEPTIDE SYNTHETASE MBTE (PEPTIDE SYNTHASE)	Lipid metabolism	3.158833	1.172777
139	Rv2381c	*mbtD*	POLYKETIDE SYNTHETASE MBTD	Lipid metabolism	2.304321	0.932392

	ID	Gene name	Function	Category	Av/FC	STDEV
140	Rv2382c	*mbtC*	INVOLVED IN THE BIOGENESIS OF THE HYDROXYPHENYLOXAZOLINE-CONTAINING SIDEROPHORE MYCOBACTINS	Lipid metabolism	3.408963	1.166422
141	Rv2383c	*mbtB*	PHENYLOXAZOLINE SYNTHASE MBTB	Lipid metabolism	1.878343	0.593032
142	Rv2386c	*mbtI*	PUTATIVE ISOCHORISMATE SYNTHASE MBTI	Lipid metabolism	1.705159	0.570991
143	Rv2500c	*fadE19*	POSSIBLE ACYL-CoA DEHYDROGENASE FADE19 (MMGC)	Lipid metabolism	1.982758	0.842339
144	Rv2524c	*fas*	PROBABLE FATTY ACID SYNTHASE FAS	Lipid metabolism	-1.33446	1.264049
145	Rv2932	*ppsB*	PHENOLPTHIOCEROL SYNTHESIS TYPE-I POLYKETIDE SYNTHASE PPSB	Lipid metabolism	2.015846	0.838399
146	Rv2933	*ppsC*	PHENOLPTHIOCEROL SYNTHESIS TYPE-I POLYKETIDE SYNTHASE PPSC	Lipid metabolism	1.628158	0.594133
147	Rv2935	*ppsE*	PHENOLPTHIOCEROL SYNTHESIS TYPE-I POLYKETIDE SYNTHASE PPSE	Lipid metabolism	-2.41067	2.457257
148	Rv2950c	*fadD29*	FUNCTION UNKNOWN, BUT INVOLVED IN LIPID DEGRADATION	Lipid metabolism	-1.60769	1.846339
149	Rv3130c	*tgs1*	INVOLVED IN SYNTHESIS OF TRIACYLGLYCEROL	Lipid metabolism	-4.4683	4.254869
150	Rv3774	*echA21*	OXIDISES FATTY ACIDS	Lipid metabolism	-0.00031	0.590971
151	Rv3804c	*fbpA*	INVOLV ED IN CELL WALL MYCOLATION	Lipid metabolism	0.014214	0.78962
152	Rv3824c	*papA1*	INVOLVED IN LIPID METABOLISM	Lipid metabolism	3.154036	1.2955
153	Rv0280	*PPE3*	UNKNOWN	PE/PPE	-1.72056	1.885468
154	Rv0285	*PE5*	UNKNOWN	PE/PPE	2.169799	0.9537
155	Rv1195	*PE13*	UNKNOWN	PE/PPE	-1.86037	1.278426
156	Rv1196	*PPe18*	UNKNOWN	PE/PPE	-1.38937	1.361668
157	Rv1386	*PE15*	UNKNOWN	PE/PPE	-7.48898	11.92575
158	Rv1387	*PPE20*	UNKNOWN	PE/PPE	-3.55211	4.378693
159	Rv1806	*PE20*	PE FAMILY PROTEIN	PE/PPE	3.346305	1.81478
160	Rv3135	*PPE50*	UNKNOWN	PE/PPE	-1.36637	1.324047
161	Rv3159c	*PPE53*	UNKNOWN	PE/PPE	5.372833	2.8863
162	Rv3478	*PPE60*	UNKNOWN	PE/PPE	-1.2902	1.206951
163	Rv0872c	*PE PGRS15*	UNKNOWN	PE/PPE)	2.161618	0.823924
164	Rv0823c	Rv0823c	THOUGHT TO BE INVOLVED IN TRANSCRIPTIONAL MECHANISM	Regulatory proteins	-1.90771	1.735217

	ID	Gene name	Function	Category	Av/FC	STDEV
165	Rv1460	Rv1460	INVOLVED IN TRANSCRIPTIONAL MECHANISM	Regulatory proteins	4.95915	2.174647
166	Rv1534	Rv1534	POSSIBLY INVOLVED IN A TRANSCRIPTIONAL MECHANISM	Regulatory proteins	2.395037	0.940763
167	Rv2358	Rv2358	INVOLVED IN TRANSCRIPTIONAL MECHANISM	Regulatory proteins	2.127472	0.885409
168	Rv2359	*furB*	PROBABLE FERRIC UPTAKE REGULATION PROTEIN FURB	Regulatory proteins	1.714664	0.678632
169	Rv2745c	Rv2745c	POSSIBLY INVOLVED IN TRANSCRIPTIONAL MECHANISM	Regulatory proteins	2.838931	0.965348
170	Rv3132c	*devS*	TWO COMPONENT SENSOR HISTIDINE KINASE DEVS	Regulatory proteins	-2.42076	2.124356
171	Rv3133c	*devR*	TWO COMPONENT TRANSCRIPTIONAL REGULATORY PROTEIN DEVR	Regulatory proteins	-2.00683	2.01749
172	Rv3160c	*Rv3160c*	POSSIBLY INVOLVED IN TRANSCRIPTIONAL MECHANISM	Regulatory proteins	27.50748	20.20303
173	Rv3219	*whiB1*	INVOLVED IN TRANSCRIPTIONAL MECHANISM	Regulatory proteins	-1.56847	0.850976
174	Rv0251c	*hsp*	RIBOSOMAL SUBUNIT. POSSIBLY A MOLECULAR CHAPERONE	Virulence, detoxification, adaptation	3.31728	1.945331
175	Rv0440	*groEl2*	PREVENTS MISFOLDING AND PROMOTES THE REFOLDING AND PROPER ASSEMBLY OF POLYPEPTIDESUNDER STRESS	Virulence, detoxification, adaptation	0.002757	0.764281
176	Rv0563	*htpX*	PROBABLE PROTEASE TRANSMEMBRANE PROTEIN HEAT SHOCK PROTEIN HTPX	Virulence, detoxification, adaptation	2.285772	0.982294
177	Rv2031c	*hspX*	HEAT SHOCK PROTEIN HSPX (ALPHA-CRYSTALLIN HOMOLOG)	Virulence, detoxification, adaptation	-5.55299	6.917586
178	Rv2190c	Rv2190c	UNKNOWN	Virulence, detoxification, adaptation	-3.30833	2.758203
179	Rv2428	*ahpC*	ALKYL HYDROPEROXIDE REDUCTASE C PROTEIN AHPC	Virulence, detoxification, adaptation	-2.81099	3.015622
180	Rv3269	Rv3269	CONSERVED HYPOTHETICAL PROTEIN	Virulence, detoxification, adaptation	3.308076	1.560983

	ID	Gene name	Function	Category	Av/FC	STDEV
181	Rv3418c	*groES*	10 KDA CHAPERONIN GROES (PROTEIN CPN10) (PROTEIN GROES)	Virulence, detoxification, adaptation	-0.00782	0.747637
182	Rv3648c	*cspA*	PROBABLE COLD SHOCK PROTEIN A CSPA	Virulence, detoxification, adaptation	-0.0016	0.683954

CHAPTER FOUR

Understanding the mechanism of action of F1082

4.1 Introduction

The gene signature profile from the micro array data (Chapter 3) provides some clues for us to understand the mechanism of action of F1082. From the data it appeared that *M. tuberculosis* "senses" a low iron concentration enviromention when treated with F1082. An organism responds to environmental changes by altering the level of expression of genes that effect metabolic changes to favour its survival and continuing growth (Boshoff *et al*., 2004). When *M. tuberculosis* is faced with low iron conditions, it up-regulates the genes involved in siderophore biosynthesis and down-regulates the genes that are involved in iron storage (Quadri *et al*., 1998), which could also be as a result of inactivation of IdeR (Schnappinger *et al*., 2003). A schematic representation of iron regulation is shown in (Figure 4.2)

4.1.1 Iron–responsive changes in gene expression

Iron limitation in bacteria induces a response aimed at increasing iron acquisition. To achieve this, the siderophore production is upregulated (Raghu *et al*., 1993) and iron is transported through the irtAB system (Rodriguez and Smith, 2006). Mycobacteria produce two classes of siderophores, mycobactins and exochelin (Ratledge and Ewing, 1996). The details of siderophore structure (Figure 4.1) and biosynthesis are known (De Voss *et al*., 1999). Pathogenic mycobacteria produce mycobactins only, whereas saprophytic mycobacteria such as *M. smegmatis* and *Mycobacterium neoarum* produce both mycobactins and exochelin (Ratledge and Ewing, 1996). Mycobactins are salicylate-containing siderophores, and exochelins are peptidic molecules. Mycobactins are found in two forms that differ in the length of the alkyl substitution and hence in polarity and solubility. The less polar form remains cell associated (mycobactins), whereas the more polar one (carboxymycobactin) is secreted into the culture medium. Mycobacterial siderophores, like most other siderophores, are synthesized by non-ribosomal peptide synthetases (Gobin *et al*., 1995).

Annotation of the complete genome sequence of *M. tuberculosis* identified a cluster of 10 genes, (the *mbt* locus) that, based on homology with other systems, encode the appropriate enzymes for the synthesis of mycobactin and the carboxymycobactin core(De Voss *et al*., 2000). Three peptide synthetases (MbtB, MbtE and MbtF), two polypeptide synthases (MbtD and MbtC), an isochorismate synthase (Mbtl) that converts chorismate to salicylate, a salicyloyl-AMP ligase (MbtA), and a hydroxylase (MbtG) are encoded by the *mbt* genes (Quadri *et al*., 1998). A common core structure isshared by the two siderophores but they differ in the length of alkyl substitution. A long alkyl chain (e.g., 10-21 carbons) is found in mycobactins, whereas a shorter one (2-9 carbons) is found in exomycobactins (Ratledge and Dover, 2000). Independent disruption of the siderophore producing enzymes is therefore necessary in order to understand their contribution in iron uptake (Rodriguez *et al*., 2008).

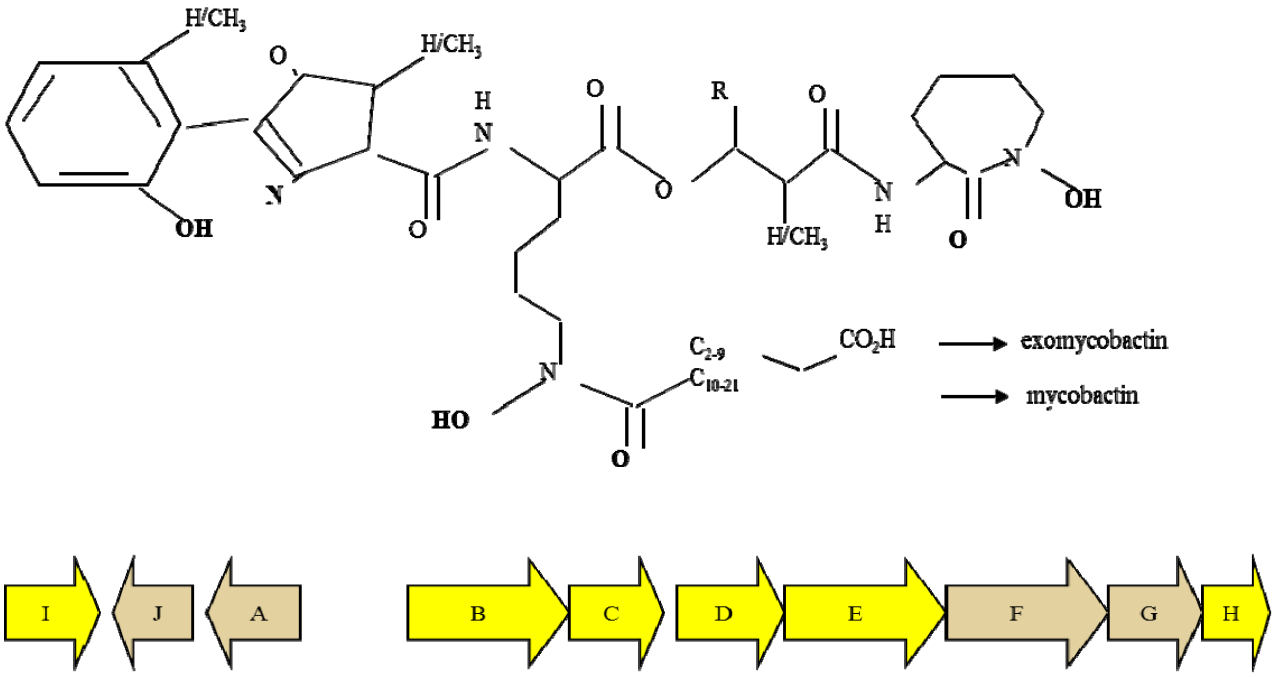

Figure 4.1. The structure of mycobactin and exomycobactin and the *mbt* gene cluster. The yellow highlighted *mbt* genes were upregulated in the microarray gene profile after F1082 treatment.

4.1.2 The IdeR protein in *M. tuberculosis*

IdeR is found in pathogenic and non-pathogenic mycobactria and is a closely related homologue of DtxR (Doukhan *et al*., 1995). In *M. tuberculosis*, when intracellular iron levels increase, IdeR combines with Fe^{2+} and binds to specific sequences (iron boxes) in the promoter region of iron-regulated genes modulating their transcription (Figure 4.2) (Rodriguez and Smith, 2003). Under these conditions, IdeR-Fe2+ down-regulates iron uptake by repressing siderophore production and increases iron storage by activating transcription of *bfrA* and *bfrB* encoding bacterioferritin and ferritin (Weinberg, 1984). In an indirect manner, IdeR also positively modulates protection against oxidative stress (Dussurget *et al*., 1998). In low-iron conditions, the IdeR-Fe^{2+} complexes are not formed, and IdeR-repressed genes are transcribed while iron storage genes are not expressed (Rodriguez *et al*., 2002).

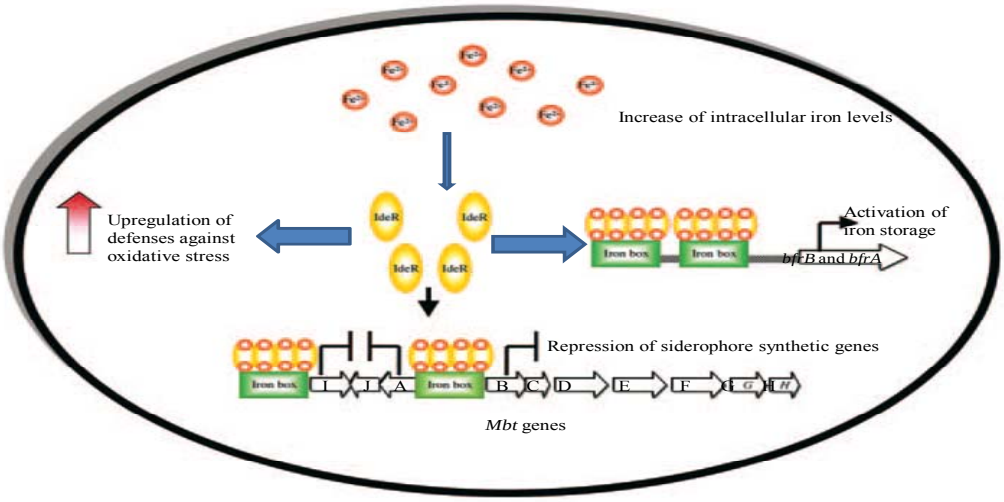

Figure 4.2 Iron-dependent regulatory function of IdeR (Adapted from Rodriguez and Smith, 2003).

4.1.3 IdeR and the oxidative stress response in Mycobacteria

Oxidative stress occurs when abnormally high levels of reactive oxygen species (ROS) are generated, causing DNA, protein and lipid damage. Iron levels and oxidative stress are closely linked in aerobic organisms (Rodriguez and Smith, 2003). On one hand, iron deficiency can lead to oxidative stress by decreasing the activity of iron containing enzymes such as superoxide dismutase and catalase involved in protection against ROS and reactive nitrogen species (RNS). Conversely, increasing intracellular free iron available to participate in a Fenton reaction results in enhanced generation of oxygen radicals and oxidative stress (Imlay *et al*., 1988). Therefore it is not surprising that many organisms couple regulation of iron metabolism with regulation of proteins against oxidative stress. Three hypotheses can be tested (1) F1082 could be more active against *M. tuberculosis* under low iron conditions; alternatively (2) F1082 could be directly interfering with the iron dependent regulators such that it up-regulates genes for iron acquisition under high iron conditions and (3) F1082 could be aiding or exacerbating the generation of intracellular oxidative stress. In this chapter the three above-mentioned scenarios will be investigated. The aim of this chapter is to understand the mechanism by which F1082 inhibits *M. tuberculosis* growth in an iron-dependent manner.

4.3 Materials and Methods

4.3.1 Bacteria, media and growth conditions

M. tuberculosis and *M. smegmatis* strains were cultured in Middlebrook 7H9 broth or on 7H10 agar (Difco), supplemented with 0.2% glycerol, 0.05% Tween 80 and 10% albumin-dextrose-NaCl complex (ADN) (Appendix 4A).The *M. tuberculosis* irtAB mutant, *M. smegmatis* sodA mutant, and *M. smegmatis* transformed strains were provided by Dr Marcela M. Rodriquez from the TB Center, The Public Health Research Institute at the International Center for Public Health. The H37Rv reference strain and H37Rv mshA mutant were obtained from Prof. WR Bill Jacobs's lab, Albert Einstein College, USA. The strains used in this study have been described (Table 4.1). Antibiotics were included when required at the following concentrations: kanamycin (Kan) at 20 µg/ml,

streptomycin (Str) at 20 µg/ml, and hygromycin (Hyg) at 150 µg/ml. For *M. tuberculosis* or *M. smegmatis* grown in low iron medium, we used a defined medium as described by Rodriquez and Smith (2006). Briefly, a defined medium (MM) containing 0.5% w/v asparagine, 0.5% w/v KH_2PO_4, 2% glycerol, 0.05% Tween 80 and 10% ADC was used. The pH was adjusted to 6.8. To reduce any trace metal contamination, the medium was treated with Chelex-100 (Bio-Rad Laboratories) according to the manufacturer's instructions. Before use the medium was supplemented with 0.5 mg/l $ZnCl_2$, 0.1 mg/l $MnSO_4$, 40 mg/l $MgSO_4$ and the desired concentration of $FeCl_3$ was also added.

Table 4.1 Bacterial strains and plasmids used in this work

Strain	Description	Mutant	Functional use
H37R v	*M. tuberculosis* laboratory strain, wild type		Baseline susceptibility testing
ST73	*irtAB-M. tuberculosis* mutant (Hyg^R)	Hyg. resistant cassette inserted in Rv1348 (Rodriguez and Smith, 2006)	Iron transport deficient mutant incapable of transporting iron into cell
SM60	*M. smegmatis*-pSM128* (Sm^R)	MC^2 155 with integrated pSM128 (Dussurget *et al*., 1999)	*IdeR*- independent regulation, serves as baseline testing
SM160	*M. smegmatis*-pSM128-*bfrB-LacZ* (Sm^R)	MC^2 155 with integrated pSM128-*bfrB-LacZ* (Sm^R), (Rodriguez *et al*., 1999)	*IdeR*-iron dependent regulation
SM193	*M. smegmatis*-pSM128-*mbtB-LacZ* (Sm^R)	MC^2 155 with integrated pSM128-*mbtB-LacZ* (Sm^R), (Rodriguez *et al*., 1999)	*IdeR*-iron dependent regulation
MC^2155	*M. smegmatis* wild type MC^2 155		Base-line screen
SM90	*M. smegmatis* superoxide dismutase mutant (Km^R)	MC^2 155 with integrated pSM299 kanamycin resistant plasmid in *sodA* gene (Dussurget *et al*., 1998)	Susceptible to oxidative stress

Strain	*Description*	Mutant	Functional use
CDC 1551	*M. tuberculosis*-CDC 1551 wild type		Baseline testing to oxidative generating compounds
ΔmshA	*M. tuberculosis*-CDC 1551 mycothiol mutant (Hm^R)	Deletion of mshA gene by specialised transduction with *phAE222* (Vilchèze *et al*., 2008)	Susceptible to oxidative stress

*pSM 128 and its derivatives contain the mycobacteriophage L5 int system that promotes integration at the chromosomal L5 at site. Km^R, kanamycin resistant; Sm^R, streptomycin resistant; Hyg^R, hygromycin resistant.

4.3.2 Alamar blue assay

Mycobacterium tuberculosis H37Rv from frozen stocks was inoculated onto 7H10 agar plates. An aliquot was taken from the 7H10 plate and liquid cultures were grown in minimal medium (MM) with no iron added. Pre-incubation in MM with no iron was done in order to exhaust the stored iron. H37Rv was grown in MM from an OD_{540} of 0.1 to 0.8 (three generations) and then diluted in MM to an OD_{540} of 0.1(1 x 10^7 cells). After two days the culture was diluted again to an OD_{540} of 0.02 (2 x 10^6 cells/ml) in MM alone or MM with iron ($FeCl_3$, 50 µm/ml) containing the different concentrations of F1082. To assay for activity of F1082 in MM with or without iron, we used the Alamar Blue assay in a 96 well plate. Different concentrations of F1082 (ranging from16 to 0.125 µg/ml) were tested in duplicate with each experiment performed at least twice. Bacterial suspension (100 µl) was added to test wells and to controls. The control wells included no drug (bacterial culture only), drug only (medium and highest drug concentration used), and medium only (serves as the blank). The plates were incubated for five days at 37°C and 20 µl of Alamar Blue solution (Trek Diagnostics, Westlake) was added to each well on the fifth day and incubated for another 24 hours. Results were read by visual detection or using fluorescence in a plate flourometer (Fluoroskan Ascent FL, Thermo, Finland) at an excitation wave-length of 490 nm and an emission wavelength of 540 nm, and the

relative fluorescence units (rfu) were recorded. Visual MIC was determined as the lowest concentration of the compound that inhibited growth (purple colour), whereas growth was recorded if the wells turned pink after 24 hour of addition of the alamar blue. Percentage growth was calculated relative to the untreated control based on the rfu. There was always a correlation between fluorometric and visual observations, i.e. pink wells represented high rfu values.

4.3.3 β-galactosidase assay

Cultures of *M. smegmatis* harbouring the different gene promoters with *LacZ* fusion (SM 60-pSM128, SM 160-*bfrB* promoter-*LacZ* and SM193-*mbtB* promoter-*LacZ*) were grown in appropriate media: in MM only (no iron-LI) or MM supplemented with 100 µM $FeCl_3$ (high iron-HI). The bacterial cultures were collected at OD_{600} of 0.5-0.7, washed twice in phosphate buffered saline (PBS), centrifuged at 14 000 rpm in a bench top centrifuge at room temperature (25°C) for five minutes and resuspended in Z buffer (Appendix 4A; Miller J.F., 1972). Suspensions were mixed with Zirconia beads (0.5 mm in diameter) and bacteria were lysed by three pulses of bead-beating for 30 s in a Mini Bead-beater (Biospec Products). The extracts were centrifuged at 14 000 rpm for 5 minutes and the supernatant was collected.

4.3.3.1The *LacZ* transcriptional fusions used

The *LacZ* transcriptional fusions in *M. smegmatis* were kindly provided by Dr Marcela Rodriquez from UMDNJ as described and published (Table 4.1). The transformed *M. smegmatis* strains were made by: amplification of a 180 base pair DNA fragment containing the putative *IdeR* binding site and promoter regions of *mbtB* and *bfrB* by PCR from *M. tuberculosis* H37Rv chromosome using primers Ppe.1 and Ppe. 2. These PCR fragments were cloned in the Scal site of pSM128 plasmid (Figure 4.3) and integrated into *M. smegmatis* chromosome to generate *M. smegmatis* strains SM160 and SM193. SM160 contained the plasmids pSM128-*bfrB* promoter-*LacZ* and SM193 contained pSM128-*mbtB* promoter-*LacZ*. SM60 contained plasmid pSM128-*LacZ* and was used for background expression activity as this strain was not controlled by the iron dependent regulator (IdeR).

4.3.3.2 Protein concentrations

Protein concentrations of the extracts were estimated by using the Bio-Rad protein assay (Bio-Rad), with bovine serum albumin (Fraction V) as a standard. Briefly, an initial stock (20 ml) of 5 mg/ml BSA was prepared in sterile distilled water. Aliquots of 100 ml BSA concentrations ranging from (5 to 0.1 mg/ml) were prepared from the stock (Appendix 4A-III, Table 4.2). Aliquots of 25 µl of BSA concentrations, water (serves as a blank) and samples tested to be tested were transferred into sterile 15 ml glass tubes. Aliquots of 125 µl of Reagent A and 1 ml of Reagent B (Bio-Rad) were added to each of the tubes and were incubated at room temperature (25°C) for 15 minutes. The optical density at 600 nm (OD_{600}) was recorded for each of the sample and a BSA standard curve was plotted using the OD_{600} values of the BSA concentration (Appendix 4A-III, Figure 4.4). Estimation of protein concentration for each sample was calculated from the curve.

4.3.3.3 β-galactosidase activity measurement

β-galactosidase activity assay (Appendix 4A): 50 µl of the supernatant of each sample was transferred into a 1,5 ml Eppendorf tube. An aliquot of 600 µl of Z-buffer with β-mercaptoethanol (complete) was added to each tube and incubated at 30°C for 5 minutes to equilibrate. Subsequently, 200 µl of o-nitrophenyl-b-D-galactopyraniside (ONPG), a substrate for β-galactosidase was added and time was recorded as reaction start time. The reaction was stopped when the reaction mixture started turning yellow by addition of 1 molar sodium carbonate (1M $NaCO_3$) and the time was recorded again as time of reaction termination. The difference between the reaction start time and the reaction termination time was recorded as the reaction for each sample. The OD_{420nm} was measured for each sample relative to the blank. β-galactosidase activity was calculated as follows.

β-galactosidase activity $= 1000 * A_{420nm}$/ Reaction time * Protein concentration (OD_{600})

β-galactosidase activity of the extracts was determined by using Miller's method (Miller J.F., 1972) and is expressed as nanomoles of nitrophenol/min/mg protein.

4.4 Results and Discussion

4.4.1 Activity testing of F1082 under low or high iron conditions.

The results presented in Chapter 3 (Table 3.4) suggest that *M. tuberculosis* "senses" low iron conditions under F1082 treatment by up-regulating the genes involved in iron acquisition and down-regulating the genes involved in iron storage. We therefore hypothesized that the activity of F1082 could be affected by varying the iron concentration. Therefore we tested *M. tuberculosis* H37Rv susceptibility to F1082 under low (MM only) and high iron (MM + 50 µM $FeCl_3$) conditions (Table 4.3). The Alamar Blue assay described in materials and methods (section 4.3.2) where *M. tuberculosis* was grown under various concentrations of F1082 was used (Table 4.3). These results show that F1082 is most active under high iron concentration, with an MIC of 2 µg/ml, compared to low iron concentration, with an MIC of 4 µg/ml. These results refute our first hypothesis that F1082 could be an iron chelator. If F1082 was an iron chelator, we expect that it would chelate the available iron, amplifying its effect under low iron concentration and with minimal activity under high iron concentration.

Table 4.3 MIC determination of F1082 treatment of *M. tuberculosis* under iron limitation.

H37Rv	F1082 (µg/ml)
Low iron (MM only)	4
High iron (MM + 50 µM/ml $FeCl_3$)	2

4.4.2 F1082 activity in an *M. tuberculosis* iron transport deficient mutant (*irtAB* mutant)

If F1082 is not an iron chelator, then it may affect iron transport in *M. tuberculosis*. We tested the activity of F1082 in an *M. tuberculosis* i*rtAB* mutant described (Table 4.1). This strain is incapable of transporting iron into the cell because the *irtAB* gene is disrupted which normally is involved in the active translocation of Fe(III)-siderophore complexes through the plasma membrane (Braun and Killmann, 1999). Whether most F1082 activity is inside the cell or outside the cell also remained to be tested. The *irtAB* mutant was tested in MM with various concentrations of $FeCl_3$ (50 to 5 µM). When the *M. tuberculosis irtAB* mutant was tested against INH, it was susceptible, with an MIC of 0.05 µg/ml. We observed that the *M. tuberculosis irtAB* mutant offered resistance to F1082, and noted an increase in MIC to 8 fold higher than the wild type H37Rv (Figure 4.5). This could suggest that most F1082 activity requires it to be transported via iron mediated active transport through the irtAB system or depends on the abundance of intracellular iron. The low inhibitory activity observed at high F1082 concentrations against irtAB mutant could be as a result of residual intracellular iron within the mycobacterium or toxic effect at high concentrations.

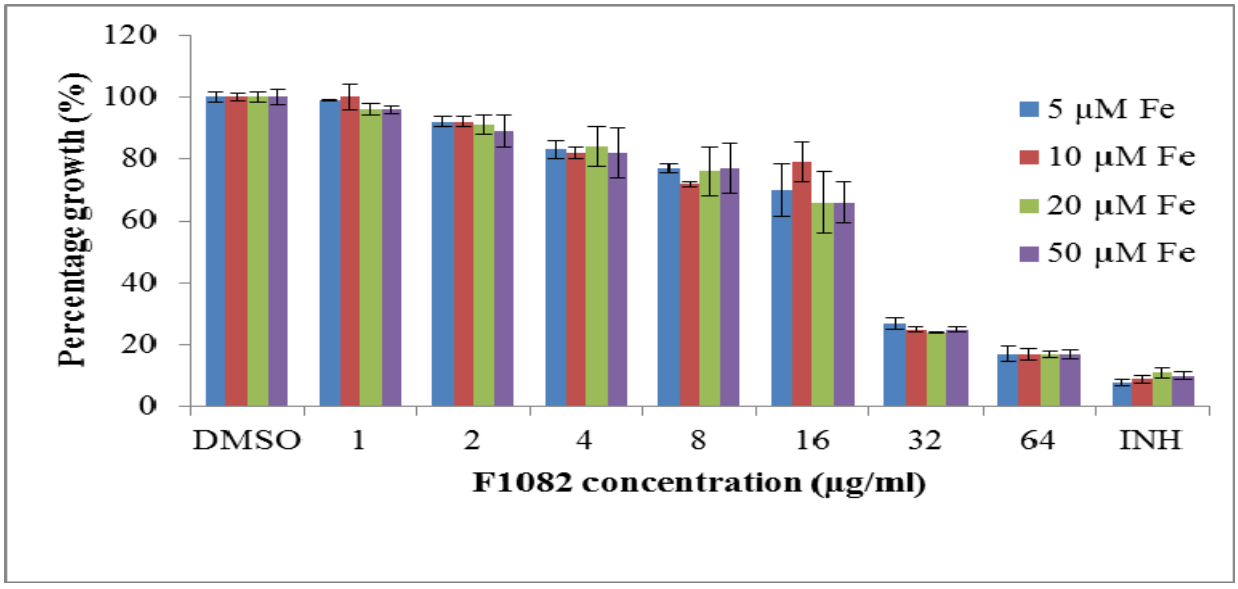

Figure 4.5 Percentage growth of *M. tuberculosis* (irtAB) mutant with F1082 in MM containing $FeCl_3$ concentrations (50-5 µM). Controls DMSO and INH (0.05 µg/ml) were used. Errors bars represent mean standard deviation of three indepent experiment with each done in duplicate.

4.4.3 Evaluation of the interference of function of the iron dependent regulator (IdeR) by F1082.

4.4.3.1 F1082 activity testing against *M. smegmatis* under low or high iron conditions

The second hypothesis was tested, viz., whether F1082 could be interfering with the iron dependent regulator (IdeR). Since we had transformed strains of *M. smegmatis* for measuring IdeR activity, it was necessary that *M. smegmatis* would be sensitive to F1082. The results show a similar pattern, in that F1082 is most active in mycobacteria that have been grown in high iron medium than in low iron (Figure 4.6).

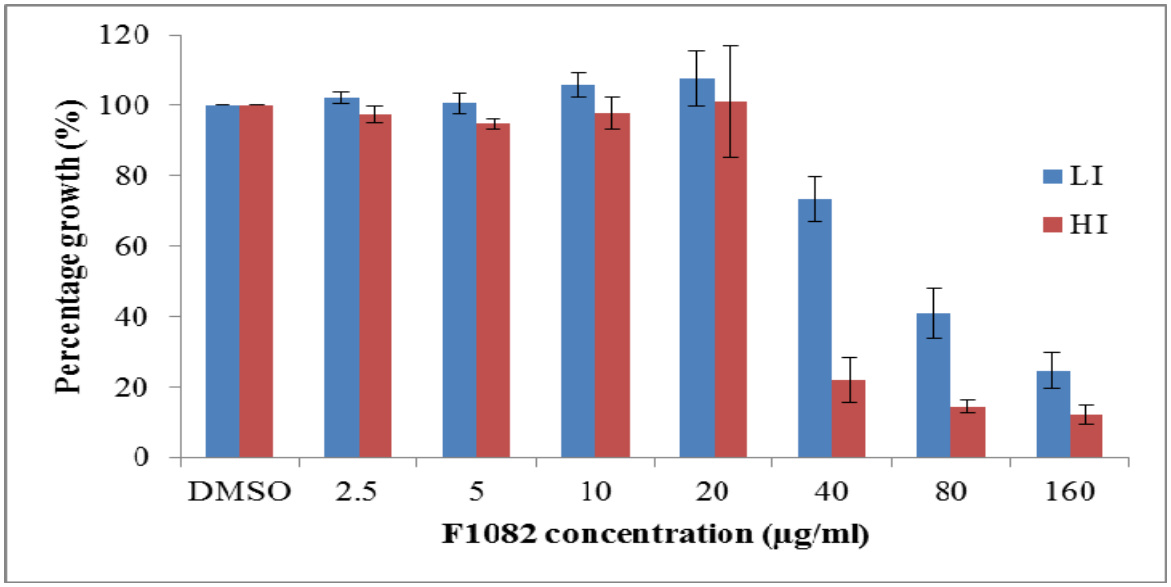

Figure 4.6 Percentage growth of *M. smegmatis* in low iron (MM only-LI) or high iron (MM + 100 µM-HI) at various concentrations of F1082. Errors bars represent mean standard deviation of three indepent experiment with each done in duplicate.

The percentage growth was calculated relative to the DMSO control with no compound and values were obtained using the cell titer flourometric assay. Three biological replicates with each performed in duplicate generated this data. These results show a similar pattern as is the case for *M. tuberculosis,* at slightly higher concentrations of F1082.

4.4.3.2 β-galactosidase activity in a transformed *M. smegmatis* strain.

It has been shown in the literature that *bfrB* and *mbtB* gene expression is iron-dependent and regulated by IdeR (Rodriguez *et al*., 2002). To test whether F1082 directly interferes with IdeR, we performed a β-galactosidase assay. The activity is driven by the promoter of *M. tuberculosis* genes whose expression is regulated by IdeR under iron availability. We used *M. smegmatis* strains that contained the *bfrB-lac-Z* and *mbtB-lac-Z* reporter genes of *M. tuberculosis* (Table 4.1). The activity of F1082 on IdeR interference was tested at a subinhibitory concentration of F1082 (10 µg/ml). For the calculation of the β-galactosidase activity we used the formula where protein concentration was determined using the BSA standard curve (Figure 4.4).

The β-galactosidase activity of SM60 (pSM128 plasmid only) did not change under any condition tested (low or high iron) (Table 4.4). This was as expected, since the plasmid did not contain any fragment regulated by IdeR and F1082 did not affect its activity. This strain was used as a base-line to measure the activities of the strains habouring IdeR regulated genes. We observed that SM160 (pSM128-bfrB-*LacZ*) had a low β-galactosidase activity (low expression of *bfrB*) under low iron and 19 times more activity under high iron conditions which was similar when F1082 was added (Table 4.4). Conversely, SM193 (pSM128-mbtB-*LacZ*) had a high β-galactosidase activity (high expression of mbtB gene) which was7 fold more under low iron conditions compared to high iron conditions.When F1082 was added, there was increased β-galactosidase activity: 8 fold more under low iron conditions, compared to high iron conditions. These results show that F1082 does not directly interfere with IdeR activity, since there was no change whether F1082 was added or not in the β-galactosidase assay (Table 4.4).

Table 4.4 Expression of *mbtB* and *bfrB* in *M. smegmatis* wild type and *ideR* mutant background

Strain	**IdeR**	**β-galactosidase specific activity**[a]			
M. smegmatis		Low iron[b]		High iron[b]	
		No compound	F1082(10µg/ml)	No compound	F1082(10µg/ml)
SM60 (pSM128)	+	0.49 ± 0.3	0.72 ± 0.07	0.54 ± 0.4	0.58 ± 0.2
SM160 (*bfrB-LacZ*)	+	7.20 ± 5	9.56 ± 7	135.40 ± 5	197.45 ± 4
SM193 (*mbtB-LacZ*)	+	133.0 ± 0.5	151.0 ± 8	19.1 ± 8	19.0 ± 6

[a]Nanomoles of nitrophenol/min/mg protein. The values obtained with strains carrying pSM128 have not been subtracted from the values obtained with other transformed strains. Values are the mean ± standard deviation of three independent experiments with each done in duplicate.

[b]Low iron, MM medium chelex treated, high iron, MM chelex treated and supplemented with 100 µM/ml $FeCl_3$.

The work done so far nullifies our first two hypotheses. The results suggest that F1082 is not an iron chelator, since it was more active in high iron than in low iron media. Secondly we have shown that F1082 requires intracellular iron for most activity, since the *irtAB* mutant offered tolerance to the compound. Finaly, the results of three independent experiments show that F1082 does not interfere directly with IdeR activity in iron regulation. The role of iron in F1082 activity is still unknown, although it appears to be key to its (F1082) activity.

4.4.3.3 Testing whether F1082 activity involves generation of oxidative stress.

A working hypothesis for F1082 is that it could be generating or exacerbating oxidative stress via modulation of iron availability. Since bacterial pathogens encounter different environments during the process of pathogenesis, adaptive responses and modulation of virulence gene expression are required

for their survival (Miller *et al*., 1989). Response to oxidative stress is a crucial factor for the survival of aerobic pathogens.

Therefore, we used *M. smegmatis* strains defective in protection against oxidative stress and tested their susceptibility to F1082. Table 4.4.17 shows the susceptibility of a *M. smegmatis* (sodA) mutant to F1082 or hydrogen peroxide (H_2O_2) when compared to the wild type. The results show that hydrogen peroxide effectively kills the mutant, since the MIC is one third (0.5 mM) that of the wild type. With F1082, it appears that the mutant survives as well as the wild type, since they have the same MICs (Table 4.5).

Table 4.5 MICs of F1082 and H_2O_2 for *M. smegmatis* WT and SOD mutant as determined by Alamar Blue**.**

Agent	MICs	
	Wild type	SM90 (sodA)
F1082	40 (µg/ml) ± 0.06	40 (µg/ml) ± 0.04
H_2O_2	1.5 (mM) ± 0.05	0.5 (mM) ± 0.08

Values are the mean ± standard deviation of two independent experiments with each done in duplicate.

A combination of the two compounds (F1082 and hydrogen peroxide) activity on the growth of *M. smegmatis* wild type was tested. A combination of the two compounds does not show enhanced activity (Figure 4.7 B) against wild type *M. smegmatis*. However we see enhanced activity of the same combination on a (sodA) mutant (Figure 4.8). It is possible that F1082 generates more oxidative stress in combination with hydrogen peroxide, which is not tolerated by the (sodA) mutant. This could

be interpreted thus: F1082 exacerbates the generation of oxidative stress in the presence of hydrogen peroxide.

In Figure 4.7 (A) it can be seen that the most growth inhibitory concentration for hydrogen peroxide appeared to be 1.6 mM whereas it was 40 µg/ml for F1082. Other (lower) concentrations gave less than 10% growth inhibition. For the combined effect of the two compounds we used the concentrations that gave minimal inhibition alone i.e. hydrogen peroxide at 0.8 mM (35% inhibition) and F1082 at 20 µg/ml (30% inhibition) (Figure 4.7 A). In combination, these two concentrations did not show much growth inhibition against *M. smegmatis* as shown in Figure 4.7 B. This can be interpreted to mean that *M. smegmatis* WT appears to cope well with the oxidative stress generated by the two compounds in combination.

A

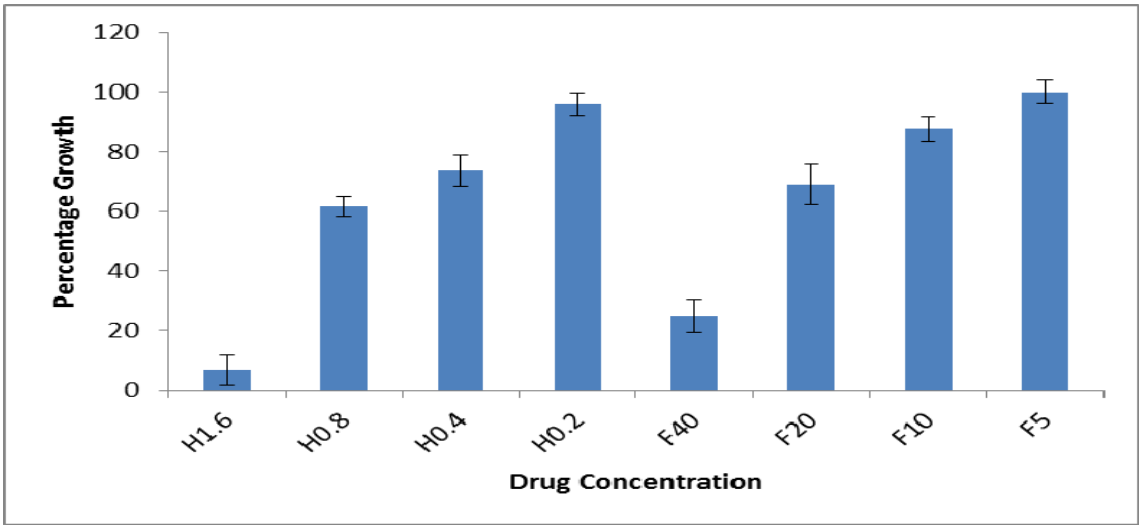

B

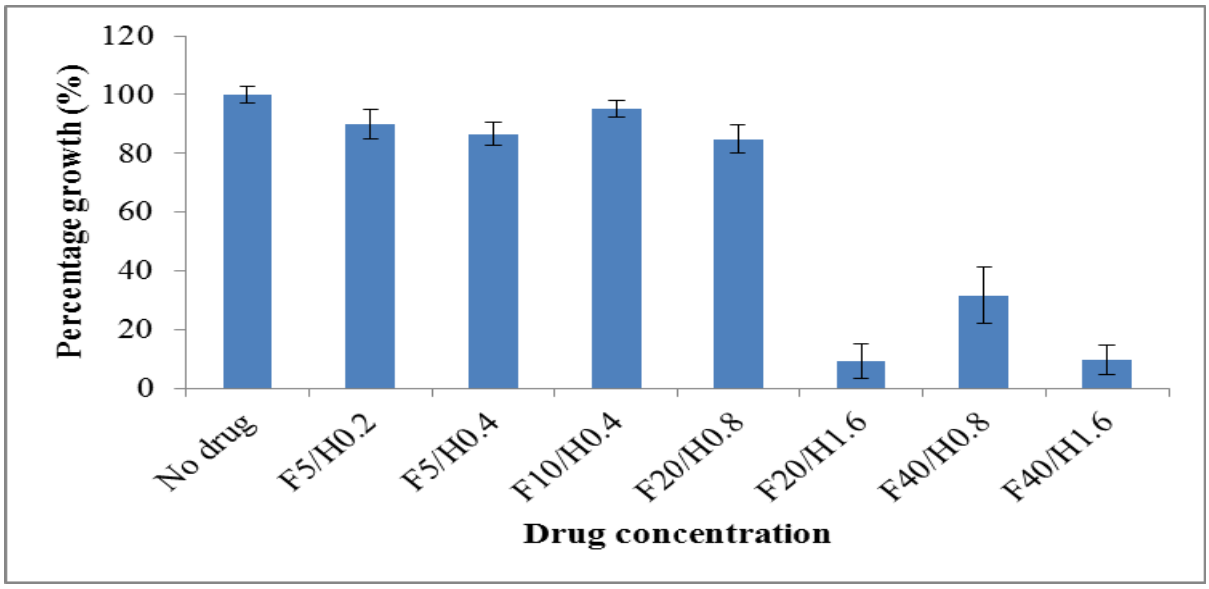

Figure 4.7 *M. smegmatis* WT grown in the presence of varying concentrations(A) of hydrogen peroxide (H) range from 0.2 to 1.6 mM alone and F1082 (F) range from 5 to 40 µg/ml alone; (B) combination effect of the (F and H) compounds. Where H: hydrogen peroxide and F: F1082**.** Errors bars represent mean standard deviation of three indepent experiment with each done in duplicate.

However when we considered the same drug combination in an *M. smegmatis* superoxide dismutase mutant (SOD), we observed a significant growth inhibitory effect of the two compounds in combination, showing more than 90% growth inhibition (Figure 4.8). Since a sodA mutant is more susceptible to oxidative stress generating molecules/compounds, it may be concluded that F1082 generates oxidative stress or exacerbates the generation of oxidative stress in combination with other oxidative stress generating molecules in *M. smegmatis.*

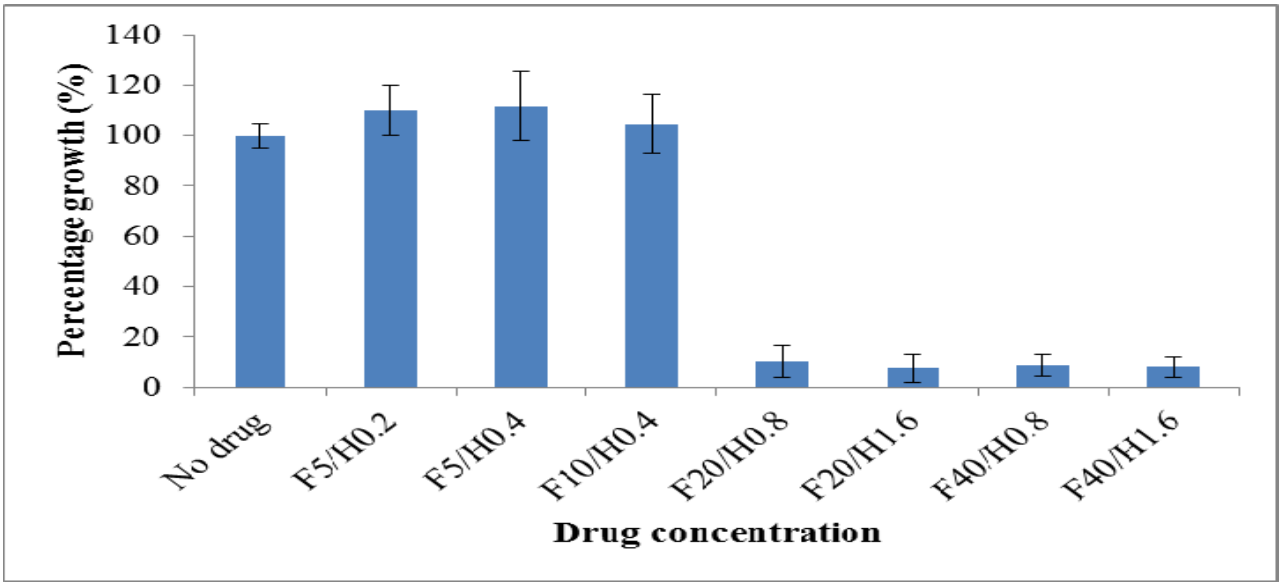

Figure 4.8 Combination effect of F1082 with H_2O_2 in *M. smegmatis* (SOD) mutant. Errors bars represent mean standard deviation of three indepent experiment with each done in duplicate.

Since it has now been shown that the *M. smegmatis* (sodA) mutant is more susceptible to F1082 in combination with hydrogen peroxide, it would be of interest to show the same or a similar effect in *M. tuberculosis* strains that are more susceptible to oxidative stress. Although *M. tuberculosis* strains with sodA deletion were not available, we used *M. tuberculosis* strains that are more susceptible to oxidative stress owing to mutations in the mycothiol genes (mshA) (Vilchèze *et al*., 2008). The mshA mutant lacks the ability to synthesize the enzyme involved in the first step of mycothiol biosynthesis (Vilchèze *et al*., 2008). Mycothiol has wide range of functions that include detoxification of electrophilic compounds, conjugation with antibiotics, and maintenance of the redox potential within the cell (Jothivasan and Hamilton, 2008) (Newton *et al*., 2008); (Rawat *et al*., 2007) and therefore susceptible to oxidative stress. *M. tuberculosis* H37Rv WT and H37Rv mshA mutant were grown in the BACTEC 460 system [described in Materials and Methods, Chapter 2 (section 2.1)] with various concentrations of F1082. The results show that the mshA mutant was more susceptible to F1082 at 2 µg/ml giving an 80% inhibition of growth compared to 20% growth inhibition in the wild type (Figure

4.9). We therefore suggest that the F0182 mode of action is via the generation of oxidative stress in mycobacteria.

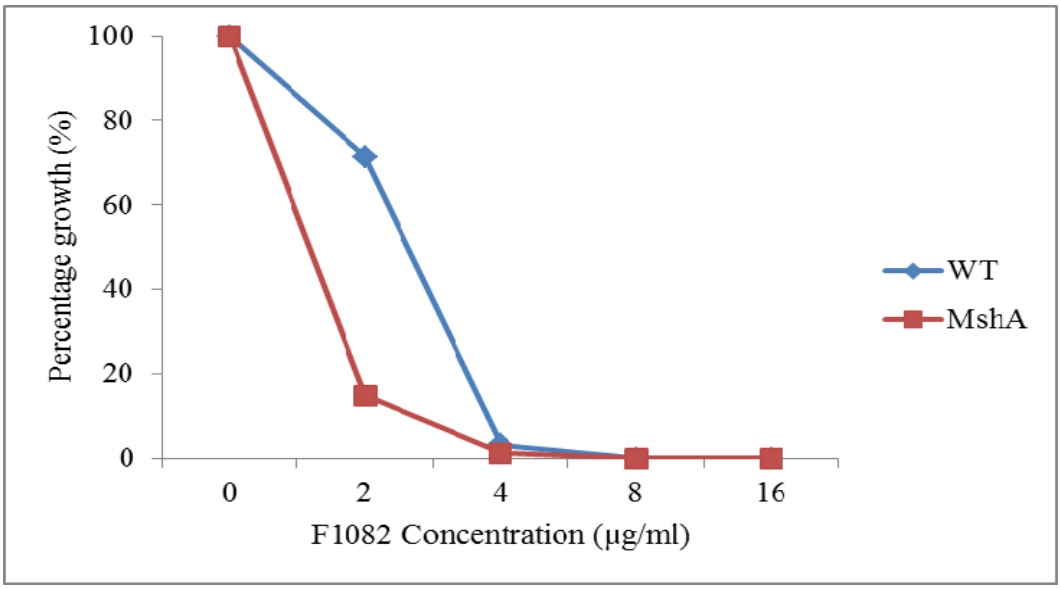

Figure 4.9 Dose response curve of *M. tuberculosis* CDC 1551 and mshA mutant strains to F1082 exposure.

Summary

In this Chapter we have explored a number of hypotheses which emerged from the results from *M. tuberculosis* microarray gene profiling. In our earlier results we have shown that F1082 is more active under high iron condition (Table 4.3). This latest work dismissed the hypothesis that F1082 could be an iron chelator as it would have been more effective in low iron conditions. This prompted us to investigate whether F1082 exerts its activity via intracellular or extracellular activity. An *irtAB* mutant (incapable of transporting iron into the cell) was resistant to F1082. This could imply that F1082 requires transportation through irtAB transport or that F1082 requires sufficient intracellular iron to exert its effect. The first hypothesis can be dismissed since F1082 was most effective against H37Rv grown under high iron conditions where the strain has efficient irtAB transport. The least activity shown under low iron conditions could be as a result of residual trace amounts of intracellular iron in the mycobacterium or probably by other less efficient/redundant iron transport systems which may

exist in the mycobacteria but are less efficient than the irtAB transport systems (Rodriguez and Smith, 2006). The results support the second hypothesis, viz. that F1082 exerts activity preferably under high intracellular iron conditions.

In *M. tuberculosis* the availability of iron is regulated by IdeR and the expression of *mbt* genes is subject to IdeR inactivation (Schnappinger *et al*., 2003) or depleted amount of intracellular iron (Rodriguez *et al*., 2002). Our results show that F1082 does not interfere with IdeR (Table 4.4). Therefore it seems that under F1082 treatment, *M. tuberculosis* reacts as if under low iron conditions. It has been published that excessive iron in mycobacteria allows generation of oxidative stress via the Fenton reaction and we have shown that F1082 requires sufficient intracellular iron to exert its effects. It could be possible that available intracellular iron is used somehow by F1082, resulting in *M. tuberculosis* sensing low iron conditions.

We have also shown that in *M. smegmatis*, F1082 in combination with hydrogen peroxide generates oxidative stress. This stress is less tolerated in a sodA mutant compared to wild type (Figure 4.9). It could then be hypothesised that in the presence of other molecules generating oxidative stress, F1082 exacerbates the generation of oxidative stress. The effect of F1082 on a *M. tuberculosis* mutant deficient in protection against oxidative stress was tested. This was a *M. tuberculosis* mshA mutant deficient in mycothiol production and was tested initially with INH and was found to be sensitive to INH at 0.06 µg/ml, consistent with published data (Vilchèze *et al*., 2008). The mycothiol (MSH) functions as general-use detoxification agent against antibiotics, alkylating agents, electrophiles and other endogenous and exogenous reactive intermediates(Rawat *et al*., 2002). The *M. tuberculosis* mshA mutant was more susceptible to F1082 compared to the wild type (Figure 4.9). This suggests that F1082 generates oxidative stress in *M. tuberculosis* which inhibits growth. The co- involvement of oxidative stress in growth which varies between *M. smegmatis* and *M. tuberculosis* could be possibly thus: *M. smegmatis* has evolved as an environmental saprophyte and may have developed alternative systems to cope with oxidative and nitrosative stressors. In contrast, *M. tuberculosis* faces a far different environment in the human host.

A definitive mechanism of action of F1082 remains to be explored through target identification; however, this work has shown the involvement of oxidative stress in F1082 activity. In addition it suggests that iron regulatory and acquisition pathways remain important for anti-TB drug development.

Appendix 4A

I. B-galactosidase activity determination

This method describes the classic colorimetric assay for ß-galactosidase widely used in early studies of *lac* gene expression. It provides a simple, reliable and economical quantitative estimate of *LacZ* expression by measuring enzyme activity directly. The assay was essential to the exploitation of the lac operon as a model system for the study of gene regulation.

β-Galactosidase is able to hydrolyze β-D-galactosides. This enzyme facilitates growth on carbon sources such as lactose by cleaving it into a molecule of glucose and a molecule of galactose, which the cells can catabolize and used for growth. In the assay described below, the artificial chromogenic substrate ortho-nitrophenyl-β-D-galactopyranoside (ONPG) is used in place of lactose. When the β-galactosidase cleaves ONPG, ortho-nitrophenol is released. ONPG is colorless, while the product compound has a yellow color, and absorbs light (λmax = 420 nm). Therefore, enzyme activity can be measured by the rate of appearance of yellow color using a spectrophotometer**.**

β-Galactosidase assay

- Strains of *M. smegmatis* grown in 15 ml LI or HI (100 µM $FeCl_3$) to OD_{600} 0.8
- Centrifuge the cells at 5000 rpm for 5 min at 4°C
- Resuspend the pellets (pellets of 15 ml bacterial cultures) in phosphate buffer saline (PBS) (30 ml), centrifuge and store the pellets at -80°C until use or proceed with the following steps
- Resuspent the pellets in 800 µl of Z-buffer
- Bead beat the cells with 200 µl of beads for 30 sec, two times
- Centrifuge at maximum speed in micro centrifuge for 5 min

- Collect the supernatant (extract). Keep 50-100 µl for protein concentration determination (OD_{600})

Reaction

- Keep 200 or 50 µl of extract in a tube at 30°C for (equilibration of the extract) for 5 min
- Add 600 µl of buffer Z with β-mecaptoethanol (30 µl of β-mecaptoethanol /15 ml Z buffer)
- Add 200 µl of o-nitrophenyl-b-D-galactopyraniside (ONPG) – substrate for β-galactosidase) (4 mg/ml stock in buffer Z with β-ME {30 µl of β-ME/15 ml Z buffer}). Record the time (time of starting the reaction)
- Stop the reaction, when the reaction mix starts turning visually yellow, by adding 400 µl of 1M Na_2CO_3 . Again record the time (time of reaction termination), this time duration will be the reaction time
- Read OD_{420nm}

Miller units: 1000 * (OD_{420}/ (T * V *OD_{600}[protein concentration])

Solutions for β-galactosidase assays

Z buffer, per 50 mL:

- O.80g $Na_2HPO_4.7H_2O$ (0.06M)
- 0.28g $NaH_2PO_4.H_2O$ (0.04M)
- 0.5 mL 1M KCl (0.01M)
- 0.05 mL 1M $MgSO_4$ (0.001M)
- 0.135 mL β -mercaptoethanol (BME) (0.05M)

- bring to approximately 40 mL with H_2O, dissolve all the salts
- adjust the pH to 7.0
- use a graduated cylinder to bring the buffer to 50 mL
- store at 4° C for no more than a few days.

ONPG (4 mg/ml) (Sufficient for 100 assays -- make fresh daily)

80 mg o-nitrophenyl-ß-D-galactoside (o-nitrophenyl-ß-D-galactopyranoside)

20 ml dH_2O

1 M Na_2CO_3 (Sufficient for 100 assays -- store in refrigerator)

5.3 g Na_2CO_3

50 ml dH_2O

β-mercaptoethanol (βME) is added to the reaction buffer to stabilize the β-galactosidase enzyme. The important part of BME is a reactive thiol (SH group). Thiols react with oxygen in the air and oxidize (inactivate) over time. Therefore, one must not make more Z buffer than will be used in a few days. Store the unused portion at 4° C.

O-nitrophenyl-b-D-galactopyraniside (ONPG) should be dissolved fresh each day. Dissolve the ONPG to a final concentration of 4mg/mL in 0.1M phosphate buffer pH 7.0.

Phosphate buffer, per 100 mL:

- 1.61g $Na_2HPO_4.7H_2O$ (0.06M)
- 0.55g $NaH_2PO_4.H_2O$ (0.04M)

- adjust the pH to 7.0
- phosphate buffer is stable at room temperature and does not need to be made fresh each time.

What is sufficient yellow colour? To get the most accurate measure of activity, the absorbance at 420 nm (A_{420}) should range from 0.6 to 0.9. Readings as low as 0.1 and as high as 1.2 are acceptable. Tubes that have become as yellow as a tube of (unused) LB broth will probably be sufficiently yellow.

If the reading is too low, the assay can be tried again with more cells or longer incubation time. When the promoter is not expressed to any meaningful extent, it will probably take hours to develop enough yellow colour. If a control starts to turn yellow (after several or more hours) it means that the substrate is beginning to auto-hydrolyze. The assay can be left overnight. The auto-hydrolysis is then accounted for by subtracting the A_{420} and A_{500} of the negative control from that of the tests before doing any further calculations.

If the reading is too high, try the assay again with fewer cells. Aim to stop the reaction after 15 minutes. For example, if in at first attempt, 0.5 mL of cells + 0.5 mL of Z buffer were added, and it was too yellow after 5 minutes, try adding 0.1 mL cells + 0.9 mL of Z buffer. Watch the tube carefully. Some cultures may have to be diluted even further.

Adding the 1 M Na_2CO_3 stops the reaction by raising the pH of the solution to 11. At this pH the enzyme is not active.

The reading at 420 nm is a combination of absorbance by o-nitrophenol and light scattering by cell debris. The absorbance at 550 corrects for light scattering. There is no absorbance from o-nitrophenol at this wavelength. The light scattering at 420 nm is proportional to that at 550 nm:

light scattering at 420 nm = 1.75 x OD_{550}

Use the following equation to calculate units of enzyme activity:

Miller Units = $1000 \times [(OD_{420} - 1.75 \times OD_{550})] / (T \times V \times OD_{600})$

- OD_{420} and OD_{550} are read from the reaction mixture.
- OD_{600} reflects cell density in the washed cell suspension.
- T = time of the reaction in minutes.
- V = volume of culture used in the assay in mLs.

The units give the change in A_{420}/min/mL of cells/OD_{600}

(Conversion of the raw data is necessary)

The sample activity of enzyme present in a sample is a rate, or velocity, value: how much yellow colour develops after incubation for a specific time. $\lambda A_{420} min^{-1}$. These total activity values alone are not very informative because two assay tubes may have different cell concentrations. Rather, it is important to know the enzyme activity level relative to the cell biomass. This quantity can be called a specific activity.

To get a specific activity from sample activity one must take into account the volume of cell culture put in the sample and the biomass concentration of the culture. Firstly standardize sample activity values on the basis of 1.0 ml of culture. So, the units of the standardized sample activity would be $\lambda A_{420} min^{-1} ml^{-1}$. Lastly, use OD_{600} readings of the culture as a standard measure of cell biomass. Therefore specific activity values are in

$\lambda A_{420} min^{-1} ml^{-1} OD_{600}^{-1}$.

For this experiment data is collected in five points:

- Sample volume in ml
- λ A_{420} (a measure of ONP produced)
- OD_{550} to correct for light scattering
- incubation time in minutes
- OD_{600} of the culture (as measure of biomass)

Typical values:

a fully induced lac^+ operon (+IPTG) = 1500 units

an uninduced lac^+ operon (no IPTG) = 1.5-3 units

II. Growth assay-Alamar Blue Assay

Inoculate *M. tuberculosis* strains from frozen stocks to 7H10 supplemented with 0.2% glycerol, 0.05% Tween 80 and 10% albumin-dextrose-NaCl-complex (ADN) agar plates and incubate at 37°C for 5-8 days. Take swab and inoculate in a MM medium with no iron to an OD_{540} 0.1 (1 x 10^7 cfu/ml).

- Add 200 µl of sterile deionised water to all outer-perimeter wells of the 96 well plate (minimize evaporation of medium in test wells during incubation.
- Wells in rows B to G in columns 3 to 11 receive 100 µl of the medium (Fe + or Fe -)
- Add 100 µl of 2 x drug solution to well in rows B to G I columns 2 and 3
- By using multichannel pipette transfer 100 µl from column 3 to 4 and mix the contents well
- Identical serial 1:2 dilution are continued through column 10, and 100 µl of excess medium is discarded from wells in column 10

- Inoculate 100 µl of *M. tuberculosis* (1 x 10^5 cfu/ml) inoculums in wells in row B to G in columns 2 to 11 (yielding a final volume of 200 µl per well), thus the wells in column 11 serve as a drug-free (inoculum only) controls.
- The plates are sealed with Parafilm and incubated at 37°C for 5 days.
- Add 50 µl of a freshly prepared 1:1 mixture of 10 x Alamar Blue reagent and 10% Tween 80 to wells in B11
- Re-incubate the plates at 37°C for 24 hours.
- If well in B11 turned pink, the reagent mixture is added to all the wells in the microplate (if the wells remained blue, the reagent mixture is added to another control well and the results will be read on the following day)
- The microplates are sealed with Parafilm and incubated at 37°C for another 24 hours, and the colours of all the wells are recorded.
- A blue colour in the well is interpreted as no growth, and a pink colour is scored as growth.
- The MIC is defined as the lowest concentration which prevented a colour change from blue to pink

III Protein concentration and pSM plasmid

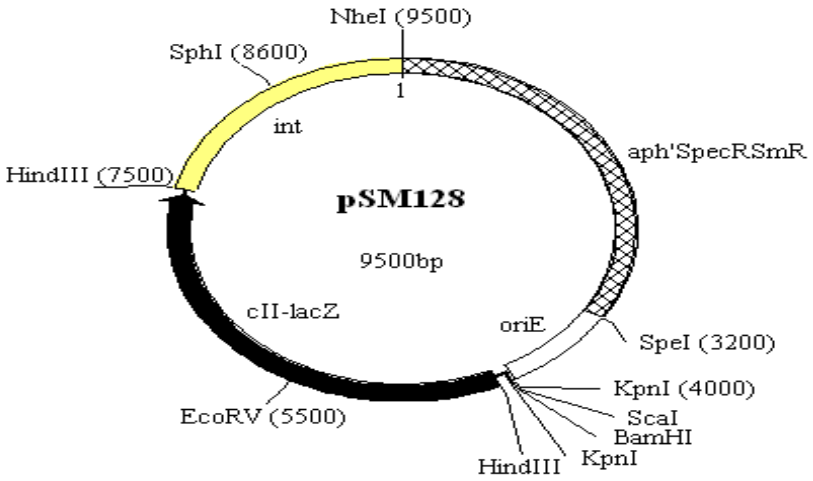

Figure 4.3 The structure of the pSM128 plasmid

Table 4.2 Standard BSA solution preparation

[BSA] µg/ml	Volume (µl) of 5mg/ml BSA Stock	Volume (µl) of MilliQ water
0.5	10	90
1.0	20	80
1.5	30	70
2.0	40	60
2.5	50	50
3.0	60	40
3.5	70	30
4.0	80	20
4.5	90	10
5.0	100	0

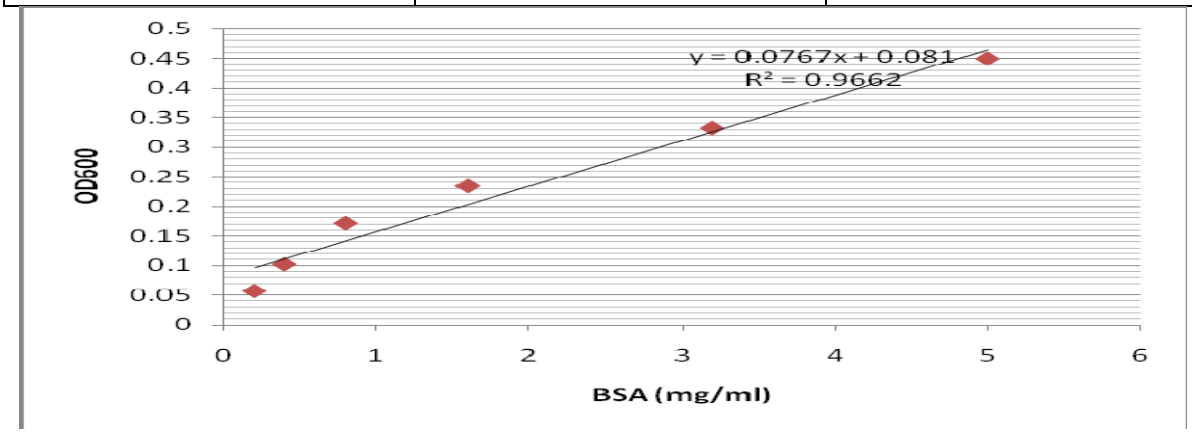

Figure 4.4 BSA standard curve for protein determination of extracts from *M. smegmatis* for β-galactosidase activity determination.

CHAPTER FIVE

Conclusions

The advent of MDR/XDR TB has highlighted the need for the discovery of novel compounds with activity against *M. tuberculosis* (Raviglione, 2007). These new compounds would ideally not only kill *M. tuberculosis*, but would also shorten regimen times, be compatible with antiretroviral drugs, active against non-replicating persisters (NRP), and act through different mechanisms of action from those employed by the existing front-line and second-line anti-TB drugs. In this study we evaluated the activity of a candidate compound (F1082) on the growth of *M. tuberculosis* and the mechanism by which it inhibits *M. tuberculosis* growth. F1082 is a furanone based compound; furanones are endowed with an array of biological activities (anti-fungal, antibacterial, anticancer activities). In the context of medicinal chemistry, a chemically tractable "hit" or "lead" molecule is one that lends itself to the synthesis of a diverse range of analogues. In this regard the mucohalic (mucobromic and mucochloric) acid furanones represent attractive starting points. These compounds are highly functionalized molecules, which makes them useful as building blocks to make functionalized and diverse new pharmacologically relevant furanones. From our starting synthetic product (F1082), a furanone, our collaborators were able to synthesise 92 furanone based compounds. These compounds were screened for anti-*M. tuberculosis* activity to improve on the activity of the original F1082. Our research efforts directed towards the development of antituberculosis agents, lie in the direction of discovering new classes of compounds, which have a different mechanism of action from known anti-TB drugs. The current work describes the identification of a novel 2(5H)-furanone (F1082) with anti-TB activity and its potential to be developed into anti-TB candidate drug.

The anti-*M. tuberculosis* activity of F1082 (MIC 8 μg/ml) and selective activity for mycobacteria provided the basis for selecting F1082 as a "hit". It did not inhibit growth of other selected Gram-positive and Gram-negative bacteria. These results are supported by published data in the literature that brominated furanones in general are known to inhibit quorum sensing by interfering with Type 1 and Type 2 auto-inducers (Ren *et al*., 2001) but do not inhibit growth of the organism at quorum sensing concentrations. Although in some published data it has been reported that brominated furanones inhibit growth of Gram –positive bacteria, such as *Bacillus subtilis*, at high concentrations

of up to 150 µg/ml (Ren *et al*., 2004), such high concentrations were not used in this work and therefore suggest that the selectivity for mycobacteria may be concentration dependent.

In order for any compound to be developed into a drug candidate, it has to satisfy a number of criteria. F1082 was tested against clinical isolates and was found to inhibit the growth of pan-susceptible and MDR/XDR clinical isolates in the same way as the *M. tuberculosis* laboratory strain H37Rv, a criterion for desired new compounds for TB drug development. This also suggests that F1082 may have a different mechanism of action since it does not show cross-resistance with the current TB drugs. Furthermore it synergizes with the rifampicin. This forms the basis of potential for a good TB candidate drug since TB is treated by combination therapy. We have shown that F1082 can be bactericidal to *M. tuberculosis* growth, although this is concentration dependent. At its (lower) bacteriostatic concentration, it has been shown to improve the mycobacterial killing effect when used in combination with some of the frontline drugs (additive effect with INH and synergistic with rifampicin). However the cytotoxic effect of F1082 to human cell lines still needs to be overcome for the compound to be effectively used for TB drug development. We hope that cytotoxicity can eventually be overcome through generation of derivatives. The derivatives synthesized so far have shown reduced cytotoxicity with concomitant increase of the killing effect of the compound (Table 2.1).

The studies of the mechanism of action by microarray gave an indication of the mechanism/s of action. These observations led to a speculation that F1082 inhibits the growth of *M. tuberculosis* via the generation of oxidative stress that is iron dependent, since this work demonstrated reduced F1082 activity under intracellular iron deprivation in both *M. tuberculosis* and *M. smegmatis*. This has been confirmed by studying mutants incapable of iron uptake and shown to be resistant to F1082 when grown under iron rich conditions. Furthermore, mutants lacking genes that provide protection against oxidative stress were more susceptible to F1082. It is possible that F1082 generates or exacerbates oxidative stress in its mode of action. When superoxide (O_2^-) and hydrogen peroxide are allowed to interact in the presence of a Harber-Weiss catalyst such as iron, hydroxyl radicals are formed (Kehrer,

2000). It could be that F1082, when taken up by mycobacteria, form intermediates that conjugate or complex with iron leading to a condition of oxidative stress. Consequences of oxidative stress are nucleic acid damage, protein damage, lipid beta-oxidation and subcellular organelle damage that could account for the transient reduction of the bacterial load. One unifying hypothesis is that membrane proteins involved in iron transport, chelation, or storage act as sites for catalysis of hydroxyl radicals (Mietzner *et al*., 1984). Hydroxyl radicals formed at these sites could cause a lethal increase in membrane permeability (Albrich *et al*., 1986) or damage to iron-rich enzyme complexes. In the absence of extracellular iron, these sites may not be subjected to oxidation. Since F1082 was shown to be bacteriostatic (concentration dependent), it is more likely that cellular protein molecules are targeted by the compound at bacteriostatic activity and do not cause direct or indirect DNA damage which is more likely a feature of bactericidal activity. Alternatively, as the fragments of the molecule are degraded (Chapter 2, section 2.3.5) it is possible that F1082 may have more than one target. However we have shown experimentally that F1082 may generate of oxidative stress.

It has been supported (Kohanski *et al*., 2007) that bacteriostatic compounds inhibit protein biosynthesis. However DNA damage is attributed to bactericidal compounds. F1082 may be generally bacteriostatic and bactericidal, depending on concentration. Interestingly, another characteristic of the brominated furanones is their anti-fungal and carcinogenic activity. It has been reported that non-mutagenic carcinogen induce oxidative DNA damage (Kawanishi *et al*., 2002) whilst weakly mutagenic carcinogen like hydrazine derivatives induce metal-dependent oxidative DNA damage (Ito *et al*., 1992). Based on the results we speculate that F1082 inhibits the growth of *M. tuberculosis* by generating oxidative stress in the presence of free iron.

This work provided a better understanding of the furanones and specifically F1082 as possible lead compounds for TB drug development. The study observations generated pave the way for future development of this compound. Resulting from this work, the four compounds (JP 206, JP210, JP216 and JP 223) in (Table 2.1 in results chapter 2) already present a positive development. Derivatives with low cytotoxicity can be further studied in an animal model for efficacy, whereafter more

derivatives can be synthesized to optimize activity and cytotoxicity. It is to be hoped that this work will be a cornerstone in driving the search for novel compounds to upscale the TB drug pipe-line and perhaps deliver one or more compounds that can enter clinical trials.

References:

Aaby, P., Shaheen, S.O., Heyes, C.B., Goudiaby, A., Hall, A.J., Shiell, A.W., Jensen, H., and Marchant, A. (2000). Early BCG vaccination and reduction in atopy in Guinea-Bissau. Clin. Exp. Allergy *30*, 644–650.

Agarwal, A.K., Rogers, P.D., Baerson, S.R., Jacob, M.R., Barker, K.S., Cleary, J.D., Walker, L.A., Nagle, D.G., and Clark, A.M. (2003). Genome-wide expression profiling of the response to polyene, pyrimidine, azole, and echinocandin antifungal agents in Saccharomyces cerevisiae. J. Biol. Chem *278*, 34998–35015.

van Agtmael, M.A., Eggelte, T.A., and van Boxtel, C.J. (1999). Artemisinin drugs in the treatment of malaria: from medicinal herb to registered medication. Trends Pharmacol. Sci *20*, 199–205.

Ahmad, Z., Minkowski, A., Peloquin, C.A., Williams, K.N., Mdluli, K.E., Grosset, J.H., and Nuermberger, E.L. (2011). Activity of the fluoroquinolone DC-159a in the initial and continuation phases of treatment of murine tuberculosis. Antimicrob. Agents Chemother. *55*, 1781–1783.

Alam, M.M., Husain, A., Hasan, S.M., Khanna, S., and Shaquiquzzaman, M. (2010). 3-arylidene-5-(4-isobutylphenyl)-2(3H)-furanones: a new series of anti-inflammatory and analgesic compounds having antimicrobial activity. J Enzyme Inhib Med Chem *25*, 323–330.

Albrich, J.M., Gilbaugh, J.H., 3rd, Callahan, K.B., and Hurst, J.K. (1986). Effects of the putative neutrophil-generated toxin, hypochlorous acid, on membrane permeability and transport systems of Escherichia coli. J. Clin. Invest. *78*, 177–184.

Alcalá, L., Ruiz-Serrano, M.J., Pérez-Fernández Turégano, C., García De Viedma, D., Díaz-Infantes, M., Marín-Arriaza, M., and Bouza, E. (2003). In vitro activities of linezolid against clinical isolates of Mycobacterium tuberculosis that are susceptible or resistant to first-line antituberculous drugs. Antimicrob. Agents Chemother. *47*, 416–417.

Ali-Vehmas, T., Louhi, M., and Sandholm, M. (1991). Automation of the resazurin reduction test using fluorometry of microtitration trays. Zentralblatt Veterinarmedizin Reihe B *38*, 358–372.

Andersen, P., and Doherty, T.M. (2005). The success and failure of BCG - implications for a novel tuberculosis vaccine. Nat. Rev. Microbiol. *3*, 656–662.

Andries, K., Verhasselt, P., Guillemont, J., Göhlmann, H.W.H., Neefs, J.-M., Winkler, H., Van Gestel, J., Timmerman, P., Zhu, M., Lee, E., *et al*. (2005). A diarylquinoline drug active on the ATP synthase of Mycobacterium tuberculosis. Science *307*, 223–227.

Ang, C.F., Ong, C.S., Rukmana, A., Pham Thi, K.L., Yap, S.F., Ngeow, Y.F., Ho, M.L., Sudiro, T.M., Bela, B., Jordaan, A.M., *et al*. (2008). An overview of the phenotypic and genotypic characteristics of multidrug-resistant Mycobacterium tuberculosis isolates from four Asian countries. J. Med. Microbiol. *57*, 1039–1040.

Aristoff, P.A., Garcia, G.A., Kirchhoff, P.D., and Hollis Showalter, H.D. (2010). Rifamycins--obstacles and opportunities. Tuberculosis (Edinb) *90*, 94–118.

Arriaza, B.T., Salo, W., Aufderheide, A.C., and Holcomb, T.A. (1995). Pre-Columbian tuberculosis in northern Chile: molecular and skeletal evidence. Am. J. Phys. Anthropol *98*, 37–45.

Ashtekar, D.R., Costa-Perira, R., Nagrajan, K., Vishvanathan, N., Bhatt, A.D., and Rittel, W. (1993). In vitro and in vivo activities of the nitroimidazole CGI 17341 against Mycobacterium tuberculosis. Antimicrob. Agents Chemother. *37*, 183–186.

Bakker-Woudenberg, I.A.J.M., van Vianen, W., van Soolingen, D., Verbrugh, H.A., and van Agtmael, M.A. (2005). Antimycobacterial agents differ with respect to their bacteriostatic versus bactericidal activities in relation to time of exposure, mycobacterial growth phase, and their use in combination. Antimicrob. Agents Chemother *49*, 2387–2398.

Balick, M.J. (1990). Ethnobotany and the identification of therapeutic agents from the rainforest. Ciba Found. Symp. *154*, 22–31; discussion 32–39.

Balunas, M.J., and Kinghorn, A.D. (2005). Drug discovery from medicinal plants. Life Sci *78*, 431–441.

Barry, C.E., 3rd, and Blanchard, J.S. (2010). The chemical biology of new drugs in the development for tuberculosis. Curr Opin Chem Biol *14*, 456–466.

Barry, C.E., 3rd, Boshoff, H.I., Dartois, V., Dick, T., Ehrt, S., Flynn, J., Schnappinger, D., Wilkinson, R.J., and Young, D. (2009). The spectrum of latent tuberculosis: rethinking the biology and intervention strategies. Nat. Rev. Microbiol. *7*, 845–855.

Barry, C.E., 3rd, Wilson, M., Lee, R., and Schoolnik, G.K. (2000). DNA microarrays and combinatorial chemical libraries: tools for the drug discovery pipeline. Int. J. Tuberc. Lung Dis *4*, S189–193.

Betts, J.C. (2002). Transcriptomics and proteomics: tools for the identification of novel drug targets and vaccine candidates for tuberculosis. IUBMB Life *53*, 239–242.

Betts, J.C., Lukey, P.T., Robb, L.C., McAdam, R.A., and Duncan, K. (2002). Evaluation of a nutrient starvation model of Mycobacterium tuberculosis persistence by gene and protein expression profiling. Mol. Microbiol *43*, 717–731.

Betts, J.C., McLaren, A., Lennon, M.G., Kelly, F.M., Lukey, P.T., Blakemore, S.J., and Duncan, K. (2003a). Signature gene expression profiles discriminate between isoniazid-, thiolactomycin-, and triclosan-treated Mycobacterium tuberculosis. Antimicrob. Agents Chemother *47*, 2903–2913.

Betts, J.C., McLaren, A., Lennon, M.G., Kelly, F.M., Lukey, P.T., Blakemore, S.J., and Duncan, K. (2003b). Signature gene expression profiles discriminate between isoniazid-, thiolactomycin-, and triclosan-treated Mycobacterium tuberculosis. Antimicrob. Agents Chemother *47*, 2903–2913.

Blaschitz, M., Hasanacevic, D., Hufnagl, P., Hasenberger, P., Pecavar, V., Meidlinger, L., Konrad, M., Allerberger, F., and Indra, A. (2011). Real-time PCR for single-nucleotide polymorphism detection in the 16S rRNA gene as an indicator for extensive drug resistance in Mycobacterium tuberculosis. J. Antimicrob. Chemother. *66*, 1243–1246.

Blumberg, H.M., Burman, W.J., Chaisson, R.E., Daley, C.L., Etkind, S.C., Friedman, L.N., Fujiwara, P., Grzemska, M., Hopewell, P.C., Iseman, M.D., *et al*. (2003). American Thoracic Society/Centers for Disease Control and Prevention/Infectious Diseases Society of America: treatment of tuberculosis. Am. J. Respir. Crit. Care Med *167*, 603–662.

Bolt, H.M. (2004). Rifampicin, a keystone inducer of drug metabolism: from Herbert Remmer's pioneering ideas to modern concepts. Drug Metab. Rev. *36*, 497–509.

Boshoff, H.I.M., Myers, T.G., Copp, B.R., McNeil, M.R., Wilson, M.A., and Barry, C.E., 3rd (2004). The transcriptional responses of Mycobacterium tuberculosis to inhibitors of metabolism: novel insights into drug mechanisms of action. J. Biol. Chem *279*, 40174–40184.

Brandt, L., Feino Cunha, J., Weinreich Olsen, A., Chilima, B., Hirsch, P., Appelberg, R., and Andersen, P. (2002). Failure of the Mycobacterium bovis BCG vaccine: some species of environmental mycobacteria block multiplication of BCG and induction of protective immunity to tuberculosis. Infect. Immun. *70*, 672–678.

Braun, V., and Killmann, H. (1999). Bacterial solutions to the iron-supply problem. Trends Biochem. Sci *24*, 104–109.

Brunborg, G., Holme, J.A., Søderlund, E.J., Hongslo, J.K., Vartiainen, T., Lötjönen, S., and Becher, G. (1991). Genotoxic effects of the drinking water mutagen 3-chloro-4-(dichloromethyl)-5-hydroxy-2[5H]-furanone (MX) in mammalian cells in vitro and in rats in vivo. Mutat. Res. *260*, 55–64.

Bryk, R., Gold, B., Venugopal, A., Singh, J., Samy, R., Pupek, K., Cao, H., Popescu, C., Gurney, M., Hotha, S., *et al*. (2008). Selective killing of nonreplicating mycobacteria. Cell Host Microbe *3*, 137–145.

Bugg, T.D.H., Lloyd, A.J., and Roper, D.I. (2006). Phospho-MurNAc-pentapeptide translocase (MraY) as a target for antibacterial agents and antibacterial proteins. Infect Disord Drug Targets *6*, 85–106.

Burman, W.J., Gallicano, K., and Peloquin, C. (1999). Therapeutic implications of drug interactions in the treatment of human immunodeficiency virus-related tuberculosis. Clin. Infect. Dis *28*, 419–429; quiz 430.

Butler, M.S. (2004). The role of natural product chemistry in drug discovery. J. Nat. Prod *67*, 2141–2153.

Calmette, A. (1931). Preventive Vaccination Against Tuberculosis with BCG. Proc. R. Soc. Med. *24*, 1481–1490.

Campbell, E.A., Korzheva, N., Mustaev, A., Murakami, K., Nair, S., Goldfarb, A., and Darst, S.A. (2001). Structural mechanism for rifampicin inhibition of bacterial rna polymerase. Cell *104*, 901–912.

Cantrell, H.F., Lombardy, E.E., Duncanson, F.P., Katz, E., and Barone, J.S. (2004). Declining susceptibility to neomycin and polymyxin B of pathogens recovered in otitis externa clinical trials. South. Med. J. *97*, 465–471.

Chambers, H.F., Turner, J., Schecter, G.F., Kawamura, M., and Hopewell, P.C. (2005). Imipenem for treatment of tuberculosis in mice and humans. Antimicrob. Agents Chemother *49*, 2816–2821.

Chandir, S., Chandir, S., Hussain, H., Salahuddin, N., Amir, M., Ali, F., Lotia, I., and Khan, A.J. (2010). Extrapulmonary tuberculosis: a retrospective review of 194 cases at a tertiary care hospital in Karachi, Pakistan. J Pak Med Assoc *60*, 105–109.

Chen, P., Gearhart, J., Protopopova, M., Einck, L., and Nacy, C.A. (2006). Synergistic interactions of SQ109, a new ethylene diamine, with front-line antitubercular drugs in vitro. J. Antimicrob. Chemother. *58*, 332–337.

Clark, G.A., Kelley, M.A., Grange, J.M., and Hill, M.C. (1987). The evolution of mycobacterial disease in human populations: a reevaluation. Curr. Anthropol *28*, 45–62.

Cohen, N.R., Garg, S., and Brenner, M.B. (2009). Antigen Presentation by CD1 Lipids, T Cells, and NKT Cells in Microbial Immunity. Adv. Immunol. *102*, 1–94.

Cole, S.T., Brosch, R., Parkhill, J., Garnier, T., Churcher, C., Harris, D., Gordon, S.V., Eiglmeier, K., Gas, S., Barry, C.E., 3rd, *et al*. (1998a). Deciphering the biology of Mycobacterium tuberculosis from the complete genome sequence. Nature *393*, 537–544.

Cole, S.T., Brosch, R., Parkhill, J., Garnier, T., Churcher, C., Harris, D., Gordon, S.V., Eiglmeier, K., Gas, S., Barry, C.E., 3rd, *et al*. (1998b). Deciphering the biology of Mycobacterium tuberculosis from the complete genome sequence. Nature *393*, 537–544.

Collins, L., and Franzblau, S.G. (1997). Microplate alamar blue assay versus BACTEC 460 system for high-throughput screening of compounds against Mycobacterium tuberculosis and Mycobacterium avium. Antimicrob. Agents Chemother *41*, 1004–1009.

Cooper, A.M., Mayer-Barber, K.D., and Sher, A. (2011). Role of innate cytokines in mycobacterial infection. Mucosal Immunol *4*, 252–260.

Costerton, J.W., Lewandowski, Z., Caldwell, D.E., Korber, D.R., and Lappin-Scott, H.M. (1995). Microbial biofilms. Annu. Rev. Microbiol *49*, 711–745.

ten Dam, H.G. (1984). Research on BCG vaccination. Adv Tuberc Res *21*, 79–106.

Daniel, T.M. (2006). The history of tuberculosis. Respir Med *100*, 1862–1870.

Dannenberg, A.M., Jr, Schofield, B.H., Rao, J.B., Dinh, T.T., Lee, K., Boulay, M., Abe, Y., Tsuruta, J., and Steinbeck, M.J. (1994). Histochemical demonstration of hydrogen peroxide production by leukocytes in fixed-frozen tissue sections of inflammatory lesions. J. Leukoc. Biol. *56*, 436–443.

Davies, G.R. (2010). Early clinical development of anti-tuberculosis drugs: science, statistics and sterilizing activity. Tuberculosis (Edinb) *90*, 171–176.

Deleu, D., Hanssens, Y., and Northway, M.G. (2004). Subcutaneous apomorphine : an evidence-based review of its use in Parkinson's disease. Drugs Aging *21*, 687–709.

Delogu, G., and Fadda, G. (2009). The quest for a new vaccine against tuberculosis. J Infect Dev Ctries *3*, 5–15.

Diacon, A.H., Dawson, R., Hanekom, M., Narunsky, K., Maritz, S.J., Venter, A., Donald, P.R., van Niekerk, C., Whitney, K., Rouse, D.J., *et al*. (2010). Early bactericidal activity and pharmacokinetics of PA-824 in smear-positive tuberculosis patients. Antimicrob. Agents Chemother. *54*, 3402–3407.

Diacon, A.H., Dawson, R., Hanekom, M., Narunsky, K., Venter, A., Hittel, N., Geiter, L.J., Wells, C.D., Paccaly, A.J., and Donald, P.R. (2011). Early bactericidal activity of delamanid (OPC-67683) in smear-positive pulmonary tuberculosis patients. Int. J. Tuberc. Lung Dis. *15*, 949–954.

Diacon, A.H., Patientia, R.F., Venter, A., van Helden, P.D., Smith, P.J., McIlleron, H., Maritz, J.S., and Donald, P.R. (2007). Early bactericidal activity of high-dose rifampin in patients with pulmonary tuberculosis evidenced by positive sputum smears. Antimicrob. Agents Chemother. *51*, 2994–2996.

Disratthakit, A., and Doi, N. (2010). In vitro activities of DC-159a, a novel fluoroquinolone, against Mycobacterium species. Antimicrob. Agents Chemother. *54*, 2684–2686.

Donoghue, H.D. (2009). Human tuberculosis--an ancient disease, as elucidated by ancient microbial biomolecules. Microbes Infect *11*, 1156–1162.

Dooley, K.E., and Chaisson, R.E. (2009). Tuberculosis and diabetes mellitus: convergence of two epidemics. Lancet Infect Dis *9*, 737–746.

Doukhan, L., Predich, M., Nair, G., Dussurget, O., Mandic-Mulec, I., Cole, S.T., Smith, D.R., and Smith, I. (1995). Genomic organization of the mycobacterial sigma gene cluster. Gene *165*, 67–70.

Douwes, E., Crouch, N.R., Edwards, T.J., and Mulholland, D.A. (2008). Regression analyses of southern African ethnomedicinal plants: informing the targeted selection of bioprospecting and pharmacological screening subjects. J Ethnopharmacol *119*, 356–364.

Drahl, C., Cravatt, B.F., and Sorensen, E.J. (2005). Protein-reactive natural products. Angew. Chem. Int. Ed. Engl *44*, 5788–5809.

Dudoit, S., and Speed, T.P. (2000). A score test for the linkage analysis of qualitative and quantitative traits based on identity by descent data from sib-pairs. Biostatistics *1*, 1–26.

Dussurget, O., Rodriguez, M., and Smith, I. (1998). Protective role of the Mycobacterium smegmatis IdeR against reactive oxygen species and isoniazid toxicity. Tuber. Lung Dis *79*, 99–106.

Dussurget, O., Timm, J., Gomez, M., Gold, B., Yu, S., Sabol, S.Z., Holmes, R.K., Jacobs, W.R., Jr, and Smith, I. (1999). Transcriptional control of the iron-responsive fxbA gene by the mycobacterial regulator IdeR. J. Bacteriol *181*, 3402–3408.

Dye, C., and Williams, B.G. (2010). The population dynamics and control of tuberculosis. Science *328*, 856–861.

Ehrt, S., and Schnappinger, D. (2009). Mycobacterial survival strategies in the phagosome: defence against host stresses. Cell. Microbiol. *11*, 1170–1178.

Ernst, J.D. (1998). Macrophage receptors for Mycobacterium tuberculosis. Infect. Immun. *66*, 1277–1281.

Fallahi-Sichani, M., El-Kebir, M., Marino, S., Kirschner, D.E., and Linderman, J.J. (2011). Multiscale computational modeling reveals a critical role for TNF-α receptor 1 dynamics in tuberculosis granuloma formation. J. Immunol. *186*, 3472–3483.

Falzon, D., Jaramillo, E., Schünemann, H.J., Arentz, M., Bauer, M., Bayona, J., Blanc, L., Caminero, J.A., Daley, C.L., Duncombe, C., *et al.* (2011). WHO guidelines for the programmatic management of drug-resistant tuberculosis: 2011 update. Eur. Respir. J. *38*, 516–528.

Farhat, M., Greenaway, C., Pai, M., and Menzies, D. (2006). False-positive tuberculin skin tests: what is the absolute effect of BCG and non-tuberculous mycobacteria? Int. J. Tuberc. Lung Dis. *10*, 1192–1204.

Fifis, T., Costopoulos, C., Radford, A.J., Bacic, A., and Wood, P.R. (1991). Purification and characterization of major antigens from a Mycobacterium bovis culture filtrate. Infect. Immun. *59*, 800–807.

Fischbach, M.A., and Walsh, C.T. (2009). Antibiotics for emerging pathogens. Science *325*, 1089–1093.

Flannagan, R.S., Cosío, G., and Grinstein, S. (2009). Antimicrobial mechanisms of phagocytes and bacterial evasion strategies. Nat. Rev. Microbiol. *7*, 355–366.

Flores, A.R., Parsons, L.M., and Pavelka, M.S., Jr (2005). Genetic analysis of the beta-lactamases of Mycobacterium tuberculosis and Mycobacterium smegmatis and susceptibility to beta-lactam antibiotics. Microbiology (Reading, Engl.) *151*, 521–532.

Flynn, J.L., Chan, J., and Lin, P.L. (2011). Macrophages and control of granulomatous inflammation in tuberculosis. Mucosal Immunol *4*, 271–278.

Fontán, P., Aris, V., Ghanny, S., Soteropoulos, P., and Smith, I. (2008). Global transcriptional profile of Mycobacterium tuberculosis during THP-1 human macrophage infection. Infect. Immun. *76*, 717–725.

Fontán, P.A., Voskuil, M.I., Gomez, M., Tan, D., Pardini, M., Manganelli, R., Fattorini, L., Schoolnik, G.K., and Smith, I. (2009). The Mycobacterium tuberculosis sigma factor sigmaB is required for full response to cell envelope stress and hypoxia in vitro, but it is dispensable for in vivo growth. J. Bacteriol *191*, 5628–5633.

Fortún, J., Martín-Dávila, P., Navas, E., Pérez-Elías, M.J., Cobo, J., Tato, M., De la Pedrosa, E.G.-G., Gómez-Mampaso, E., and Moreno, S. (2005). Linezolid for the treatment of multidrug-resistant tuberculosis. J. Antimicrob. Chemother. *56*, 180–185.

Fox, W., Ellard, G.A., and Mitchison, D.A. (1999). Studies on the treatment of tuberculosis undertaken by the British Medical Research Council tuberculosis units, 1946-1986, with relevant subsequent publications. Int. J. Tuberc. Lung Dis *3*, S231–279.

Frieden, T.R., Sterling, T.R., Munsiff, S.S., Watt, C.J., and Dye, C. (2003). Tuberculosis. Lancet *362*, 887–899.

Fu, L.M., and Shinnick, T.M. (2007). Understanding the action of INH on a highly INH-resistant Mycobacterium tuberculosis strain using Genechips. Tuberculosis (Edinb) *87*, 63–70.

Gagneux, S., DeRiemer, K., Van, T., Kato-Maeda, M., de Jong, B.C., Narayanan, S., Nicol, M., Niemann, S., Kremer, K., Gutierrez, M.C., *et al*. (2006). Variable host-pathogen compatibility in Mycobacterium tuberculosis. Proc. Natl. Acad. Sci. U.S.A. *103*, 2869–2873.

Gallegos, A.M., Pamer, E.G., and Glickman, M.S. (2008). Delayed protection by ESAT-6-specific effector CD4+ T cells after airborne *M. tuberculosis* infection. J. Exp. Med. *205*, 2359–2368.

Gandhi, N.R., Nunn, P., Dheda, K., Schaaf, H.S., Zignol, M., van Soolingen, D., Jensen, P., and Bayona, J. (2010). Multidrug-resistant and extensively drug-resistant tuberculosis: a threat to global control of tuberculosis. Lancet *375*, 1830–1843.

Garn, H., Krause, H., Enzmann, V., and Drössler, K. (1994). An improved MTT assay using the electron-coupling agent menadione. J. Immunol. Methods *168*, 253–256.

Gerson, S.L., Kaplan, S.L., Bruss, J.B., Le, V., Arellano, F.M., Hafkin, B., and Kuter, D.J. (2002). Hematologic effects of linezolid: summary of clinical experience. Antimicrob. Agents Chemother. *46*, 2723–2726.

Gobin, J., Moore, C.H., Reeve, J.R., Jr, Wong, D.K., Gibson, B.W., and Horwitz, M.A. (1995). Iron acquisition by Mycobacterium tuberculosis: isolation and characterization of a family of iron-binding exochelins. Proc. Natl. Acad. Sci. U.S.A *92*, 5189–5193.

Golden, M.P., and Vikram, H.R. (2005). Extrapulmonary tuberculosis: an overview. Am Fam Physician *72*, 1761–1768.

Goletti, D., Weissman, D., Jackson, R.W., Graham, N.M., Vlahov, D., Klein, R.S., Munsiff, S.S., Ortona, L., Cauda, R., and Fauci, A.S. (1996). Effect of Mycobacterium tuberculosis on HIV replication. Role of immune activation. J. Immunol *157*, 1271–1278.

Gómez i Prat, J., and de Souza, S.M.F.M. (2003). Prehistoric tuberculosis in america: adding comments to a literature review. Mem. Inst. Oswaldo Cruz *98 Suppl 1*, 151–159.

Gondela, E., and Walczak, K.Z. (2011). Convenient synthesis of 3,4-dichloro-5-hydroxy-2(5H)-furanone glycoconjugates. Molecules *16*, 1011–1020.

Goodwin, B., Hodgson, E., and Liddle, C. (1999). The orphan human pregnane X receptor mediates the transcriptional activation of CYP3A4 by rifampicin through a distal enhancer module. Mol. Pharmacol *56*, 1329–1339.

Grange, J.M. (1996). The biology of the genus Mycobacterium. Soc. Appl. Bacteriol. Symp. Ser. *25*, 1S–9S.

Grange, J.M., Gibson, J., Osborn, T.W., Collins, C.H., and Yates, M.D. (1983). What is BCG? Tubercle *64*, 129–139.

Gumbo, T., Louie, A., Deziel, M.R., Liu, W., Parsons, L.M., Salfinger, M., and Drusano, G.L. (2007). Concentration-dependent Mycobacterium tuberculosis killing and prevention of resistance by rifampin. Antimicrob. Agents Chemother. *51*, 3781–3788.

Haas, C.E., Brazeau, D., Cloen, D., Booker, B.M., Frerichs, V., Zaranek, C., Frye, R.F., and Kufel, T. (2005). Cytochrome P450 mRNA expression in peripheral blood lymphocytes as a predictor of enzyme induction. Eur. J. Clin. Pharmacol. *61*, 583–593.

Harrington-Brock, K., Doerr, C.L., and Moore, M.M. (1995). Mutagenicity and clastogenicity of 3-chloro-4-(dichloromethyl)-5-hydroxy-2(5H)-furanone (MX) in L5178Y/TK+/(-)-3.7.2C mouse lymphoma cells. Mutat. Res. *348*, 105–110.

Hashem, A.I., Youssef, A.S.A., Kandeel, K.A., and Abou-Elmagd, W.S.I. (2007). Conversion of some 2(3H)-furanones bearing a pyrazolyl group into other heterocyclic systems with a study of their antiviral activity. Eur J Med Chem *42*, 934–939.

Hentzer, M., Riedel, K., Rasmussen, T.B., Heydorn, A., Andersen, J.B., Parsek, M.R., Rice, S.A., Eberl, L., Molin, S., Høiby, N., *et al*. (2002). Inhibition of quorum sensing in Pseudomonas aeruginosa biofilm bacteria by a halogenated furanone compound. Microbiology (Reading, Engl.) *148*, 87–102.

Herbert, D., Paramasivan, C.N., and Prabhakar, R. (1994). Protective response in guinea pigs exposed to Mycobacterium aviumintracellulare/M. scrofulaceum, BCG & south Indian isolates of M. tuberculosis. Indian J. Med. Res *99*, 1–7.

Hershfield, E. (1999). Tuberculosis: 9. Treatment. CMAJ *161*, 405–411.

Hesseling, A.C., Schaaf, H.S., Hanekom, W.A., Beyers, N., Cotton, M.F., Gie, R.P., Marais, B.J., van Helden, P., and Warren, R.M. (2003). Danish bacille Calmette-Guérin vaccine-induced disease in human immunodeficiency virus-infected children. Clin. Infect. Dis. *37*, 1226–1233.

Hirsh, A.E., Tsolaki, A.G., DeRiemer, K., Feldman, M.W., and Small, P.M. (2004). Stable association between strains of Mycobacterium tuberculosis and their human host populations. Proc. Natl. Acad. Sci. U.S.A *101*, 4871–4876.

HOBBY, G.L., and LENERT, T.F. (1957). The in vitro action of antituberculous agents against multiplying and non-multiplying microbial cells. Am Rev Tuberc *76*, 1031–1048.

Hoffner, S.E., Svenson, S.B., and Källenius, G. (1987). Synergistic effects of antimycobacterial drug combinations on Mycobacterium avium complex determined radiometrically in liquid medium. Eur. J. Clin. Microbiol *6*, 530–535.

Holland, D.P., Sanders, G.D., Hamilton, C.D., and Stout, J.E. (2009). Costs and cost-effectiveness of four treatment regimens for latent tuberculosis infection. Am. J. Respir. Crit. Care Med. *179*, 1055–1060.

Holmberg, S.D. (1990). The rise of tuberculosis in America before 1820. Am. Rev. Respir. Dis. *142*, 1228–1232.

Hopewell, P.C., Pai, M., Maher, D., Uplekar, M., and Raviglione, M.C. (2006). International standards for tuberculosis care. Lancet Infect Dis *6*, 710–725.

Hugonnet, J.-E., Tremblay, L.W., Boshoff, H.I., Barry, C.E., 3rd, and Blanchard, J.S. (2009). Meropenem-clavulanate is effective against extensively drug-resistant Mycobacterium tuberculosis. Science *323*, 1215–1218.

Hurdle, J.G., Lee, R.B., Budha, N.R., Carson, E.I., Qi, J., Scherman, M.S., Cho, S.H., McNeil, M.R., Lenaerts, A.J., Franzblau, S.G., *et al*. (2008). A microbiological assessment of novel nitrofuranylamides as anti-tuberculosis agents. J. Antimicrob. Chemother. *62*, 1037–1045.

Igarashi, M., Nakagawa, N., Doi, N., Hattori, S., Naganawa, H., and Hamada, M. (2003). Caprazamycin B, a novel anti-tuberculosis antibiotic, from Streptomyces sp. J. Antibiot. *56*, 580–583.

Imlay, J.A., Chin, S.M., and Linn, S. (1988). Toxic DNA damage by hydrogen peroxide through the Fenton reaction in vivo and in vitro. Science *240*, 640–642.

Ito, K., Yamamoto, K., and Kawanishi, S. (1992). Manganese-mediated oxidative damage of cellular and isolated DNA by isoniazid and related hydrazines: non-Fenton-type hydroxyl radical formation. Biochemistry *31*, 11606–11613.

Jia, L., Tomaszewski, J.E., Hanrahan, C., Coward, L., Noker, P., Gorman, G., Nikonenko, B., and Protopopova, M. (2005). Pharmacodynamics and pharmacokinetics of SQ109, a new diamine-based antitubercular drug. Br. J. Pharmacol. *144*, 80–87.

Jones, W.P., Chin, Y.-W., and Kinghorn, A.D. (2006). The role of pharmacognosy in modern medicine and pharmacy. Curr Drug Targets *7*, 247–264.

Jothivasan, V.K., and Hamilton, C.J. (2008). Mycothiol: synthesis, biosynthesis and biological functions of the major low molecular weight thiol in actinomycetes. Nat Prod Rep *25*, 1091–1117.

Kant, L. (2009). Gradual filling up of TB drug pipeline: how can we play our role better? Indian J Tuberc *56*, 1–4.

Karakousis, P.C., Williams, E.P., and Bishai, W.R. (2008). Altered expression of isoniazid-regulated genes in drug-treated dormant Mycobacterium tuberculosis. J. Antimicrob. Chemother. *61*, 323–331.

Kaufmann, S.H.E. (2005). Recent findings in immunology give tuberculosis vaccines a new boost. Trends Immunol *26*, 660–667.

Kaur, P., Agarwal, S., and Datta, S. (2009). Delineating bacteriostatic and bactericidal targets in mycobacteria using IPTG inducible antisense expression. PLoS ONE *4*, e5923.

Kawanishi, S., Oikawa, S., Inoue, S., and Nishino, K. (2002). Distinct mechanisms of oxidative DNA damage induced by carcinogenic nickel subsulfide and nickel oxides. Environ. Health Perspect. *110 Suppl 5*, 789–791.

Keating, G., and Figgitt, D. (2003). Caspofungin: a review of its use in oesophageal candidiasis, invasive candidiasis and invasive aspergillosis. Drugs *63*, 2235–2263.

Kehrer, J.P. (2000). The Haber-Weiss reaction and mechanisms of toxicity. Toxicology *149*, 43–50.

Kelly, S.L., Lamb, D.C., Jackson, C.J., Warrilow, A.G., and Kelly, D.E. (2003). The biodiversity of microbial cytochromes P450. Adv. Microb. Physiol. *47*, 131–186.

Kinghorn, A.D. (1994). The discovery of drugs from higher plants. Biotechnology *26*, 81–108.

Kmentova, I., Sutherland, H.S., Palmer, B.D., Blaser, A., Franzblau, S.G., Wan, B., Wang, Y., Ma, Z., Denny, W.A., and Thompson, A.M. (2010). Synthesis and Structure-Activity Relationships of Aza- and Diazabiphenyl Analogues of the Antitubercular Drug (6S)-2-Nitro-6-{[4-(trifluoromethoxy)benzyl]oxy}-6,7-dihydro-5H-imidazo[2,1-b][1,3]oxazine (PA-824). J. Med. Chem.

Koehn, F.E., and Carter, G.T. (2005). The evolving role of natural products in drug discovery. Nat Rev Drug Discov *4*, 206–220.

Kohanski, M.A., Dwyer, D.J., Hayete, B., Lawrence, C.A., and Collins, J.J. (2007). A common mechanism of cellular death induced by bactericidal antibiotics. Cell *130*, 797–810.

Koul, A., Arnoult, E., Lounis, N., Guillemont, J., and Andries, K. (2011). The challenge of new drug discovery for tuberculosis. Nature *469*, 483–490.

Koul, A., Dendouga, N., Vergauwen, K., Molenberghs, B., Vranckx, L., Willebrords, R., Ristic, Z., Lill, H., Dorange, I., Guillemont, J., *et al*. (2007). Diarylquinolines target subunit c of mycobacterial ATP synthase. Nat. Chem. Biol *3*, 323–324.

Koumis, T., and Samuel, S. (2005). Tiotropium bromide: a new long-acting bronchodilator for the treatment of chronic obstructive pulmonary disease. Clin Ther *27*, 377–392.

L'homme, R.F., Nijland, H.M.J., Gras, L., Aarnoutse, R.E., van Crevel, R., Boeree, M., Brinkman, K., Prins, J.M., Juttmann, J.R., and Burger, D.M. (2009). Clinical experience with the combined use of lopinavir/ritonavir and rifampicin. AIDS *23*, 863–865.

Lalloo, U.G., and Ambaram, A. (2010). New antituberculous drugs in development. Curr HIV/AIDS Rep *7*, 143–151.

Lenaerts, A.J., Gruppo, V., Marietta, K.S., Johnson, C.M., Driscoll, D.K., Tompkins, N.M., Rose, J.D., Reynolds, R.C., and Orme, I.M. (2005a). Preclinical testing of the nitroimidazopyran PA-824 for activity against Mycobacterium tuberculosis in a series of in vitro and in vivo models. Antimicrob. Agents Chemother *49*, 2294–2301.

Lenaerts, A.J., Gruppo, V., Marietta, K.S., Johnson, C.M., Driscoll, D.K., Tompkins, N.M., Rose, J.D., Reynolds, R.C., and Orme, I.M. (2005b). Preclinical testing of the nitroimidazopyran PA-824 for activity against Mycobacterium tuberculosis in a series of in vitro and in vivo models. Antimicrob. Agents Chemother *49*, 2294–2301.

Leroy, V., Salmi, L.R., Dupon, M., Sentilhes, A., Texier-Maugein, J., Dequae, L., Dabis, F., and Salamon, R. (1997). Progression of human immunodeficiency virus infection in patients with tuberculosis disease. A cohort study in Bordeaux, France, 1988-1994. The Groupe d'Epidémiologie Clinique du Sida en Aquitaine (GECSA). Am. J. Epidemiol *145*, 293–300.

Levin, B.R., and Rozen, D.E. (2006). Non-inherited antibiotic resistance. Nat. Rev. Microbiol. *4*, 556–562.

Lin, P.L., Rodgers, M., Smith, L., Bigbee, M., Myers, A., Bigbee, C., Chiosea, I., Capuano, S.V., Fuhrman, C., Klein, E., *et al*. (2009). Quantitative comparison of active and latent tuberculosis in the cynomolgus macaque model. Infect. Immun. *77*, 4631–4642.

Lönn-Stensrud, J., Petersen, F.C., Benneche, T., and Scheie, A.A. (2007). Synthetic bromated furanone inhibits autoinducer-2-mediated communication and biofilm formation in oral streptococci. Oral Microbiol. Immunol *22*, 340–346.

Ma, Z., Lienhardt, C., McIlleron, H., Nunn, A.J., and Wang, X. (2010). Global tuberculosis drug development pipeline: the need and the reality. Lancet *375*, 2100–2109.

Makarov, V., Manina, G., Mikusova, K., Möllmann, U., Ryabova, O., Saint-Joanis, B., Dhar, N., Pasca, M.R., Buroni, S., Lucarelli, A.P., *et al*. (2009). Benzothiazinones kill Mycobacterium tuberculosis by blocking arabinan synthesis. Science *324*, 801–804.

Malik, Z.A., Iyer, S.S., and Kusner, D.J. (2001). Mycobacterium tuberculosis phagosomes exhibit altered calmodulin-dependent signal transduction: contribution to inhibition of phagosome-lysosome fusion and intracellular survival in human macrophages. J. Immunol. *166*, 3392–3401.

Manefield, M., Rasmussen, T.B., Henzter, M., Andersen, J.B., Steinberg, P., Kjelleberg, S., and Givskov, M. (2002). Halogenated furanones inhibit quorum sensing through accelerated LuxR turnover. Microbiology (Reading, Engl.) *148*, 1119–1127.

Manganelli, R., Voskuil, M.I., Schoolnik, G.K., Dubnau, E., Gomez, M., and Smith, I. (2002). Role of the extracytoplasmic-function sigma factor sigma(H) in Mycobacterium tuberculosis global gene expression. Mol. Microbiol *45*, 365–374.

Manjunatha, U., Boshoff, H.I., and Barry, C.E. (2009). The mechanism of action of PA-824: Novel insights from transcriptional profiling. Commun Integr Biol *2*, 215–218.

Manjunatha, U.H., Boshoff, H., Dowd, C.S., Zhang, L., Albert, T.J., Norton, J.E., Daniels, L., Dick, T., Pang, S.S., and Barry, C.E., 3rd (2006). Identification of a nitroimidazo-oxazine-specific protein involved in PA-824 resistance in Mycobacterium tuberculosis. Proc. Natl. Acad. Sci. U.S.A. *103*, 431–436.

Marais, B.J., Parker, S.K., Verver, S., van Rie, A., and Warren, R.M. (2009). Primary and postprimary or reactivation tuberculosis: time to revise confusing terminology? AJR Am J Roentgenol *192*, W198; author reply W199–200.

Margulies, D.H. (2009). Antigen-processing and presentation pathways select antigenic HIV peptides in the fight against viral evolution. Nat. Immunol. *10*, 566–568.

Mathema, B., Kurepina, N.E., Bifani, P.J., and Kreiswirth, B.N. (2006). Molecular epidemiology of tuberculosis: current insights. Clin. Microbiol. Rev *19*, 658–685.

Matsumoto, M., Hashizume, H., Tomishige, T., Kawasaki, M., Tsubouchi, H., Sasaki, H., Shimokawa, Y., and Komatsu, M. (2006). OPC-67683, a nitro-dihydro-imidazooxazole derivative with promising action against tuberculosis in vitro and in mice. PLoS Med. *3*, e466.

McCune, R.M., Feldmann, F.M., Lambert, H.P., and McDermott, W. (1966). Microbial persistence. I. The capacity of tubercle bacilli to survive sterilization in mouse tissues. J. Exp. Med. *123*, 445–468.

McLean, K.J., Clift, D., Lewis, D.G., Sabri, M., Balding, P.R., Sutcliffe, M.J., Leys, D., and Munro, A.W. (2006). The preponderance of P450s in the Mycobacterium tuberculosis genome. Trends Microbiol. *14*, 220–228.

Mietzner, T.A., Luginbuhl, G.H., Sandstrom, E., and Morse, S.A. (1984). Identification of an iron-regulated 37,000-dalton protein in the cell envelope of Neisseria gonorrhoeae. Infect. Immun. *45*, 410–416.

Migliori, G.B., De Iaco, G., Besozzi, G., Centis, R., and Cirillo, D.M. (2007). First tuberculosis cases in Italy resistant to all tested drugs. Euro Surveill. *12*, E070517.1.

Miller, J.F., Mekalanos, J.J., and Falkow, S. (1989). Coordinate regulation and sensory transduction in the control of bacterial virulence. Science *243*, 916–922.

Mitchell, G., Bartlett, D.W., Fraser, T.E., Hawkes, T.R., Holt, D.C., Townson, J.K., and Wichert, R.A. (2001). Mesotrione: a new selective herbicide for use in maize. Pest Manag. Sci *57*, 120–128.

Mitchison, D.A. (2004). The search for new sterilizing anti-tuberculosis drugs. Front. Biosci. *9*, 1059–1072.

Mitnick, C., Bayona, J., Palacios, E., Shin, S., Furin, J., Alcántara, F., Sánchez, E., Sarria, M., Becerra, M., Fawzi, M.C.S., *et al*. (2003). Community-based therapy for multidrug-resistant tuberculosis in Lima, Peru. N. Engl. J. Med *348*, 119–128.

Moran, M. (2005). A breakthrough in R&D for neglected diseases: new ways to get the drugs we need. PLoS Med. *2*, e302.

Muñoz-Elías, E.J., Timm, J., Botha, T., Chan, W.-T., Gomez, J.E., and McKinney, J.D. (2005). Replication dynamics of Mycobacterium tuberculosis in chronically infected mice. Infect. Immun. *73*, 546–551.

Myers, J.P. (2005). New recommendations for the treatment of tuberculosis. Curr. Opin. Infect. Dis. *18*, 133–140.

Nathan, C. (2008). Microbiology. An antibiotic mimics immunity. Science *322*, 1337–1338.

Newman, D.J., Cragg, G.M., and Snader, K.M. (2000). The influence of natural products upon drug discovery. Nat Prod Rep *17*, 215–234.

Newman, D.J., Cragg, G.M., and Snader, K.M. (2003). Natural products as sources of new drugs over the period 1981-2002. J. Nat. Prod *66*, 1022–1037.

Newton, G.L., Buchmeier, N., and Fahey, R.C. (2008). Biosynthesis and functions of mycothiol, the unique protective thiol of Actinobacteria. Microbiol. Mol. Biol. Rev *72*, 471–494.

Niemi, M., Backman, J.T., Fromm, M.F., Neuvonen, P.J., and Kivistö, K.T. (2003). Pharmacokinetic interactions with rifampicin : clinical relevance. Clin Pharmacokinet *42*, 819–850.

Nikonenko, B.V., Protopopova, M., Samala, R., Einck, L., and Nacy, C.A. (2007). Drug therapy of experimental tuberculosis (TB): improved outcome by combining SQ109, a new diamine antibiotic, with existing TB drugs. Antimicrob. Agents Chemother. *51*, 1563–1565.

North, R.J., and Jung, Y.-J. (2004). Immunity to tuberculosis. Annu. Rev. Immunol *22*, 599–623.

de Nys, R., Givskov, M., Kumar, N., Kjelleberg, S., and Steinberg, P.D. (2006). Furanones. Prog. Mol. Subcell. Biol *42*, 55–86.

O'Reilly, L.M., and Daborn, C.J. (1995). The epidemiology of Mycobacterium bovis infections in animals and man: a review. Tuber. Lung Dis *76 Suppl 1*, 1–46.

Palma, C., Vendetti, S., and Cassone, A. (2010). Role of 4-1BB receptor in the control played by CD8(+) T cells on IFN-gamma production by Mycobacterium tuberculosis antigen-specific CD4(+) T Cells. PLoS ONE *5*, e11019.

Palmer, C.E., and Long, M.W. (1966). Effects of infection with atypical mycobacteria on BCG vaccination and tuberculosis. Am. Rev. Respir. Dis *94*, 553–568.

Palomino, J.C., Ramos, D.F., and da Silva, P.A. (2009). New anti-tuberculosis drugs: strategies, sources and new molecules. Curr. Med. Chem. *16*, 1898–1904.

Paterson, I., and Anderson, E.A. (2005). Chemistry. The renaissance of natural products as drug candidates. Science *310*, 451–453.

Payne, D.J., Gwynn, M.N., Holmes, D.J., and Pompliano, D.L. (2007). Drugs for bad bugs: confronting the challenges of antibacterial discovery. Nat Rev Drug Discov *6*, 29–40.

Pethe, K., Sequeira, P.C., Agarwalla, S., Rhee, K., Kuhen, K., Phong, W.Y., Patel, V., Beer, D., Walker, J.R., Duraiswamy, J., *et al*. (2010). A chemical genetic screen in Mycobacterium tuberculosis identifies carbon-source-dependent growth inhibitors devoid of in vivo efficacy. Nat Commun *1*, 57.

Pillay, P., Vleggaar, R., Maharaj, V.J., Smith, P.J., Lategan, C.A., Chouteau, F., and Chibale, K. (2007). Antiplasmodial hirsutinolides from Vernonia staehelinoides and their utilization towards a simplified pharmacophore. Phytochemistry *68*, 1200–1205.

Projan, S.J. (2003). Why is big Pharma getting out of antibacterial drug discovery? Curr. Opin. Microbiol. *6*, 427–430.

Protopopova, M., Hanrahan, C., Nikonenko, B., Samala, R., Chen, P., Gearhart, J., Einck, L., and Nacy, C.A. (2005). Identification of a new antitubercular drug candidate, SQ109, from a combinatorial library of 1,2-ethylenediamines. J. Antimicrob. Chemother. *56*, 968–974.

Quadri, L.E., Sello, J., Keating, T.A., Weinreb, P.H., and Walsh, C.T. (1998). Identification of a Mycobacterium tuberculosis gene cluster encoding the biosynthetic enzymes for assembly of the virulence-conferring siderophore mycobactin. Chem. Biol *5*, 631–645.

Rae, J.M., Johnson, M.D., Lippman, M.E., and Flockhart, D.A. (2001). Rifampin is a selective, pleiotropic inducer of drug metabolism genes in human hepatocytes: studies with cDNA and oligonucleotide expression arrays. J. Pharmacol. Exp. Ther. *299*, 849–857.

Raghu, B., Sarma, G.R., and Venkatesan, P. (1993). Effect of iron on the growth and siderophore production of mycobacteria. Biochem. Mol. Biol. Int *31*, 341–348.

Ramachandran, G., and Gurumurthy, P. (2002). Effect of rifampicin & isoniazid on cytochrome P-450 in mycobacteria. Indian J. Med. Res. *116*, 140–144.

Ratledge, C., and Dover, L.G. (2000). Iron metabolism in pathogenic bacteria. Annu. Rev. Microbiol. *54*, 881–941.

Ratledge, C., and Ewing, M. (1996). The occurrence of carboxymycobactin, the siderophore of pathogenic mycobacteria, as a second extracellular siderophore in Mycobacterium smegmatis. Microbiology (Reading, Engl.) *142 (Pt 8)*, 2207–2212.

Raviglione, M.C. (2007). The new Stop TB Strategy and the Global Plan to Stop TB, 2006-2015. Bull. World Health Organ. *85*, 327.

Rawat, M., Johnson, C., Cadiz, V., and Av-Gay, Y. (2007). Comparative analysis of mutants in the mycothiol biosynthesis pathway in Mycobacterium smegmatis. Biochem. Biophys. Res. Commun *363*, 71–76.

Rawat, M., Newton, G.L., Ko, M., Martinez, G.J., Fahey, R.C., and Av-Gay, Y. (2002). Mycothiol-deficient Mycobacterium smegmatis mutants are hypersensitive to alkylating agents, free radicals, and antibiotics. Antimicrob. Agents Chemother. *46*, 3348–3355.

Reddy, V.M., Einck, L., Andries, K., and Nacy, C.A. (2010). In vitro interactions between new antitubercular drug candidates SQ109 and TMC207. Antimicrob. Agents Chemother. *54*, 2840–2846.

Ren, D., Bedzyk, L.A., Setlow, P., England, D.F., Kjelleberg, S., Thomas, S.M., Ye, R.W., and Wood, T.K. (2004). Differential gene expression to investigate the effect of (5Z)-4-bromo- 5-(bromomethylene)-3-butyl-2(5H)-furanone on Bacillus subtilis. Appl. Environ. Microbiol. *70*, 4941–4949.

Ren, D., Sims, J.J., and Wood, T.K. (2001). Inhibition of biofilm formation and swarming of Escherichia coli by (5Z)-4-bromo-5-(bromomethylene)-3-butyl-2(5H)-furanone. Environ. Microbiol. *3*, 731–736.

Reynes, J., Perez, C., Lamaury, I., Janbon, F., and Bertrand, A. (1989). Bacille Calmette-Guérin adenitis 30 years after immunization in a patient with AIDS. J. Infect. Dis *160*, 727.

Rice, S.A., McDougald, D., Kumar, N., and Kjelleberg, S. (2005). The use of quorum-sensing blockers as therapeutic agents for the control of biofilm-associated infections. Curr Opin Investig Drugs *6*, 178–184.

Rodriguez, G.M., Gardner, R., Kaur, N., and Phanstiel, O., 4th (2008). Utilization of Fe3+-acinetoferrin analogs as an iron source by Mycobacterium tuberculosis. Biometals *21*, 93–103.

Rodriguez, G.M., Gold, B., Gomez, M., Dussurget, O., and Smith, I. (1999). Identification and characterization of two divergently transcribed iron regulated genes in Mycobacterium tuberculosis. Tuber. Lung Dis *79*, 287–298.

Rodriguez, G.M., and Smith, I. (2003). Mechanisms of iron regulation in mycobacteria: role in physiology and virulence. Mol. Microbiol *47*, 1485–1494.

Rodriguez, G.M., and Smith, I. (2006). Identification of an ABC transporter required for iron acquisition and virulence in Mycobacterium tuberculosis. J. Bacteriol *188*, 424–430.

Rodriguez, G.M., Voskuil, M.I., Gold, B., Schoolnik, G.K., and Smith, I. (2002). ideR, An essential gene in mycobacterium tuberculosis: role of IdeR in iron-dependent gene expression, iron metabolism, and oxidative stress response. Infect. Immun *70*, 3371–3381.

Rothschild, B.M., Martin, L.D., Lev, G., Bercovier, H., Bar-Gal, G.K., Greenblatt, C., Donoghue, H., Spigelman, M., and Brittain, D. (2001). Mycobacterium tuberculosis complex DNA from an extinct bison dated 17,000 years before the present. Clin. Infect. Dis *33*, 305–311.

Rozman, K.K., and Doull, J. (2001). Paracelsus, Haber and Arndt. Toxicology *160*, 191–196.

Ruslami, R., Nijland, H.M.J., Adhiarta, I.G.N., Kariadi, S.H.K.S., Alisjahbana, B., Aarnoutse, R.E., and van Crevel, R. (2010). Pharmacokinetics of antituberculosis drugs in pulmonary tuberculosis patients with type 2 diabetes. Antimicrob. Agents Chemother *54*, 1068–1074.

Russell, D.G. (2011). Mycobacterium tuberculosis and the intimate discourse of a chronic infection. Immunol. Rev. *240*, 252–268.

Rustomjee, R., Lienhardt, C., Kanyok, T., Davies, G.R., Levin, J., Mthiyane, T., Reddy, C., Sturm, A.W., Sirgel, F.A., Allen, J., *et al*. (2008). A Phase II study of the sterilising activities of ofloxacin, gatifloxacin and moxifloxacin in pulmonary tuberculosis. Int. J. Tuberc. Lung Dis. *12*, 128–138.

Saeed, A.I., Sharov, V., White, J., Li, J., Liang, W., Bhagabati, N., Braisted, J., Klapa, M., Currier, T., Thiagarajan, M., *et al*. (2003). TM4: a free, open-source system for microarray data management and analysis. BioTechniques *34*, 374–378.

Sasaki, H., Haraguchi, Y., Itotani, M., Kuroda, H., Hashizume, H., Tomishige, T., Kawasaki, M., Matsumoto, M., Komatsu, M., and Tsubouchi, H. (2006). Synthesis and antituberculosis activity of a novel series of optically active 6-nitro-2,3-dihydroimidazo[2,1-b]oxazoles. J. Med. Chem. *49*, 7854–7860.

SCHMITZ, P., and KLEINE-ALLEKOTTE, B. (1960). [Treatment of pulmonary tuberculosis with PAS infusions associated with INH and streptomycin]. Med Welt *42*, 2206–2211.

Schnappinger, D., Ehrt, S., Voskuil, M.I., Liu, Y., Mangan, J.A., Monahan, I.M., Dolganov, G., Efron, B., Butcher, P.D., Nathan, C., *et al*. (2003). Transcriptional Adaptation of Mycobacterium tuberculosis within Macrophages: Insights into the Phagosomal Environment. J. Exp. Med. *198*, 693–704.

Scott, L.J., Curran, M.P., and Figgitt, D.P. (2004). Rosuvastatin: a review of its use in the management of dyslipidemia. Am J Cardiovasc Drugs *4*, 117–138.

Shikano, S., Yamashita, Y., and Sato, T. (2009). [Anatomical names of skeletal tubers and tubercles: analysis and classification of Latin names, and comparison with corresponding English and Japanese names]. Kaibogaku Zasshi *84*, 11–15.

Siddiqi, S.H., Libonati, J.P., and Middlebrook, G. (1981). Evaluation of rapid radiometric method for drug susceptibility testing of Mycobacterium tuberculosis. J. Clin. Microbiol. *13*, 908–912.

Slayden, R.A., Lee, R.E., and Barry, C.E., 3rd (2000). Isoniazid affects multiple components of the type II fatty acid synthase system of Mycobacterium tuberculosis. Mol. Microbiol *38*, 514–525.

Sly, L.M., Lopez, M., Nauseef, W.M., and Reiner, N.E. (2001). 1alpha,25-Dihydroxyvitamin D3-induced monocyte antimycobacterial activity is regulated by phosphatidylinositol 3-kinase and mediated by the NADPH-dependent phagocyte oxidase. J. Biol. Chem. *276*, 35482–35493.

Smith, C.V., Huang, C., Miczak, A., Russell, D.G., Sacchettini, J.C., and Höner zu Bentrup, K. (2003). Biochemical and structural studies of malate synthase from Mycobacterium tuberculosis. J. Biol. Chem. *278*, 1735–1743.

Smith, D.W. (1985). Protective effect of BCG in experimental tuberculosis. Adv Tuberc Res *22*, 1–97.

Smith, N.H., Gordon, S.V., de la Rua-Domenech, R., Clifton-Hadley, R.S., and Hewinson, R.G. (2006). Bottlenecks and broomsticks: the molecular evolution of Mycobacterium bovis. Nat. Rev. Microbiol. *4*, 670–681.

Spigelman, M.K. (2007). New tuberculosis therapeutics: a growing pipeline. J. Infect. Dis. *196 Suppl 1*, S28–34.

Stanford, J.L., Shield, M.J., and Rook, G.A. (1981). How environmental mycobacteria may predetermine the protective efficacy of BCG. Tubercle *62*, 55–62.

Steingart, K.R., Jotblad, S., Robsky, K., Deck, D., Hopewell, P.C., Huang, D., and Nahid, P. (2011). Higher-dose rifampin for the treatment of pulmonary tuberculosis: a systematic review. Int. J. Tuberc. Lung Dis. *15*, 305–316.

Strohl (2000). The role of natural products in a modern drug discovery program. Drug Discov. Today *5*, 39–41.

Tanaka, Y., Morita, C.T., Tanaka, Y., Nieves, E., Brenner, M.B., and Bloom, B.R. (1995). Natural and synthetic non-peptide antigens recognized by human gamma delta T cells. Nature *375*, 155–158.

Taniguchi, M., and Kubo, I. (1993). Ethnobotanical drug discovery based on medicine men's trials in the African savanna: screening of east African plants for antimicrobial activity II. J. Nat. Prod. *56*, 1539–1546.

Teixeira, H.C., Abramo, C., and Munk, M.E. (2007). Immunological diagnosis of tuberculosis: problems and strategies for success. J Bras Pneumol *33*, 323–334.

Temple, M.E., and Nahata, M.C. (1999). Rifapentine: its role in the treatment of tuberculosis. Ann Pharmacother *33*, 1203–1210.

Thwaites, G., Caws, M., Chau, T.T.H., D'Sa, A., Lan, N.T.N., Huyen, M.N.T., Gagneux, S., Anh, P.T.H., Tho, D.Q., Torok, E., *et al*. (2008). Relationship between Mycobacterium tuberculosis genotype and the clinical phenotype of pulmonary and meningeal tuberculosis. J. Clin. Microbiol. *46*, 1363–1368.

Touré, N.O., Dia Kane, Y., Diatta, A., Ba Diop, S., Niang, A., Ndiaye, E.M., Thiam, K., Mbaye, F.B.R., Badiane, M., and Hane, A.A. (2007). [Tuberculosis and diabetes]. Rev Mal Respir *24*, 869–875.

Trefzer, C., Rengifo-Gonzalez, M., Hinner, M.J., Schneider, P., Makarov, V., Cole, S.T., and Johnsson, K. (2010). Benzothiazinones: prodrugs that covalently modify the decaprenylphosphoryl-β-D-ribose 2'-epimerase DprE1 of Mycobacterium tuberculosis. J. Am. Chem. Soc. *132*, 13663–13665.

Tsuchiya, S., Kobayashi, Y., Goto, Y., Okumura, H., Nakae, S., Konno, T., and Tada, K. (1982). Induction of maturation in cultured human monocytic leukemia cells by a phorbol diester. Cancer Res *42*, 1530–1536.

Tsuchiya, S., Yamabe, M., Yamaguchi, Y., Kobayashi, Y., Konno, T., and Tada, K. (1980). Establishment and characterization of a human acute monocytic leukemia cell line (THP-1). Int. J. Cancer *26*, 171–176.

Tusher, V.G., Tibshirani, R., and Chu, G. (2001). Significance analysis of microarrays applied to the ionizing radiation response. Proc. Natl. Acad. Sci. U.S.A *98*, 5116–5121.

Udwadia, Z.F., Amale, R.A., Ajbani, K.K., and Rodrigues, C. (2012). Totally drug-resistant tuberculosis in India. Clin. Infect. Dis. *54*, 579–581.

Velayati, A.A., Masjedi, M.R., Farnia, P., Tabarsi, P., Ghanavi, J., Ziazarifi, A.H., and Hoffner, S.E. (2009). Emergence of new forms of totally drug-resistant tuberculosis bacilli: super extensively drug-resistant tuberculosis or totally drug-resistant strains in iran. Chest *136*, 420–425.

Vilchèze, C., Av-Gay, Y., Attarian, R., Liu, Z., Hazbón, M.H., Colangeli, R., Chen, B., Liu, W., Alland, D., Sacchettini, J.C., *et al*. (2008). Mycothiol biosynthesis is essential for ethionamide susceptibility in Mycobacterium tuberculosis. Mol. Microbiol *69*, 1316–1329.

Vilchèze, C., Morbidoni, H.R., Weisbrod, T.R., Iwamoto, H., Kuo, M., Sacchettini, J.C., and Jacobs, W.R., Jr (2000). Inactivation of the inhA-encoded fatty acid synthase II (FASII) enoyl-acyl carrier protein reductase induces accumulation of the FASI end products and cell lysis of Mycobacterium smegmatis. J. Bacteriol *182*, 4059–4067.

Voskuil, M.I., Schnappinger, D., Visconti, K.C., Harrell, M.I., Dolganov, G.M., Sherman, D.R., and Schoolnik, G.K. (2003). Inhibition of respiration by nitric oxide induces a Mycobacterium tuberculosis dormancy program. J. Exp. Med. *198*, 705–713.

De Voss, J.J., Rutter, K., Schroeder, B.G., and Barry, C.E., 3rd (1999). Iron acquisition and metabolism by mycobacteria. J. Bacteriol *181*, 4443–4451.

De Voss, J.J., Rutter, K., Schroeder, B.G., Su, H., Zhu, Y., and Barry, C.E., 3rd (2000). The salicylate-derived mycobactin siderophores of Mycobacterium tuberculosis are essential for growth in macrophages. Proc. Natl. Acad. Sci. U.S.A. *97*, 1252–1257.

Wassenaar, T.M., Bohlin, J., Binnewies, T.T., and Ussery, D.W. (2009). Genome comparison of bacterial pathogens. Genome Dyn *6*, 1–20.

Wayne, L.G. (1994). Dormancy of Mycobacterium tuberculosis and latency of disease. Eur. J. Clin. Microbiol. Infect. Dis. *13*, 908–914.

Wayne, L.G., and Hayes, L.G. (1996). An in vitro model for sequential study of shiftdown of Mycobacterium tuberculosis through two stages of nonreplicating persistence. Infect Immun *64*, 2062–2069.

Weinberg, E.D. (1984). Iron withholding: a defense against infection and neoplasia. Physiol. Rev *64*, 65–102.

Wilson, M., DeRisi, J., Kristensen, H.H., Imboden, P., Rane, S., Brown, P.O., and Schoolnik, G.K. (1999). Exploring drug-induced alterations in gene expression in Mycobacterium tuberculosis by microarray hybridization. Proc. Natl. Acad. Sci. U.S.A *96*, 12833–12838.

Winau, F., Weber, S., Sad, S., de Diego, J., Hoops, S.L., Breiden, B., Sandhoff, K., Brinkmann, V., Kaufmann, S.H.E., and Schaible, U.E. (2006). Apoptotic vesicles crossprime CD8 T cells and protect against tuberculosis. Immunity *24*, 105–117.

Yajko, D.M., Madej, J.J., Lancaster, M.V., Sanders, C.A., Cawthon, V.L., Gee, B., Babst, A., and Hadley, W.K. (1995). Colorimetric method for determining MICs of antimicrobial agents for Mycobacterium tuberculosis. J. Clin. Microbiol. *33*, 2324–2327.

Zhang, J., Blazecka, P.G., Belmont, D., and Davidson, J.G. (2002). Reinvestigation of mucohalic acids, versatile and useful building blocks for highly functionalized alpha,beta-unsaturated gamma-butyrolactones. Org. Lett. *4*, 4559–4561.

Zhao, X., and Drlica, K. (2008). A unified anti-mutant dosing strategy. J. Antimicrob. Chemother. *62*, 434–436.